40ª REUNIÃO IBÉRICA DE ADSORÇÃO

LIVRO DE RESUMOS

Universidade de Évora

Évora, 2016

Título: 40ª Reunião Ibérica de Adsorção – Livro de Resumos
Editores: Manuela Ribeiro Carrott e Peter Carrott
Design da Capa: Gabinete de Comunicação da Universidade de Évora
Impressão: Reprografia da Universidade de Évora
Tiragem: 100 exemplares
ISBN: 978-989-8550-34-7
Depósito Legal nº 414298/16

40ª REUNIÃO IBÉRICA DE ADSORÇÃO

COMISSÃO ORGANIZADORA

Manuela Ribeiro Carrott

Peter Joseph Carrott

João Manuel Nabais

Isabel Paixão Cansado

Paulo Mira Mourão

José Rubén García

COMISSÃO CIENTÍFICA

Alírio Egídio Rodrigues (Universidade do Porto)

Carmen Blanco Delgado (Universidad de Cantabria)

Filipa Gomes Ribeiro (Universidade de Lisboa)

João Pires da Silva (Universidade de Lisboa)

José Bernardo Parra (INCAR-CSIC)

José Luís Figueiredo (Universidade do Porto)

José María Guil (IQFR-CSIC)

José Rubén García (Universidad de Oviedo)

Julián Garrido Segovia (Universidad Pública de Navarra)

Manuela Ribeiro Carrott (Universidade de Évora)

Peter Joseph Carrott (Universidade de Évora)

Sofía Calero Díaz (Universidad Pablo de Olavide)

APOIOS

UNIVERSIDADE DE ÉVORA

CQE
Centro de Química de Évora

PRECISION

Dias de Sousa
INSTRUMENTAÇÃO ANALÍTICA E CIENTÍFICA, S.A.

paralab

CÂMARA MUNICIPAL DE ÉVORA

SOCIEDADE PORTUGUESA DE QUÍMICA

RSEQ
Real Sociedad Española de Química

ÍNDICE

CONFERÊNCIAS PLENÁRIAS

Adsorption Deformation of Nanoporous Materials: from Single Crystals to Hierarchical Structures

Alexander V. Neimark
Department of Chemical and Biochemical Engineering,
Rutgers University, 98 Brett Road, Piscataway, New Jersey 08854-8058, USA
Email: aneimark@rutgers.edu; Web: http://sol.rutgers.edu/~aneimark/

Phenomenon of adsorption-induced deformation attracted recently a considerable attention owing to its relevance to practical problems of mechanical stability and integrity of novel nanoporous materials and their adsorption properties. Guest molecules adsorbed in nanopores cause a substantial stress in the host matrix leading to its contraction or swelling depending on the specifics of host-guest interactions. Although various experimental manifestations of adsorption-induced deformation have been known for a long time since Leonardo da Vinci's studies of water sorption on human hair, a rigorous theoretical description of this phenomenon is lacking. I will present a general thermodynamic approach to predicting adsorption stress and respective deformation in various microporous and mesoporous materials based on molecular models of adsorption within elastic nanoscale confinements. Examples include metal-organic frameworks, zeolites, mesoporous crystals, and hierarchical micro-mesoporous carbons [1-12]. As a topical practical application, I will also discuss the deformation of coal during CO_2 sequestration at geological conditions [7,8].

Selected references

1. P. Kowalczyk, C. Balzer, G. Reichenauer, A.P. Terzyk, P.A. Gauden, A.V. Neimark, Using in-situ Adsorption Dilatometry for Assessment of Micropore Size Distribution in Monolithic Carbons, Carbon 103 (2016) 263-272.
2. F.X. Coudert, A.H. Fuchs, A.V. Neimark, Adsorption Deformation of Microporous Composites, Dalton Transactions 45 (2016) 4136-4140.
3. H.S. Cho, H. Deng, K. Miyasaka, Z. Dong, M. Cho, A.V. Neimark, J.K. Kang, O.M. Yaghi, O. Terasaki, Extra adsorption and adsorbate superlattice formation in metal-organic frameworks, Nature 527 (2015) 503-508.
4. F.X. Coudert, A.H. Fuchs, A. Boutin, A.V. Neimark, Adsorption Deformation and Structural Transitions in Metal-Organic Frameworks: From the Unit Cell to the Crystal, Journal of Physical Chemistry Letters 4 (2013) 3198−3205.
5. G.Yu. Gor, O. Paris, J. Prass, P.A. Russo, M.M.L. Ribeiro Carrott, A.V. Neimark, Adsorption of n-Pentane on Mesoporous Silica and Adsorbent Deformation, Langmuir 29 (2013) 8601–8608.
6. A.V. Neimark, F.X. Coudert, C. Triguero, A. Boutin, A.H. Fuchs, I. Beurroies, R. Denoyel, Structural Transitions in MIL-53 (Cr): View from Outside and Inside, Langmuir 27 (2011) 4734-4741.
7. K. Yang, X. Lu, Y. Lin, A.V. Neimark, Effects of coal deformation upon CO_2 adsorption and sequestration, Journal of Geophysical Research – Solid Earth 116 (2011) B08212.
8. K. Yang, X. Lu, Y. Lin, A.V. Neimark, Deformation of coal induced by methane adsorption at geological conditions, Energy & Fuel 24 (2010) 5955–5964.

9. G.Yu. Gor, A.V. Neimark, Adsorption-Induced Deformation of Mesoporous Solids, Langmuir 26 (2010) 13021–13027.
10. A.V. Neimark, F.X. Coudert, A. Boutin, A.H. Fuchs, Stress-based model for the breathing of metal–organic frameworks, Journal of Physical Chemistry Letters 1 (2010) 445–449.
11. P. Kowalczyk, A. Ciach, A.V. Neimark, Adsorption-induced deformation of microporous carbons: pore size distribution effect, Langmuir 24 (2008) 6603-6608.
12. P.I. Ravikovitch, A.V. Neimark, Density Functional Theory Model of Adsorption Deformation, Langmuir 22 (2006) 11171-11179.

Zeolite-Type Transition Metal/Lanthanide Silicates Adsorbents and Metal Organic Frameworks

João Rocha
Department of Chemistry, CICECO-Aveiro Institute of Materials
University of Aveiro, 3810-193 Aveiro, Portugal
rocha@ua.pt

I shall review some of the work carried out in Aveiro on nanoporous transition-metal [1] and lanthanide (Ln) silicates [2] and on Ln-bearing coordination polymers (or metal organic frameworks, MOFs) [3]. The main focus will be on the design of (nano) materials for light emission sensing small molecules [4] and temperature [5-8] and for drug delivery [9], treating bone tissue disorders [10] and use as pharmaceuticals [11].

While nanoporous (zeolite-like) silicates are highly robust (thermal and chemical) systems, allowing applications in relatively harsh conditions, it is very challenging to synthesise the desired architectures and modify them post-synthesis. In contrast, MOFs operate in milder conditions and often lack robustness but they are much more amenable to 'rational synthesis' and post-synthetic modification. Thus, together, metal silicates and MOFs provide a wonderful playground for chemists and a tool box for engineering applications.

Acknowledgements

This work was developed in the scope of the project CICECO-Aveiro Institute of Materials (Ref. No. FCT UID /CTM /50011/2013), financed by national funds through FCT/MEC and when applicable co-financed by FEDER under the PT2020 Partnership Agreement.

References

1. M.W. Anderson, O. Terasaki, T. Ohsuna, A. Philippou, S.P. MacKay, A. Ferreira, J. Rocha, S. Lidin, Nature 367 (1994) 347.
2. D. Ananias, A. Ferreira, J. Rocha, P. Ferreira, J.P. Rainho, C. Morais, L. Carlos, J. Am. Chem. Soc. 123 (2001) 5735-5742.
3. F.N. Shi, L. Cunha-Silva, R.A. Sá Ferreira, L. Mafra, T. Trindade, L.D. Carlos, F.A. Almeida Paz, J. Rocha, J. Am. Chem. Soc. 130 (2008) 150-167.
4. B.V. Harbuzaru, A. Corma, F. Rey, P. Atienzar, J.L. Jordá, H. García, D. Ananias, L.D. Carlos, J. Rocha, Angew. Chem. Int. Ed. 47 (2008) 1080-1083.
5. A. Cadiau, C.D.S. Brites, P.M.F.G. Costa, R.A.S. Ferreira, J. Rocha, L.D. Carlos, ACS Nano 7 (2013) 7213-7218.
6. Z. Wang, D. Ananias, A. Carné-Sánchez, C.D.S. Brites, I. Imaz, D. Maspoch, J. Rocha, L.D. Carlos, Adv. Funct. Mater. 25 (2015) 2824-2830.
7. D. Ananias, F.A. Almeida Paz, D.S. Yufit, L.D. Carlos, J. Rocha, J. Am. Chem. Soc. 137 (2015) 3051-3058.
8. C.D.S. Brites, X. Xie, M.L. Debasu, X. Qin, J. Rocha, X. Liu, X., L.D. Carlos, Nature Nanotech (2016) (doi: 10.1038/nnano.2016.111)

9. M.L. Pinto, J. Rocha, J.R.B. Gomes, J.R.B. Pires, J. Am. Chem. Soc. 133 (2011) 6396–6402.
10. F.N. Shi, J.C. Almeida, L.A. Helguero, M.H.V. Fernandes, J.C. Knowles, J. Rocha, Inorg. Chem. 54 (2015) 9929-9935.
11. Z. Lin, A. Ferreira, M.R. Soares, J. Rocha, Inorg. Chim Acta 356 (2003)19-26.

COMUNICAÇÕES ORAIS

Photoassisted Preparation of Pore Controlled Metal-Decorated Nanoporous Carbons

María C. Fernández de Córdoba[a*], Mohamed Zaier[b], Inmaculada Velo Gala[a], Lavinia Balan[b], Conchi O. Ania[a]

[a]ADPOR Group, Instituto Nacional del Carbón (INCAR, CSIC), 33011 Oviedo, Spain

[b]Institut de Sciences des Matériaux de Mulhouse (IS2M, CNRS), rue Jean Starcky, 68057 Mulhouse Cedex, France

**m.fernandezdecordoba@incar.csic.es*

Introduction

Nanocomposite systems that combine nanoporous carbon materials, with well-defined and controlled architectures, and metal nanoparticles properties are of great importance in many different fields like adsorption, sensing, energy storage, catalysis... [1-6]. In this work, we have explored the potentialities of the use of light activation to promote the polycondensation of different precursors for the synthesis of nanoporous carbons. We have investigated the incorporation of either silver or gold salts to produce metal-polymer nanoassemblies and Ag/Au-decorated nanoporous. The textural, structural and chemical properties, as well as the effect of the dispersion of the metallic nanoparticles within the carbon matrix have been discussed in terms of the experimental conditions (e.g., light source, pH, electrolyte, chromophores).

Materials and Methods

We selected various polymeric precursors for the photoassisted synthesis of the nanoporous carbons: gallacetophenone (GA), 2,3-dyhydroxynaphtalene (NP), pyrogallol (PY) and bisphenol A (BP). The precursors are dissolved in ethanol containing HCl (37%). Then, the solutions are transferred to glass dishes and at that time they are exposed to UV light for 60 min. The distance between the light source and the solution was optimized to avoid heating of the sample during the irradiation (temperature monitored was constant). For the samples incorporating metals, either $AgNO_3$ or $AuBr_4$ were added to the precursor's mixture (in the presence of an electrolyte and a chromophore) and the irradiation as indicated above. The nomenclature of the obtained materials along with selected characteristics is compiled in Table 1. The brownish viscous solids obtained after the irradiation were dried at room temperature, scratched from the dishes and further pyrolyzed at 600 ºC to allow the decomposition of the organic resins in carbon materials, and the generation of porosity. The textural properties of the samples were determined by means of gas adsorption/desorption isotherms (i.e., N_2 and CO_2 at -196 °C and 0ºC, respectively). Before the experiments, samples were outgassed at 120 °C overnight to constant vacuum (10^{-4} Torr). The main textural parameters such as specific surface area, S_{BET}, pore volumes and distribution of pore sizes were evaluated from the nitrogen adsorption isotherms. The carbon materials were further characterized by elemental analysis and surface pH, X-Ray diffraction, Raman spectroscopy, SEM and TEM.

Results and Discussion

For all the series and regardless the precursor, the colorless initial solutions become gradually dark upon 60 min irradiation, either in the absence and presence of metallic salts. The darkening of the solution was more remarkable when 2,3-dyhydroxynaphtalene was used as precursor, and in the presence of the metallic salts (either $AgNO_3$ or $AuBr_4$). The main textural features of the samples after the thermal treatment at 600 ºC (to render the carbon material) are shown in Table 1. As seen, all the samples presented as well-defined pore structure with the exception of the sample prepared using bisphenol A as precursor. Moreover, gallacetophenone lead to carbon materials with a well-developed mesoporosity, whereas the photopolymerization of 2,3-dyhydroxynaphtalene resulted in a compact microporous network. Furthermore, all the samples presented a low surface functionalization, with quite hydrophobic nature (surface pH between ca. 8-9).

Table 1. Nomenclature and selected physicochemical and textural characteristics of the synthesized nanoporous carbons.

Precursor		**S_{BET} [m^2g^{-1}]**	**V_{TOTAL}[A] [$cm^3\ g^{-1}$]**	**$V_{MICROPORES}$ [B] [$cm^3\ g^{-1}$]**	**$V_{MESOPORES}$[B] [$cm^3\ g^{-1}$]**
gallacetophenone	**GA**	620	0.89	0.20	0.57
pyrogallol	**PY**	720	0.69	0.22	0.46
bisphenol A	**BP**	10	0.006	--	--
2,3-dyhydroxynaphtalene	**NP**	486	0.28	0.19	0.09
gallacetophenone	**GA-Ag**	548	0.49	0.15	0.35
gallacetophenone	**GA-Au**	557	0.58	0.16	0.34
[A] Total pore volume evaluated from the N_2 adsorption isotherms at -196 °C at p/p_0 ~0.99.					
[B] Evaluated from the NLDFT-HS method applied to N_2 adsorption isotherms					

References

1. D.D. Kulkarni et al., *Adv. Funct. Mater.,* vol. 22 (2012) 2129-2139.
2. Matei Ghimbeu C. *et al., RSC Adv.,* vol. 5 (2015) 2861-8.
3. J.P. Fouassier, Photoinitiation, Photopolymerization, and Photocuring: Fundamentals and Applications , Hanser Publishers , Munich, 1995 .
4. L. Cao, *et al. Nano Lett.,* vol. 7 (2007) 3523-3525.
5. Y.T. Liao et al., *ChemCatChem*, vol. 8 (2016) 502-509
6. N. Ashfaq et al., *Mater. Sci. Eng. C*, vol. 59 (2016) 938-947

Effect of Si/Al Ratio on Water Hydration in LTA-Type Zeolites

J. Perez-Carbajo[a], S. R. G. Balestra[a], P. Gómez-Álvarez [a], S. Calero[a,*]
[a] Department of Physical, Chemical, and Natural Systems, Universidad Pablo de Olavide, Ctra. Utrera km 1, 41013 Seville, Spain
**scalero@upo.es*

Introduction

Water and zeolites go together in several environmental and industrial applications, including catalytic processes, water treatment and purification, or ion exchange softening [1,2]. Therefore, to explore water adsorption in zeolites at the molecular level becomes relevant. Zeolites are built up from the covalent linkage of TO_4 tetrahedra, where the central atoms (T) are usually silicon or aluminium atoms. In the latter case, the presence of a trivalent atom instead a tetravalent one induces a net negative charge which that has to be compensated by introducing cations.

In this work, we have considered Linde Type A (LTA) zeolites to evaluate the effect on the water mechanisms of the gradual reduction of Al content, from lattices with Si/Al ratio of 1 (LTA-4A) down to almost pure silica structures. The systems were charge-balanced with sodium cations. LTA-type zeolites are well known and widely used in industry due their well-defined structure, large surface area and high porosity. Alongside, we have comparatively studied how confined water behaves in structures allowed to relax after the Al/Na^+ reduction (from LTA-4A initial structure) and in those where the crystallographic positions were strictly kept.

Methods

We performed Monte Carlo simulations in the Grand Canonical ensemble to compute adsorption isotherms at 298K, using RASPA [3] code. Crystallographic positions for non-optimized structures were taken from literature [4], and these structures allowed to relax were computed using energy minimisations with the shell-model potentials of Sanders et al. [5]. Structures are consistent with these reported in the literature [6] and all of them are considered as rigid lattices during the simulations.

The potential energy consists on Lennard-Jones (L-J) and coulombic interactions. Water was defined through TIP5P/Ew model [7]. Extra-framework cations were defined as point charges allowed to move by interacting with the lattice and the adsorbate. Interactions between water molecules, cations and with the zeolite atoms were taken from literature [8,9,10].

The structure of adsorbed water was evaluated by computing Radial Distribution Functions (RDFs) and Hydrogen-Bonded (HB) statistics. We used a geometric criterion [11] to define HB formation.

Results and Discussion

Adsorption isotherms indicate the relevance of letting the zeolite get relaxed. As can be seen in figure 1.a, this affects, not only to the amount of water adsorbed but also in the pressure in which the molecules of water enter the structure, especially in the lowest Al-containing zeolites. The reduction of loading capacity at high pressures is

consequence of volume exclusion by the presence of cations, which shifts likewise the onset pressures of adsorption to lower values.

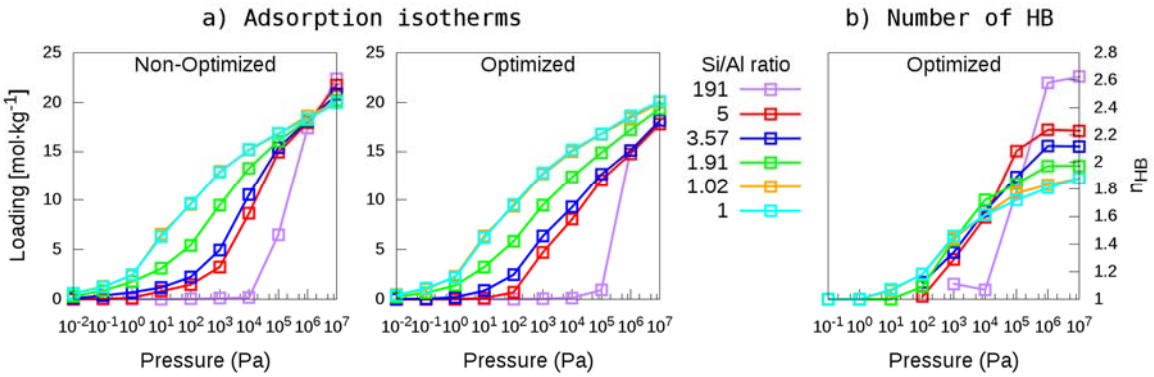

Fig. 1. a) Simulated adsorption isotherms of water in LTA-type zeolites. b) Average number of HB per water molecule as a function of pressure. Each color in the shared key represents a Si/Al ratio.

Although there are different trends depending on loading, not aparent divergences for water molecules RDF data arise between the non- and optimized structures but it is clear that hydrogen bonding occurs for all the structures.

For HB analysis we used the optimized structures. We found, for similar water uptakes, a clear enhancement of hydrogen bonding with increasing Si/Al ratio (figure 1.b).

On the basis of our results, the presence of cations clearly affects the aggregation of the molecules of water, but makes the structural optimization of simulation lattices is needed. Therefore, LTA-zeolites could be suitable to tune and even to reverse water adsorption by adding or removing aluminium atoms to the framework.

Acknowledgements

Work supported by the ERC Starting Grant (ERC2011-StG-279520-RASPA). S.R.G. Balestra thanks Spanish MEC (CTQ2013-48396-P) for his predoctoral fellowship.

References

1. R. Gounder and M. E. Davis, AIChE Journal 29 (2013) 3349–3358.
2. L. X. Li, J. H. Dong, and T. M. Nenoff, Sep. Purif. Tech. 53 (2007) 42-48.
3. D. Dubbeldam, S. Calero, D. E. Ellis, R. Q. Snurr, Mol. Simul. 42 (2016) 81-101.
4. J. J. Pluth and J. V. Smith, J. Am. Chem. Soc. 102 (1980) 4704-4708.
5. M. J. Sanders, M. Leslie, and C. R. A. Catlow., Chem. Commun. (1984) 1271–1273
6. Ch. Baerlocher and L. B. McCusker, Database of Zeolite Structures http://www.iza-database.org/databases/
7. S. Rick, J. Chem. Phys. 120 (2004) 6085-6093.
8. S. Calero and P. Gómez Alvarez, J. Phys. Chem. C 118 (2014) 9056–9065.
9. J. M. Castillo, J. Silvestre-Albero, F. Rodriguez-Reinoso, T. J. H. Vlugt, S. Calero, Phys. Chem. Chem. Phys. 15 (2013) 17374-17382.
10. A. García-Sánchez, C. O. Ania, J. B. Parra, D. Dubbeldam, T. J. H. Vlugt, R. Krishna, and S. Calero, J. Phys. Chem. C 113 (2009) 8814-8820.
11. A. Luzar and A. Chandler, J. Chem. Phys. 98 (1993) 8160–8173.

Influencia de las Condiciones de Activación en la Obtención de Carbones Activados de Bajo Costo para la Remoción de Plaguicidas

Claudia Amézquita-Marroquin[a,*], Patricia Torres-Lozada[a], Liliana Giraldo[b], Juan Carlos Moreno-Piraján[c]

[a] Escuela de Ingeniería de los Recursos naturales y del Ambiente, Facultad de Ingeniería, Universidad del Valle. Calle 13 100-00, Cali – Colombia.

[b] Departamento de Química, Facultad de Ciencias, Universidad Nacional de Colombia, Carrera 45, Bogotá, Colombia

[c] Departamento de Química, Facultad de Ciencias , Universidad de los Andes, Carrera 1 18A-12, Bogotá, Colombia

**claudia.amezquita@correounivalle.edu.co*

Introducción

En países en desarrollo, es común que las fuentes de abastecimiento se encuentren deterioradas debido a fenómenos naturales y actividades antrópicas que aportan diferentes contaminantes, generando riesgos en los Sistemas de Abastecimiento de Agua Potable –SAAP si no realizan un adecuado tratamiento [1]. La producción y uso de compuestos orgánicos emergentes-COE como los plaguicidas, generan una gran preocupación por la escorrentía y potencial lixiviación a través del suelo, contaminando las fuentes de abastecimiento [1]. Estudios han documentado la persistencia de estos compuestos en los SAAP generando riesgos a la salud humana [1, 2]. La adsorción mediante carbón activado granular –CAG, es considerada como una excelente opción de tratamiento de aguas con presencia de plaguicidas, pero este es relativamente costoso por lo que diversos estudios se han centrado en el desarrollo de carbón activado de bajo costo a partir de residuos agrícolas [3]. Su uso, ha permitido obtener resultados prometedores en cuanto a la eficiencia de remoción de plaguicidas como la atrazina [3,4]. Por lo tanto, se planteó analizar la obtención de carbones activados mediante la cáscara de mangostino bajo diferentes condiciones de activación para evaluar su influencia en la remoción de atrazina.

Materiales y Métodos

Materiales de partida Se empleó cáscara de mangostino (*Garcinia mangostana*) adquirida en centros de acopio en Colombia, como residuo agrícola para la obtención de carbón activado de bajo costo.

Obtención de carbones activados Los carbones activados fueron obtenidos de acuerdo a las condiciones que se muestran en la Tabla 1 (impregnaciones v/v 1:2).

Tabla 1. Condiciones de activacion de los diferentes precursores

Precursor	Activación Física	Denominación	Activación química	Denominación
Cáscara de mangostino	700°C/3h; N_2	ACM-7	700°C/3h; N_2;40%H_3PO_4	ACM-7-4H
	800°C/3h; N_2	ACM-8	800°C/3h; N_2;40%H_3PO_4	ACM-8-4H
	900°C/3h; N_2	ACM-9	900°C/3h; N_2; 40%H_3PO_4	ACM-9-4H

Caracterización de los carbones activados Los carbones activados se caracterizaron mediante la toma de isotermas de N_2 a -196°C, isotermas de CO_2 a 0°C, Microscopía Electrónica de Barrido SEM y difracción de rayos X DRX. En este trabajo se presentan los resultados obtenidos con las técnicas de análisis termogravimétrico TGA, espectroscopia infrarroja FTIR [5], titulaciones utilizando el método modificado de Boehm [6], y el punto de carga cero PZC [7].

Resultados y Discusión

El PZC presento valores que oscilan entre 11,3 y 9,8 unidades. De acuerdo con lo observado en los FTIR de la Figura 1 para los mismos carbones activados, es de resaltar que presenta una banda amplia a media que aumenta la tempratura de activación, la cual corresponde a grupos –OH y grupos carboxílicos.

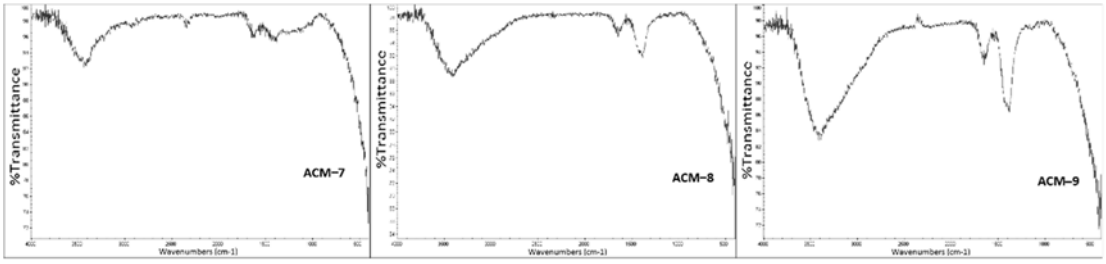

Fig. 1. Espectroscopia infrarroja FTIR carbones activados de Mangostino

Estas carcateristicas quimicas de los carbones son de gran importancia ya que determinan la capacidad particular de adsorcion del contaminante.

Agradecimientos

Los autores agradecen a COLCIENCIAS por la financiación de becas de Doctorado Nacional Convocatoria 567, a la Universidad del Valle por la financiación del proyecto CI 2869 de 2015 y al Grupo de Solidos Porosos y Calorimetría de la Universidad de los Andes.

Referencias

1. World Health Organization (WHO). 2011. Guidelines for Drinking Water Quality. Fourth edition. ISBN 978-92-4-154815-1.
2. Stackelberg P., Furlong, E., Meyer M., Zaugg S., Henderson A., Reissman D. 2004. Persistence of pharmaceutical compounds and other organic wastewater contaminants in a conventional drinking-water-treatment plant. Sci. Total Environ. 329, 1-3, pp.99-113.
3. Ioannidou A., Zabaniotou A., Stavropoulos G., Islam M, Albanis T. 2010. Preparation of activated carbons from agricultural residues for pesticide adsorption, Chemosphere. 80 (11) pp 1328-1336.
4. Ignatowicz K. 2009. Selection of sorbent for removing pesticides during water treatment, Journal of Hazardous Materials. 169(1–3), 953-957.
5. Rodríguez-Reinoso; M. Molina-Sabio (1998).Textural and chemical characterization of microporous carbons. Advances in Colloid and Interface Science. 76: 271-294.
6. Boehm, H.P.: Surface oxides on carbon and their analysis: a critical assessment. Carbon 40, 145–149 (2002)
7. Giraldo L.; Moreno J.C. (2004). Determinación de la entalpía de inmersión y capacidad de adsorción de un carbón activado en soluciones acuosas de plomo. Revista Colombiana de Química 33 (2): 87-97.

Continuous Purification Platforms for Viral Vectors Based on Multicolumn Simulated Countercurrent Chromatography

Luís Grossinho Dias da Silva[a,b,c,†], Snezana Reljic[a,d,†], Abimaelle Silva Chibério[a,†], Ricardo J. S. Silva[b,c], Cristina Peixoto[b,c], José P. B. Mota[a,c,*]

[a] LAQV-REQUIMTE, Department of Chemistry, Faculty of Science and Technology, Universidade NOVA de Lisboa, 2829-516 Caparica, Portugal.

[b] Instituto de Tecnologia Química e Biológica António Xavier, Universidade Nova de Lisboa, Av. da República, 2780-157 Oeiras, Portugal

[c] iBET, Instituto de Biologia Experimental e Tecnológica, Apartado 12, 2780-901 Oeiras, Portugal

[d] Department of Biochemical Engineering and Biotechnology, Faculty of Technology and Metallurgy, University of Belgrade, Karnegijeva 4, 11000 Beograd, Serbia

** pmota@fct.unl.pt*

† These authors contributed equally to this work.

Introduction

The advent of advanced therapies in the pharmaceutical industry has moved the spotlight into virus-like particles (VLPs) and viral vectors produced in cell culture, holding great promise in a myriad of clinical targets, including cancer prophylaxis and treatment.

Currently, the challenge for a widespread application of these new biopharmaceuticals is the development of bioprocesses where they can be cost-effectively produced while maintaining their bioactivity. With increasing cell culture expression levels, the capacity bottleneck in biomanufacturing has shifted from the upstream to the downstream process.

Although chromatography is currently the workhorse in downstream bioprocessing, because of its powerful ability to remove contaminants, chromatographic processes have a few disadvantages. In general, multi-step batch processes exhibit poor productivity, and in some cases recovery, and this leads to scalability limitations. This has generated a need to address the limitations of batch chromatography in biopharmaceutical applications. Moreover, there is an increasing interest in process intensification through conversion of traditional batch biomanufacturing to that of a compressed, integrated, and continuous model.

Materials and Methods

We present a computer-aided strategy for the design of (quasi-)continuous purification platforms of viral vectors and virus-like particles. These platforms combine batch processing and simulated counter-current (SMB) operation to produce highly efficient hybrid processes, wherein some columns are dynamically interconnected, so that non-pure product cuts are internally and counter-currently recycled, while other columns are short circuited to operate in pure batch mode, and others frozen to introduce time lags between the positions of the various concentration fronts and decouple the migrating velocities of the various solutes. This way some fractions can be separated by a SMB approach (the switching and remixing with the feed keep the mass-transfer zone inside the system), whereas the separation of other fractions can be

chromatographic (the mass-transfer zone leaves the system).

Results and Discussion

It is shown that these new process configurations substantially reduce the chromatographic media volume and buffer consumption per unit of productivity and increase product recovery. The proposed processes are validated experimentally with the purification of adenovirus vectors and retro VLPs on different chromatography media, including gel permeation (Sepharose FF), multimodal chromatography (CaptoCore 700), and ion exchange (Sartobind STIC PA).

Acknowledgements

This work was supported by the Associate Laboratory for Green Chemistry LAQV which is financed by national funds from FCT/MEC (UID/QUI/50006/2013) and co-financed by the ERDF under the PT2020 Partnership Agreement (POCI-01-0145-FEDER - 007265).

The authors also acknowledge CNPq-Brasil, Erasmus Mundus Action 2-Sigma Agile and FCT/MCTES for financial support through grants 234180/2014-5 (Abimaelle Silva Chibério), 2014-0848/ 001-001 (Snezana Reljic), PD/BD/114419/2016 (Luís Grossinho Dias da Silva).

References

1. P Nestola, C Peixoto, PM Alves, MJT Carrondo, JPB Mota, Rational development of two flowthrough purification strategies for adenovirus type 5 and retro virus-like particles, J. Chromatogr. A 1426 (2015) 91-101.
2. RJS Silva, JPB Mota, C Peixoto, PM Alves, MJT Carrondo, Improving the downstream processing of vaccine and gene therapy vectors with continuous chromatography, Pharm. Bioproc. 3 (2015) 489-505.
3. P Nestola, C Peixoto, RJS Silva, PM Alves, MJT Carrondo, JPB Mota, Robust design of adenovirus purification by two-column, simulated moving-bed, size-exclusion chromatography, J. Biotechnol. 213 (2015) 109-119
4. P Nestola, C Peixoto, RJS Silva, PM Alves, JPB Mota, MJT Carrondo, Improved Virus Purification Processes for Vaccines and Gene Therapy, Biotechnol. Bioeng. 112 (2015) 843-857
5. P Nestola, RJS Silva, C Peixoto, PM Alves, MJT Carrondo, JPB Mota, Adenovirus purification by two-column, size-exclusion, simulated countercurrent chromatography, J. Chromatogr. A 1347 (2014) 111-121.

Light Olefin/Paraffin Separation on Cu-BTC MOF: VPSA vs. gas-SMB

Vanessa F. D. Martins[a], Ana M. Ribeiro[a], João C. Santos[b], U-Hwang Lee[c], Young Kyu Hwang[c], Jong-San Chang[c,d], José M. Loureiro[a], Alexandre Ferreira[a,*], Alírio E. Rodrigues[a]

[a] Laboratory of Separation and Reaction Engineering – Laboratory of Catalysis and Materials (LSRE-LCM), Dept. of Chemical Engineering, University of Porto, Rua Dr. Roberto Frias, s/n, 4200-465 Porto, Portugal

[b] Jacobs Engineering Group Inc., Haven 190, Noorderlaan 127, Antwerp 2030, Belgium

[c] Catalysis Center for Molecular Engineering, Korea Research Institute of Chemical Technology (KRICT), Jang-dong 100, Yuseong, Daejeon, Republic of Korea

[d] Department of Chemistry, Sungkyunkwan University, Suwon 440-476, Republic of Korea

**aferreir@fe.up.pt*

Ethylene is an important light olefin used to manufacture a wide variety of commodities. This light olefin is the major worldwide industrial feedstock and it has widespread use as a precursor for other organic compounds such as polyethylene, that accounts approximately for 60% of the total use of the olefin [1]. Ethylene is mainly produced in the petrochemical industry by steam cracking of naphtha, gas oil, propane, ethane and others derived from crude oil and/or natural gas. For most end uses, and mainly in the polymer manufacture, ethylene is required at a high purity (>99.9%) [2].

The production of pure ethylene is complex because the ethylene/ethane pair has similar physical properties. Distillation is still the conventional process employed to achieve the required high purity of ethylene [3]. The high energy requirements have led to intense research into new technologies such as pressure swing adsorption (VPSA) and simulated moving bed (SMB).

This work aims to study the separation of ethane/ethylene mixtures on the copper based MOF (Cu-BTC beads) synthesized at the Korea Research Institute of Chemical Technology (KRICT).

The required adsorption equilibrium isotherms of ethane, ethylene, and propane on the Cu-BTC MOF were previously reported by our group at temperatures of 50, 75 and 100 ºC and pressures of 0–7 bar [4]. The adsorbed amount data was regressed against the Dual Site Langmuir (DSL) model. Dynamic studies were performed to provide important information, not only for process modelling, but also for the VPSA and SMB cyclic experiments. Additionally, in the present study, a 5-steps VPSA cycle and a SMB cycle were proposed and performed experimentally to produce ethylene from 0.50/0.50 ethane/ethylene feed mixture. The SMB cycle was performed at 100 ºC using a gas phase SMB bench unit with eight columns detailed elsewhere [5]. Propane was used as desorbent and a 2-3-3 configuration, in an open loop circuit by suppressing section IV was proposed, as can be seen in Figure 1a. The VPSA cycle schemes comprises the following steps: counter-current pressurization, adsorption, rinse, counter-current blowdown and purge (see Figure 1b). The VPSA experimental part was carried out, at 100 ºC and 1.5 bar, on a single-column VPSA unit described in detail by Da Silva and Rodrigues [6]. Ethylene purity and recovery obtained are very similar for both

technologies tested (see Table 1). However, the direct comparison may not be the fairest, since the results obtained by SMB are experimental ones (may not be the optimal ones) obtained at bench scale, while the VPSA study reports simulation results with optimization.

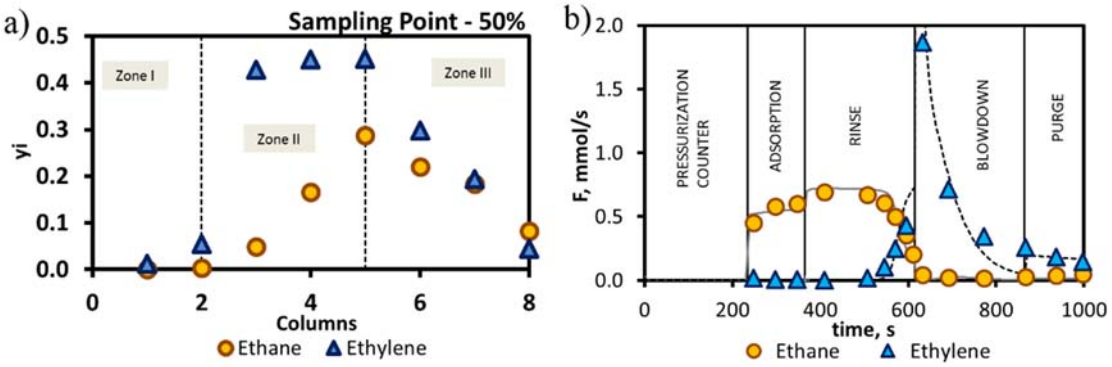

Fig. 1. (a) SMB internal profile at step half time as function of column number and (b) zoom to the 10th VPSA cycle performed. Lines represent the simulation results.

Table 1. Performance parameters of the VPSA and SMB cycles.

Run	Technology	PurC2H6/%	PurC2H4/%	RecC2H6/%	RecC2H4/%
1	VPSA	89.3	97.8	84.6	41.0
2	SMB	56.5	97.5	98.7	39.8

Acknowledgements

The authors acknowledge financial support provided by Fundação para a Ciência e a Tecnologia (FCT, Portugal) and FEDER under Programme COMPETE through the Project FCOMP-01-0124-FEDER-027458 (Ref. FCT EXCL/QEQPRS/0308/2012) and Project POCI-01-0145-FEDER-006984 – Associate Laboratory LSRE-LCM funded by FEDER funds through COMPETE2020 - Programa Operacional Competitividade e Internacionalização (POCI) – and by national funds through FCT - Fundação para a Ciência e a Tecnologia

References

1. K.M. Sundaram, M.M. Shreehan, E.F. Olszewski, Kirk-Othmer Encyclopedia of Chemical Technology, Wiley, (2000).
2. V.D. Martins, A. Ribeiro, J.C. Santos, J.M. Loureiro, K. Gleichmann, A. Ferreira, A.E. Rodrigues, Development of Gas Phase SMB Technology for Light Olefin Paraffin Separations, Aiche J, (2016).
3. E.D. Bloch, W.L. Queen, R. Krishna, J.M. Zadrozny, C.M. Brown, J.R. Long, Hydrocarbon Separations in a Metal-Organic Framework with Open Iron(II) Coordination Sites, Science, 335 (2012) 1606-1610.
4. V.F.D. Martins, A.M. Ribeiro, A. Ferreira, U.H. Lee, Y.K. Hwang, J.S. Chang, J.M. Loureiro, A.E. Rodrigues, Ethane/ethylene separation on a copper benzene-1,3,5-tricarboxylate MOF, Sep Purif Technol, 149 (2015) 445-456.
5. V.F.D. Martins, A.M. Ribeiro, M.G. Plaza, J.C. Santos, J.M. Loureiro, A.F.P. Ferreira, A.E. Rodrigues, Gas-phase simulated moving bed: Propane/propylene separation on 13X zeolite, J Chromatogr A, 1423 (2015) 136-148.
6. F.A. Da Silva, A.E. Rodrigues, Propylene/propane separation by vacuum swing adsorption using 13X zeolite, Aiche J, 47 (2001) 341-357.

Diseño de Materiales Mesoporosos para la Formación de Hidratos de Metano Confinados

Carlos Cuadrado Collados[a], Mirian E. Casco[a], Deicy Barrera[a], Enrique V. Ramos Fernández[a], Joaquín Silvestre Albero[*a]

[a]Laboratorio de materiales avanzados, Departamento de Química Inorgánica, Universidad de Alicante. Apartado 99; E-03080, España.

**joaquin.silvestre@ua.es*

Introducción

En las últimas décadas, el consumo de metano (CH_4) como combustible se ha visto incrementado debido a su alto poder energético y bajas emisiones de gases de efecto invernadero en comparación con las fuentes tradicionales de energía (carbón y petróleo). Al ser un gas, la tecnología actual para su almacenamiento basada en comprimir el CH_4 a 200 bar y temperatura ambiente, o transportarlo en estado líquido a-165ºC y 1 atm dista mucho de ser la solución factible debido al riesgo que supone almacenar gases a alta presión y al elevado consumo energético que conlleva transportar el CH_4 líquido[1]. No obstante, en la naturaleza existe una tercera vía de almacenamiento de CH_4 que aun no ha sido explotada y que consiste en la formación de hidratos de gas, en los cuales el CH_4se encuentra rodeado por una malla de moléculas de agua en la relación 1:5,75. Estas estructuras solidas cristalinas se forman principalmente en los fondos marinos y en el permafrost en condiciones de alta presión y baja temperatura. Recientemente se han encontrado grandes depósitos de estos hidratos que duplican las reservas actuales de combustibles fósiles [2].

Estudios recientes del grupo LMA (Laboratorio de Materiales Avanzados) de la Universidad de Alicante han demostrado que, mediante el uso de materiales de carbón activado con una porosidad muy desarrollada, es posible mimetizar a la naturaleza y sintetizar hidratos de CH_4 con una estequiometría idéntica a los naturales, bajo condiciones más suaves de presión (40 bar) y temperatura (2ºC) y, con una cinética de formación muy superior a los procesos naturales. Estos estudios fueron realizados con carbones activados microporosos [3,4]. En base a estos antecedentes, el objetivo del presente trabajo es evaluar de forma detallada y con mayor profundidad el mecanismo de crecimiento de hidratos de CH_4 en espacio confinado, y más concretamente, en materiales mesoporosos de diferente composición química (sílice y carbones).

Materiales y métodos

Se emplearon sílices mesoporosas ordenadas y materiales de carbón obtenidos por replicación del material de sílice anterior. Como se observa en la Tabla 1, la selección de los materiales se hizo para comprender el efecto que ejercen variables como el tamaño y forma del poro, naturaleza y morfología del material y química superficial, en el proceso de formación de hidratos confinados.

Tabla 1. Características de los materiales usados para la formación de hidratos de CH_4

Carbón	Replica	Φ_{Poro}(nm)	Forma del poro
CMK-3	SBA-15	6	Canales cilíndricos y ordenamiento hexagonal
CMK-8	KIT-6	8	Canalesdesordenados y ordenamiento cúbico

Los materiales sintetizados fueron evaluados textural, química y morfológicamente mediante diferentes técnicas analíticas. Éstas incluyen la adsorción de gases a bajas temperaturas, mediante isotermas de N_2,CO_2 y vapor de agua; técnicas de microscopia (SEM y TEM), con el propósito de observar la morfología de las muestras a nivel superficial y atómico, respectivamente, y difracción de Rayos X (DRX) para analizar la estructura ordenada de largo alcance del material. La evaluación de la capacidad de adsorción de CH_4 en forma de hidrato se llevó a cabo a diferentes temperaturas: 0ºC, -5ºC y-10ºC hasta 100 bar variando la cantidad de agua incorporada en el material.

Resultados y discusión

Las isotermas de adsorción de CH_4 se realizaron primero en materiales secos y después en presencia de humedad. En todos los casos se observó que la capacidad de adsorción del CH_4 fue mayor en las muestras húmedas frente a los valores obtenidos en ausencia de humedad, es decir, procesos convencionales de adsorción física. La estructura cristalina de estos hidratos fue confirmada mediante radiación de sincrotrón (Rayos-X) en el acelerador ALBA (Barcelona) tal y como refleja la figura 1, donde además se obtuvo el difractograma del carbón CMK-3 (propio de materiales amorfos) así como la estructura hexagonal del hielo (antes de inyectar el CH_4**).**

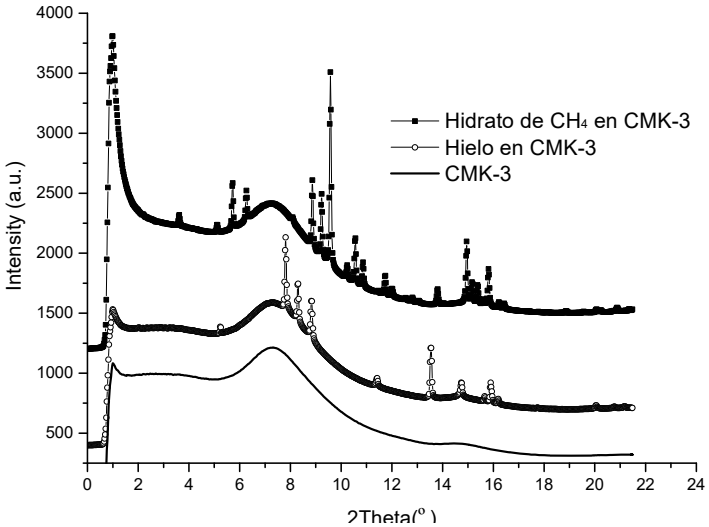

Fig. 1. Difraccion de Rayos X de hidratos de CH_4 y hielo en CMK-3

Agradecimientos

Los autores de este trabajo agradecen la ayuda económica del MINECO a través del proyecto: MAT2013-45008-p.

Bibliografía

1. Sang-Yong Lee, Gerald D. Holder. *Fuel Processing Technology.* **2001,** 181–186
2. Sloan E. D., Koh C. 2008. *Clathrate Hydrates of Natural Gases, Tercera Edición, CRC Press, U.S.A.* **2013**
3. Mirian E. Casco, Joaquín Silvestre-Albero, Aníbal J. Ramirez-Cuesta, Fernando Rey, Jose L. Jordá. Atul Bansode, Manuel Martínez-Escandell, Inma Peral, Atushi Urakawa, Katsumi Kaneko, Francisco Rodríguez-Reinoso. *Nature Communications*. **2015**, 6:6432
4. Mirian E. Casco, Manuel Martínez-Escandell, Enrique Gadea-Ramos, Katsumi Kaneko, Joaquín Silvestre-Albero, Francisco Rodríguez-Reinoso. *Chem. Mater. 27*, **2015**, 959-964

Predicción de la Capacidad de Adsorción de CO_2 en Sílice Mesoestructurada a partir de sus Propiedades Texturales

E.S. Sanz-Pérez, A. Arencibia, G. Calleja, R. Sanz*
Grupo de Ingeniería Química y Ambiental.
Universidad Rey Juan Carlos, Móstoles, Madrid, España.
** raul.sanz@urjc.es*

Introducción

El aumento en la concentración atmosférica de CO_2 proveniente del empleo masivo de combustibles fósiles durante más de un siglo está provocando un significativo Cambio Climático a escala mundial [1]. Según ha señalado el IPCC, la tecnología de captura de CO_2 en grandes fuentes emisoras es una tecnología clave para reducir las emisiones de este gas de efecto invernadero [2].

En la actualidad, una opción prometedora es la adsorción de CO_2 sobre materiales porosos. Principalmente se han empleado sólidos microporosos como zeolitas, carbones activos o MOFs, así como sílices y alúminas y mesoporosas. En el caso de los materiales microporosos, varios autores han obtenido correlaciones satisfactorias entre su capacidad de adsorción de CO_2 y el diámetro de poro [3-5]. Sin embargo, en el caso de los sólidos mesoestructurados los resultados son menos abundantes y concluyentes. Además, hay que tener en cuenta que algunos soportes mesoestructurados han sido funcionalizados con grupos amino con objeto de incrementar su capacidad de adsorción de CO_2 y ésta ya no se restringe sólo a fisisorción sino que también presentan quimisorción en dichos grupos amino.

En el presente trabajo se ha estudiado la adsorción de CO_2 sobre 30 sólidos adsorbentes mesoporosos diferentes, obteniendo las isotermas de adsorción de CO_2 45 ºC y las capacidades de adsorción de CO_2 a 1 bar y se han correlacionado éstas con las propiedades texturales de los sólidos considerados.

Materiales y Métodos

Se sintetizaron sólidos mesoestructurados tipo SBA-15 convencional y de poro expandido, Al-SBA-15, varios soportes tipo HMS y MCM-41 y un gel de sílice comercial. También se utilizaron materiales funcionalizados con grupos amino por anclaje o impregnación, aunque dichos grupos funcionales no presentan afinidad por el CO_2.

Se realizaron isotermas de adsorción-desorción de CO_2 a 45 ºC entre 0 y 6 bar, calculando la capacidad de adsorción a 1 bar por interpolación. Estas condiciones se emplearon por ser las típicas de los gases de post-combustión de centrales térmicas de carbón tras la unidad de desulfuración. También se obtuvieron isotermas de adsorción-desorción de N_2 a 77K, determinando la superficie específica y el parámetro C mediante el método BET, el diámetro de poro mediante el método BJH en la rama de adsorción y el volumen total de poros a una presión relativa de 0,98.

Resultados y Discusión

Con objeto de encontrar una posible relación entre la capacidad de adsorción de CO_2 de los 30 sólidos mesoporosos estudiados y alguna de sus propiedades texturales, se

realizaron regresiones simples y múltiples entre la capacidad de adsorción de CO_2 y las propiedades texturales tales como la superficie específica, el diámetro de poro, el volumen total de poros y el parámetro C de la ecuación BET. En todos los casos se obtuvieron coeficientes de correlación muy bajos, inferiores a 0,58.

Posteriormente, se evaluó si la capacidad de adsorción de CO_2 correlacionaba con el producto $C{\cdot}S_{BET}$, obteniendo un ajuste adecuado y una correcta dispersión de los datos, como se observa en la Figura 1. El producto de variables empleado tiene en cuenta la superficie disponible para la adsorción así como su naturaleza química [6].

Varias de las muestras consideradas contienen grupos amino que no son activos en captura de CO_2, por lo que la adsorción de CO_2 es simplemente física, sin que haya ninguna contribución de quimisorción [7]. Esto es coherente con el hecho de que sean las propiedades texturales y no otras variables como el contenido en grupos amino las que correlacionen correctamente con la capacidad de adsorción de CO2.

La correlación entre la capacidad de adsorción de CO_2 y el producto C·SBET obtenida en este trabajo ($y = 5{,}37958 + 1{,}71419\ E^{-4}\ x$) presenta una gran relevancia ya que permite conocer a priori cual será el comportamiento de materiales mesoestructurados en adsorción de CO_2.

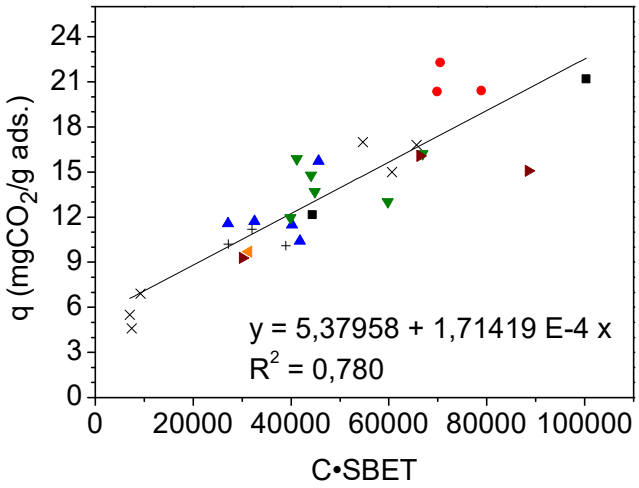

Fig. 1. Regresión lineal entre $C{\cdot}S_{BET}$ y la capacidad de adsorción de CO_2 a 45 ºC y 1 bar. Materiales: SBA-15 (■), Al-SBA-15 (●), SBA-15 de poro expandido (▲), HMS (▼), gel de sílice (◀), MCM-41 (▶), SBA-15-anclaje (X) y SBA-15-co-condensación (+).

Referencias

1. R.K. Pachauri and L.A. Meyer (Eds.), Fifth Assessment Report of the Intergovernmental Panel on Climate Change, IPCC, Geneva, Switzerland, 2014.
2. B. Metz, O. Davidson, H.C. de Coninck, M. Loos, L.A. Meyer, (Eds.), Special Report on Carbon Dioxide Capture and Storage. Cambridge University Press, Cambridge, UK, 2005.
3. M. Sevilla, J.B. Parra and A.B. Fuertes, ACS Appl. Mater. Interfaces 5 (2013) 6360-8.
4. V. Presser, J. McDonough, S.-H. Yeon and Y. Gogotsi, Energy Environ. Sci. 4 (2011) 3059-66.
5. A. Silvestre-Albero, S. Rico-Francés, F. Rodríguez-Reinoso, A.M. Kern, M. Klumpp, B.J.M. Etzold and J. Silvestre-Albero, Carbon 59 (2013) 221-8.
6. E.S. Sanz-Pérez, A. Arencibia, R. Sanz and G. Calleja, RSC Adv. 5 (2015) 103147-54.
7. R. Sanz, G. Calleja, A. Arencibia and E.S. Sanz-Pérez, Microporous Mesoporous Mater. 158 (2012) 309-17.

Modelización de la Regeneración mediante Oxidación Húmeda de Carbón Activado. Estudio de Reactividad en la Interfase

S. Román*, B. Ledesma, A. Álvarez, E. Sabio, C.M. González
[a]Dpto. Física Aplicada, Universidad de Extremadura, Avda. de Elvas s/n, Badajoz, España
**sroman@unex.es*

Introducción

La consolidación de los carbones activados (CAs) como adsorbentes versátiles y eficientes, unido a la creciente preocupación por el carácter finito de los recursos materiales y energéticos, han llevado a la búsqueda de metodologías alternativas de producción de CAs, así como la mejora de las técnicas de regeneración de los mismos.

Mediante la regeneración por oxidación húmeda (RgOxH), el carbón agotado, en el seno de una disolución acuosa, se somete a calentamiento con alimentación simultánea de un agente oxidante (generalmente O_2 o H_2O_2), bajo temperaturas y presiones moderadas. De este modo, el adsorbato se desorbe del carbón y se convierte por medio de un mecanismo de radicales libres a productos finales intermedios con una reducción significativa de toxicidad implicando por tanto una ventaja medioambiental muy importante en comparación con otros procesos de regeneración térmicos.

La RgOxH tiene lugar mediante una secuencia de pasos: 1→Inicio del proceso de desorción del adsorbato desde el CA y transferencia de masa desde la superficie interna a la externa; 2→Transferencia de masa desde la superficie externa de la película a la totalidad del líquido; 3→Transferencia de masa de O_2 desde la totalidad del gas a la fase líquida; 4→ Reacción entre el O_2 disuelto y el adsorbato en la totalidad del líquido. Si bien el mecanismo descrito ha sido propuesto y aceptado por la comunidad científica, no contempla otros modos de oxidación que el que tiene lugar en la fase líquida.

En este estudio se ha investigado el proceso de oxidación de p-Nitrofenol (PNF) comparativamente en los sistemas PNF-O_2 y CA-PNF-O_2. Los resultados de la cinetica de desorción junto con la caracterización superficial de los adsorbentes permitieron identificar existencia de reacciones de oxidación en la interfase sólido-líquido. A partir de los datos experimentales, el proceso fue modelizado utilizando el software COMSOL, estimándose diferentes parámetros energéticos y cinéticos.

Materiales y Métodos

El adsorbente usado ha sido un carbón comercial, Carsorb (CB) proporcionado por Chemviron (material microporoso, área superficial 930 m^2g^{-1} y punto de carga cero 10,2). Se ha empleado como adsorbato p-nitrofenol (PNF) suministrado por Sigma.

Los estudios de RgOxH se realizaron a T = 140, 160, 180 y 200 ^oC y P parciales de O_2, de 3, 6, 9 y 12 bar; la velocidad de agitación se fijó en 600 rpm. Una vez la temperatura seleccionada era alcanzada se introducía el O_2 en el reactor y se tomaba como tiempo cero de reacción. Previo a ello, CB había sido saturado con PNF (CB_{sat}).

Todos los experimentos se realizaron en un autoclave PARR (0,5 L de capacidad), dotado con alimentación de oxígeno. En dicho reactor, una masa de 0,5 g de carbón saturado previamente de PNF se puso en contacto con un volumen de agua de 0,433 L.

Los ensayos de oxidación de PNP (0,1 g L^{-1}), sin presencia de carbón activo se realizaron en idénticas condiciones.

Resultados y Discusión

El análisis de los resultados obtenidos durante la regeneración húmeda del carbón activado, reveló que el proceso no puede ser descrito como la simple adición de las etapas de desorción y oxidación de PNF. Se encontró que la presencia de carbón cataliza el proceso de oxidación del PNF, disminuyendo la energía de activación de reacción que inicia el proceso radicálico [1]. A modo de ejemplo, en la Figura 1.a se muestran las curvas correspondientes a los ajustes realizados a las series experimentales de oxidación de PNF (sin CA), para la temperatura de 200 ºC. En la Figura 1.b se muestran los datos experimentales para la muestra RH/200/12 en la que se sometió al CA saturado a oxidación. En ambos casos se revela el buen ajuste del modelo.

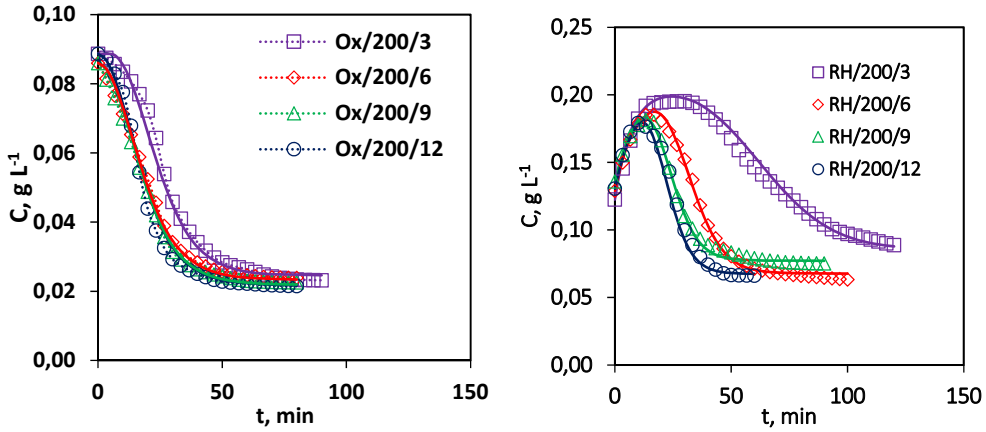

Fig. 1. Oxidación de PNP a) en ausencia de carbón; b) carbón saturado.

Por otra parte, la alimentación de oxígeno en disolución conlleva una mejoría de la regeneración, en comparación con la simple desorción, logrando eficiencias de retención superiores al 100%. Se dedujo por tanto que además de la modificación del equilibrio de desorción debida a "la retirada" de PNF de la fase líquida propiciada por la oxidación, el oxígeno debe acceder a la matriz porosa del carbón, reaccionando de este modo con el adsorbato quimisorbido.

Acknowledgements

Los autores agradecen la financiación recibida de la Junta de Extremadura a través del proyecto GR15034, en el marco de las "Ayudas para el fortalecimiento de los de Grupos de Investigación de Extremadura" y al Ministerio de Economía y Competividad por el proyecto CTM2014-55998-R.

References

1. Ashish Yadav, Agni K. Teja, Nishith Verma, J Env. Chem Eng. 4(2) (2016) 1504-1513

Síntesis y Caracterización de un Polímero Poroso de Coordinación Compuesto por Hierro y Ácido Gálico

A. Briz[a], J.M. Oliva[a], M.J. Sayagués[b], S. Calero[a], A.P. Zaderenko[a,*]
[a]*Departamento de Sistemas Físicos, Químicos y Naturales, Universidad Pablo de Olavide, Sevilla, España*
[b] *Instituto de Ciencias de los Materiales-CSIC, Sevilla, España*
[*]*apzadpar@upo.es*

Introducción

Los Polímeros Porosos de Coordinación (PCPs) son materiales híbridos formados por centros metálicos unidos a través de ligandos orgánicos, que crean redes de interconexión porosas [1,2]. La naturaleza porosa del material lo hace especialmente útil en aplicaciones de adsorción y separación, siendo la de captura y liberación controlada de moléculas de interés biomédico una de las más recientes y prometedoras. En este sentido, el PCP debe cumplir una serie de requisitos en cuanto a tamaño y biocompatibilidad. En este trabajo describimos la síntesis de un PCP compuesto por Fe(III) y ácido gálico, *Fe-Galato*, que cumple los anteriores requisitos para su uso en aplicaciones biomédicas. El hierro es un oligoelemento esencial, participa en la catálisis oxidativa de biocomponentes, y es fundamental en el transporte de oxígeno y en la cadena de transporte de electrones [3]. Por su parte, el ácido gálico, es un polifenol que destaca por su gran poder antioxidante [4].

La capacidad de adsorción de Fe-Galato se ha ensayado utilizando fluoróforos orgánicos como moléculas modelo.

Materiales y Métodos

La síntesis de *Fe-galato* se llevó a cabo en condiciones suaves (presión y temperatura ambiente) por adición de una disolución acuosa de $FeCl_3$ a una disolución acuosa de ácido gálico ($(HO)_3C_6H_2CO_2H$) cuyo pH se ajustó previamente a 8,7 por adición de NaOH. El sólido azul obtenido se purificó mediante procesos secuenciales de centrifugación/lavado en agua y se liofilizó (obteniéndose un rendimiento del 60%), manteniéndose en desecador hasta su posterior uso en ensayos de captación. *Fe-Galato* se caracterizó mediante dispersión dinámica de luz (DLS), espectroscopia de infrarrojo (FT-IR) y microscopia electrónica.

Los estudios de la capacidad de adsorción se realizaron por incubación acuosa del *PCP Fe-galato* con los fluorófos. El perfil de liberación del fluoróforo se realizó a 2, 6, 12 y 24 horas en cultivo celular sobre la línea tumoral A-431 (Carcinoma epidermoide).

Resultados y Discusión

La caracterización de PCP Fe-galato se recoge en la Fig. 1. En la imagen A, se muestran los espectros FT-IR de los precursores y del PCP, observándose la diferencia fundamental en la aparición de la banda a 1580 cm^{-1} característica de carboxilatos aromáticos. La Fig.1 B muestra la imagen TEM, donde se observa que las estructuras poseen un tamaño entorno a los 100nm. El análisis del PCP Fe-galato por DLS revela cierto grado de agregación al establecer el tamaño hidrodinámico en 200 ± 20 nm, así como una buena

homogeneidad media (Índice de polidispersión de 0,21) y un alto grado de estabilidad coloidal con un potencial ζ de -22 mV.

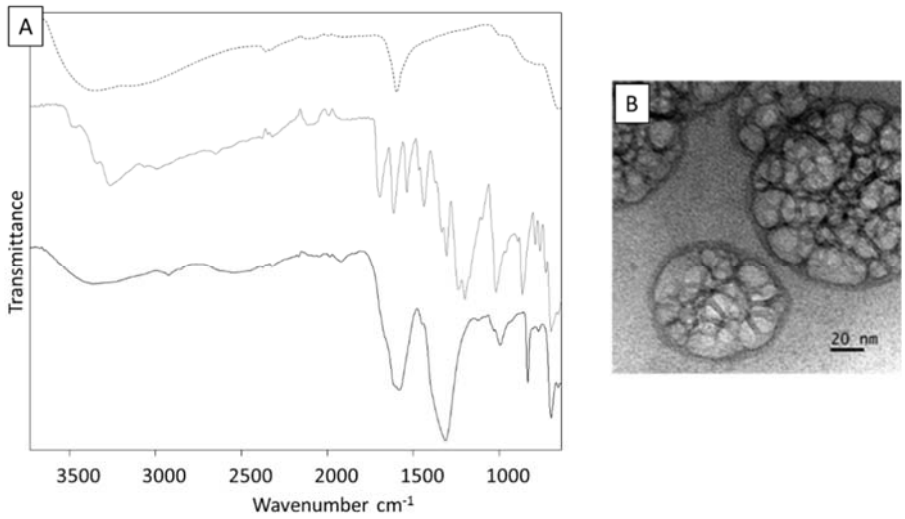

Fig. 1 (A) Espectros de FTIR del $FeCl_3$ (línea punteada), galato (línea gris) y *PCP Fe-galato* (línea negra). (B) Imagen TEM de *PCP Fe-galato*.

Agradecimientos

Esta investigación ha sido financiada por el proyecto CTQ-2013-48396P MINECO.

Referencias

1. C. Janiak, J.K., Vieth. MOFs, MILs and more: Concepts, properties and applications for porous coordination networks (PCNs). New J Chem 2010;34(11):2366-2388.
2. A.K. Cheetham, C.N.R. Rao, R.K. Feller. Structural diversity and chemical trends in hybrid inorganic-organic framework materials. Chem Commun 2006(46):4780-4795.
3. A.T. Iffat, Z.T. Maqsood, N. Fatima. Study of complex formation of Fe(III) with tannic acid. J Chem Soc Pak 2005;27(2):174-177.
4. B. Badhani, N. Sharma, R. Kakkar. Gallic acid: A versatile antioxidant with promising therapeutic and industrial applications. RSC Adv 2015;5(35):27540-27557.

Preparation of Activated Carbons from Apple Tree Bark Char for Water Treatment

Susana Marques[a]*, Ana S. Mestre[a], Andreja Z. Gotvajn[b], Ana P. Carvalho[a]
[a]Centro de Química e Bioquímica, Faculdade de Ciências, Universidade de Lisboa, 1749-016 Lisboa, Portugal
[b]Faculty of Chemistry and Chemical Technology, University of Ljubljana, Slovenia
**scrmarques@fc.ul.pt*

Introduction

Nowadays, an increasing number of pharmaceuticals is used for the treatment and prevention of various diseases. These drugs are only partially absorbed by the body, reaching domestic wastewater and, since the conventional water treatment processes are ineffective in removing these compounds, they are continuously introduced in the aquatic system [1]. To solve this problem, advanced technologies, such as adsorption onto carbon materials, have been developed. However, there are still improvements to be made in order to make their application more economic and efficient [2]. One way to achieve this goal is to produce adsorbents from biomass wastes under optimized conditions to maximize their performance as adsorbents of recalcitrant compounds.

The objective of this work was to prepare activated carbons from the char of apple tree bark residues, evaluating the influence of different experimental conditions in the textural properties of the materials. Selected samples were tested as adsorbents of a β-blocker medicine (atenolol) and a veterinary antibiotic (tiamulin fumarate).

Materials and Methods

The activated carbons were produced by impregnation of apple tree bark char, with K_2CO_3 and KOH solutions in the weight proportions of 1:3, at room temperature. The dried samples were activated at 800 °C for 1, 2, and 3 h under N_2 flow of 5 cm^3 s^{-1} (heating rate 10 °C min^{-1}), then cooled down under N_2 flow. The samples were finally washed with distilled water until pH 7, dried overnight at 100 °C and stored. The obtained carbon samples are designated by activated agent (**C**, for K_2CO_3, and **H**, for KOH)A800/activation time (h).

The materials were characterized by N_2 (ASAP 2010 from Micromeritics) and CO_2 (conventional volumetric apparatus, equipped with an MKS-Baratron 310BHS-100 pressure sensor) adsorption isotherms at, respectively, -196 and 0 °C. The pH at the point of zero charge (pH_{PZC}) was also determined, using a microelectrode (Symphony SP70P pH Meter) following the reversed mass titration procedure.

The removal efficiency of the pharmaceuticals was studied adding 20 cm^3 of pollutant solution (120 mg dm^{-3}) to 6 mg of carbon (30 °C). Samples were collected after 18 h of contact time, and quantification of remaining solute was made by UV-Vis spectrophotometry. For comparison purposes, powdered commercial carbons used in water treatment were also tested (CP –ChiemiVall CCP 900, NS – Norit NSAE Super).

Results and Discussion

The materials prepared have a very well developed pore network, composed almost

exclusively by micropores. In any case the micropore volume is higher than those presented by the commercial samples but one of the commercial samples has a large mesopore structure that is absent in the lab-made carbons (Table 1).

The samples produced with KOH have A_{BET} values higher than 2000 $m^2\ g^{-1}$, being the microporosity mainly (and for longer treatments exclusively) composed by supermicropores. The activation with K_2CO_3 produced carbons with less developed porosity (lower values of A_{BET} and V_{total}). As it was already reported for other precursors [2] this activating agent enables a more controllable development of the porosity than what is observed with KOH, thus allowing to "design" the micropore network of the final samples. Regarding the activation yield is interesting to notice that with exception of sample HA800/1 all the other materials present values around 40 %. The lab-made samples have a pH_{PZC} value of 5.5, whereas the commercial carbons are basic (10.3 and 8.4 for CP and NS, respectively).

Table 1. Nanotextural properties of the lab-made and commercial activated carbons. Activation yield (η) of the lab-made samples also presented.

Sample	A_{BET} ($m^2\ g^{-1}$)	V_{total}[a] ($cm^3\ g^{-1}$)	V_{meso}[b] ($cm^3\ g^{-1}$)	Method α_S			η[c] (%)
				$V_{\alpha\ total}$ ($cm^3\ g^{-1}$)	$V_{\alpha\ ultra}$ ($cm^3\ g^{-1}$)	$V_{\alpha\ super}$ ($cm^3\ g^{-1}$)	
HA800/1	2029	0.93	0.05	0.88	0.12	0.76	46
HA800/2	2345	1.14	0.08	1.06	0.00	1.06	38
HA800/3	2445	1.24	0.08	1.16	0.00	1.16	22
CA800/1	1169	0.48	0.01	0.52	0.27	0.25	44
CA800/2	1455	0.69	0.06	0.64	0.15	0.49	42
CA800/3	1900	0.91	0.08	0.83	0.09	0.74	38
CP	907	0.43	0.03	0.40	0.16	0.24	-
NS	1065	0.70	0.30	0.40	0.02	0.38	-

[a] N_2 volume adsorbed at $p/p^0 = 0.95$; [b] $V_{meso} = V_{total} - V_{\alpha\ total}$; [c] Activation yield.

The data concerning atenolol adsorption showed that lab-made carbons are highly efficient since removal efficiencies ≈ 90 % were attained against 62 % obtained with commercial samples. The better performance of the lab-made activated carbons is most likely due to their high volume of supermicropores. The study will proceed in order to obtain kinetic and equilibrium data for atenolol and also tiamulin fumarate adsorption.

Acknowledgements

The authors thank FCT for the project UID/MULTI/00612/2013 to CQB and for fellowships to SM (SFRH/BD/91767/2012) and ASM (SFRH/BPD/86693/2012). Quimitejo and Salmon & Cia are also acknowledged for kindly supplying the carbons CP and NS, respectively.

References

1. Beek, T.; Weber, F.; Bergamn, A.; Hickmann, S.; Ebert, I.; Hein, A.; Küster, A. J. Hazard. Mat. 282 (2015) 141-149.
2. Mestre, A.S.; Tyszko, E.; Andrade, M.A.; Galhetas, M.; Freire, C.; Carvaho, A.P. RSC Adv. 5 (2015) 19696-19707.

Equilibrio y Cinética de Adsorción de n-Parafinas de Cadena Larga sobre Zeolita 5A

V.I. Águeda[1], M.A. Uguina[1], J.A. Delgado[1], M.T. Holik[1], D. Aranda[1,*], I.D. López[3], J.J. Lázaro[2], J. Peláez[2]

[1]Departamento de Ingeniería Química Universidad Complutense de Madrid, Madrid/SPAIN

[2]Centro de Investigación Cepsa, [3]Cepsa Química, Madrid/SPAIN

** daniaran@ucm.es*

Introducción

Las n-parafinas se utilizan ampliamente en la fabricación de detergentes. Estos hidrocarburos lineales pueden separarse selectivamente de fracciones petrolíferas mediante adsorción utilizando los adsorbentes apropiados empleando la tecnología de lecho móvil simulado (SMB) [1]. Para el desarrollo y el diseño de procesos de adsorción, son necesarios parámetros de equilibrio y cinéticos. Estos parámetros están disponibles en la bibliografía para parafinas ligeras en fase vapor, sin embargo, hay poca información para sistemas en fase líquida de parafinas de elevado peso molecular.

El objetivo de este trabajo es el estudio del equilibrio y la cinética de adsorción de n-parafinas de cadena larga sobre zeolita 5A. Las parafinas representativas utilizadas son las siguientes: *n-decano, n-dodecano, n-tetradecano, n-hexadecano y n-octadecano.* También se ha analizado el *n-pentano*, ya que se utiliza como desorbente en el proceso industrial de lecho móvil simulado (SMB) para la separación de parafinas. Se ha desarrollado un modelo teórico para describir la cinética de adsorción de los sistemas estudiados. El modelo se ha incluido en un programa de simulación de SMB (SMBSIM), y las predicciones del modelo se han comparado con los datos de la separación real de una unidad comercial de SMB que separa n-parafinas de una fracción de queroseno hidrotratado [2].

Materiales y Procedimientos

Se han llevado a cabo experimentos de adsorción de n-parafinas en lecho fijo a 175^{o}C y a 21 barg empleando como adsorbente un tamiz molecular 5A comercial aglomerado [2]. Aunque la operación a escala comercial se realiza en un lecho móvil simulado (SMB), los parámetros cinéticos y de equilibrio necesarios para su diseño deben ser los mismos, independientemente del sistema utilizado en su determinación.

El procedimiento experimental consiste en una activación del adsorbente a elevada temperatura (350ºC), seguida de un acondicionamiento con una mezcla de *isooctano-n-pentano* con una proporción 40-60% en peso. Posteriormente se alimentan las mezclas de adsorción constituidas por *isooctano* que se emplea como disolvente, *trimetilbenceno* en una concentración del 0,5% como trazador y la parafina en concentraciones variables entre el 0,1 y el 10% en peso. Las curvas de rotura se obtienen por análisis en cromatógrafo de gases de las muestras recogidas periódicamente a la salida del lecho mediante un colector de muestras.

Resultados y discusión

En la figura 1 se presentan a modo de ejemplo las curvas de rotura de *n-dodecano* (n-C12). Se ha observado que al aumentar la concentración de la parafina a caudal constante, el tiempo de rotura disminuye, mientras que la capacidad de adsorción aumenta (kg de parafina/kg de adsorbente).

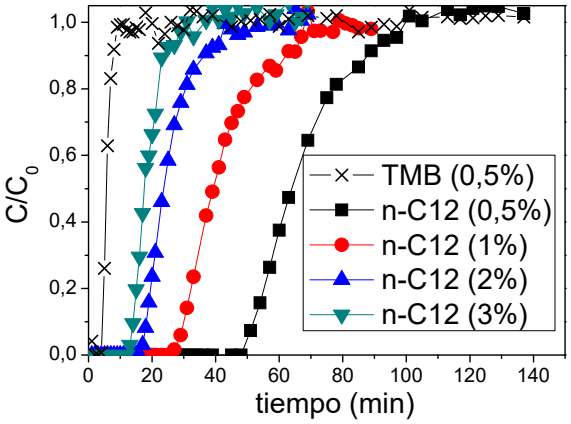

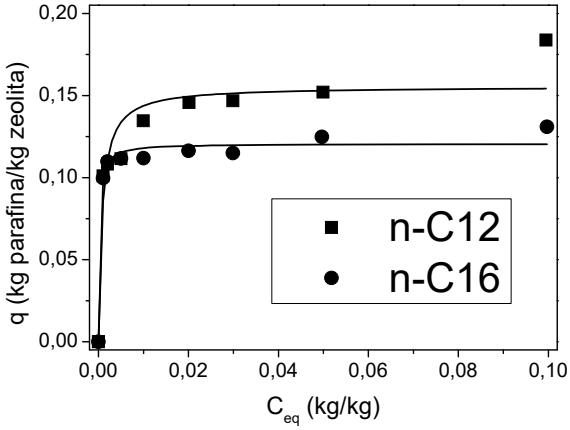

Fig. 1. Curvas de rotura de n-C12 a distintas concentraciones (Q=6mL/min).
Fig. 2. Ejemplo de ajustes a la isoterma de Langmuir de las parafinas C12 y C16.

En la figura 2 se presentan las isotermas de adsorción de n-C12 y n-C16 así como el ajuste obtenido empleando el modelo de Langmuir. Todas las parafinas presentan un comportamiento de isoterma de tipo I. La parafina n-C12 presenta una mayor capacidad de adsorción debido a su menor tamaño y mejor acoplamiento en el interior de los poros de zeolita 5A. Por otra parte, el parámetro K_L, representativo de la afinidad del adsorbato por el adsorbente, es mayor en el caso de la parafina C16 debido a su mayor masa molecular.

Además, las curvas de rotura se han ajustado empleando un modelo cinético isotermo basado en ecuaciones de conservación. Se han considerado tres resistencias en serie a la transferencia de materia. De los resultados obtenidos se concluye que la resistencia a la transferencia de materia en los microporos de la zeolita es la etapa limitante.

Los parámetros cinéticos, junto con las isotermas ajustadas al modelo de Langmuir, se han utilizado para el desarrollo del modelo de lecho móvil simulado, con el propósito de optimizar una unidad industrial y predecir los efectos de las variaciones en la alimentación al proceso. Se ha validado el modelo con los resultados obtenidos de bibliografía [2], obteniéndose un error menor del 10% en las concentraciones de parafinas en el extracto y de isoparafinas en el refinado.

Referencias

1. K. Kosswig, in: Wiley-VCH, Ullmann's encyclopedia of industrial chemistry, Surfactants, 7ª Ed., pp. 1-18.
2. H.J. Bieser, Process for separating normal paraffins, U.S. Patent 4006197 (1977).

Adsorción de N_2, Ar, O_2, CH_4 e H_2 a 77 K para la Caracterización Textural de Materiales Mesoporosos

Jhonny Villarroel-Rocha[a], Deicy Barrera[a], Karim Sapag[a*]
[a]INFAP, Universidad Nacional de San Luis, CONICET, Ej. de los Andes 950, San Luis, Arg.
**sapag@unsl.edu.ar*

Introducción

En la mayoría de las aplicaciones, la eficiencia y selectividad de los materiales porosos en un determinado proceso (de adsorción o de catálisis heterogénea) tiene una relación directa con sus propiedades texturales. Esta dependencia ha sido mostrada y estudiada en diversos trabajos de investigación para diferentes tipos de aplicaciones, como la adsorción de gases, vapores, compuestos orgánicos, colorantes, proteínas, y aplicaciones catalíticas diversas, entre otras. Por esta razón es que las propiedades texturales de los materiales porosos son algunas de las características más importantes a ser evaluadas, dentro de las cuales están la superficie específica, la porosidad y la distribución de tamaño de poros. La técnica experimental más utilizada para estudiar la textura de los materiales porosos es la adsorción de gases, en particular la ads-des de N_2 a 77 K [1,2]. Sin embargo, diversos investigadores [3-5] sostienen que el momento cuadrupolar de la molécula de N_2 presenta interacciones específicas con los grupos silanol superficiales presentes en materiales de sílice, causando así un efecto de orientación preferencial a la molécula de N_2 adsorbida [4], siendo éste el caso de los materiales mesoporosos ordenados (MMO) de sílice. En este sentido, además de la ads-des de N_2 a 77 K, el estudio de la adsorción de otros gases o vapores orgánicos, sería útil para complementar la información de la textura y/o estructura del MMO. Teniendo en cuenta todo lo anteriormente planteado, en este trabajo se presenta el estudio de la adsorción de N_2, Ar, O_2, CH_4 e H_2 a 77 K sobre MCM-41, MCM-48, SBA-15 y SBA-16, con el fin de obtener la información más completa acerca de la textura y estructura de poro de dichos MMO.

Materiales y Métodos

Se sintetizaron cuatro tipos de MMO de sílice (MCM-41, MCM-48, SBA-15 y SBA-16), vía proceso sol-gel bajo condiciones no hidrotérmicas. Las medidas de ads–des de N_2, Ar, O_2 y CH_4 a 77 K, se realizaron en un equipo de adsorción manométrico ASAP-2000 mientras que las de H_2 a 77 K hasta 10 atm se realizaron en un ASAP-2050 (Micromeritics). Las muestras se desgasificaron previamente a 150 °C durante 12 h.

Resultados y Discusión

La Fig. 1 muestra las isotermas de ads–des de N_2, Ar, O_2, CH_4 e H_2 a 77 K para los distintos MMO de sílice estudiados. Dichas isotermas (tipo IV) son típicas de materiales mesoporos que presentan un alto grado de ordenamiento, debido a que en todos los casos la etapa de condensación capilar está bien definida. Los resultados más importantes del análisis textural fueron: ***i)*** *Superficie específica*: tomando como referencia los valores de S_{BET} obtenidos a partir de datos de adsorción de Ar a 77 K, se encontró que (para que haya un acuerdo entre las S_{BET} determinadas con los otros

adsorbibles) los valores del área transversal de la molécula adsorbida sobre la superficie (A_m) del N_2 y CH_4 a 77 K varían en función de la cantidad de grupos silanol presentes en los MMO, sin embargo, los valores de A_m del O_2 a 77 K fueron prácticamente constantes (≈ 0.123 nm^2), sugiriendo que este último puede ser considerado como un adsorbible alternativo para la caracterización de sólidos porosos; ***ii)*** *Volumen de poros*: usando la regla de Gurvich y el método α_S-plot, los cuatro adsorbibles utilizados (N_2, Ar, O_2 y CH_4 a 77 K) proporcionan valores muy similares de volúmenes de poro; y ***iii)*** *Distribución de tamaño de mesoporos (PSD)*: utilizando el método VBS y datos de adsorción-desorción de N_2, Ar, O_2 y CH_4 a 77 K, se encontró que las PSD son muy consistentes entre sí y además concuerdan con el método de NLDFT.

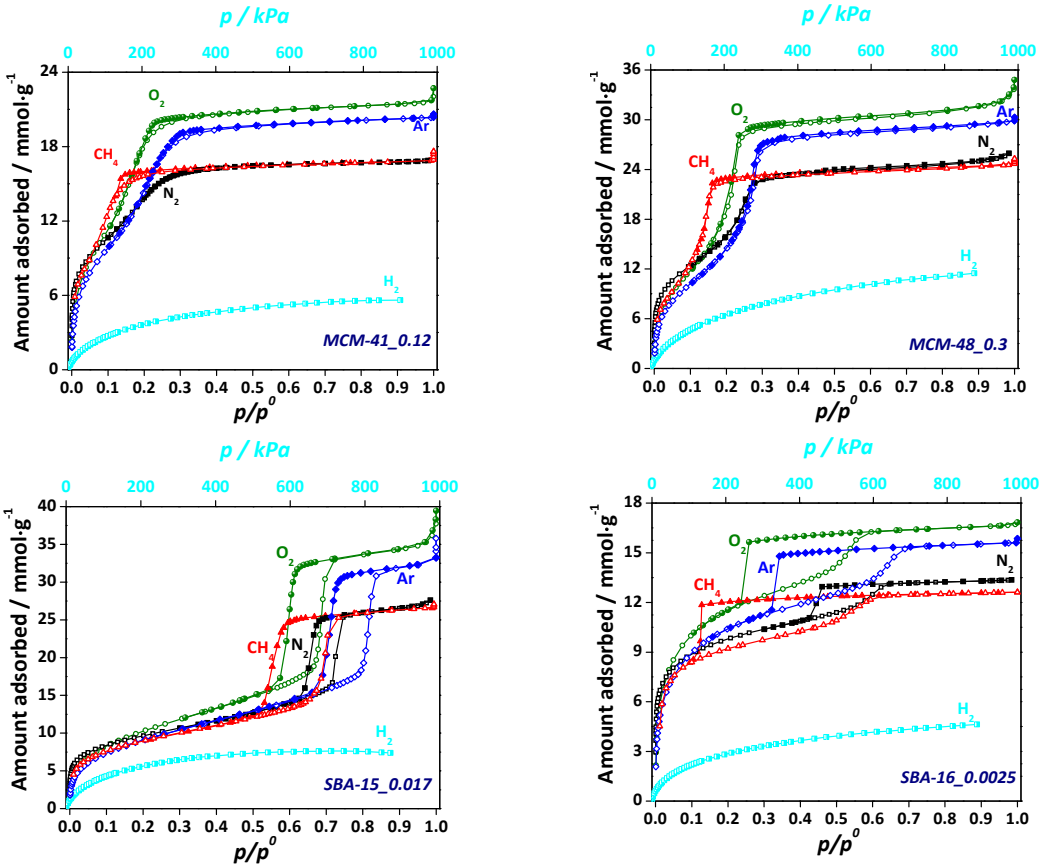

Fig. 1. Isotermas de ads.-des. de N_2, Ar, O_2, CH_4 e H_2 a 77 K de distintos MMO de Si

Agradecimientos

Universidad Nacional de San Luis, Agencia Nacional de Promoción Científica y Tecnológica (ANPCyT) y Consejo Nacional de Investigaciones Científicas y Técnicas (CONICET) de Argentina.

Referencias

1. Gregg SJ, Sing KSW, Adsorption, surface area and porosity, Academic Press, N. York, 1982.
2. Rouquerol F, Rouquerol J, Sing KSW, Llewellyn P, Maurin G, Adsorption by powders and porous solids: Principles, methodology and applications, Academic Press, San Diego, 2014.
3. McClellan AL, Harnsberger FH, J. Colloid Interf. Sci. 23 (1967) 577-599.
4. Rouquerol J, Rouquerol F, Grillet Y, Boudellal M, en: Gregg SJ, Sing KSW, Stoeckli HF (Eds.), Characterization of porous solids, The Society of Chemical Industry, Luton, 1979, 107.
5. Cascarini de Torre LE, Flores ES, Bottani EJ, Langmuir 16 (2000) 1896-1901.

Adsorption: the Key in Response Surface Methodology for the Synthesis of Bespoke Carbon Xerogels

Natalia Rey-Raap*, J. Angel Menéndez, Ana Arenillas
Instituto Nacional del Carbón, CSIC, Apartado 73, 33080 Oviedo, Spain
**nreyraap@gmail.es*

Introduction

Carbon gels are porous materials which properties can be tailored by modifying the synthesis conditions in order to fit the requirements of a specific application [1]. In particular, the concentrations of reagents are the ones that have the greatest influence on the final properties of carbon gels [2, 3]. These concentrations are reported in the literature to be related to the pH of the precursor solution, the dilution ratio (D) and the molar ratio between the main reagents (resorcinol and formaldehyde (R/F)) [2]. Each of these three variables not only has a significant effect on the properties of carbon gels but also synergy effects between them must be taken into account [1, 2, 3]. In these cases, statistical techniques are particularly useful for assessing the significance of these effects. Among all, there is one powerful and convenient technique known as Response Surface Methodology (RSM). This methodology allows obtaining mathematical models from which it is possible to calculate the concentration of each reagent to be used in order to synthesize materials with the desired properties [4]. In this scenario, the adsorption techniques allow obtaining the key response parameters for using RSM and hence, designing bespoke porous carbon xerogels.

Materials and Methods

Accurate and reliable mathematical models were obtained by generating an extensive database, which was achieved following the scheme shown in Figure 1.

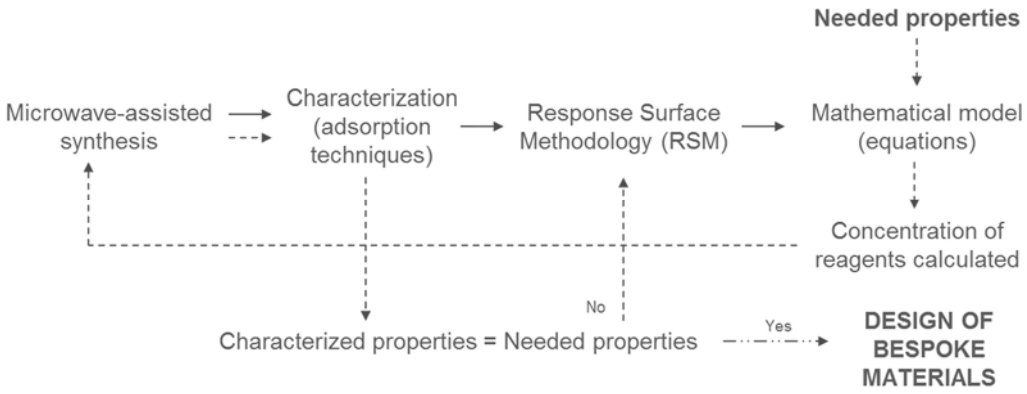

Fig. 1. Experimental methodology for design bespoke porous materials.

Carbon gels were obtained by drying and carbonizing organic polymer-based gels. The Organic xerogels were synthesized by the polycondensation of resorcinol (R) and formaldehyde (F) using deionized water as solvent and sodium hydroxide as catalyst. Different pH, dilution ratio and R/F molar ratio values were used to prepare the precursor solutions. These values ranged from 5.0 to 7.0, from 5 to 10 and from 0.1 to 1.0, respectively; which involves the synthesis of more than 200 materials. The dried gels obtained were then carbonized in order to obtain the carbon gels. The syntheses were performed in a microwave oven while the carbonizations were performed in a horizontal tubular furnace, following the methods described

elsewhere [2, 3, 4]. All the carbon xerogels were characterized from the point of view of their porous structure by means of nitrogen adsorption-desorption isotherms. Response Surface Methodology (RSM) was applied to the characterization results by using the software Design-Expert 8 trial version.

Results and Discussion

The application of RSM to all the parameters obtained by nitrogen adsorption-desorption isotherms allows the interaction between the pH, the dilution ratio and the R/F molar ratio and their effect on the main porous properties to be evaluated. The evolution of mesopore volume by modifying the concentration of all reagents is shown in Figure 2. However, more information on the evolution of all the other porous properties can be found elsewhere [2, 3, 4]. A maximum mesopore volume (0.65 ± 0.05 cm^3/g) is obtained by adjusting the pH between 5.6 and 6.0 and the dilution ratio between 5.5 and 7.0. This range is not altered by a decrease in the R/F molar ratio below the stoichiometric value (Figure 2b). However, the volume is enhanced by 37% when the molar ratio is fixed at 0.2. From these results, different mathematical models were obtained, from which, from now on, the values of the final porous properties within the range of combinations of pH-D-R/F studied can be determined. Hence, carbon xerogels can be directly synthesised and tailored to have porous properties that fit specific application requirements.

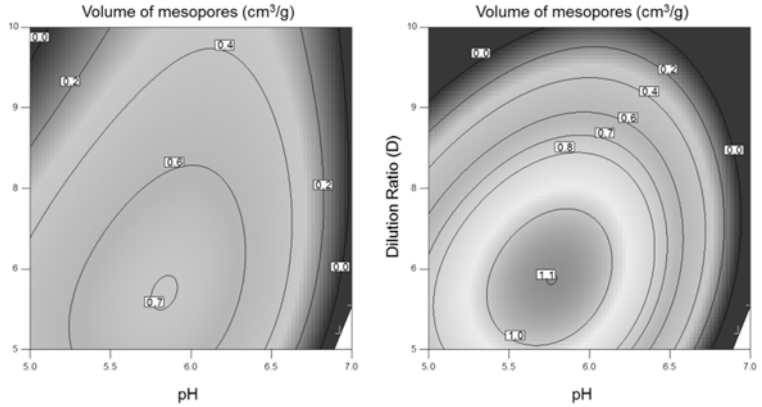

Fig. 2. Contour plot representing the simultaneous effect of pH and D on mesoporosity when the R/F molar ratio is fixed at 0.5 (a) and 0.2 (b).

Acknowledgements

Financial support from the Ministerio de Economía y Competitividad of Spain MINECO (under Projects CTQ2013-49433-EXP and CTQ2014-54772-P) is greatly acknowledged. NRR is also grateful to MINECO for her predoctoral research grant.

References

[1] N. Rey-Raap, A. Arenillas, J.A. Menéndez, Formaldehyde in the Synthesis of Resorcinol-Formaldehyde Carbon Gels. Amy Patton Ed., Nova Science Publishers, 2015.
[2] N. Rey-Raap, J.A. Menéndez, A. Arenillas, Carbon, 78 (2014) 490-499.
[3] N. Rey-Raap, J.A. Menéndez, A. Arenillas, Micropor. Mesopor. Mater., 195 (2014) 266-275.
[4] N. Rey-Raap, Síntesis de xerogeles de carbono inducida por microondas. Diseño de materiales porosos a la carta, Universidad de Oviedo (2016). http://digital.csic.es/handle/10261/130096

Zeolites as Sieves for Butene Isomers Separation

Ana Martín-Calvo[a,b,*], Sofía Calero[b]
[a]*Vrije Universiteit Brussel, Pleinlaan 2, 1050, Brussels, Belgium*
[b] *Universidad Pablo de Olavide, Ctra. Utrera km.1, 41013, Sevilla, Spain*
**amarcal@upo.es*

Introduction

Separation of parafins and olefin has attracted important attention since their uses have several industrial applications such as the production of detergents or of multi-branched alkanes with high octane numbers (1). However, the separation of short olefins is particularly complex as it is a highly energy-demanding process. Such is the case of butene isomers, as all compounds have very similar boiling points their separation is achieved through extractive distillations and several reactions, making the process energetically and economically expensive. It is for this reason that the use of molecular sieves has been study for this separation process (2).

Materials and Methods

Among the variety of materials used as molecular sieves, zeolites are the most interesting structures due to their low cost, high thermal stability, bulk density, or adjustable composition. We focus on pure silica structures such as MOR (1D channels), MFI (intersecting channels), LTA (cavities), FAU (cavities), and RWY (cavities).

Monte Carlo simulations are computed in the Gibbs-, Canonical-, and Grand Canonical ensemble to obtain vapor-liquid coexistence curves, heats of adsorption, and adsorption isotherms, respectively, using the RASPA code (3).

Results and Discussion

In this work we approach the separation of butene isomers from the molecular simulation point of view. With this aim in mind, we provide new models for 1-butene, cis/trans-2-butene, and isobutene that reproduce experimental properties of the molecules such as their polarity and vapor-liquid coexistence curves. Pure component adsorption isotherms and heats of adsorption are calculated and compared to experimental data to corroborate the accuracy of the interaction force field parameters. On a third step, the adsorption of different mixtures of both geometric isomers is analyzed in a variety of zeolites to understand the influence that their topology (MFI, MOR, LTA) and pore volume (LTA, FAU, RWY) have on the separation process (figure 1). Finally, all isomers are studied in mixtures to evaluate the effect that their different conformation has on the adsorption behavior.

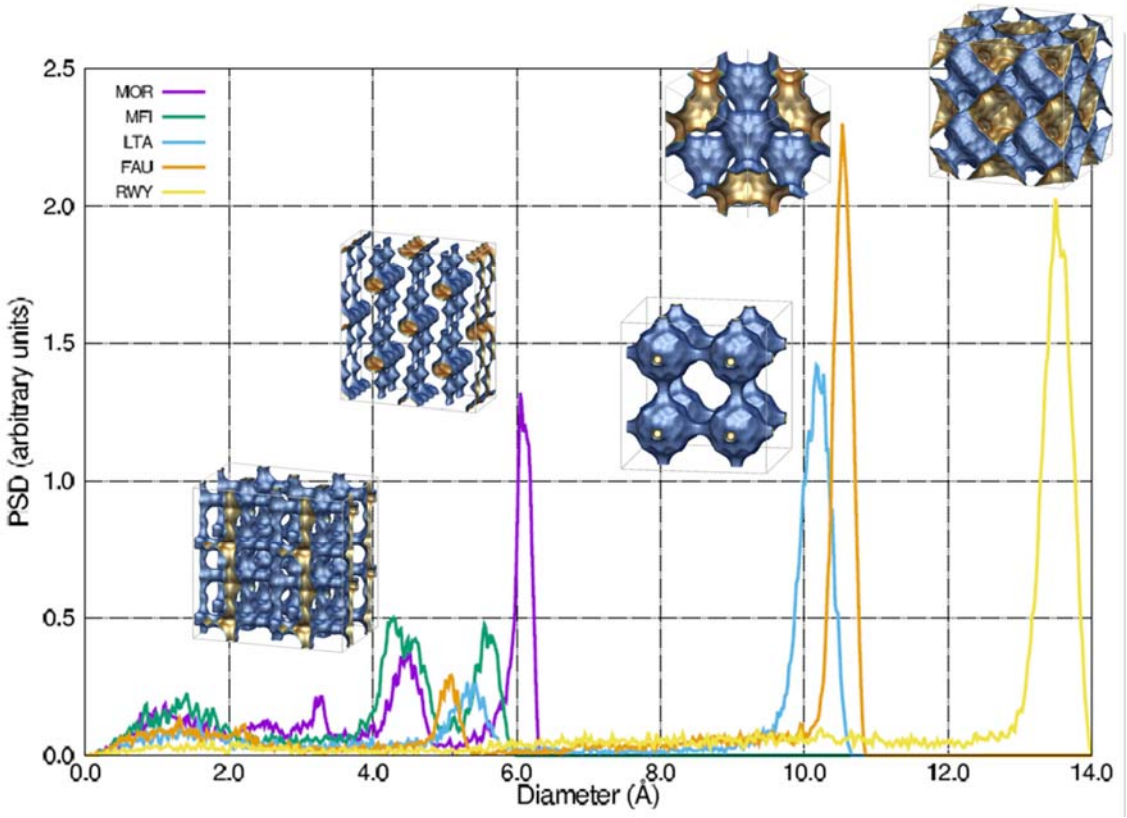

Figure 1: Pore Size Distribution and energy profiles of the zeolites under study. Brown and blue represent the accessible and the non-accessible parts of the structures, respectively.

Acknowledgements

This work has been supported by the European Research Council (ERC2011-StG-279520-RASPA) and the Spanish MINECO (CTQ2013-48396-P).

References

1. F. Tielens, J. F. M. Denayer, I. Daems, G. Baron, W. J. Mortier, and P. Geerlings. J.Phys. Chem. B, 2003, 107, 11065-11071
2. M. Palomino, A. Cantin, A. Corma, S. Leuva, F. Rey, S. Valencia. Chem. Commun., 2007, 12, 1233-1235
3. D. Dubbeldam, S. Calero, D. E. Ellis, and R. Q. Snurr, Mol. Simul., 2016, 42, 81-101.

Preparación de Adsorbentes Carbonosos a partir de Plástico Industrial. Adsorción de Solutos en Disolución

Juan Manuel Ladera López[a], María Alexandre Franco[a], Carmen Fernández González[a], Manuel Alfaro Domínguez[b,*], Vicente Gómez Serrano[a]

[a]Departemento de Química Orgánica e Inorgánica, Facultad de Ciencias, Universidad de Extremadura, Avda. de Elvas, s/n, 06006-Badajoz, España

[b]Departamento de Ingeniería Mecánica, Energética y de los Materiales, Escuela de Ingenierías Industriales, Universidad de Extremadura, Avda. de Elvas s/n, 06006-Badajoz, España

**malfaro@unex*

Introducción

Debido a su bajo coste de producción y excelentes propiedades mecánicas y de moldeo, el propileno (PP) es el plástico más utilizado en la industria del automóvil. De hecho, más de la mitad de todos los materiales plásticos empleados en automóviles son de PP. Debido a ello, según datos del año 2007, sobre cuatro millones de toneladas de PP, de un consumo total que era entonces de más de 45 millones de toneladas, tenía como destino la citada industria del automóvil [1]. Las mezclas de PP y el monómero etileno-propileno-dieno (EPDM) tienen una gran importancia desde el punto de vista comercial [2].Tras la vida útil del automóvil, la enorme cantidad generada de este plástico termina como un material de desecho que es muy difícil de procesar y por tanto reciclar. Como una posibilidad, dada su constitución química con un contenido muy elevado de carbono, el citado plástico podría aprovecharse y valorizarse mediante su empleo como material de partida en la preparación de materiales carbonosos (MC) para su posterior uso como adsorbentes en tratamientos de descontaminación del agua. Con dichas miras, en esta comunicación se presentan algunos resultados obtenidos al llevar a cabo la preparación de MC a partir de goma de PP-EPDM, caracterización y uso en la adsorción de tres solutos en disolución acuosa. En estudios anteriores, se ha investigado la utilización de la goma de neumáticos usados para la preparación también de MC [3,4].

Materiales y Métodos

El material empleado, un elastómero plástico vulcanizado PP-EPDM, fue suministrado por la empresa regional Catelsa Cáceres, S.A, dedicada a la fabricación de componentes de automóviles de varias marcas comerciales, con la consiguiente generación de residuos plásticos. Los datos obtenidos en los análisis del producto (% en peso) son: C, 88; H, 11.8; N, = 0.00; S, 0.37; contenido de cenizas, 0.93. El plástico fue primero reducido de tamaño hasta 1-3 mm. Después, se procedió a la preparación de los MC por el método de activación química con $ZnCl_2$, H_3PO_4 y KOH. La impregnación se realizó con los agentes activantes tanto en disolución acuosa como en estado sólido. Dependendo de dicho agente, la carbonización se efectuó a 500-600, 500 u 800 ºC. Los MC obtenidos fueron caracterizados mediante adsoción física de N_2 a -196 ºC, porosimetría de mercurio y espectrocospia FT-IR así como mediante medida del pH del punto de carga cero (pH_{pcc}). El estudio de adsorción en disolución se llevó a cabo utilizando alguna muestra seleccionada de los MC como adsorbente; naranja de metilo,

p-nitrofenol y el ion Cd^{2+} como adsorbatos en disolución acuosa 10^{-3} M, y procediendo en la forma habitual.

Resultados y Discusión

Los datos obtenidos en el estudio de caracterización de los MC ponen claramente de manifiesto la existencia de una gran influencia sobre todo del agente activante y el método de impregnacióny la temperatura de carbonización sobre sus propiedades texturales y químico superficiales. A modo orientativo, la Figs. 1 muestra las isotermas de adsorción de N_2 para tres muestras preparedas con $ZnCl_2$, H_3PO_4 y KOH. A la vista de la misma es evidente la presencia de micro- y mesoporosidad en las tres muestras, pero especialmente en la preparada con KOH. Los volúmes de poros varían según: W_0 (por adsorción de N_2), KOH > $ZnCl_2$ > H_3PO_4 y V_{me-p} y V_{ma-p} (por porosimetría de mercurio), KOH > H_3PO_4 > $ZnCl_2$. V_{ma-p} >> V_{me-p} y W_0, y por tanto los MC son sólidos esencialmente macroporosos. De hecho, V_{ma-p} es 1.55 $cm^3\ g^{-1}$ para la muestra de KOH.

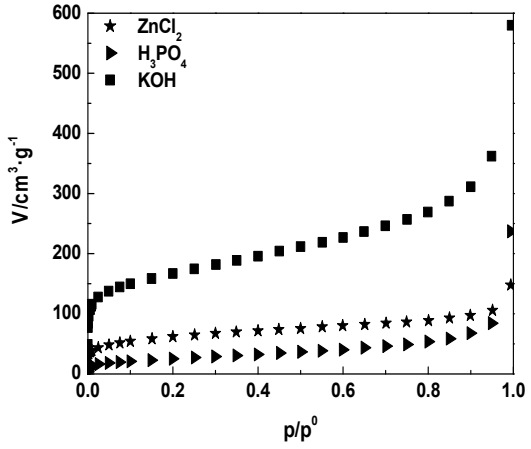

Fig. 1. Isotermas de adsorción de N_2 a -196 ºC.

El pH_{pcc} sigue el orden KOH > $ZnCl_2$ >> H_3PO_4. La cinética del proceso de adsorción es muy rápida con naranja de metilo y con p-nitrophenol y más lenta con el ion Cd^{2+}. La cantidad rentenida en condiciones de equilibrio varía según naranja de metilo > p-nitrofenol > ion Cd^{2+}.

Agradecimientos

Los autores del presente trabajo agradecen al Gobierno de la Comunidad Autónoma de Extremadura la ayuda recibida, con la cofinanciación de FEDER, a Grupos de Investigación.

Referencias

1. S. Moritomi, T. Watanabe, S. Kanzaki, R&D Report, Sumitomo Kagaku Jan., 2010, pp. 1-16.
2. K. Naskar, U. Gohs, G. Wagenknecht, G. Heinrich. Express Polym. Lett. 3 (2009) 677-683.
3. E. Manchón-Vizuete, A. Macías-García, A. Nadal Gisbert, C. Fernández-González, V. Gómez-Serrano, Micropor. Mesopor. Mat. 67 (2004) 35-41.
4. E. Manchón-Vizuete, A. Macías-García, A. Nadal Gisbert, C. Fernández-González, V. Gómez-Serrano, J. Hazard. Mater. B119 (2005) 231-238.

Hollow Silica Microspheres Functionalized with TEPA for the CO_2 Capture at High Temperature

E. Vilarrasa-Garcia[a], J.A. Cecilia[b], C. Garcia-Sancho[b], R.M.A. Saboya[a], C.L. Cavalcante Jr., D.C.S. Azevedo[a], E. Rodríguez-Castellón[b]

[a] Universidade Federal do Ceará, Dep. Eng. Química, Grupo de Pesquisa em Separações por Adsorção – GPSA, Campus do Pici, Bl. 709, 60455-760 Fortaleza, CE, Brasil

[b] Universidad de Málaga, Dep. Química Inorgánica, Cristalografía y Mineralogía. Facultad de Ciencias, Campus de Teatinos s/n, 29071 Málaga, España

** castellon@uma.es*

Introduction

According to the last report about greenhouse gases emissions in 2014 [1], CO_2 appears as the highest concentration, reaching 65% of emissions. In the last two centuries, the concentration of CO_2 in atmosphere has increased up to reach 402.6 ppm while prior 1800, atmospheric CO_2 averaged concentration was 280 ppm. This global issue has led to the governments to propose laws to minimize the CO_2 impact. Taking into account that fossil fuels will continue as the main energy source, avoid the release of CO_2 into the atmosphere is vital. CO_2 adsorption using materials functionalized with amino groups has been proposed as an alternative to the traditional absorption process due to minor energy consumption. The aim of this work is the synthesis and characterization of hollow silica microspheres with a narrow particle size distribution. In addition, the use of swelling agents such as 1,3,5-triisopropylbenzene (TiPB) and fluoride species (NH_4F) limit the aggregation of silica in the synthetic procedure decreasing diffusional resistances. Tetraethylenpentamine (TEPA) was incorporated post-synthesis by impregnation as amino source to improve the CO_2 capacity.

Materials and Methods

HMS materials were synthesized following the method described by Araujo et al. (2009) [2] with some modifications as the incorporation of a swelling agent such as TiPB and NH_4F. Thereby HMS, HMS-F, HMS-TiPB and HMS-F-TiPB were synthesized. The addition of a swelling agent causes an increase of the volume of the hollow silica spheres due to TiPB moves into the hydrophobic core and enlarges the size of the surfactant micelle [3]. The impregnation with TEPA was carried out according previous research [4]. Samples were characterized by N_2 adsorption/desorption isotherms at 77K. X-Ray diffraction, scanning and transmission electron microscopy, Fourier Transformed infrared spectroscopy and elemental analysis. CO_2 adsorption/desorption isotherms were obtained up to 1 bar and at 298, 318 and 338K.

Results and Discussion

DRX, TEM and SEM verified the success of the sytnheses. The incorporation of swelling agents leads to an increase of the size of the hollow silica microspheres and higher dispersion of them, which causes an increase of the external surface area as can be observed in Table 1.

Table 1. Textural properties obtained from N_2 adsorption/desorption isotherms at 77K.

Sample	S_{BET} (m^2g^{-1})	S_{MIC} (m^2g^{-1})	V_P (cm^3g^{-1})	V_{MIC} (cm^3g^{-1})	Pore size (nm)
HMS	1119	978	0.94	0.61	3.6
HMS-F	636	436	0.42	0.20	4.1
HMS-TiPB	1227	341	1.63	0.25	5.3
HMS-F-TiPB	1005	227	1.43	0.22	5.1

CO_2 adsorption/desorption isotherms were measured at three different temperatures up to 1 bar. No hysteresis loop was observed, which it confirms the reversibility of adsorption process. Porous material with higher CO_2 adsorption capacity was HMS-F (1.05 mmol CO_2 g^{-1} at 298K and 1 bar), probably due to its smaller pore diameter and higher microporous surface in comparison with the other adsorbents. These facts favor the interaction of the porous silica with the CO_2 due to a physical process by van der Waals interactions.

Samples were functionalized by impregnation from 20 to 50 wt % of TEPA. The incorporation of TEPA molecules improves the CO_2 capacity at the studied temperature range. Higher TEPA loadings increase the density of amino species on the HMS surface, reaching N contents above to 14% for HMS-F-TiPB. The highest CO_2 adsorption capacity obtained was 3.4 mmol g^{-1} at 1 bar and 298K for the before called sample.

The study of the CO_2 adsorption at different temperatures revealed that the adsorbents without amines species are governed by physisorption (26 kJ/mol). HMS-F-TiPB impregnated with TEPA showed an increase of CO_2 capacity at high temperature (3.6 mmol CO_2 g^{-1} at 338K and 1 bar). However, for high TEPA loadings the working capacity tends to minimize. Hence, with the aim to hold an important working capacity, it would be necessary the use combined of pressure and temperature with a view to application of these materials in a continuous adsorption/desorption process

Finally, the stability of the adsorbent under temperature swing was also evaluated. The CO_2 capacity remained constant after 5 cycles.

Acknowledgements

We thank project CTQ2015-68951-C3-3-R (Ministerio de Economía y Competitividad) and FEDER funds, project P12-RNM-1565 (Excelencia, Junta de Andalucía) and European project 295156 FP7-PEOPLE-2011-IRSES for financial support. E. Vilarrasa-Garcia thanks to CAPES (Brazilian Ministry of Education) for fellowship.

References

1. IPCC, 2014: Climate Change 2014: Synthesis Report. Contribution of Working Groups I, II and III to the Fifth Assessment Report of the Intergovernmental Panel on Climate Change [Core Writing Team, R.K. Pachauri and L.A. Meyer (eds.)]. IPCC, Geneva, Switzerland, 151 pp.
2. R.S. Araújo, D.A.S. Maia, D.C.S. Azevedo, C.L. Cavalcante Jr., E. Rodríguez-Castellón, A. Jiménez-López, Appl. Surf. Sci. 255 (2009) 6205-6209
3. E. Vilarrasa-García, J.A. Cecilia, E.M. Ortigosa-Moya, C.L. Cavalcante Jr., D.C.S. Azevedo, E. Rodríguez-Castellón, Materials 8 (2015) 2495-2513
4. E.S.Sanz-Pérez, M. Olivares-Marín, A. Arencibia, R. Sanz, G. Calleja, M.M. Maroto-Valer, Int. J. Greenh. Gas Con. 17 (2013).366-375.

Experimental Realization of Single-Column Batch Chromatography with Recycle Lag

Abimaelle Silva Chibério[a], Luís Grossinho Dias da Silva[a], Snezana Reljic[a,d], Rui P. P. L. Ribeiro[a], Ricardo J. S. Silva[b,c], José P. B. Mota[a,*]

[a] *LAQV-REQUIMTE, Department of Chemistry, Faculty of Science and Technology, Universidade NOVA de Lisboa, 2829-516 Caparica, Portugal.*

[b] *Instituto de Tecnologia Química e Biológica António Xavier, Universidade Nova de Lisboa, Av. da República, 2780-157 Oeiras, Portugal*

[c] *iBET, Instituto de Biologia Experimental e Tecnológica, Apartado 12, 2780-901 Oeiras, Portugal*

[d] *Department of Biochemical Engineering and Biotechnology, Faculty of Technology and Metallurgy, University of Belgrade, Karnegijeva 4, 11000 Beograd, Serbia*

**pmota@fct.unl.pt*

Introduction

In previous work (AIChE J. 2005;51:1641-1653) we demonstrated that the periodic state of the simulated-moving-bed (SMB) process is reproduced by a single-column chromatographic process with a recycle lag of (N-1)×τ time units, where N is the number of columns of the equivalent SMB unit and τ is the switching interval. The operation of this ideal single-column process is formulated by selecting an arbitrary column of the SMB and following its operation over a complete cycle. To implement the recycle lag in practice, a special type of plug-flow tube was proposed. It includes internal elements to make the flow as close as possible to plug flow, and a piston to compensate for the difference between the inlet and outlet flow rates. This is necessary because the recycle lag is not a multiple of the overall cycle duration. The proposed system is a more compact, less expensive, and simpler-to-operate alternative to the SMB. Depending on the efficiency of the recycle tube, it was shown that the single-column process can achieve the same purities as the analogous SMB unit while keeping the specific productivity constant.

Materials and Methods

Here we present an experimental realization of the single-column process with recycle lag that uses a simplified version of the plug-flow device. The experimental proof of concept uses the separation of nucleosides by reverse phase and protein capture by protein-A affinity chromatography as case studies to demonstrate the effectiveness of the proposed chromatography apparatus.

Acknowledgements

This work was supported by the Associate Laboratory for Green Chemistry LAQV which is financed by national funds from FCT/MEC (UID/QUI/50006/2013) and co-financed by the ERDF under the PT2020 Partnership Agreement (POCI-01-0145-FEDER - 007265).

The authors also acknowledge CNPq-Brasil, Erasmus Mundus Action 2-Sigma Agile, and FCT/MCTES for financial support through grants 234180/2014-5 (Abimaelle Silva Chibério), 2014-0848/ 001-001 (Snezana Reljic), and SFRH/BPD/103533/2014 (Rui Ribeiro).

Physical Activation of Wood Pellets for CO_2 Selective Adsorption

J.F. Vivo-Vilches[a*], A.F. Pérez-Cadenas[a], F.J. Maldonado-Hódar[a], F. Carrasco-Marín[a], R.P.V. Faria[b], A.M. Ribeiro[b], A.F.P. Ferreira[b], A.E. Rodrigues[b]

[a](Carbon Materials Research Group, Department of Inorganic Chemistry, Science Faculty, University of Granada, Campus Fuentenueva s/n, ES18071-Granada,Spain)

[b](Laboratory of Separation and Reaction Engineering - Laboratory of Catalysis and Materials, Department of Chem. Eng., Faculty of Engineering, University of Porto, Rua Dr. Roberto Frias, PT4200-465-Porto, Portugal)

** joseviv@ugr.es*

Introduction

There is an increasing interest on finding alternatives to fossil fuels, especially in countries which are energetically dependent on others. Biogas and natural gas in general (methane) is a cleaner energy source than other heavier hydrocarbons. Nevertheless, in the case of biogas, the main drawback is its high content on carbon dioxide (it might be as high as 40% or more) which significantly reduces its heating capacity. Therefore, for biogas to be used, a previous separation step in order to reduce the CO_2 content is needed. Separation can be performed by several techniques, but selective adsorption is the one with lower energetic requirements for regeneration[1,2].

Materials and Methods

Pine wood pellets for domestic heating applications were used as raw material. Two samples were obtained; carbonization was performed in N_2 (300 cm^3min^{-1}) and once at 900°C pellets were either kept at this temperature for two hours (PINPEL); or the inlet gas was switched to CO_2 and the temperature maintained for five hours in the case of physically activated sample (PINPEL20).

N_2 adsorption-desorption isotherms at -196°C and CO_2 adsorption ones at 0°C, as well as Mercury Intrusion Porosimetry were performed. Scanning Electron Microscopy (SEM) microphotographs of sample were also obtained.

After characterizing the samples, isotherms of target compounds (CH_4 and CO_2) were obtained at 30, 50 and 70°Cin a pressure range from 0 to 10 bar by using a magnetic suspension balance (Rubotherm, Germany). Breakthroughs were performed in the case of PINPEL20 at P=1.5 bar, x_{CO2}=0.6, x_{CH4}=0.4, T=30°C and Q=0.3SLPM.

Results and Discussion

CO_2 activation generated a large volume of micropores regarding carbonized sample. An increment on macropore volume measured by Mercury Intrusion Porosimetry was also observed, and these macropores are similar in size to the ones of the carbonized sample, so CO_2 activation made accessible part of porosity which was blocked in the non-activated sample. Therefore, a reduction on bulk density and an increment on S_{BET} was observed for PINPEL20 (Table 1).

Once porous texture of samples was characterized, adsorption-desorption isotherms for the target gases, CO_2 and CH_4 were obtained. Experimental data were fitted with Langmuir or Toth model depending on the suitability of each one. Figure 1 illustrates the

CO_2 and CH_4 adsorption-desorption isotherms at 30°C for PINPEL20. From them, different parameters were calculated and variation of isosteric heat of adsorption with loading was also obtained by analyzing isotherms at different temperatures.

Breakthrough experiments were performed only with the activated sample PINPEL20 since it was the one with the highest CO_2/CH_4 selectivity. When binary adsorption breakthrough curves (Figure 2) are analyzed and compared with single component experiments, several differences are observed. For methane the adsorbed amount became smaller, due the competition with CO_2. Additionally, for CO_2 the adsorption front becomes more dispersed. Nevertheless, it was clearly pointed out that PINPEL20 was able to adsorb CO_2 preferentially regarding CH_4, so this sample is a good candidate to be used as selective adsorbent for biogas upgrading.

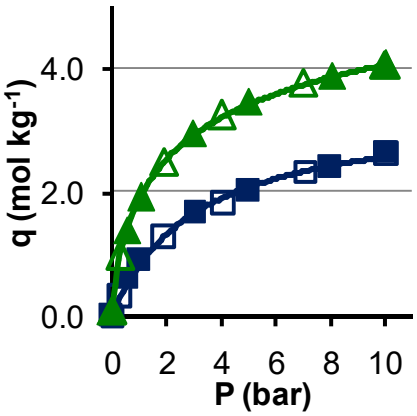

Fig. 1. CO_2 (▲) and CH_4 (■) isotherms at 30°C for PINPEL20

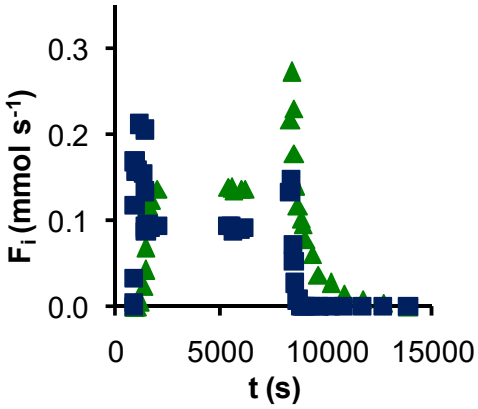

Fig. 2. Breakthrough curves for binary adsorption of CO_2 (▲) and CH_4 (■).

Table 1. Textural properties of samples.

Sample	S_{BET} / $m^2 \cdot g^{-1}$	$W_0(N_2)$ / $cm^3 \cdot g^{-1}$	$W_0(CO_2)$ / $cm^3 \cdot g^{-1}$	$L_0(CO_2)$ / nm	ρ_{Hg} / $g \cdot cm^{-3}$
PINPEL	0	0.00	0.21	0.61	0.83
PINPEL20	561	0.22	0.31	0.84	0.52

Acknowledgements

This research is supported by the FEDER and Spanish projects CTQ2013-44789-R (MINECO) and P12-RNM-2892 (Junta de Andalucía). This work was partially financially supported by: Project POCI-01-0145-FEDER-006984 – Associated Laboratory LSRE-LCM funded by FEDER funds through COMPETE2020 - Programa Operacional Competitividade e Internacionalização (POCI). The author Vivo-Vilches is grateful to Spanish MECD for his FPU grant.

References

1. P. Serra-Crespo, R. Berger, W. Yang, J. Gascón, F. Kapteijn, *Chem Eng Science* 124(2015) 96-108.
2. N. Álvarez-Gutiérrez, M.V. Gil, F. Rubiera, C.Pevida, *Fuel Processing Tech* 142(2016) 361-369.

Enhancement of the Photochemical Conversion Tuning the Surface Chemistry and Structure of Nanoporous Carbons

Alicia Gomis-Berenguer[a*], Jesús Iniesta[b], João C. Lima[c], Conchi O. Ania[a]
[a]*Instituto nacional del carbon (INCAR, CSIC), 33080 Oviedo, Spain*
[b]*Instituto de electroquímica, Universidad de Alicante, 03080 Alicante, Spain*
[c]*Universidade Nova de Lisboa, Lisboa, Portugal*
**alicia.gomis@incar.csic.es*

Introduction

The incorporation of carbon materials in carbon/semiconductor composites is an interesting strategy to attain high photoconversion efficiencies. First investigations in the field focused on their use as additives to TiO_2 and the enhanced performance of the photocatalysts was attributed to the porosity of the carbon support [1]. More recently, the self photochemical activity of semiconductor-free nanoporous carbons under different irradiation conditions was demonstrated [2-3], showing their ability to photogenerate radical oxygen species in aqueous environments, that are capable of converting high and low energy photons in chemical reactions. This has opened new perspectives in the field of applied photochemistry based on carbon materials covering environmental remediation, water splitting, enhanced adsorption/oxidation, or photoluminescence [2-3]. Aiming to understand the mechanisms governing the conversion of light in chemical reactions in the pore space of nanoporous carbons, we report the combined effect of O- and S-doping and nanopore size on the light conversion efficiency of the studied nanoporous carbons.

Materials and Methods

A nanoporous carbon was selected and modified to obtain i) a series of materials with well-defined and increasing pore size, and ii) different composition and nature of O- and S-containing surface. Briefly, the pristine carbon was activated under CO_2 atmosphere (i.e., 850 ºC, 10 mL/min) for variable periods of time (samples are labelled as F, F1 and F4, where the number represents the increasing burn-off degree). To introduce S-containing functional groups, the carbons were exposed to H_2S (ca. 1000 ppm balanced in nitrogen, flow rate 150 mL/min) for 3 h at 800 °C (heating rate 10 °C/min). The S-doped carbons are labelled F-S, F1-S and F4-S. The photochemical activity of the carbons towards the photooxidation of phenol in aqueous environments was explored using monochromatic light, to determine the wavelength onset of the photochemical activity. Further details are given in references 3-5. The experiments were designed to suppress secondary reactions other than photooxidation in the constricted pore space by irradiating aqueous suspensions of the carbons pre-loaded with phenol [3].

Results and Discussion

Fig. 1 shows the normalized phenol conversion values of the nanoporous carbons at different wavelengths. The gathered data has confirmed the photoassisted degradation of the pollutant retained inside the porosity for all the studied samples and all selected wavelengths. This is most remarkable considering that carbons are strong light

absorbers, hence a large fraction of the light is not expected to reach the target molecule in the adsorbed state. Furthermore, the photooxidation yields inside the porosity of the carbons are higher than that of direct photolysis from solution, corroborating the outstanding role of the confinement of the pollutant in enhancing the light conversion into a chemical reaction. Most importantly, when the adsorbed species commensurate the average pore size of the nanoporous carbon, the conversion of low energy photons increased significantly, achieving photochemical quantum yields for photooxidation reactions upon close to those of high energy photons. Outstanding conversion values are obtained at 400, 450 and 500 nm when the photochemical reaction is carried out in the confined carbon pore space. This corresponds to over 100-200 nm redshift in the wavelength onset for the photochemical reaction compared to photolysis, and clearly demonstrates the ability of these carbons to convert visible light into a chemical reaction in aqueous medium [4,5].

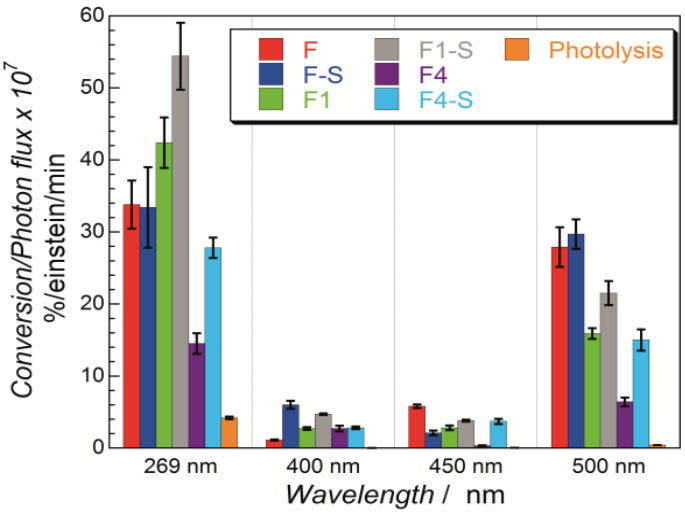

Fig. 1. Normalized phenol conversion per incident flux at different wavelengths for the studied nanoporous carbons.

Acknowledgements

This study is supported by the Spanish MINECO (grant CTM2014-56770-R) and the European Research Council through an ERC-Consolidator Grant (648161-PHOROSOL). AGB thanks MINECO for her PhD fellowship (BES-2012-060410).

References

1. Matos J., Laine J., Hermann J-M. Appl. Catal. B Environ. 18 (1998) 281-291.4.
2. Velasco L.F., Maurino V., Laurenti E., Fonseca I.M., Lima J.C., Ania C.O. Appl Catal A 452 (2013) 1-8.
3. Velasco L.F., Lima J.C, Ania C.O., Angew. Chem.Int. Ed. 5 (2014) 4146-48.
4. Gomis-Berenguer A., Iniesta J., Moro A., Maurino V., Lima J.C., Ania C.O. Carbon 96 (2016) 98-104.
5. Gomis-Berenguer A., Seredych M., Iniesta J., Lima J.C., Bandosz T.J., Ania C.O. Carbon (2016) In press.

Chemical Warfare Agents *S*- and *R*-Sarin Isomers Adsorption and Separation in Chiral Metal-Organic Frameworks

Francisco D. Lahoz-Martín[a], Ana Martín-Calvo[a,b], Sofía Calero[a]*

[a] *Department of Physical, Chemical, and Natural Systems, University Pablo de Olavide, Seville, Spain*

[b] *Department of Chemical Engineering, Vrije Universiteit Brussel, Brussels, Belgium*

**scalero@upo.es*

Introduction

The use and synthesis of the potent nerve agent sarin (isopropyl methylphosphonofluoridate) have been extremely restricted since the 1920s. However, its use as a chemical weapon has been reported ever since. [1] There are two isomeric forms of sarin, *S*- and *R*-, being the *S*-sarin isomer the most neurotoxic variant. In the human body, these molecules inhibit the action of the acetylcholinesterase (AChE). As this enzyme eliminates the excess of acetylcholine neurotransmitter, the presence of sarin results on uncontrolled muscular spasms and possible death. [2, 3]

We explore the use of Metal-Organic Frameworks to adsorb sarin from the air. Our first approach involves chiral Boron Imidazolate Frameworks (BIFs) such as BIF-8 and BIF-22. [4] To complete our study, we also focus on novel MOFs with chiral centers such as a BINOL based MOF [5] and BINAF dMOF [6], studying both the absolute intake of sarin in different conditions and the differential behavior that both isomers may feature.

Materials and Methods

To understand the behavior of both isomers we employ computational techniques. We carry out Monte Carlo simulations to study the adsorption loading and selectivity, as well as Molecular Dynamics to estimate self-diffusion coefficients at 10^5 Pa and 298 K. Molecular models of sarin isomers are based on a *S*-sarin model reported by Sokkalingam *et al.* [7]. Atomic positions and structure descriptions are derived from experimental crystalographic work.

Results and Discussion

Our results show differential adsorption behavior for both isomers at 50:50 starting fractions at 10^5 Pa and 298 K in BIF-22. Figure 1 shows that this structure favors the adsorption of *S*-sarin in mixture with more than 40% of this isomer. The chiral nature of the structure makes possible the differentiation of both isomers at equimolar conditions. We also study the presence of sarin in air using vapor mixtures of *S*- and *R*-sarin (3.7%, both isomers), oxygen (20.2%), nitrogen(75.1%), and argon (1.0%). We vary the relative amount of both isomers and then we compare these results with those obtained for the binary mixture. As observed in Figure 1, there is a stronger preference for the *S*- isomer in BIF-22 from air mixture compared to the binary mixture. The adsorption of *S*-sarin remains almost unaffected, while the adsorption of *R*-isomer is reduced, increasing therefore the selectivity of the structure towards the *S*-isomer. Figure 2 shows the occupation of the framework by *S*-sarin at different relative fractions of the adsorbate. We observe a similar behavior for *R*-sarin, as both isomers compete

for the adsorption sites inside the structure. Overall, our results stress the importance of understanding the adsorptive behavior of sarin and other hazardous compounds in MOFs and highlight the applicability of these structures in adsorption and separation proccesses.

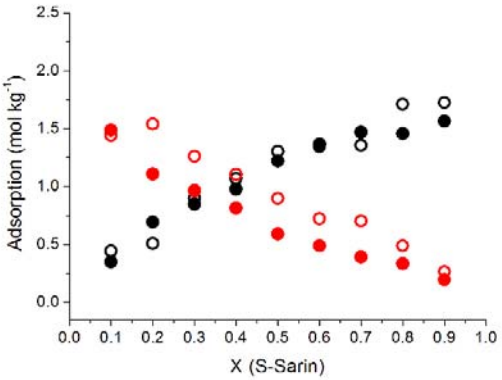

Figure 1. Adsorption loading of binary mixtures of *S*- (red) and *R*-sarin (black) isomers as a function of the molar fraction of *S*-sarin at 298 K and 10^5 Pa in BIF-22. Binary mixtures (empty symbols), mixtures with air (full symbols).

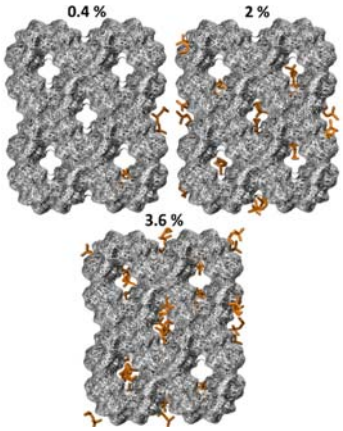

Figure 2. Location of *S*-sarin molecules (orange) inside BIF-22 at different concentrations of the isomer in air.

Acknowledgements

This work is supported European Research Council through an ERC Starting Grant (ERC2011-StG-279520-RASPA), by the MINECO (CTQ2013-48396-P) and by the Andalucía Region (FQM-1851).

References

1. A.P. Volans. *J. Accid. Emerg. Med.*, 13 (1996) 202-6
2. A.C. Hemmert *et al., Mol. Pharmacol.*, 77 (2010) 508-16
3. R. Iyer *et al., Toxicol. Lett.,* 233 (2015) 200-6
4. F. Wang *et al., Chemistry*, 18 (2012) 11876-9
5. M. M. Wanderley *et al., J. Am. Chem. Soc.*, 134 (2012) 9050-3
6. T. Sawano *et al., J. Am. Chem. Soc.*, 137 (2015) 12241-8
7. N. Sokkalingam *et al., J. Phys. Chem. B*, 113 (2009) 10292-7

Selective Liquid Phase Adsorption and Separation of *p*-Xylene with Shaped MIL-125(Ti)_NH_2

M. A. Moreira [a], M. P. Santos [a], J. M. Loureiro [a], J. C. Santos [a], U-Hwang Lee [b], Young Kyu Hwang [b], Jong-San Chang [b], A. F. P. Ferreira [a,*], Alírio E. Rodrigues [a]

[a] Laboratory of Separation and Reaction Engineering, Associate Laboratory LSRE-LCM, Department of Chemical, Engineering, Faculty of Engineering, University of Porto, Rua Dr. Roberto Frias s/n, 4200-465 Porto, Portugal.

[b] Catalysis Center for Molecular Engineering, Korea Research Institute of Chemical Technology (KRICT), P.O. Box 107, Yusung, Taejon 305–600, Korea.

**aferreir@fe.up.pt*

Metal-organic frameworks (MOFs) combine high chemical and thermal stability, large surface areas and tunable surface properties [7]; thus are good candidates as adsorbents for several separation processes. Vermoortele *et al.* reported that MIL-125(Ti)_NH_2 presents high *p*-xylene selectivity in xylene mixtures, in liquid phase [8]. Later it was reported by Moreira *et al.* the synthesis optimization of the MIL-125(Ti)_NH_2, at the laboratory scale, in order to be evaluated as powder for the selective adsorption and separation of xylene isomers including ethylbenzene also in liquid phase, and using *n*-heptane as eluent [9].

Although MOFs have not yet found their way into industrial separation applications, it is clear that they show potential for liquid phase separations [10].

The main objective of the present work was to study the adsorption behaviour of the xylene isomers on MIL-125(Ti)_NH_2 in order to evaluate its potential for xylenes separation. Therefore, a detailed experimental study of binary and multicomponent adsorption equilibrium of xylene isomers in MIL-125(Ti)_NH_2 pellets is presented, at three different temperatures.

Binary (xylene isomers in the presence of the eluent) breakthrough experiments were performed in order to determine the adsorption equilibrium isotherms for *o*-, *m*-, *p*-xylene and ethylbenzene at 299 K, 313 K and 343 K using n-heptane as eluent. Several experiments were carried out in order to screen a wide range of concentrations. In Fig. 1 are presented the adsorption isotherms for *p*-xylene at three different temperatures.

Multicomponent breakthrough experiments were also carried out and the selectivity values were calculated. In the presence of ethylbenzene, MIL-125(Ti)_NH_2 have revealed a *p*-xylene or an ethylbenzene selectivity depending on the feed mixture concentration. At low ethylbenzene concentrations, MIL-125(Ti)_NH_2 solid was *para*-xylene selective in liquid phase, whereas selectivity was reversed to ethylbenzene selectivity at higher concentrations.

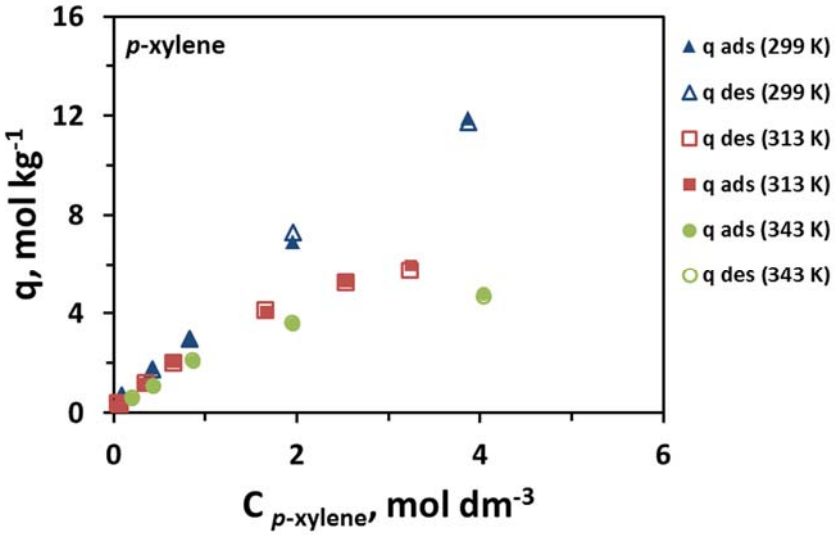

Fig. 1. Adsorption equilibrium isotherms on MIL-125(Ti)_NH_2 for bi-component mixtures of *p*-xylene in n-heptane at 299 K, 313 K and 343 K.

Acknowledgements

This work was financially supported by: Project POCI-01-0145-FEDER-006984 – Associated Laboratory LSRE/LCM funded by FEDER funds through COMPETE2020 - Programa Operacional Competitividade e Internacionalização (POCI) – and by national funds through FCT - Fundação para a Ciência e a Tecnologia; Bolsa FCT SFRH/BPD/93167/2013.

References

1. G. Férey, C. Mellot-Draznieks, C. Serre, F. Millange, Crystallized Frameworks with Giant Pores: Are There Limits to the Possible?, Accounts of Chemical Research, 38 (2005) 217-225.
2. F. Vermoortele, M. Maes, P.Z. Moghadam, M.J. Lennox, F. Ragon, M. Boulhout, S. Biswas, K.G.M. Laurier, I. Beurroies, R. Denoyel, M.B.J. Roeffaers, N. Stock, T. Duren, C. Serre, D.E. De Vos, para-Xylene selective Metal-Organic Frameworks: a case of topology-directed selectivity, J. Am. Chem. Soc., ASAP (2011).
3. M.A. Moreira, J.C. Santos, A.F.P. Ferreira, J.M. Loureiro, F. Ragon, P. Horcajada, P.G. Yot, C. Serre, A.E. Rodrigues, Effect of ethylbenzene in p-xylene selectivity of the porous titanium amino terephthalate MIL-125(Ti)_NH2, Micropor Mesopor Mater, 158 (2012) 229-234.
4. B. Van de Voorde, B. Bueken, J. Denayer, D. De Vos, Adsorptive separation on metal-organic frameworks in the liquid phase, Chem. Soc. Rev., 43 (2014) 5766-5788.

Two-Column Relay Simulated Moving Bed Concept for Gas Separation

Rui P. P. L. Ribeiro, Isabel A. A. C. Esteves, José P. B. Mota*
LAQV-REQUIMTE, Department of Chemistry, Faculty of Science and Technology, Universidade NOVA de Lisboa, 2829-516 Caparica, Portugal.
**pmota@fct.unl.pt*

Introduction

Simulated moving bed (SMB) technology is a robust and well-established adsorption-based separation process which has been increasingly employed in the biotechnology, pharmaceutical and fine chemistry industries [1], since it allows obtaining large recoveries of high-purity products. Although the SMB concept has been mainly employed for liquid-phase separations, recently several studies focusing in gas phase separations have appeared in the literature, namely in the separation of olefins/paraffins and volatile inhalation anesthetic enantiomers [2 - 5].

The SMB consists in a counter-current chromatographic process in which *N* identical columns are connected in series to build a closed loop. During the process the input and withdrawal ports are moved one column ahead, in the direction of fluid flow, at fixed intervals, and this way the counter-current contact of adsorbent and fluid is simulated. Recent advances in the cycle engineering of liquid phase SMB include the development of two-column schemes which allow the decreasing cycle complexity, the use of less stationary phase, and the pressure-drop [6].

In this work, we evaluate the performance of a two-column SMB system for the separation of CO_2/CH_4 mixtures, using a new experimental two-column prototype. The system employed uses recent liquid-phase operation schemes to gas-phase systems, operating as a relay SMB unit [7]. The two-column scheme performance working in relay mode is compared with the performance of a classical four-zone SMB process.

Acknowledgements

Financial support from FCT/MCTES (Portugal) through projects EXCL/QEQ-PRS/0308/2012, PTDC/AAC-AMB/108849/2008, and PTDC/CTM/104782/2008 is gratefully acknowledged. The authors also acknowledge FCT/MCTES for financial support through grant SFRH/BPD/103533/2014 (Rui P. P. L. Ribeiro) and FCT Investigator contract IF/01016/2014 (Isabel A. A. C. Esteves).

This work was partially supported by the Associate Laboratory for Green Chemistry LAQV which is financed by national funds from FCT/MEC (UID/QUI/50006/2013) and co-financed by the ERDF under the PT2020 Partnership Agreement (POCI-01-0145-FEDER - 007265).

References

1. R. P. V. Faria, A. E. Rodrigues, J. Chromatogr. A. 1421 (2015) 82-112.
2. M. Juza, O. Di Giovanni, G. Biressi, V. Schurig, M. Mazzotti, M. Morbidelli, J. Chromatogr. A. 813 (998) 333-347.
3. M.C. Campo, M.C. Baptista, A.M. Ribeiro, A. Ferreira, J.C. Santos, C. Lutz, J.M. Loureiro, A.E. Rodrigues, Adsorption. 20 (2013) 61-75.
4. J.P.B. Mota, I.A.A.C. Esteves, Ind. Eng. Chem. Res. 46 (2007) 6978-6988.
5. J.P.B. Mota, I.A.A.C. Esteves, M.F.J. Eusébio, AIChE J., 53 (2007) 1192-1203.

6. R. C. R. Rodrigues, T. J. S. B. Canhoto, J. M. M. Araújo, J. P. B. Mota, J. Chromatogr. A. 1180 (2008) 42-52.
7. R. J. S. Silva, R. C. R. Rodrigues, J. P. B. Mota, J. Chromatogr. A. 1260 (2012) 132-142.

Analysis of Photocatalytic Activity in Activated Carbon during its Interaction with UV Light and Solar Simulated Radiation

Inmaculada Velo Gala[a,b] *, Jesús J. López Peñalver[a], Manuel Sánchez Polo[a], José Rivera Utrilla[a]

[a]Department of Inorganic Chemistry, Faculty of Pharmacy. University of Granada. Granada, Spain.

[b]ADPOR Group, Instituto Nacional del Carbón (INCAR, CSIC), Oviedo, Spain.

**i.velo@incar.csic.es*

Introduction

Advanced Oxidation Processes (AOPs) appear to be a promising technology for removing organic compounds that are resistant to conventional treatments. Activated carbon (AC) has the capacity to improve some AOPs. Photocatalytic processes are well-known AOPs, which require the use of luminous radiation capable of producing electronic activation of the catalyst. This process can be improved by the presence of ACs with adequate physical and chemical properties. In earlier investigations [1-4], it has been reported that some ACs have an important photocatalytic activity by themselves under solar and UV radiations, so it is necessary to clarify the action mechanism and which are the decisive properties of ACs for this behavior.

The main objective of this study was to demonstrate the photocatalytic behavior of ACs in the presence of UV light and solar radiation analyzing the mechanism of the photocatalytic processes. For this purpose we studied and analyzed: (i) the influence of the amount of AC in the process of solar and UV photocatalysis, (ii) the existence of photogenerated positive holes, (iii) the concentrations of both superoxide and hydroxyl radicals formed, (iv) the role of dissolved oxygen in the medium and (v) the influence of the chemical properties of ACs in the concentrations of the radical species obtained.

Materials and Methods

Experiments were conducted in a photoreactor equipped with a low-pressure mercury lamp (Hg 253.70 nm) Heraeus Noblelight, model TNN 15/32 (15 W), and a solar simulator, model 1500 Solarbox, equipped with a Xenon lamp (Brand NEURTEK instruments), in an irradiance of 450 W/m^2. We used a commercial activated carbon Witco (W) in its original form and the samples obtained after its gamma radiation treatment in five different experimental conditions [5]. The model of emerging contaminant used to evaluate the capacity of photocatalytic degradation was sodium diatrizoate, a contrast media applied in hospitals in radiodiagnostic tests.

Results and Discussion

The presence of activated carbon during the contaminant photodegradation considerably increased its removal rate when using UV light (UV/AC) and solar radiation (Solar/AC). The values of band gap (Eg) of ACs showed these materials to behave as semiconductors and, therefore, as photoactive materials. Our analysis of the hydroxyl radicals and superoxide anions in these systems demonstrated that activated carbons act as photocatalyst materials (Fig. 1). Concentrations of superoxide anion and hydroxyl

radical photogenerated depended on the surface chemistry of the activated carbons and the hydroxyl radical concentration was favored when their value of Eg was lower.

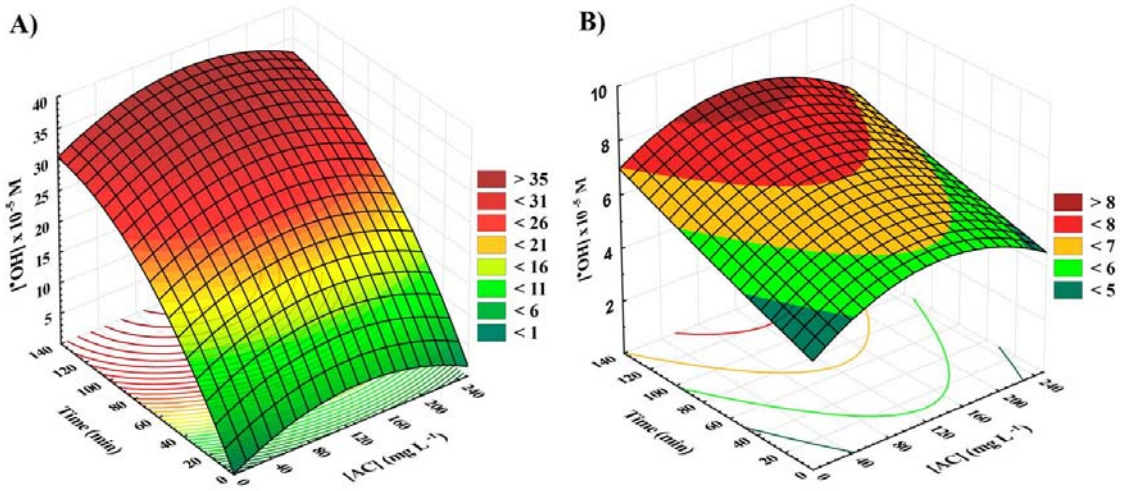

Fig 1. Response surface which connects the hydroxyl radical concentration with the reaction time and the AC amount in the system. A) Systems UV/AC and B) Solar/AC. Amount of AC (mg L^{-1}): 35, 100, 170, 235. AC = W; pH = 6.5; T = 298 K.

The photocatalytic role of AC was favored by the presence of ester/anhydride groups on its surface, as well as by a higher percentage of carbon atoms with sp^2 hybridization. We have detected that oxygen dissolved in the medium plays a significant role in the photoactive behavior of the activated carbon, thus, its removal from the solution favored the recombination of electron-hole pairs, preventing the formation of superoxide anion and, therefore, annulling the generation of hydroxyl radicals. We also found that the presence of oxygen on the activated carbon surface promoted the formation of radical species, thus, carbon with a high surface oxygen content could result in materials with higher photoactive character.

Acknowledgements
We are grateful for the financial support provided by the Junta de Andalucía (RNM7522) and the Spanish Ministry of Science and Innovation (CTQ2011-29035-C02-02). We thank ADPOR Group (INCAR, CSIC) for its support to our attendance in the 40th Iberian Adsorption Meeting (RIA).

References
[1] L.F. Velasco, J.B. Parra, C.O. Ania, Appl Surf Sci 256 (2010) 5254-5258.
[2] L.F. Velasco, I.M. Fonseca, J.B. Parra, J.C. Lima, C.O. Ania, Carbon 50 (2012) 249-258.
[3] I. Velo-Gala, J.J. López-Peñalver, M. Sánchez-Polo, J. Rivera-Utrilla, Appl Catal B-Environ 142–143 (2013) 694-704.
[4] M. Haro, L.F. Velasco, C.O. Ania, Catal Sci Tech 2 (2012) 2264-2272.
[5] I. Velo-Gala, J.J. López-Peñalver, M. Sánchez-Polo, J. Rivera-Utrilla, Carbon 67 (2014) 236-249.

The Structure of CO_2 Species Adsorbed in Amine-Functionalized Mesoporous Silicas for CO_2/CH_4 Separation

Luís Mafra[a], Tomaž Čendak[a], Sarah Schneider[a], Paul Wiper[a], João Pires[b], José R. B. Gomes[a], Moisés L. Pinto[c]*

[a]CICECO - Aveiro Institute of Materials, Department of Chemistry, University of Aveiro, Campus Universitário de Santiago, 3810-193 Aveiro, Portugal

[b]Center of chemistry and biochemistry, Faculdade de Ciências, Universidade de Lisboa, 1749-016 Lisboa, Portugal

[c]CERENA, Instituto Superior Técnico, Universidade de Lisboa, Av. Rovisco Pais, n° 1, 1049-001 Lisboa, Portugal

** moises.pinto@tecnico.ulisboa.pt*

Introduction

In recent years, several adsorbent materials have been studied for the selective adsorption/capture of CO_2 in order to substitute the classical scrubbing of gases with aqueous amine solutions. Among the materials that are being developed, amine-functionalized porous sorbents are the most significant ones as they have high selectivity and capacity towards CO_2 at low partial pressures. A large number of works exists in the literature about the CO_2 adsorption on amine-modified mesoporous silicas, although only few are focused on understanding the interaction of the CO_2 with the amines and understanding the species formed at the materials' surface. In the present work, we use a combination of adsorption of ^{13}C labeled CO_2 [1], computational models and adsorption of gases at high pressures to study the adsorption of CO_2 on SBA-15 functionalized with primary, secondary and mixed amines. We were able to unveil the complexity of the interactions at molecular level and explain the very high selectivities in the separation of CO_2/CH_4 mixtures.

Materials and Methods

SBA-15 was functionalized with [3-aminopropyltriethoxysilane (APTES)], secondary [trimethoxy[3-(methylamino)propyl]silane (TMMAP)] and tertiary ([3-(diethylamino)propyl]trimethoxysilane (3-DEAPTES)) amines, and also in a diamine containing primary and secondary amine groups [N-[3-(trimethoxysilyl)propyl]ethylenediamine (N-3)] under dry toluene reflux. The materials were characterized by nitrogen adsorption and TG-DSC.

Adsorption of CO_2 and CH_4 laboratory made stainless steel volumetric apparatus up to 1000 kPa. DFT cluster calculations have been computed using Gaussian 09 software considering the molecules in the gas phase, using the hybrid functional M06-2X with the 6-31G(d,p) basis set. ^1H and ^{13}C magic angle spinning (MAS) NMR spectra were acquired on a Bruker Avance III 400 and 700 spectrometers operating at B_0 fields of 9.4 and 16.4 T. Before NMR spectra acquisition, samples were prepared in a lab made high vacuum line capable of heating the zirconia rotors filled with the samples, introducing $^{13}CO_2$ and closing the rotors under controlled environment.

Results and Discussion

The selectivity of the CO_2/CH_4 binary mixture adsorption on the materials shows that the functionalization with the primary amine (APTES) increases the selectivity of the material to values between 10 and 25. The increase is even higher for the secondary amines TMMAP and N-3, where the values are between 119 and 1114, and between 3300 and 15000, for the former and latter, respectively.

The strong affinity of the functionalized materials for CO_2 is a consequence of the reaction of the CO_2 molecule with the amines on the surface, forming species that were identified by NMR. These species were stabilized by strong lateral interactions with neighboring amine groups, giving rise to different ^{1}H and ^{13}C chemical shifts.

The assignment of the observed chemical shifts was supported by cluster model calculations, for the different studied amine groups. The molecular models obtained agreed remarkably with the observed chemical shifts (see Fig.1 for the example with APTES) and depict the importance of the hydrogen bonds with lateral amine groups and with the surface hydroxyl groups. These complex conjugated hydrogen bonds are responsible for stabilizing the labile carbamic acid species formed at the surface. These are however sufficiently unstable to be reversibly removed with vacuum and their stability was studied by NMR with variable $^{13}CO_2$ pressure.

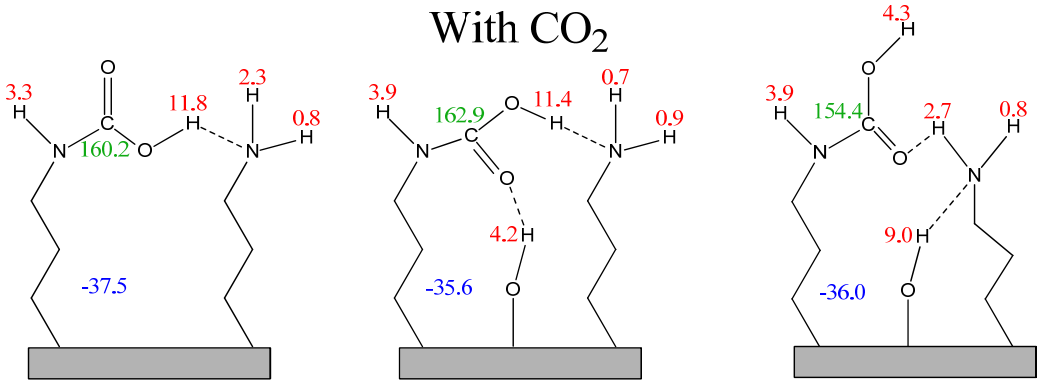

Fig. 1. Comparison of ^{1}H (red) and ^{13}C (green) chemical shifts of possible structures of APTES functionalized silica with and without CO_2, obtained from cluster model calculations. ΔE (kJ/mol) of the structures in blue

Acknowledgements

The work was financed by Fundação para a Ciência e a Tecnologia (FCT) through projects IF/00993/2012/CP0172/CT0013 and PTDC/QEQ-QAN/6373/2014. This work was developed in the scope of the Projects POCI-01-0145-FEDER-007679 | UID/CTM/50011/2013 (CICECO), UID/MULTI/00612/2013 (CQB), UID/ECI/04028/2013 (CERENA), financed by national funds through the FCT/MEC and cofinanced by FEDER under the PT2020 Partnership Agreement. The authors are also grateful to Investigador FCT program and to the Portuguese NMR Network (RNRMN).

References

1. Pinto, M. L.; Mafra, L.; Guil, J. M.; Pires, J.; Rocha, J. Adsorption and Activation of CO2 by Amine-Modified Nanoporous Materials Studied by Solid-State NMR and 13CO2 Adsorption. Chem. Mater. 23 (2011) 1387–1395.

Computational Study on Ethanol/Butanol/Pentanol/Water Separation in Hierarchical Pure Silica Zeolites

Salvador R. G. Balestra, José Manuel Ortiz-Roldan, Said Hamad, A. Rabdel Ruiz-Salvador*, Sofía Calero*

Área de Química−Física, Universidad Pablo de Olavide*, Ctra. Utrera km 1, 41013 Seville,* Spain

* rruisal@upo.es *(ARRS),* scalero@upo.es *(SC)*

Introduction

Hierarchical (or mesoporous) zeolites have attracted significant attention during the last years [1-5]. These materials sustain the physical characteristics of zeolites, adding a tuneable degree of mesoporosity (see Fig. 1). In this work, we have evaluated hierarchical zeolites as a molecular sieve for biofuel/water separation using theoretical and simulation methods.

Materials and Methods

Topology is crucial in the transport of molecules. A variety of strategies have been used for the theoretical structural modeling of the experimental pore architecture [2, 3]: interconnectivity, pore-size/space distribution, and the mesopore/bulk interface. We have selected the LTA (3D channel type) and STW (1D) zeolites to model the microporosity. Monte Carlo (MC) simulations have been carried out with the RASPA code for reproduce the adsorption of molecules while constant volume Molecular Dynamics (MD) simulations have been carried out with the LAMMPS program to study the transport properties. The framework has been modeled as flexible in order to catch both the intracrystalline distortions and those distortions at the bulk/mesopore interface, for which the force field of Ramsahye and Bell was used [6]. Water molecule and biofuel molecules (methanol, ethanol and butanol isomers) were modelled with N. de Leew and OPLS-AA force field, respectively.

Results and Discussion

In order to characterize the modeled structures we have calculated the void fractions, PLC and LCD. To calculate the transport properties we have calculated the mean squared displacement of water, ethanol and butanol isomers through the structures and the self-diffusion coefficient. We have found differences in the diffusion for the isomers of butanol (n-butanol, sec-butanol, isobutanol and tert-butanol). We have studied the role of the hydrogen bonds of water/alcohol in the mesopore/bulk interface and its effect in the diffusion of molecules. The strong attractive interaction between the oxygen atoms of the zeolite and the H-bond of water and alcohols exerts a large force on the framework that is likely to be the cause. There is a complex interplay between structural flexibility and water molecules, modulated by the presence of these polar adsorbates.

In order to get a better representation of the effect of the mesoporosity, we compare the results with those of traditional non-herarchical zeolites. We have found that the mesopore/bulk interface is relevant in controlling the different behavior of the two cases. The surface resistance, known in the surface diffusion context, plays a special role

here. We found that the balance between the micro and macroporosity is a simple dial for tuning the separation behavior.

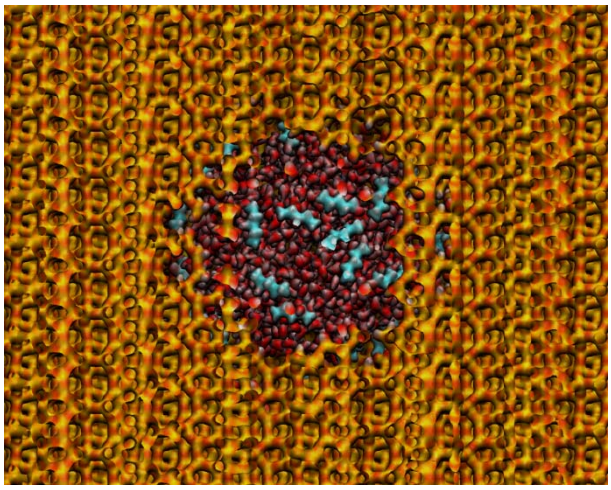

Fig. 1. Snapshot of water molecules and biofuel molecules crossing the mesopore/bulk interface.

Acknowledgements

This work was supported by the European Research Council and ERC Starting Grant (Sofía Calero, ERC2011-StG-279520-RASPA) and the spanish *Ministerio de Economía y Competitividad* (Sofía Calero, CTQ2010-16077 and CTQ2013-48396-P). S.R.G. Balestra thanks Spanish MEC (CTQ2013-48396-P) for his predoctoral fellowship.

References

1. Y. Wei, T. E. Parmentier, K. P. de Jong, J. Zecevic, Chem. Soc. Rev. 44 (2015) 7234-7261.
2. T. Prasomsri, W. Jiao, S. Z. Wenga and J. García-Martinez, Chem. Commun., 51 (2015) 8900.
3. J García-Martínez, M Johnson, J Valla, K Li, JY Ying, Catal. Sci. Technol. 2 (2012) 987-994
4. J. G. Martinez E. Senderov, R. Hinchey, U. S. Patent App., 13 (2012) 440-781.
5. A. Galarneau, F. Guenneau, A. Gédéon, D. Mereib, J. Rodriguez, F. Fajula, B. Coasne J. Phys. Chem. C, Just Accepted Manuscript.
6. N. A. Ramsahye and R. G. Bell, J. Phys. Chem. B, 109 (2005) 4738-4747.

Preparación de Biosorbentes a partir de Cáscaras de Toronja Modificadas mediante Descompresión Instantánea Controlada y Posterior Tratamiento Químico: Remoción de Cu(II) en Solución en Modo Batch y Continuo

Luis A. Romero Cano [a, c*], Linda V. González Gutiérrez [a], Leonardo A. Baldenegro Pérez [b], Francisco Carrasco Marín [c]

[a] Centro de Investigación y Desarrollo Tecnológico en Electroquímica (CIDETEQ) S.C. Parque Tecnológico Sanfandila, Pedro Escobedo, Querétaro, C.P. 760703, MEXICO

[b] Centro de Ingeniería y Desarrollo Industrial (CIDESI), Av. Playa Pie de la Cuesta No. 702, Desarrollo San Pablo, Querétaro, C.P. 76130, MEXICO

[c] Grupo de Investigación en Materiales de Carbón, Facultad de Ciencias, Universidad de Granada, Av. Fuente Nueva s/n. Granada, C.P. 18071, ESPAÑA

**lromero@cideteq.mx*

Introducción

En años recientes se han publicado numerosos estudios donde se muestran el uso de desechos agroindustriales como alternativa para la preparación de biosorbentes, los cuales son baratos y efectivos en la remoción de iones metálicos [1]. Los estudios hasta ahora publicados reportan que empleando estos biosorbentes es posible adsorber metales en solución, sin embargo es necesario realizar tratamientos físicos y/o químicos durante su preparación para obtener mayores capacidades de adsorción, incluso mejores que las alcanzadas por los carbones activados comerciales, razón por lo que tienen un especial interés como alternativa para resolver problemáticas ambientales. Sin embargo, para que el uso de estos biosorbentes pueda ser factible como tecnología de tratamiento de aguas residuales es necesario: a) Que los biosorbentes sean preparados a partir de materiales fácilmente disponibles, b) que presenten altas capacidades de adsorción y c) que el proceso se lleve a cabo en modo continuo, generalmente en columnas de lecho fijo [2]. Por tal razón, el presente estudio muestra una nueva metodología para preparar biosorbentes a partir de cáscaras de toronja (*Citrus x paradisi*), desechos de la industria alimentaria que tienen problemas para su disposición. La preparación consiste en un tratamiento empleando Descompresión Instantánea Controlada (DIC). Posterior al DIC se realiza un tratamiento químico para acondicionar el biosorbente para la adsorción de cationes. Con la finalidad de evaluar el efecto de este nuevo método de preparación en la capacidad de adsorción del biosorbente se eligió como adsorbato modelo Cu(II) en solución acuosa, de tal forma que los resultados obtenidos pudieran compararse con las modificaciones reportadas hasta ahora en la literatura.

Materiales y Métodos

Se prepararon materiales biosorbentes empleando cáscaras de toronja, muestra *GP*, modificadas con: a) un tratamiento químico empleando Hidróxido de Sodio 0.1 M y Ácido Cítrico 0.6 M a 80 °C, muestra *GP-AC*, b) Descompresión Instantánea Controlada (DIC), muestra *GP-DIC*, y c) la combinación de DIC con tratamiento químico, muestra *GP-DIC-AC*. Los biosorbentes preparados fueron caracterizados previo y posterior a la adsorción del metal y se evaluaron para la adsorción de Cu(II) en solución en modo *batch*

a 25°C y pH 5 empleando $CuSO_4$-$5H_2O$ como adsorbato para obtener las isotermas de adsorción. Los estudios de caracterización consistieron en determinación de sitios activos, el pH de punto de carga cero, estudios de microscopia electrónica de barrido, espectroscopia de energía dispersiva, porosimetría de intrusión de mercurio y espectroscopia infrarroja. A partir de los resultados obtenidos se discutió el mecanismo de adsorción y posteriormente se estudió la adsorción en modo continuo empleando una columna de lecho fijo de 1 cm de diámetro interno.

Resultados y discusión

La Fig. 1 muestra la distribución de tamaño de poro obtenida mediante porosimetría de mercurio para cada uno de los biosorbentes preparados. Se puede observar que el tratamiento DIC otorga al material propiedades adsorbentes tales como mayor porosidad y en consecuencia existirá mayor cantidad de sitios activos disponibles. Las isotermas de adsorción de Cu(II) sobre los biosorbentes preparados en modo *batch* muestran un buen ajuste al modelo de Langmuir y las capacidades de adsorción obtenidas se encuentran en el orden: *GP-DIC-AC*, 106.95 mg g^{-1} > *GP-AC*, 87.38 mg g^{-1} > *GP-DIC*, 76.80 mg g^{-1} > *GP*, 62.04 mg g^{-1}. La Fig. 2 muestra las curvas de ruptura obtenidas a diferentes alturas de lecho del biosorbente *GP-DIC-AC*, se puede observar que para las condiciones experimentales probadas: flujo 1.3 mL min^{-1}, concentración inicial de 100 mg L^{-1} y un condición de tiempo de ruptura de C/C_o = 0.02, todas las alturas de relleno se obtienen tiempos de ruptura que van desde los 6 min hasta los 130 min para la altura de 16 cm. A partir de las curvas de ruptura, los datos experimentales se ajustaron a los modelos de *Bed Depht Service Time* y *Empty bed contact time* para determinar parámetros de diseño de las columnas. Se realizaron estudios de adsorción a distintas concentraciones iniciales y se determinó la capacidad máxima de adsorción del lecho fijo en flujo continuo, la cual fue de 52.48 mg g^{-1}. Igualmente se realizaron estudios para evaluar la reutilización del biosorbente, una vez saturado, alcanzando una regeneración del 92% y hasta 17 ciclos de adsorción - desorción

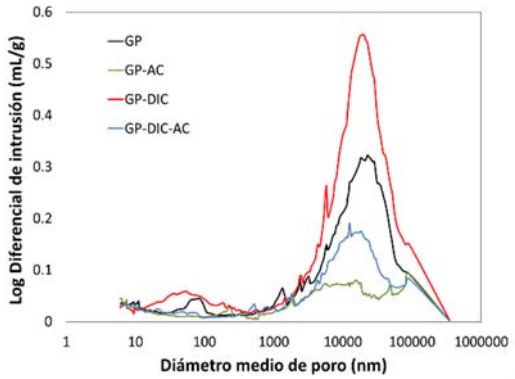

Fig. 1.- Distribución de tamaño de poro de los biosorbentes preparados

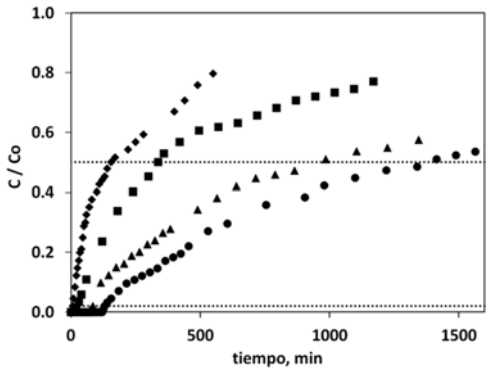

Fig. 2.- Curvas de ruptura para adsorción de Cu(II) a distintas alturas de lecho: ◆ 4 cm, ■ 6 cm, ▲ 12 cm, ● 4 cm

Agradecimientos

Luis A. Romero Cano agrade al CONACyT por el apoyo recibido a través de la beca No. 378307

Referencias

1. Fu, F., & Wang, Q. J. *Environ Manage*, Vol. 92 (2011), p. 407-418
2. Vijayaraghavan, K. & Balasubramanian, R. J. *Environ Manage*, Vol. 160 (2015), p. 283-296

Application of Thermally Exfoliated g-C_3N_4 for a Green Selective Photocatalytic Oxidation of 5-Hydroxymethyl-2-Furfural

Igor Krivtsov[a*], Elisa García-López[b], Giuseppe Marcì[b], Leonardo Palmisano[b], José R. García[a], Eva Díaz[c], Salvador Ordóñez[c]

[a]University of Oviedo-CINN, Department of Organic and Inorganic Chemistry, 33006, Julian Claveria 8, Oviedo, Spain.

[b]University of Palermo, DEIM, Viale delle Scienze Ed. 6, Palermo 90128, Italy.

[c]University of Oviedo, Department of Chemical Engineering and Environmental Technology, 33006, Julian Claveria 8, Oviedo, Spain.

**uo247495@uniovi.es*

Introduction

Catalytic valorization of biomass platform molecules is one of the major challenges in the field of sustainable chemistry. Conversion of 5-hydroxymethyl-2-furfural (HMF), a compound deriving from the oxidation of sugars, to 2,5-furandicarboxaldehyde (FDC) represents a significant interest for biopolymers production. A catalytic reaction allowing to obtain this molecule is known [1], however the studies describing photooxidation pathways of its production are almost absent [2].

Photocatalytic process benefits from almost free energy source, the solar radiation, and it does not demand the application of toxic oxidative agents. Therefore, we present the application of this environmentally benign method for UV-assisted photocatalytic oxidation of HMF to FDC in presence of thermally exfoliated graphitic carbon nitride (g-C_3N_4).

Materials and Methods

Carbon nitride photocatalysts were synthesized *via* thermal condensation of melamine in a closed crucible at 520 ^oC for 2 h. Thermal exfoliation procedure was carried out by treating the as-prepared g-C_3N_4 in air at 450, 500, 520, and 550 ^oC in a muffle furnace during 4 h, the samples were assigned correspondingly as g-C_3N_4, TE_450, TE_500, TE_520, and TE_550. The properties of the g-C_3N_4 were investigated using XRD, FTIR, SEM, TEM, DR UV, XPS and nitrogen physisorption methods. The performance of the prepared materials in the selective UV-assisted oxidation of HMF to FDC in an aqueous phase was evaluated.

Results and Discussion

Thermal exfoliation of g-C_3N_4 is a simple and powerful mean of enhancing its specific surface [3]. The dramatic change of this property occurred at treatment temperatures equal or higher than 500 ^oC (Fig. 1a). It is worth noting that this oxidative treatment did not result in the destruction of the g-C_3N_4 structure, which is confirmed by XRD and FTIR studies (Fig.1b). However, certain changes in the surface functionalization and electronic properties, revealed by the spectroscopic techniques, might have a significant impact on the reaction performance of the photocatalyst. The absorption edge of carbon nitride suffered a blue shift at the increased exfoliation temperature, thus the band gap energy changes from 2.8 eV for the as-prepared sample to 3.0 eV for that treated at 550 ^oC.

The photooxidation of HMF in the presence of the prepared photocatalysts is reported in Figure 2. Considering that the reaction was carried out in an aqueous solution, environment seldom favourable to selective photocatalytic processes, all the tested samples showed more than a satisfactory selectivity values that were higher than those previously reported for the case of TiO_2-assisted HMF photooxidation [2]. The lowest treatment temperature applied did not enhance SSA of carbon nitride, hence no increase of the activity is observed, but at the same time the selectivity towards FDC formation rises up to 35-40 % (Fig. 2). The HMF conversion rate steadily increased with the enhancement of SSA of the photocatalysts, while the selectivity reached its highest values (40-45 %), when carbon nitride was exfoliated at 520 °C (Fig. 2). The increase of the selectivity could be attributed to the elimination of the uncondensed species and surface NH_2-groups, which is obvious from the FTIR data, where a significant decrease in the relative intensity of N-H bonds vibration at 3160 cm^{-1} is observed (Fig. 1b).

The obtained results allow to conclude that graphitic carbon nitride is a promising candidate for selective photocatalytic oxidation reactions in an aqueous media considering that its selective performance is stable with time and superior to that observed for inorganic semiconductor photocatalysts [2].

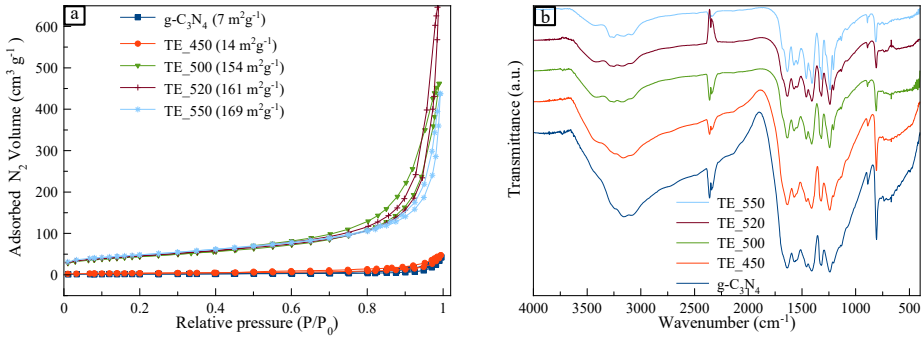

Fig. 1. (a) N_2 adsorption-desorption isotherms and (b) FTIR spectra of g-C_3N_4 samples.

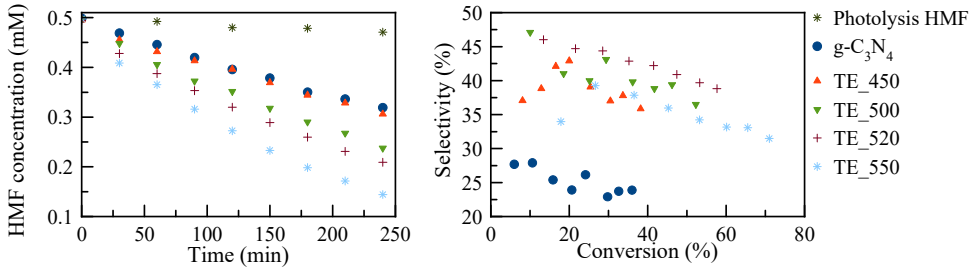

Fig. 2. Photocatalytic oxidation plots of HMF to FDC over g-C_3N_4.

Acknowledgements

We acknowledge the financial support from MINECO (MAT2013-40950-R).

References

1. J. Ma, Z. Du, J. Xu, Q. Chu, Y. Pang, ChemSusChem 4 (2011) 51–54.
2. S. Yurdakal, B.S. Tek, O. Alagoz, V. Augugliaro, V. Loddo, G. Palmisano, L. Palmisano, ACS Sustainable Chem. Eng. 1 (2013) 456−461.
3. F. Dong, Y. Li, Z. Wang, W-K. Ho, Appl. Surface Sci. 358 (2011) 393-403.

Waste-Based Adsorbents for a Cocktail of Psychiatric Pharmaceuticals

Vânia Calisto[a*], Guilaine Jaria[a], Carla Patrícia Silva[a], Catarina I.A. Ferreira[a], Marta Otero[b], Valdemar I. Esteves[a]

[a]Department of Chemistry/CESAM, University of Aveiro, Campus de Santiago, 3800-193 Aveiro, Portugal

[b]Department of Applied Chemistry and Physics, IMARENABIO, University of Léon, Campus de Vegazana, Léon, Spain

**vania.calisto@ua.pt*

Introduction

The presence of pharmaceuticals in water is an environmental emerging concern as the number of studies reporting their presence in surface, ground and even drinking waters continues to grow. The development of effective methodologies to be applied in Sewage Treatment Plants as tertiary treatment is a need to minimize their environmental impact. Adsorption has been considered as an interesting option due to its versatility and efficiency; yet, the high costs of commercially available activated carbons are a disadvantage, motivating the search for alternative adsorbents. In this context, this work uses primary pulp mill sludge as a new raw material for carbon production. Globally, the pulp and paper industry generate millions of tons of solid wastes per year. The use of these wastes as new resources constitutes an innovative management strategy, transforming a residue into an added value product.

This work evaluates the performance of pulp mill sludge-based carbon for the removal of 3 psychiatric pharmaceuticals from water (oxazepam (OXZ), carbamazepine (CBZ) and paroxetine (PAR)), under single and competitive conditions.

Materials and Methods

The paper mill sludge-based carbon (PS800-150-HCl) was produced by the controlled pyrolysis (at 800ºC, 10ºC/min, 150 min of residence time under N_2 atmosphere) of primary pulp mill sludge followed by an acid washing step. PS800-150-HCl and the corresponding raw material were characterized by means of elemental and proximate analyses, total organic carbon, specific surface area (N_2 isotherms) and FTIR. PS800-150-HCl was used in single, binary and ternary batch experiments in order to determine the adsorption kinetics and equilibrium isotherms of OXZ, CBZ and PAR (C_i=20 μmol L^{-1}).

Results and Discussion

For the three drugs, the equilibrium was quickly attained (with maximum equilibrium times of 15 min) even in binary and ternary systems.

Single component equilibrium data were adequately described by the Langmuir model, with maximum adsorption capacities of 64 ± 2, 70 ± 1 and 74 ± 1 μmol g^{-1} for PAR, OXZ and CBZ, respectively. Multi-component equilibrium data were also best fitted by the single component Langmuir isotherm. Single maximum adsorption capacities of each pharmaceutical decreased in the multi-component systems, suggesting the existence of competition between these pharmaceuticals; however, the decrease in the individual maximum adsorption capacities between single and multi-component

systems was not higher than 50% in any case. On the other hand, cumulative maximum adsorption capacities for binary and ternary systems were consistently higher than the single maximum adsorption capacities, indicating an actual increase in the total amount of pharmaceuticals adsorbed by the carbon (see Fig. 1).

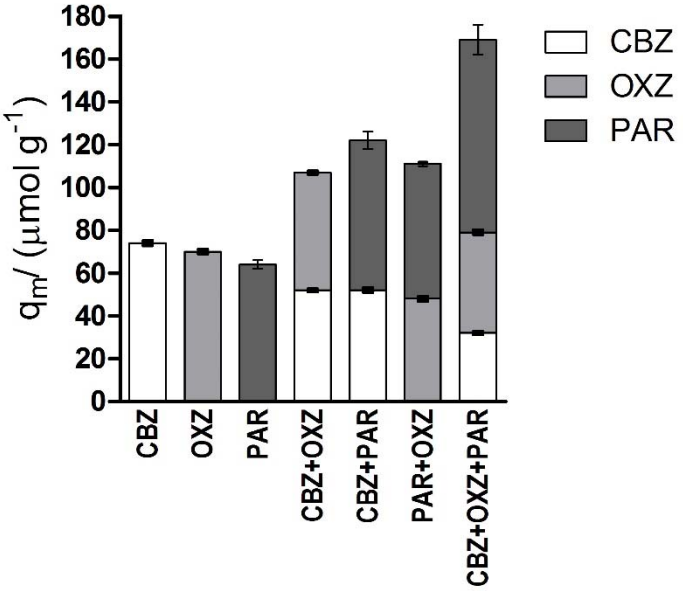

Fig. 1. Cumulative maximum adsorption capacities of PS800-150-HCl for single, binary and ternary systems.

Acknowledgements

Thanks are due, for the financial support to CESAM (UID/AMB/50017), to FCT/MEC through national funds, and the co-funding by the FEDER, within the PT2020 Partnership Agreement and Compete 2020. This work is funded by the research project PTDC-AAG-TEC-1762-2014 (FCT and Compete). Vânia Calisto thanks L'Oréal, UNESCO and FCT for funding through the "*Honor Medal for Women in Science 2014*". Catarina I.A. Ferreira and Vânia Calisto thank FCT for their PhD (SFRH/BD/88965/2012) and postdoctoral (SFRH/BPD/78645/2011) grants, respectively. The authors also thank the kind collaboration of *RAIZ – Instituto de Investigação da Floresta e do Papel*.

Effect of Nanostructure on the Supercapacitor Performance of Activated Carbon Xerogels Obtained from Hydrothermally Carbonized Glucose-Graphene Oxide Hybrids

M. Enterría*[a], F.J. Martín-Jimeno[b], F. Suárez-García[b], J.I. Paredes[b], M.F.R. Pereira[a], J.I. Martins[c], A. Martínez-Alonso[b], J. M. D. Tascón[b], J.L. Figueiredo[a]

[a] Laboratório de Processos de Separação e Reacção - Laboratório de Catálise e Materiais (LSRE-LCM), Departamento de Engenharia Química, Faculdade de Engenharia, Universidade do Porto. R. Dr Roberto Frias s/n, 4200-465 Porto, Portugal.

[b]Instituto Nacional del Carbón, INCAR-CSIC, Apartado 73, 33080, Oviedo, Spain.

[c]Departamento de Engenharia Química, Faculdade de Engenharia, Universidade do Porto. R. Dr Roberto Frias s/n, 4200-465, Porto, Portugal.

**menterria@fe.up.pt*

Introduction

The intrinsic principle of charge storage in supercapacitors (SC) consists of electrostatic adsorption of electrolyte ions on the electrode surface and, consequently, the surface area is the main factor influencing the capacitance. However, suitable nanostructure, enhancing both electrolyte diffusion and electronic conduction, has also demonstrated to determine the electrochemical performance of SC electrodes. A suitable electrode material gathering all these features would consist on coating the highly conductive surface of graphene sheets with a very thin layer of porous carbon. In the present work, activated carbon xerogels with a specific cellular morphology were obtained from hydrothermally carbonized glucose-graphene oxide (GO) hybrids. The effect of the chemical activation (using KOH) on the nanometer-scale morphology and the porous texture of the resulting carbon materials was investigated and correlated with their electrochemical behaviour.

Materials and Methods

The activated carbon xerogels were prepared by a recently reported procedure that makes use of GO sheets as morphology-directing agents in the hydrothermal carbonization of glucose, affording hydrothermal carbon xerogels that are then chemically activated with KOH [1]. Xerogels were denoted as Kx_Ty, were x is the proportion of activating agent (1 or 4) and y refers to the temperature of activation (700 or 800 ºC, T7 or T8, respectively). A control sample, prepared in absence of GO and fixing the activation parameters, was named as Glu_ K1_T8. The electrode preparation and the electrochemical cell assembly were also reported in a previous work [2]. The electrochemical characterization was performed on a PGZ 402 Voltalab potentiostat (Radiometer Analytical).

Results and Discussion

The xerogels activated with lower KOH amounts (K1 series) showed higher surface areas (1400-1500 m^2/g) and mesopore volumes (0.16-0.30 cm^3/g) than those activated at higher KOH proportions (K4 series). Curiously, Glu_K1_T8 sample presented very low mesopore volume (0.03 cm^3/g). Larger differences were observed in the morphological

features: K1 xerogels exhibited a cellular morphology, comprising a high density of rounded voids (~200 and 800 nm) enclosed by very thin walls (15 nm thick, Fig. 1a). In contrast, K4 xerogels incorporated much larger voids between thicker and loosely connected platelet-like walls (Fig. 1b). On the other hand, the hydrothermal carbonization of glucose by exclusion of GO from the production process led to 1-2 µm sized spheres, instead of a xerogel structure (Fig. 1c). Hence, the presence of GO sheets during the hydrothermal carbonization, as well as the utilization of low KOH proportions in the activation step, seem to be critical parameters in achieving the peculiar cellular nanomorphology observed for K1 samples.

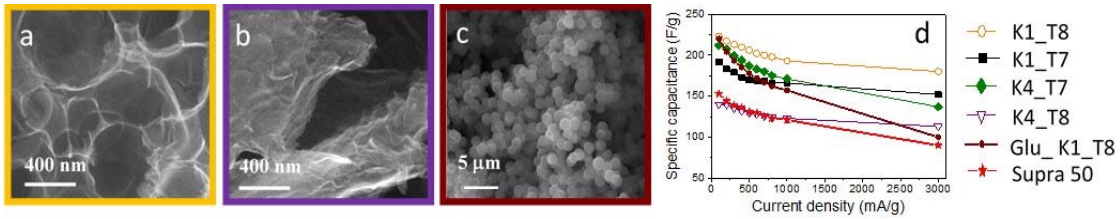

Fig. 1. FE-SEM images of samples a) K1_T8, b) K4_T8 and c) Glu_ K1_T8. d) Evolution of the specific capacitance with current load by charging-discharging the electrodes up to 0.8 V from 100 to 3000 mA/g.

The electrochemical performance of the prepared xerogels was tested in a two-electrode cell. The performance of K4_T7 and Glu_K1_T8 deteriorated significantly with increasing current density, while K4_T8 showed low capacitance values in the entire range of studied current densities. In contrast, K1_T8 presented high capacitance values and retentions when charged from 100 to 3000 mA/g (Fig. 1d). For comparison purposes, an electrode made from a commercial activated carbon (Norit DLC Supra 50) was also tested in the same set-up. Despite its much higher surface area (2090 m^2/g), the commercial activated carbon exhibited much lower capacitance and capacitance retention than the prepared xerogels. The key role played by the nanostructural features of K1_T8 xerogel on its electrochemical performance was therefore highlighted. Thus, the presence of very thin and highly accessible porous carbon walls enhancing diffusion, together with a boosted electronic conduction provided by graphene sheets, address the performance limitations of conventional SC electrodes derived from purely microporous activated carbons.

Acknowledgements

This work was financially supported by Project POCI-01-0145-FEDER-006984 – Associated Laboratory LSRE-LCM funded by FEDER funds through COMPETE2020 - Programa Operacional Competitividade e Internacionalização (POCI) – and by national funds through FCT - Fundação para a Ciência e a Tecnologia. Partial funding of this work by the Spanish MINECO and the European Regional Development Fund (projects MAT2015-69844-R and MAT2012-34011) is also gratefully acknowledged.

References

1. F.J. Martín-Jimeno, F. Suárez-García, J.I. Paredes, A. Martínez-Alonso, J.M.D. Tascón, Carbon. 81 (2015) 137-147.
2. M. Enterría, M.F.R. Pereira, J.I. Martins, J.L. Figueiredo, Carbon. 95 (2015) 72-83.

Chemical Modification of Venezuelan Delayed Petroleum Coke: Effect on the Development of Porosity

Hilmar Guzmán[a], Raquel García-González[a]*, José B. Parra[a], Luis F. D'Elia Camacho[b], Conchi Ania[a]

[a]ADPOR Group, Instituto Nacional del Carbón (INCAR–CSIC) 33011, Oviedo, España.

[b]Petróleos de Venezuela (PDVSA)–Intevep, Gerencia General de Refinación e Industrialización, Gerencia Departamental de Investigación Estratégica, Apartado 76343, Caracas 1070-A, República Bolivariana de Venezuela.

**garcia.raquel@incar.csic.es*

Introduction

Venezuela has one of the largest oil deposits in the world, characterise by high contents of asphaltenes, sulphur, metals and others. The upgrading of heavy oil fractions (ca. thermal cracking), to produce lighter fractions, involves the well-known delayed coking process, which produces a carbon-rich solid (petcoke). This solid, known as delayed petroleum coke (DPC), mainly consists in carbon with hydrogen, nitrogen, sulphur, oxygen, and other trace elements. Venezuelan petcoke production is about 20,000 tonnes per day in 2015. Thus, Venezuelan delayed petcoke represents a large and inexpensive resource with a great potential in a variety of applications. Depending on the selected precursor, the preparation of nanoporous carbons usually involves various steps (i.e., oxidation, pyrolysis, activation), and the porous texture of the final products is strongly conditioned by the pre-treatments (oxidation and pyrolysis) carried out on the precursor [1-3]. For instance, coals with thermoplastic properties must be previously oxidised in order to reduce or eliminate the plastic behaviour, and ensure a char with suitable porous development during pyrolysis step [3]. Elimination of the plastic behaviour in the preparation of activated carbons from anthracites is not necessary, anthracites has a harder structural network leading to materials with restricted surface areas [2,3]. Due to the DPC characteristics, oxidations may be necessary. The aim is to fabricate high value carbons with a well-developed pore structure using Venezuelan delayed coke as precursor; herein it is reported the effect of chemical and thermochemical modifications on the composition and textural properties of obtained petcoke-derived materials.

Materials and Methods

DPC was collected from the one of the oil upgrading facilities located in Venezuela. The as-received material was oxidised at 325 ^{0}C in an oven with a forced air circulation for different periods of time. In order to compare different activating procedures, materials were further pyrolysed and/or activated to develop a porous structure. Pyrolysis was performed under nitrogen up to 900 ^{0}C. Physical activation was carried out under CO_2 (10 mL/min, 900 ^{0}C) using different activation times to obtain variable burn-off degrees. Furthermore, chemical activation was also performed using K_2CO_3 and KOH (in N_2, 300 mL/min) at various temperatures, coke:activating agent ratios and impregnation protocols (wet and dry). Textural characterisation of obtained materials was carried out by means of gas adsorption-desorption isotherms (i.e., N_2 and CO_2 at

-196 and 0 ^{0}C, respectively) on outgassed samples (vacuum at 120 ^{0}C for overnight). Surface areas and total pore volumes were calculated from gas adsorption isotherms. Oxygen content was determined by difference from elemental analysis.

Results and Discussion

Selected characteristics of DPC used in this study are presented in Table 1; such characteristics are expected to influence DPC reactivity towards gasification and activation reactions taking place during porous generation. Also, it has been reported that oxidation produces important transformations in the composition and textural properties of bituminous coals [1]. Therefore, an oxidation treatment was applied to pristine DPC and the effect on the development of porosity, using various activation procedures, was explored.

Table 1 shows that as oxidation progressed, oxygen content increased significantly, reaching values around 27 wt. % after 96 h. Data corresponding to pyrolysed delayed petroleum coke (DPC char) are also included for comparison. The oxidation also led to a slight opening of the porosity, being more pronounced for the samples oxidized for 48 and 96 hours. Indeed, surface areas values obtained from the analysis of the N_2 adsorption isotherms (S_{BET}-N_2) slightly increased upon oxidation, showing its positive effect on the evolution of the porosity. This effect is much more remarkable in the CO_2-derived surface area (S_{DR}-CO_2), with rather constant values after 72-96 h. The oxidation also had a strong influence on the porosity of the corresponding chars, leading to S_{BET} values ranging from 4 to 7 m^2/g after the pyrolysis (not shown in Table 1). Despite of the modest values, this is most outstanding since it confirms the creation of porosity during the oxidation step. As a result, a noteworthy effect on physical (CO_2) and chemical (KOH or K_2CO_3) activations of DPC precursors may be expected.

Table 1. Selected physicochemical characteristics of the as-received and oxidised delayed petroleum cokes

Sample	Oxygen (wt.%)	Surface area, N_2, S_{BET} (m^2/g)	Pore Volume, N_2 (cm^3/g)	Surface area, CO_2, S_{DR} (m^2/g)
Delayed petroleum coke (DPC)	0.93	0.3	0.001	149
DPC char	NA	2	0.001	9
DPC-oxidized 12 hours	10.23	0.4	0.001	168
DPC-oxidized 24hours	15.80	1	0.001	206
DPC-oxidized 48 hours	20.82	2	0.001	220
DPC-oxidized 72 hours	22.90	2	0.001	221
DPC-oxidized 96 hours	27.30	1	0.001	220

NA- Not available

Acknowledgements

Authors thank PDVSA-Intevep for the permission of publishing this contribution.

References

1. H. Marsh, F. Rodriguez-Reinoso, Activated Carbon, Elsevier, New York, 2006.
2. B. Ruiz, J.B. Parra, T. Alvarez, A.B. Fuertes, J.A. Pajares, J.J. Pis, Appl. Catal. A98 (1993) 115.
3. B. Ruiz, J.B. Parra, J.A. Pajares, J.J. Pis, J. Anal. Appl. Pyrol. 58–59 (2001) 873–886.

Caracterización Textural de MOFs mediante Combinación de Adsorción de Gases a Temperatura Criogénica y Calorimetría de Inmersión

Beatriz Saavedra Guillem,[a] Carlos Cuadrado Collados,[a] Cintia K. Rojas Mayorga,[a] Mirian E. Casco,[a] Enrique V. Ramos Fernández[a], Joaquín Silvestre Albero[a,*]
[a]Laboratorio de materiales avanzados, Departamento de Química Inorgánica, Universidad de Alicante. Apartado 99; E-03080, España.
** joaquin.silvestre@ua.es*

Introducción

Los materiales híbridos metalo-orgánicos MOFs (*metal-organic frameworks*, en inglés) son una nueva y prometedora clase de sólidos porosos que han despertado un creciente interés en el mundo de la nanotecnología. Los MOFs son materiales híbridos formados por unidades metálicas (átomos o agregados metálicos) unidos entre sí mediante ligandos orgánicos, conformando en su conjunto estructuras cristalinas bien definidas y ordenadas. Su principal ventaja con respecto a otros sólidos adsorbentes como el carbón activado o las zeolitas es su versatilidad para modificar la estructura de su red cristalina mediante la combinación apropiada entre el bloque orgánico e inorgánico, obteniéndose un grado de porosidad y una química superficial ajustable e idónea dependiendo de su aplicación final [1]. Uno de los aspectos más importantes para comprender el comportamiento de estos materiales en una aplicación determinada es la caracterización de su estructura porosa. El tamaño, forma y volumen de esas cavidades va a condicionar su comportamiento cuando se aplique en procesos como el intercambio iónico, separación y almacenamiento de gases, administración de fármacos y catálisis heterogénea, entre otros [1,2].

Tradicionalmente la caracterización textural se ha evaluado mediante la adsorción física de una molécula sonda como N_2 a temperatura criogénica (77 K). Las isotermas de adsorción de esta molécula permiten cuantificar parámetros texturales como la superficie específica, volumen de microporos y volumen total de poros. Paralelamente se han propuesto nuevas moléculas sonda para complementar la caracterización textural como son el CO_2 a 273K, el cual permite determinar la porosidad más estrecha y el Ar a 87 K, dado que no presenta momento cuadrupolar [3]. A partir de estos métodos experimentales se han desarrollado modelos matemáticos para cuantificar y estimar la distribución y tamaños de poro (DFT) en carbones y zeolitas.

Una técnica experimental alternativa también utilizada en la caracterización de sólidos porosos es la calorimetría de inmersión. Esta técnica permite estimar el calor de inmersión o mojado de sólidos porosos en contacto con disolventes de diferentes diámetros cinéticos. La selección de moléculas sonda de diferente tamaño permite evaluar la distribución de tamaño de poros del material, siempre y cuando no haya interacciones de tipo específicas. En base a estos antecedentes, el objetivo del presente trabajo es evaluar la caracterización textural de una serie de MOFs, ampliamente conocidos en la literatura, mediante combinación de las técnicas mencionadas anteriormente.

Materiales y métodos

Se han seleccionado cuatro MOFs diferentes tanto comerciales como sintetizados en el grupo LMA (MIL-100, UiO-66, ZIF-8 y HKUST-1). Las isotermas de adsorción de N_2 a 77 K, Ar a 77 K y CO_2 a 273 K, se llevaron a cabo en un equipo manométrico. Las medidas de calorimetría de inmersión, se llevaron a cabo a 30.5ºC usando un calorímetro Setaram Tian-Calvet C80D y empleando como disolventes diclorometano (0. 33nm), n-Hexano (0.43 nm), 2-Metilpentano (0.50 nm), α-Pineno (0.70 nm) y 1,3,5-Triisopropilbenceno (0.85 nm).

Resultados y discusión

Los resultados comparados de adsorción de N_2 y Ar a 77 K en estos materiales MOFs demuestran que a bajas presiones relativas la adsorción de N_2 es superior a Ar debido a la presencia del momento cuadrupolar N_2. Aunque la estimación de la superficie aparente para estas dos moléculas da resultados bastante coincidentes en algunos MOFs, la presencia de interacciones específicas con los centros metálicos expuestos (p. ej. HKUST-1) y la presencia de alteraciones estructurales (fenómenos de apertura de ventana) generan incertidumbre en la cuantificación de estos parámetros. Como se aprecia en la figura 1, el material ZIF-8 presenta diferentes saltos en la isoterma de N_2, atribuidos a la presencia de movimientos estructurales del ligando orgánico, que dificultan la aplicación de teorías como BET o Dubinin-Radushkevich [4]. La textura porosa en términos de tamaño de ventana ha podido ser confirmada mediante los estudios de calorimetría de inmersión.

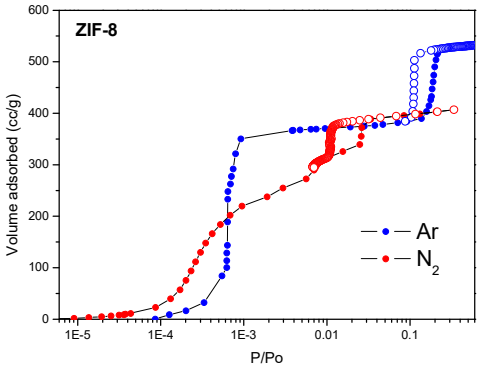

Fig. 1. Isotermas de N_2 y Ar (ZIF-8), en escala logarítmica

Agradecimientos

Los autores de este trabajo agradecen la ayuda económica del MINECO a través del proyecto: MAT2013-45008-p.

Bibliografía

1. Furukawa, H., Cordova, K.E., O´Keeffe, M., Yagui, O.M. *Science* **2013**, 341, DOI: 10.1126/science.1230444.
2. Long, J. R. *Chem. Sci.* **2014**, *5*, 32–51.
3. Silvestre-Albero, J., Silvestre-Albero, A., Rodriguez-Reinoso, F., Thommes, M. *Carbon 50* **2012**, 3128-3133
4. Casco, M.E., Cheng, Y.Q., Daemen, L.L., Fairen-Jimenez, D., Ramos-Fernandez, E.V., Ramirez-Cuesta, A.J., Silvestre-Albero, J. *Chem. Commun.* **2016**, 52, 3639-3642

Evaluation of the Optimum Activated Carbon Properties for a Sorption Cooler using a Combined Simulation and Experimental Methodology

J. P. B. Mota[a,*], R. P. P. L. Ribeiro[a], I. A. A. C. Esteves[a], F. A. Teixeira[a], D. Martins[b], M. B. C. Branco[b], T. Tirolien[c], J. Barreto[d], G. Bonfait[d]

[a]LAQV-REQUIMTE, Department of Chemistry, Faculty of Science and Technology, Universidade NOVA de Lisboa, 2829-516 Caparica, Portugal.

[b]Active Space Technologies S.A., Parque Industrial de Taveiro, Lote 12, 3045-508 Coimbra, Portugal.

[c]European Space Agency, ESTEC, E0053A, 2200 AG Noordwijk, The Netherlands

[d]LIBPhys-UNL – Department of Physics, Faculdade de Ciências e Tecnologia da Universidade Nova de Lisboa, 2829-516 Caparica, Portugal.

** pmota@fct.unl.pt*

Introduction

Cryogenic environments are necessary on-board spacecrafts for diverse purposes. For example, the signal-to-noise ratio of several detectors (e.g. IR detectors) or microelectronics devices (e.g. low-noise amplifiers) benefit from being cooled down to cryogenic temperatures since this way the noise production can be mitigated.

Nowadays, the Stirling or Pulse tube cryocoolers are widely used for this type of applications although the commonly used mechanical compressors bring undesired vibrations that can be harmful for diverse equipment.

Thermal compressors i.e. sorption cooling allows providing low temperatures without the inherent vibrations and electromagnetic interference of mechanical compressors. The gas (low pressure) is stored by cooling a sorbent bed and subsequently released at high pressure by heating the adsorbent. Several adsorbent beds work cyclically to allow the cooler to deliver continued refrigeration, i.e. while some compressor elements are desorbing the gas at high pressure (due to the temperature raise), other part is adsorbing the low pressure gas by cooling the sorbent. Therefore, the properties of the chosen adsorbent are of paramount importance for the successful and efficient operation of the cooler.

In this work the adsorption of neon and nitrogen on activated carbons were studied with the objective of developing a sorption cooler. For this purpose, experimental measurements and molecular simulation techniques were combined to determine the properties of the optimum activated carbon to be employed in a sorption cooler for the desired temperature range.

Acknowledgements

Financial support from the European Space Agency is gratefully acknowledged.

Rui P. P. L. Ribeiro and Isabel A. A. C. Esteves acknowledge FCT/MCTES for financial support through grant SFRH/BPD/103533/2014 and FCT Investigator contract IF/01016/2014, respectively.

This work was partially supported by the Associate Laboratory for Green Chemistry LAQV which is financed by national funds from FCT/MEC (UID/QUI/50006/2013) and co-financed by the ERDF under the PT2020 Partnership Agreement (POCI-01-0145-FEDER - 007265).

COMUNICAÇÕES EM POSTER

Underlying Adsorption Mechanisms of Water in Hydrophobic and Hydrophilic Zeolite Imidazolate Frameworks: ZIF-71 and ZIF-90

Sofía Calero[a], Paula Gómez-Álvarez[a,*]
[a]*Department of Physical, Chemical and Natural Systems, Universidad Pablo de Olavide, ES-41013 Seville, Spain*
** pgomalv1@upo.es*

Introduction

The hydration of porous materials is relevant for separation, transport, and catalysis purposes, among others. In this respect, zeolitic imidazolate frameworks (ZIFs) have received considerable attention since they have shown remarkable resistance to water [1] as well as to other organic solvents. Studies on water adsorption in ZIFs are however relatively scarce and primarily focused on the effect of the host composition and porosity on their hydrophobic or hydrophilic nature. In this work,[2] we explore by using molecular simulation the microscopic behavior governing the water adsorption process in ZIF-71 and ZIF-90, which are experimentally known structures reported as hydrophobic and hydrophilic, respectively. Although the polar functional group in ZIF-90 leads to adsorption in the gas phase, a following rapid cage filling occurs as in ZIF-71. A consistent description of this phenomenon is provided in terms of hydrogen bonding formation between water molecules. In the low-coverage regime, the preferential adsorption sites are identified and interactions with water comprehensively characterized.

Materials and Methods

We conducted Monte Carlo simulations using previously validated models and force fields [3,4] and RASPA code [5] to compute the adsorption performance of water in both ZIFs at room temperature.

Results and Discussion

Although the radial distribution functions reveal that the interaction of water molecules with the chlorine functional group *Cl* in ZIF-71 is remarkable in relation to the remaining framework atoms, it is weakly polar and water adsorption in ZIF-71 occurs in the liquid phase (hydrophobic nature). In ZIF-90, the aldehyde oxygen atom O_{ald} was distinctly found to be the strongest interacting site surely involving hydrogen bonds with water molecules, and thus responsible for the water intrusion below the bulk saturation pressure (hydrophilic nature). The affinity of water to these preferential sites in each ZIF, *Cl* and O_{ald}, was quantitatively evaluated in terms of the adsorption energy and the average minimum distances in the low-coverage regime from NVT calculations. We found the heat of adsorption to be 16 kJ·mol^{-1} in ZIF-71 and 36 kJ·mol^{-1} in ZIF-90, approximately, and the distance values from a single water molecule to *Cl* and O_{ald} sites of about 3.7 Å and 3 Å, respectively. The abrupt condensation transition observed in the water adsorption isotherms in both ZIFs was demonstrated, by means of energetic and structural factors, a consequence of rapid water clustering even in ZIF-90. Instead of nucleation around the O_{ald} high-energy sites, self-association of water dominates the

adsorption process, as in hydrophobic materials such as ZIF-71 (Figure 1). This suggests an amphiphilic more than hydrophilic character of ZIF-90. Indeed, the adsorption energy in the dilute regime was found to be even slightly lower than the heat of vaporization of water and significantly decreases with water uptake. In the highly hydrated structures, the hydrogen-bonded properties of water reveal the absence of the tetrahedral ordering typical of the bulk in both ZIFs and the formation of higher-order water clusters in ZIF-71 despite its lower accessible space in comparison with ZIF-90 (Table 1). This is ascribed to the weaker interactions with the pore surface, which enhances hydrogen bonding formation between water molecules.

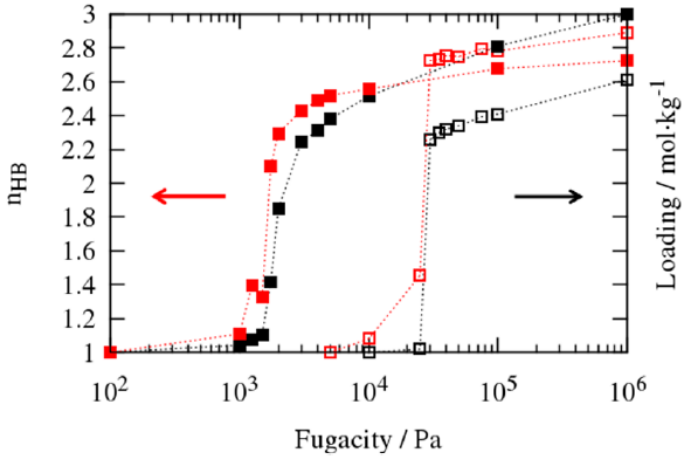

Fig. 1. Average number of hydrogen bonds per molecule n_{HB} (in red) together with the water loading (in black) as a function of fugacity in ZIF-71 (empty squares) and ZIF-90 (full squares)

Table 1. Hydrogen-bonded statistics (fraction of associated molecules f_{ass}, of molecules engaged in *i* bonds f_i, and average number of hydrogen bonds per molecule n_{HB}) of bulk water and of water adsorbed in ZIF-71 and ZIF-90 at 10^6 Pa

	f_{ass}	f_1	f_2	f_3	f_4	f_5	n_{HB}
Bulk	0.99	3.9	17.4	38.3	38.0	2.4	3.2
ZIF-71	0.97	7.1	23.6	40.9	25.6	2.7	2.9
ZIF-90	0.98	7.8	30.9	43.6	16.4	1.25	2.7

Acknowledgements

This work is supported by the European Research Council through an ERC Starting Grant (ERC2011-StG-279520-RASPA), by the MINECO (CTQ2013-48396-P) and by the Andalucia Region (FQM-1851)

References

1. K. S. Park, Z. Ni, A. P. Cote, J. Y. Choi, R. D. Huang, F. J. Uribe-Romo, H. K. Chae, M. O'Keeffe, O. M. Yaghi, *Proc. Natl. Acad. Sci. U.S.A.* 103 (2006) 10186-10191.
2. S. Calero, P. Gómez-Álvarez, *J. Phys. Chem. C* 119 (2015) 23774–23780.
3. S. A. Rick, *J. Chem. Phys.* 120 (2004) 6085-6093.
4. K. Zhang, A. Nalaparaju, Y. Chen, J. Jiang, *Phys. Chem. Chem. Phys*. 16 (2014) 9643-9655.
5. D. Dubbeldam, S. Calero, E. Donald, R. Snurr, *Mol. Simulat.* 42 (2015) 81-101.

Separation of a H_2, CH_4, CO and CO_2 Mixture with BPL Activated Carbon by PSA

J. A. Delgado[a], V. I. Águeda[a], M. A. Uguina[a], P. Brea[a,*]
[a] *Departamento de Ingeniería Química, Facultad de Ciencias Químicas, Universidad Complutense de Madrid, Avenida Complutense S/N,Madrid, Spain*
** pbprieto@ucm.es*

Introduction

Hydrogen is obtained from the methane steam reforming (SMR) nowadays. Methane and water react resulting in a gas mixture were the majority compound is hydrogen, mixed with carbon dioxide, carbon monoxide, methane, nitrogen and water as main impurities. The adsorption technology based on pressure swing adsorption (PSA) appears as one of the most efficient techniques, resulting in high hydrogen purity and low energy consumption. Activated carbon is one of the most extended adsorbents used for hydrogen purification because it is capable to remove carbon dioxide from the mixture more easily than other adsorbents. In this work, the purification of hydrogen from a gas mixture containing H_2, CH_4, CO and CO_2 has been studied in a cyclic PSA process using BPL activated carbon as adsorbent. A model based on conservation equations has been developed in order to describe the adsorption dynamics in this process.

Materials and Methods

Pure component isotherms of H_2, CO, CO_2 and CH_4 were obtained in a volumetric equipment (Micromeritics ASAP2000). Breakthrough experiments at a total pressure of 3 bar were performed on a fixed bed. The adsorbate concentration was measured at the bed exit with a mass spectrometer detector. The adsorption capacity has been calculated from the mass balance and pure component isotherms have been obtained. Dynamic and volumetric isotherms have been compared. Breakthrough curves have been fitted onto a dynamic adsorption model [1] in order to obtain the mass transfer coeficients of each gas in the adsorbent. Multicomponent gas mixture (H_2 75,89%, CO 3,03%, CH_4 4,01% and CO_2 17,07%) adsorption experiments have been carried out at three different temperatures. Pure component isotherms and the mass transfer coeficients were used to reproduce the experimental breakthrough curves.

Finally, experimental Skartstrom PSA cycles in a BPL activated carbon fixed bed have been done. The influence of different variables (high cycle pressure, step time, gas velocity) over the amount of hydrogen produced, hydrogen purity and hydrogen recovery have been studied.

Results and Discussion

Breakthrough curve compared with the equilibrium isotherm obtained in the volumetric equipment have been compared in Figure 1.a. Figure 1 b presents the experimental and simulated CO_2 breakthrough curves at different partial pressures. Simulations have proven that in the studied experimental conditions mass transfer has no influence on the shape of the breakthrough curve.

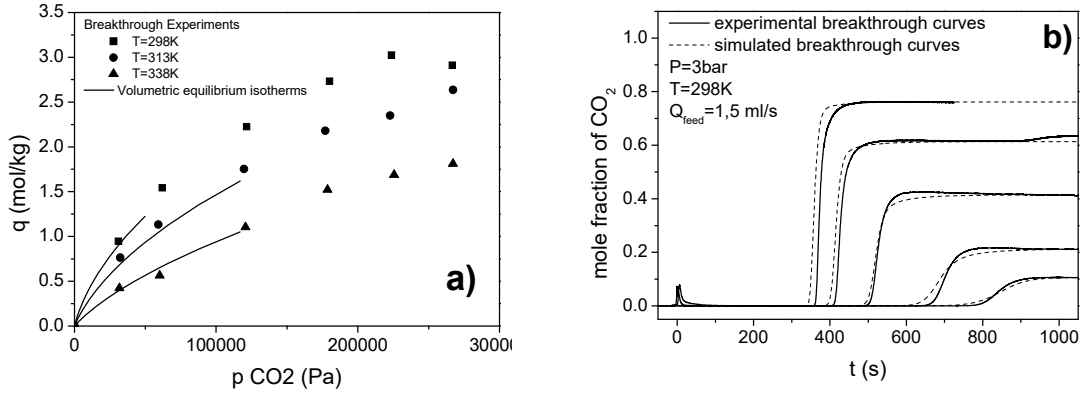

Fig. 1. Adsorption of CO2 onto BPL activated carbon. a) Equilibrium isotherms, b) experimental and simulated breakthrough curves

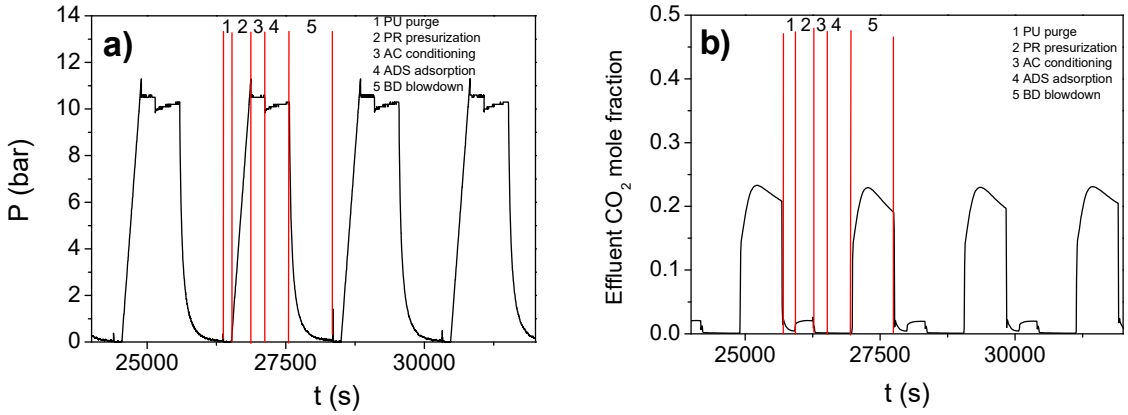

Fig. 2. Skarstrom PSA adsorption cycles. a) pressure, b) CO_2 concentration in the effluent

Skarstrom cycles have been performed with a BPL activated carbon fixed bed and the influence of the operation parameters as the high pressure, depresurization time, presurization time and feed flowrate have on the hydrogen purity in the light product, hydrogen recovery and hydrogen productivity have been studied. Hydrogen purity higher than 99,5% has been achieved at the cyclic steady state after 30 cycles.

Acknowledgements

Financial support from the ‘‘Ministerio de Ciencia e Innovación’’ of Spain through project CTQ2009-08838 (PPQ) is gratefully acknowledged.

References

1. Adsorption and diffusion of H_2, CO, CH_4 and CO_2 in BPL activated carbon and13X zeolite: Evaluation of performance in pressure swing adsorption hydrogen purification by simulation. J. A. Delgado. V. I. Águeda, M. A. Uguina, J. L. Sotelo, P. Brea and C. Grande. *Ind. Eng. Chem. Res.*, **2014**, *53* (40), pp 15414–15426.

Molecular Simulation and Spectroscopic Studies (FT-IR, Raman, ^{29}Si NMR) of Hybrid-Xerogels using Density Functional Theory

Isaura Ospino[a,*], Asunción Luquin[a,*], Jesús Echeverría[a], Mariano Laguna[b], Julian Garrido[a]

[a] *Institute for Advanced Materials (InaMat)-Public University of Navarre, Pamplona, Campus Arrosadia-31006 Pamplona, Spain.*

[b] *Instituto de Síntesis Química y Catálisis Homogénea (ISQCH)-Universidad de Zaragoza, Pedro Cerbuna-50009, Zaragoza, Spain.*

**isauraospino@yahoo.com.mx; a.luquin@unavarra.es*

Introduction

Recently, quantum chemistry studies have helped to advance significantly in the understanding of amorphous materials properties. In general, the computational modeling of amorphous materials using periodic supercell models is usually considered as the most relevant approach [1]. Nevertheless, a study carried out has shown that the experimental characteristic data are well reproduced and nearly identical for molecular models [2]. In order to achieve a better understanding of structure formation in xerogels and thus be able to better influence the properties of these materials, which is the key for most of the applications of this amorphous material, it is of great importance to get insight into the xerogel structure. In this study, we have chosen the molecular approach to model the hybrid-xerogel surface structure using the density functional theory (DFT) on a well-studied silicate-xerogel proposed by some of us in the past [3]. The basic aim of this work is therefore to understand the structure of the hybrid-xerogel. The evolution of cluster and the effects in the structure of the organic functional groups incorporated on the host structure network are investigated using a theoretical spectroscopic study.

Materials and Methods

For all calculations, with Gaussian 03, we have used the PBEPBE density functional [4] and 6–31G(d,p) basis set for all atoms [5]. Shieldings are calculated using the GIAO method and 6–311+G(2d,p) basis set for all atoms [6].

Results and Discussion

The most commonly encountered picture about the sol-gel process is that of an SN_2 like mechanism with a pentacoordinated silicon atom in the transition state and where ring closure reactions are possible and preferred. In addition, the most stable species in the following reaction cascade are probably a cyclic tetramer, the hexagonal prism, and the cubic octamer, which is assumed to be the predominant starting point of particle growth [7]. In this work, a cyclic tetramer was our starting point to perform a cage model of hybrid xerogels of methyltriethoxysilane (MTEOS) and tetraethoxysilane (TEOS). These models were optimized for configuration: 0% of MTEOS (J4-0), 30% of MTEOS (J4-3), 70% of MTEOS (J4-70) (Fig. 1).

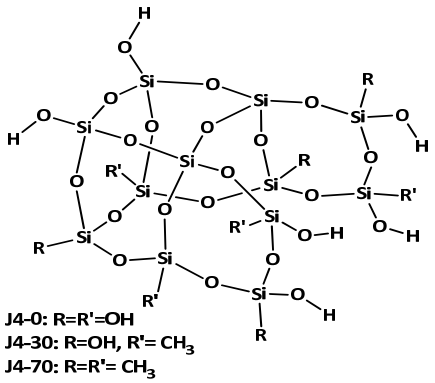

Fig. 1. Different Cage models

We observed that methyl groups incorporated on the cage network of the cage model give structures 0.15 kcal/mol less stable (Table 1). This is related with the experimental observations that show that the gelation time exponentially increases when the organic functional groups are incorporated [3].

Table 1. Optimized energy

Cage-Model	Nº of Q, T	kcal/mol (x10⁶)
J4-0	$4Q_2, 6Q_3, 2Q_4$	-3.65
J4-30	$2Q_2, 4Q_3, 2Q_4, 2T_2, 2T_3$	-3.56
J4-70	$3Q_3, 2Q_4, 4T_2, 3T_3$	-3.47
J4-100	$2T_2, 10T_3$	-3.38

The structural band around 1090 cm^{-1} associated with siloxane bonds (Si–O) in the IR spectra shifted to lower wavenumbers, the same behavior is observed both in experimental and theoretical results (Fig. 2a). Gas phase optimizations give structures close enough to experiment for reliable NMR shielding calculations (Fig 2b). A transition from Q_n to T_n signals detected in the ^{29}Si NMR spectra, show an reliable shift predictions can thus be made using gas phase geometries and gas phase shielding calculations for comparison with solid state NMR.

Finally, the whole set of results discussed shows that, by combining spectroscopic measurements with appropriate DFT-calculations on a cluster model, detailed interpretation of IR and ^{29}Si NMR can be attained with nearly accuracy.

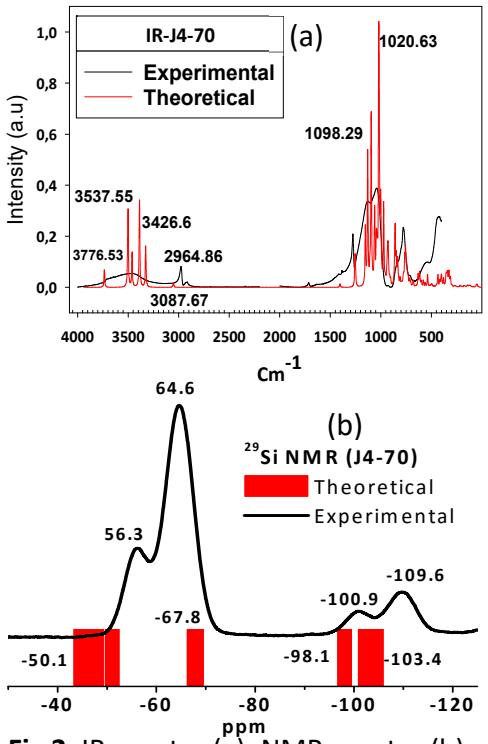

Fig 2. IR spectre (a); NMR spectre (b) of J4-70 as example.

Acknowledgements

Isaura Ospino is thankful to the Public University of Navarre for Postdoc-fellowships. The authors also thank the Galicia Supercomputing Technological Center (CESGA-CSIC), Spain, for the computer resources provided.

References

1. a) A. Rimola, M. Sodupe, S. Tosoni, B. Civalleri, and P. Ugliengo. *Langmuir*. 22(2006), 6593-6604; b) K. H. Lim, O. Zakharieva, A. M. Shor, N. Rösch. *Chem. Phys. Lett*. 444(2007), 280-286; c) H. Henschel, A. M. Schneider and M. H. Prosenc. *Chem. Mater*. (22)2010, 5105-5111
2. a) Blanc, F.; Basset, J.-M.; Copéret, C.; Sinha, A.; Tonzetich, Z. J.; Schrock, R. R.; Solans-Monfort, X.; Clot, E.; Eisenstein, O.; Lesage, A.; Emsley, L. *J. Am. Chem. Soc*. 2008, 130, 5886-5900; b) I. Del Rosal, I. C. Gerber, R. Poteau, and L. Maron. *J. Phys. Chem. A*. 114(2010), 6322-6330
3. a) X. Rios, P. Moriones, J. C. Echeverría, A. Luquín, M. Laguna and J. J. Garrido. *Adsorption*. 17 (2011), 583-593; b) X. Rios, P. Moriones, J. C. Echeverría, A. Luquín, M. Laguna and J. J. Garrido. *Materials Chemistry and Physics* 141 (2013), 166-174
4. J. P. Perdew, K. Burke, and M. Ernzerhof, *Phys. Rev. Lett*. 77(1996), 3865-3868
5. P. C. Hariharan and J. A. Pople, *Theor. Chim. Acta*. 28 (1973), 213
6. a) R. Ditchfied, Mol. Phys., 27(1974), 789-807; b) R. Krishnan, J.S. Binkley, R. Seeger and J.A. Pople, *J. Chem. Phys*. 72(1980), 650
7. a) Hench, L. L.; West, J. K. *Chem. Rev*. 90(1990), 33–72; b) Schaack, B. B.; Schrader, W.; Schuth, F. *Angew. Chem., Int. Ed*. 47(2008), 9092-9095

Efectos Sinérgicos, Antagónicos y de No Interacción Presentes en la Adsorción de Mezclas Binarias de un Colorante Catiónico, uno Aniónico, un Metal Pesado y un Anión empleando un Carbón Modificado con HNO_3

M. T. Hernández Eudave[a], R. Tovar Gómez[a], C. J. Durán Valle[b], V. Hernández Montoya[a], Ma. R. Moreno Virgen[a]

[a] Departamento de Ingeniería Química y Bioquímica. Instituto Tecnológico de Aguascalientes. Av. Adolfo López Mateos No. 1801 Ote. Fracc. Bona Gens. C.P. 20256. Aguascalientes, Ags., México.

[b] Departamento de Química Orgánica e Inorganica y IACYS. Universidad de Extremadura. Avda. de Elva, s/n ES-06006 Badajoz, Spain. carlosdv@unex.es

Introducción

La contaminación ambiental afecta la calidad del aire, agua y suelo, y como consecuencia, tiene impacto en los ecosistemas y organismos vivos. En forma particular, la presencia de los contaminantes que emiten las industrias se encuentran en concentraciones altas y su disposición incorrecta en cuerpos de agua causan daños para el medio ambiente y la salud del ser humano. En particular, algunas industrias descargan colorantes, metales pesados y algunos aniones dentro de sus aguas residuales y esta mezcla dificulta el tratamiento del agua ya que el color persiste aún después de los procesos de remoción convencionales, y los metales pesados y los aniones son no degradables (*Visa et al., 2010*). Es conveniente indicar que es complicado seleccionar algún método para tratar soluciones de mezclas de dos, tres o cuatro especies completamente diferentes en cuanto a su estructura química, debido a que los métodos utilizados frecuentemente se emplean para un mismo tipo de contaminante. Sin embargo, el método de adsorción empleando diversos tipos de carbones activados es una alternativa para remover contaminantes, ya sea en soluciones monocomponente como en mezclas; es por eso que el proceso de adsorción se considera un proceso efectivo para la remoción de colorantes, metales pesados y otras especies peligrosas orgánicas e inorgánicas de soluciones acuosas. En este contexto, diversos investigadores que trabajan con el método de adsorción buscan constantemente estrategias para incrementar la capacidad de adsorción de los materiales adsorbentes. Una de ellas es la modificación superficial de los adsorbentes para favorecer las interacciones adsorbato-adsorbente e incrementar la cantidad adsorbida (*Tovar-Gómez et al., 2012*). Además, se pueden presentar efectos de adsorción antagónicos, sinérgicos y de no interacción durante el proceso de remoción dependiendo de las características fisicoquímicas de las especies presentes en la solución (*Tovar-Gómez et al., 2012; Deng et al., 2013; Luo et al, 2015*).

Materiales y Métodos

En este trabajo se reporta la modificación química de un carbon comercial utilizando HNO_3. 1 g de carbon se puso en contacto con 10 mL de HNO_3 concentrado (69-70%w), y en agitación por 5 min a 40°C. Enseguida se lavó con agua desionizada y finalmente se secó a 110°C durante 24 h. Una vez modificado el carbon, se utilizó en la adsorción de mezclas binarias de 4 contaminantes: Procion Red MX-5B (RR2), Brilliant Green 1 (BG1),

cadmio (Cd^{2+}) y Cr^{6+} en forma de cromato (CrO_4^{2-}). Los estudios de adsorción se realizaron en sistema monocomponente y binario, siendo la variable de respuesta la capacidad de adsorción. La concentración inicial de los colorantes RR2 y BG1 fueron de 60, 125, 250 y 500 mg/L; de 25, 50, 100 y 200 mg/L para el Cd^{2+}, y de 12.5, 25, 50 y 75 mg/L para el Cr^{6+}. Las mezclas binarias fueron RR2+Cd^{2+}, RR2+ CrO_4^{2-}, RR2+BG1, BG1+Cd^{2+}, BG1+ CrO_4^{2-} y Cd^{2+}+ CrO_4^{2-}. Los tubos de vidrio que contenían 0.0200 g de carbón modificado y 10 mL de solución de cada contaminante, se mantuvieron a 30°C y en agitación durante 24 h. La concentración de los colorantes y del CrO_4^{2-} se determinó con un espectrofotómetro UV-Vis DR5000; mientras que para el Cd^{2+} se utilizó un espectrofotómetro de absorción atómica Perkin Elmer AAnalist 100.

Discusión y Resultados

Los resultados de los estudios de adsorción muestran que para la mezcla RR2+Cd^{2+}, la capacidad de adsorción de ambos contaminantes incrementa con respecto a su adsorción en solución monocomponente; es decir, se presentan efectos sinérgicos. Algo similar ocurre para la mezcla RR2+ CrO_4^{2-}, ya que se observa que conforme aumenta la concentración inicial de ambos contaminantes, la capacidad de adsorción también incrementa, observándose efectos sinérgicos. Sin embargo, cuando el colorante RR2 esta presente en solución con el colorante BG1, la capacidad de adsorción de ambos colorantes disminuye conforme la concentración inicial aumenta; es decir, se presentan efectos antagónicos. Por otra parte, en la mezcla BG1+Cd^{2+}, los resultados indican que cuando el BG1 se encuentra en mezcla con el Cd^{2+}, la adsorción del colorante BG1 no es afectada, es decir, se observa efecto de no interación; por el contrario, la presencia del colorante BG1 afecta la adsorción del Cd^{2+}, presentando efecto antagónico. Referente a la mezcla BG1+ CrO_4^{-}, el colorante BG1 presenta efecto antagónico ya que la adsorción BG1 disminuye al estar presente el CrO_4^{2-}; sin embargo, al CrO_4^{2-} le beneficia la presencia del BG1 ya que conforme aumenta la concentración del BG1, la capacidad de adsorción del CrO_4^{2-} incrementa. Finalmente, la mezcla Cd^{2+}+ CrO_4^{2-} muestra que ambos contaminantes son favorecidos con un incremento en la capacidad de adsorción, es decir, se observan efectos sinérgicos. Lo anterior es debido a las interacciones electrostáticas, ya sea de atracción o repulsión, entre las diferentes especies presenten en las mezclas: catión-catión, catión-anión, anión-anión.

Referencias

1. Visa, M., Bogatu, C., Duta, A. Simultaneous adsorption of dyes and heavy metals from multicomponent solutions using fly ash. *Applied Surface Science*. 2010, 256, 5486-5491.

2. Tovar-Gómez, R., Rivera-Ramírez, D.A., Hernández-Montoya., V., Bonilla-Petriciolet, A., Dúran-Valle, C.J., Montes-Morán, M.A. Synergic adsorption in the simultaneous removal of acid blue 25 and heavy metals from water using $Ca(PO_3)^2$-modified carbon. *Journal of Hazardous Materials*. 2012, 199-200, 290-300.

3. Deng., J.H., Zhang, X.R., Zeng, G.M., Gong, J.L., Niu, Q.Y., Liang, J. Simultaneous removal of Cd(II) and ionic dyes from aqueous solution using magnetic graphene oxide nanocomposite as an adsorbent. *Chemical Engineering Journal*. 2013, 226, 189-200.

4. Luo X., Zhang Z., Zhou P., Liu Y., Ma G., Lei Z. Synergic adsorption of acid blue and heavy metal ions (Cu^{2+}/Ni^{2+}) onto activated carbon and its mechanisms. *Journal of Industrial and Engineering Chemistry*. 2015.

Characterization of the Surface Chemistry of Carbon Nanotubes

Raquel P. Rocha*, O. Salomé G.P. Soares, José J.M. Órfão, M. Fernando R. Pereira, José L. Figueiredo
Laboratory of Separation and Reaction Engineering - Laboratory of Catalysis and Materials (LSRE-LCM)
Faculty of Engineering, University of Porto, Rua Dr. Roberto Frias, 4200-465 Porto, Portugal
**rprocha@fe.up.pt*

Introduction

Carbon materials are currently used as adsorbents, as catalysts or catalyst supports in the fields of renewable energy (storage and generation) and environmental technologies (oxidation/remediation/adsorption). The ability to tune their physicochemical properties by suitable thermal or chemical post-treatments provides a major asset for these applications [1]. Furthermore, the increasing role assumed by carbon nanomaterials in recent decades is intrinsically linked to the better understanding of the carbon surface chemistry, as a result of reliable methods of analysis. Several techniques are available to explore the chemical and structural properties of carbon nanotubes (CNTs): scanning tunneling microscope (STM), transmission electron microscopy (TEM), X-ray diffraction (XRD), X-ray photoelectron spectroscopy (XPS), infrared (IR) and Raman spectroscopies, chemical titration methods, electron energy loss spectroscopy (EELS), temperature programmed desorption (TPD), thermogravimetry [2-4]. Some techniques do not allow quantitative characterization, others require relatively large amounts of sample and are time consuming or difficult to implement as a routine analysis. In some cases, data interpretation is quite subjective [4].

In the present work, the surface characterization of oxidized CNTs is studied using a combination of relatively accessible analytical techniques, namely the interpretation of the relevant XPS spectra and peak-fitting of the profiles of gases evolved during TPD analysis. For that purpose, commercial multi-walled carbon nanotubes were modified by different chemical and thermal treatments, different surface groups being incorporated onto the pristine carbon nanotubes. The systematic study of the presence/absence of such groups allows a less ambiguous interpretation of the data, and improved characterization of the carbon surface chemistry.

Materials and Methods

Commercial multi-walled carbon nanotubes (CNT-O) purchased from NANOCYL^{TM} (NC3100 series) were oxidized by a liquid-phase treatment with nitric acid followed by thermal treatments at different temperatures in order to modify the original surface properties. 4 g of the CNT-O sample was treated with a 7 M nitric acid solution at boiling temperature during 3 h, resulting in sample CNT-N. In order to obtain samples with successively lower acid character, portions of the CNT-N sample (1 g) were heated at 10 °C min^{-1} under N_2 flow (100 cm^3 min^{-1}) up to selected temperatures (200, 400, 600 and 900 °C) and kept at the desired temperature for 1 h. Samples were labelled

according to the treatment temperature: CNT-N200, CNT-N400, CNT-N600 and CNT-N900.

Textural and chemical properties of the prepared samples were investigated using suitable methods: N_2 adsorption isotherms determined at -196 °C, temperature programmed desorption (TPD) analysis, X-ray photoelectron spectroscopy (XPS), point of zero charge (pH_{pzc}), thermogravimetric analysis (TGA) and elemental analysis (EA).

Results and Discussion

The chemical and thermal treatments applied to the pristine CNTs promote modifications in their textural and surface chemical properties. Oxidation with nitric acid results in an increase of the surface area, as well as the consequent thermal treatments. Large amount of oxygenated surface groups are introduced onto the carbon surface: carboxylic acids, carboxylic anhydrides, lactones, phenols and carbonyls. The thermal treatments applied to CNT-N remove selectively those surface groups. Thus, the sample treated at 200 °C presents less carboxylic groups than the CNT-N sample, such groups being completely absent in sample CNT-N400. After the treatment at 600 °C, the surface only contains phenols and carbonyl groups, all groups being removed at 900 °C. Those modifications are also observed in terms of the decrease of the volatiles released during TGA analysis, of the change in the acidity/basicity of the carbon surface measured by the pH_{pzc}, of the oxygen content determined by a direct oxygen analyzer, through the samples composition determined by elemental analysis and by analysis of the XPS O1s spectra of the samples. The combination of these techniques allows a clear interpretation of the different data leading to a rigorous characterization of carbon nanotubes with different surface chemistries, the qualitative and quantitative assessment of the surface groups being possible using small amounts of sample.

Acknowledgements

This work was supported by Project POCI-01-0145-FEDER-006984 – Associate Laboratory LSRE-LCM funded by FEDER funds through COMPETE2020 - Programa Operacional Competitividade e Internacionalização (POCI) – and by national funds through FCT - Fundação para a Ciência e a Tecnologia. O.S.G.P. Soares and R.P. Rocha acknowledge grants received from FCT (SFRH/BPD/97689/2013 and SFRH/BD/95411/2013, respectively).

References

1. P. Serp and J.L. Figueiredo (Eds.), Carbon Materials for Catalysis, John Wiley & Sons, Inc, Hoboken, NJ, 2009.
2. T. Belin, F. Epron, Mater. Sci. Eng., B 119 (2005) 105-118.
3. C. Herrero-Latorre et al., Anal. Chim. Acta 853 (2015) 77-94.
4. K. A. Wepasnick et al., Anal Bional Chem 396 (2010) 1003-1014.

Application of the Peroxo Method for Synthesis of Photoactive Mesoporous TiO_2 Spheres

M. Ilkaeva[a*], I. Krivtsov[a], Z. Amghouz[b], S. Khainakov[b], J.R. García[a], E. Díaz[c], S. Ordóñez[c]

[a] *University of Oviedo-CINN, Department of Organic and Inorganic Chemistry, 33006, Julian Claveria 8, Oviedo, Spain.*

[b] *Scientific Technical Services, University of Oviedo, Oviedo, Spain*

[c] *University of Oviedo, Department of Chemical Engineering and Environmental Technology, 33006, Julian Claveria 8, Oviedo, Spain.*

** ilkaevamarina@uniovi.es, UO247496@uniovi.es*

Introduction

Titanium dioxide is the most widespread photocatalyst, which is due to its low-cost, non-toxicity and chemical stability. Presently the researchers' attention is focused on the formation of complex architectures, one of such is TiO_2 spheres. Submicron- and micron-size spheres provide a desirable form for a solid catalyst facilitating its reusability, while dealing with TiO_2 of nanometric sizes causes difficulties with recovery of the nanosized catalyst from aqueous suspension. However, the preparation of spherical titania particles demands special experimental setups or expensive (and occasionally volatile and toxic) organic structure-directing agents. Peroxo method is a good alternative to alkoxide-based or template-assisted procedures, since no toxic organic solvents or inert atmosphere are necessary. In the present study we apply peroxo-mediated procedure for preparation of TiO_2 spheres with controlled particle size and porosity, which is achieved by regulating a type of solvent used for the synthesis and by post-synthetic treatment.

Materials and Methods

The photocatalysts have been prepared via the modified previously reported solvent-exchange method [1]. The interaction between titania peroxo complexes and some organic solvents leads to the formation of amorphous TiO_2 precursor, which is crystallized under reflux or heat treatment. The as-prepared materials as well as the those calcined at 500, 650 and 800°C have been characterized using XRD, N_2 physisorption, SEM, TEM analysis. Both the prepared TiO_2 materials and commercial Aeroxide P25 have been studied in the reaction of photodecomposition of MPET under UV irradiation. The evaluation of MPET concentration and determination of its decomposition products have been carried out by means of GC-MS analysis.

Results and Discussion

The formation of titania spherical particles is achieved by tuning the earlier described synthetic method [1]. The size and porosity of the spheres are easily controlled synthetically as well as via post-synthetic procedures. The carbon chain length of an alcohol used for precipitating the hydrous titania from the peroxo complex determines the size of spherical aggregates. A spheres size in case if methanol is used is only 50-100 nm, while for n-propanol this value reaches 400 nm. Furthermore, the proposed

technique favors formation of titania particles having high thermal stability of the photocatalytically active anatase phase. High-temperature treatment promotes the increase of the photocatalytic activity of the titania spheres, despite the reduction of surface area to 11-33 m^2/g. A nonporous character of the prepared spherical aggregates having pore volume of only 0.03 cm^3/g can be modified by applying a post-synthetic treatment procedure. The N_2 adsorption-desorption isotherm of the sample that underwent post-synthetic treatment shows prominent hysteresis loop of H1-type at P/P_0 0.65-0.9, indicating the presence of the mesopores likely to be attributed to the internal particle porosity (Fig 1A). The post-synthetic treatment leads to the formation of the mesopores with a mean size of 10 nm and enhances pore volume up to 0.14 cm^3/g, which presence appears to play a crucial role in the improved photocatalytic performance of the titania spheres.

It has been established that the nonporous TiO_2 spheres possess moderate photocatalytic activity, while commercial photocatalyst Aeroxide P25 and the synthesized mesoporous TiO_2 spheres within 6-8 h of irradiation totally decompose as MPET (Fig 1B), as well as toxic intermediate (p-cresol). However, considering the total organic carbon (TOC) removal, P25 shows significantly better mineralization ability. Nevertheless, the prepared materials have an advantage over P25, since they are easily separated from the reaction mixture and can be reused in many consecutive photocatalytic cycles without losing activity contrary to P25, which is composed of nanometer-sized particles.

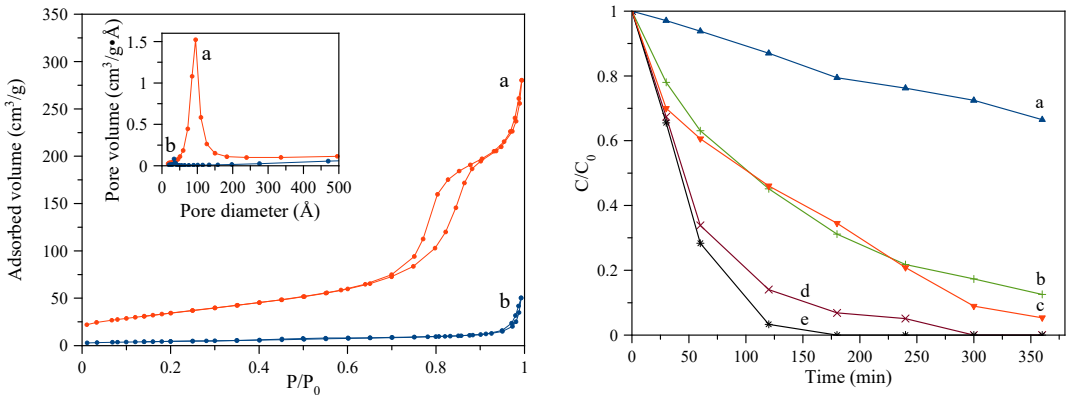

A B

Fig. 1. A - N_2 adsorption-desorption isotherms and average pore size distribution of porous (a) and nonporous titania spheres (b) calcined at 500 °C; B - Photocatalytic degradation of MPET in presence of: nonporous titania spheres treated at (a) 500°C, (b) 800°C; and porous spheres calcined at (c) 500°C, (d) 800°C; (e) Aeroxide P25.

Acknowledgements

We gratefully acknowledge financial support from the Spanish MINECO (MAT2013-40950-R) and the Government of the Principality of Asturias (Severo Ochoa PhD grant BP-14-029 to M.I.).

References

1. I. Krivtsov, M. Ilkaeva, V. Avdin, Z. Amghouz, S. Khainakov, J. R. García, E. Díaz, S. Ordóñez, RSC Adv., 5 (2015) 36634–36641.

Amino Acid Intercalated Clays as Green Materials for Carbon Dioxide Adsorption

João Pires[a*], Joanna Juźków[a,b], Ana C. Fernandes [a] and Moisés L. Pinto[b]
[a] Centro de Química e Bioquímica, Faculdade de Ciências, Universidade de Lisboa, 1749-016 Lisboa, Portugal
[b] CERENA, Instituto Superior Técnico, Universidade de Lisboa, Av. Rovisco Pais, nº 1, 1049-001 Lisboa, Portugal
jpsilva@fc.ul.pt

Introduction

The global awareness of changes in biosphere has increased considerably in recent years, especially concerning the problematics of climate change. The majority of climate researchers agree that this phenomenon is associated with the high concentration of greenhouse gases in the atmosphere, particularly carbon dioxide [1]. Carbon sequestration, a relatively new concept, has been proposed to reduce atmospheric CO_2, especially from stationary sources. Technology may be relatively complex but the basic idea is to separate the CO_2 from flue gas streams and to trap it in oceans, terrestrial ecosystems, and geological formations including depleted gas, oil, and coal formations. Also, the use of CO_2 as a raw material in chemical processes has been investigated [1,2]. Amine modified materials have been proposed for CO_2 adsorption, since the amounts of CO_2 adsorbed are known to increase due to the specific interaction with amine groups [3].

In the present work, and in the search for low-cost sustainable materials for carbon dioxide adsorption, and for the separation carbon dioxide /methane, clay based materials were prepared by the intercalation of a montmorillonite with amino acids.

Materials and Methods

A montmorillonite from Wyoming, USA was used as starting material. The clay was intercalated with aqueous solutions of glycine (Gly), arginine (Arg) and Histidine (His) at two different pH values (5 or 7). The materials were characterized by XRD, TG and N_2 adsorption at -196 °C.

The adsorption isotherms of carbon dioxide and methane were measured up to 1000 kPa (10 bar), at 25 and 45 °C. These experiments were carried out on a custom made volumetric apparatus, made-up of stainless steel, which is comprised a pressure transducer (Pfeiffer Vacuum, APR 266) equipped with a vacuum system that allows a vacuum better than 10-2 Pa.

Results and Discussion

The obtained carbon dioxide adsorption isotherms are exemplified in Figure 1a. The intercalation at pH = 5 revelled to better to prepare materials with higher adsorption capacity than at pH = 7.

The materials were also evaluated for the CO_2/CH_4 separation and the results are exemplified in Figure 1b with a phase diagram. The presence of amino acids in the materials increased the selectivity for CO_2 adsorption in CO_2/CH_4 separations.

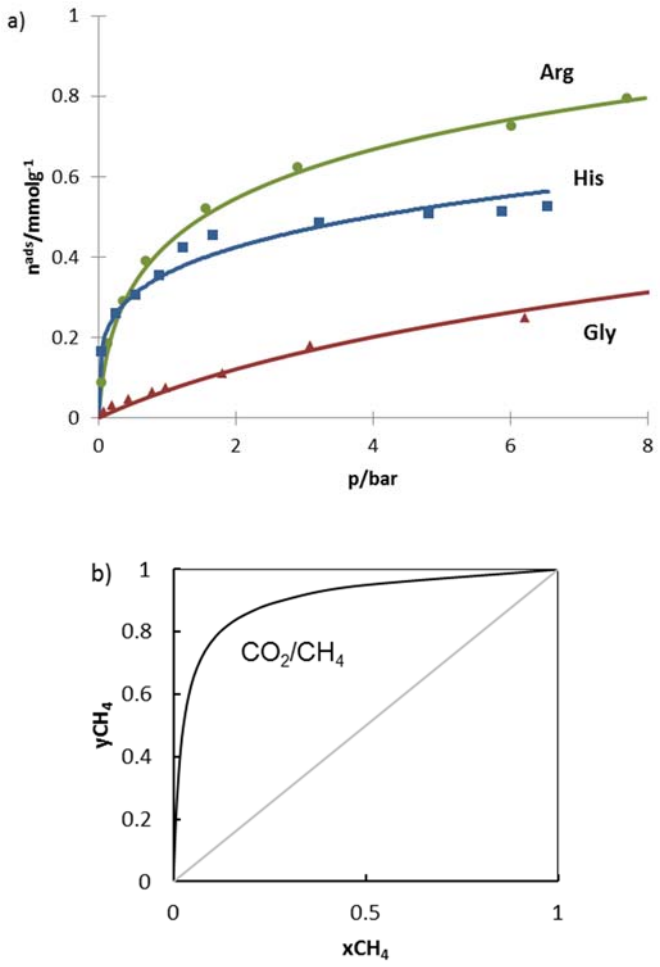

Figure 1 (a) Adsorption isotherms of CO_2 at 25 °C for montmorillonite intercalated with the indicated amino acids at pH=7; **(b)** Phase diagram for the CO_2/CH_4 separation for montmorillonite intercalated with Arg at pH = 7.

Acknowledgements

The authors thank the Foundation for Science and Technology (FCT) for funding CQB UID/MULTI/00612/2013 and CERENA (UID/ECI/04028/2013).

References

[1] C. S Song. Catal. Today 115 (2006) 1-4 2–32.
[2] R. Srivastava, D.Srinivas, P. Ratnasamy, J. Catal. 233 (2005) 1–15.
[3] M.L. Pinto, L. Mafra, J.M. Guil, J. Pires, J. Rocha. Chem. Mater. 23 (2011) 1387-1395.

Eliminación de Bisfenoles del Agua mediante Adsorción/Bioadsorción sobre Tela de Carbón Activada

M. V. López-Ramón[a], I. Bautista-Toledo[b], R. Ocampo-Pérez[c], J. Rivera-Utrilla[b], M. A. Álvarez[a*], M. Sánchez-Polo[b]

[a]Departamento de Química Inorgánica y Orgánica, Universidad de Jaén, 23071 Jaén
[b]Departamento de Química Inorgánica, Universidad de Granada, 18071 Granada.
[c]Facultad de Ciencias Químicas, Universidad Autónoma de San Luis de Potosí, 78260 San Luis Potosí, México.
**malvarez@ujaen.es*

Introducción

En los últimos años, la contaminación ambiental de las fuentes de agua y efluentes industriales por los productos químicos conocidos como disruptores endocrinos ha despertado un creciente interés. Entre estos productos químicos antropogénicos se encuentra el bisfenol A (BPA), usado ampliamente en la industria del plástico. Muchos países, incluido España, han regulado ya el uso de este compuesto, y en la mayoría de los casos (latas, biberones de plástico, resinas epoxi) el BPA ha sido sustituido por bisfenol S (BPS), encontrándose estos productos etiquetados como "BPA-free". Sin embargo, estudios recientes han demostrado que el BPS presenta una toxicidad similar a la del BPA [1]. El objetivo de este trabajo ha sido estudiar la eliminación de estos bisfenoles del agua mediante procesos de bioadsorción, usando para ello la bacteria Escherichia coli soportada en una tela de carbón activada y su correspondiente oxidada (TCA y TCAox, respectivamente) con objeto de relacionar este proceso de eliminación con las características químicas y texturales de los soportes empleados. A continuación se presentan algunos de los resultados obtenidos con BPA.

Materiales y Métodos

La tela empleada en este estudio fue suministrada por Kynol Europe. Dicha muestra fue oxidada con una disolución de $(NH_4)_2S_2O_8$ en H_2SO_4 1M. Estos adsorbentes se caracterizaron por adsorción de N_2 a 77 K, análisis elemental y valoración potenciométrica. El BPA se caracterizó por valoración potenciométrica y medidas de su tamaño molecular. Previo a la obtención de las isotermas de adsorción, se llevó a cabo el estudio cinético, pH disolución y 298 K, con objeto de determinar la velocidad de adsorción del BPA sobre TCA. Para ello, se emplearon diferentes masas de adsorbentes (0.01g – 0.04g) y 100 mL de disolución. Las isotermas de adsorción se determinaron a 298 K empleando 0.04 g de carbón y 200 mL de disolución de BPA (20 a 200 mg/L). En el caso del estudio de adsorción en régimen estático en presencia de bacterias, éstas fueron previamente inmovilizadas en ambas telas [2]. Las concentraciones de equilibrio del BPA se determinaron espectrofotométricamente a λ = 276.5 nm.

Resultados y Discusión

En la Tabla 1 se recogen las características de los adsorbentes empleados. La TCA-ox presenta una menor área superficial y menor porosidad que la muestra TCA, lo cual se atribuye a la destrucción de las paredes de parte de los microporos durante la oxidación.

El proceso de oxidación también produce un aumento del contenido de grupos ácidos en la tela oxidada y, por tanto, un pH_{PCC} ácido (3.3).

Tabla 1.- Características de las telas de carbón activadas

Carbón	S_{BET} m^2/g	S_{ext} m^2/g	W_0 cm^3/g	V_{meso} cm^3/g	E_0 kJ/mol	L_0 nm	pH_{PCC}
TCA	2128	40	0.91	0.02	15.2	1.69	8.0
TCA-ox	1636	94	0.71	0.03	14.6	1.80	3.3

La aplicación del modelo difusional a las curvas de decaimiento de la concentración de BPA sobre TCA reveló que este modelo interpreta adecuadamente los datos experimentales y que el coeficiente de difusión molecular de BPA sobre la tela de carbón es independiente de la masa de BPA adsorbido, siendo $D_{ep} = 6.16\times10^{-9}$ cm^2/s.

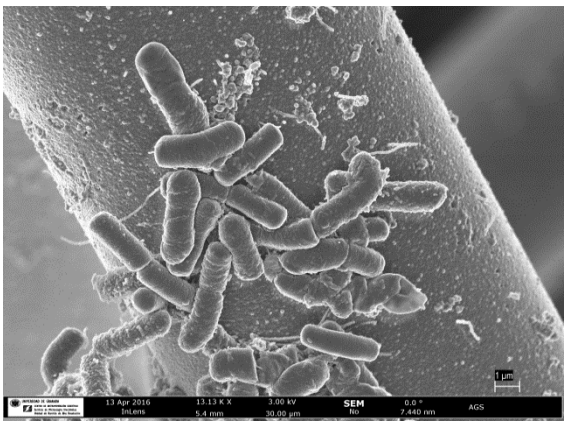

Fig. 1. Bacteria Escherichia coli soportada (adsorbida) sobre TCA

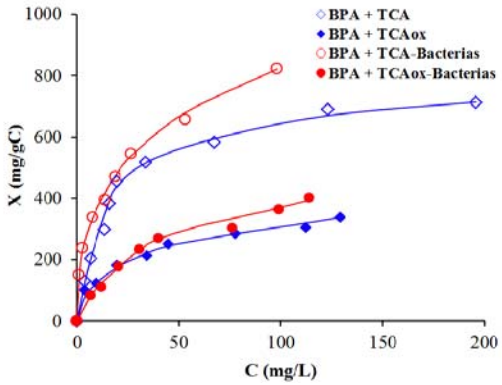

Fig. 2. Isotermas de adsorción de BPA sobre los diferentes soportes empleados a pH ≈ 7

En la Figura 1 se muestra una microfotografía de las bacterias adsorbidas en la tela original. Las isotermas de adsorción de BPA obtenidas con los diferentes adsorbentes (Fig. 2) muestran como el adsorbente más eficaz fue TCA. De acuerdo con el diagrama de distribución de especies del BPA a pH≈7 [3], éste se encuentra como especie neutra y la superficie de TCA estará cargada positivamente y la de TCAox negativamente, por lo que predominarán las interacciones no electrostáticas. Por ello, la mayor capacidad de adsorción de la TCA es debida a su mayor área superficial. En la Figura 2 también se muestra claramente el efecto de la mejora de la capacidad de adsorción en ambos adsorbentes debido a la presencia de las bacterias inmovilizadas sobre ellos.

Agradecimientos

Los autores agradecen a MICINN y FEDER (proyecto CTQ2011-29035-C02-01) y a la Universidad de Jaén (Proyecto UJA 2015/06/01) por la financiación recibida.

Bibliografia

1. J. R. Rochester, A.L. Bolden, Environmental Health Perspectives 123 (2015) 643-650.
2. C. Moreno-Castilla, I. Bautista-Toledo, M.A. Ferro-García, J. Rivera-Utrilla, Carbon 41 (2003) 1743-1479.
3. I. Bautista-Toledo, M.A. Ferro-García, J. Rivera-Utrilla, C. Moreno-Castilla, F.J. Vegas-Fernández, Environ. Sci. Technol. 39 (2005) 6246-6250.

Tuning the Pore Size Distribution of Mesoporous Carbons: the Key Role of Alkaline Chlorides in Mixtures with Zinc Chloride

Ana S. Mestre[a,b]*, Raquel Gonçalves[a], Valentine Vigneron[a], Cristina Freire[b], Ana P. Carvalho[a]
[a] Centro de Química e Bioquímica, Faculdade de Ciências, Universidade de Lisboa, 1749-016 Lisboa, Portugal
[b] REQUIMTE/LAQV, Departamento de Química e Bioquímica, Faculdade de Ciências, Universidade do Porto, 4169-007 Porto, Portugal
**asmestre@fc.ul.pt*

Introduction

Activated carbons are unique materials due to their high adsorption properties, tunable pore size distribution and rich surface chemistry, being so crucial in various industrial processes. However, the sustainability, stability and versatility of these materials still stimulates continuous efforts in the development of improved or new synthetic routes leading to better performances or even new properties. Particularly, the synthesis of mesoporous carbons has had significant advances in the last decades, due to their importance in applications involving large molecules, such as, adsorbents for dyes, catalyst supports for biomolecules, or as electrodes for biosensors [1,2].

A recent study reported the synthesis of highly mesoporous carbons from biomass using a eutectic salt mixture $KCl/ZnCl_2$ [3]. The control of the activation conditions allowed to produce materials with total pore volumes up to 2.7 $cm^3\ g^{-1}$ ($A_{BET} \approx 1300\ m^2\ g^{-1}$) with more than 90 % of mesopores. The present work aims to explore the potentialities of alkaline and zinc chlorides mixtures (in eutectic and non-eutectic conditions), as porogens for the control of the mesopore size distribution in glucose-derived activated carbons.

Materials and Methods

Glucose was used as carbon precursor for the preparation of the mesoporous carbons. The activation was made with eutectic and non-eutectic mixtures of $LiCl/ZnCl_2$, $NaCl/ZnCl_2$ and $KCl/ZnCl_2$, designated, respectively, by LiZn, NaZn and KZn, and also only with $ZnCl_2$ for comparison purposes. Briefly, 1 g of glucose was milled with 3 g of the salt mixture and was activated under N_2 flow (5 $cm^5\ s^{-1}$) with the following heating scheme: from room temperature up to 240 °C at 10 °C min^{-1}, this temperature was maintained during 2 h, further increased up to 800 or 1000 °C (10 ºC min^{-1}), and final held for more 2 h. The furnace was cooled (N_2 flow), the resultant mixture was ground, washed with distilled water until no detection of chlorine ions in the supernatant, dried and stored.

Characterization of the carbon materials was made by SEM, N_2 and CO_2 adsorption isotherms at, respectively, -196 and 0 °C, elemental analysis, ash content, determination of the pH at the point of zero charge (pH_{PZC}) and apparent density, DRIFT and DRX.

Results and Discussion

The use of salt mixtures as porogens during the carbonization of glucose allowed to obtain porous carbons with yields between 23 and 31 %. Salt mixtures play a crucial role in the porosity development as illustrated in the N_2 adsorption isotherms shown in

Fig. 1. All curves belong to the type IV(a) according to the IUPAC classification [4], being characteristic of mesoporous solid materials. Hysteresis loops close at $p/p^0 \approx 0.4$, but while samples obtained with the eutectic salt mixtures LiZn and NaZn present type H2(b) loops associated with pore blocking and large size distribution of neck widths, sample prepared with KZn has a type H4 loop usually found in micro-mesoporous carbons.

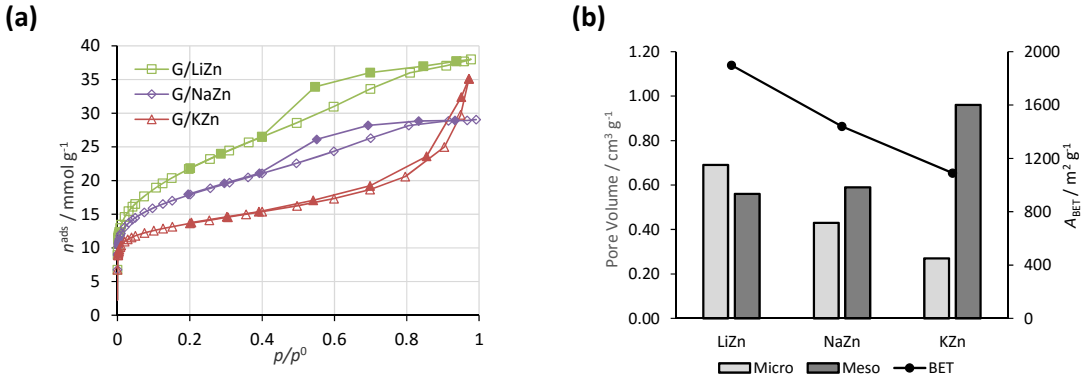

Fig. 1. Textural characterization of materials obtained at 800 °C with the mentioned eutectic mixtures (a) N_2 isotherms; (b) textural parameters (bars: volumes; line: A_{BET}).

Fig. 1(b) summarizes the textural parameters obtained from the N_2 adsorption data. In all cases superactivated carbons were obtained since total pore volumes (V_{total}) are higher than 1.0 cm^3 g^{-1} and apparent surface areas (A_{BET}) range from 1000 to 2000 m^2 g^{-1}. The materials present well developed micro and mesopore networks, with V_{meso} accounting to 45-60 % of the V_{total} when LiZn and NaZn were used as porogens, and reaching 80 % when KZn was employed. Sample prepared only with zinc, in the same amount of zinc used in the eutectic mixture KZn, has the double of the A_{BET} but only 18 % of mesopores, proving that, in fact, alkaline chlorides play a fundamental role in the development of micro and mesopores thought this methodology.

The results obtained so far reveal that the mesopore size distribution can be tuned by the salt mixture: LiZn leads to materials with high volume of mesopores with diameters in the range of 2 – 10 nm; NaZn originates mesopores up to 20 nm, and KZn results in high volume of large mesopores (20 – 50 nm). The work will proceed to evaluate the effect of other salt mixture compositions and these results will be correlated with morphological and surface chemistry data.

Acknowledgements

This study was funded by projects PEst-OE/QUI/UI0612/2013 (CQB) and UID/QUI/50006/2013 - POCI/01/0145/FERDER/007265 (REQUIMTE) from FCT/MEC through national funds and co-financed by FEDER, under the Partnership Agreement PT2020. ASM thanks FCT for Post-doc grant (SFRH/BPD/86693/2012).

References

1. Lee, J., Kim, J., Hyeon, T., Adv. Mater. 18 (2006) 2073-94.
2. Xin, W. and Song, Y.H., 2015. RSC Adv. 5 (2015) 83239-85.
3. Ma, Z., Zhang, H., Yang, Z., Zhang, Y., Yu, B., Liu, Z., 2014. J. Mater. Chem. A 2 (2014) 19324-9.
4. Thommes, M., Kaneko, K., Neimark, A.V., Olivier, J.P., Rodriguez-Reinoso, F., Rouquerol, J., Sing, K.S.W., Pure Appl. Chem. 87 (2015) 1051-69.

Performance of the MAF-6 Metal Organic Framework on the Separation of C_4, C_5, and C_6 Hydrocarbon Isomers

A. Luna-Triguero[a], J. J. Gutiérrez-Sevillano*[a,b], Sofía Calero[a,*]
[a]*Dpt. of Physical, Chemical, and Natural Systems, Universidad Pablo de Olavide, 41013-Sevilla (Spain)*
[b] *Center for Molecular Modeling (CMM), Ghent university, 9000 Ghent (Belgium)*
**jjgutierrez@upo.es, scalero@upo.es*

Introduction

The efficiency of combustion engines is related to the amount and type of isomers present in the fuel. Some hydrocarbon isomers are likely to be present while other decrease the efficiency of the process. For this reason, the separation of isomers of alkanes is an important process with high interest in the petrochemical industry. To carry out this separation by adsorption is a challenging task due to the similar chemical nature of the species. Differences between isomers are practically reduced to the length of the chain, shape, and size.

Metal-organic frameworks offer a huge variety of topologies and pore geometries. In addition they can be tuned[1] to achieve specifics features. The MAF-6 framework has RHO based topology[2] and relatively long linkers resulting on a topology of big cavities connected by straight channels, that can be suitable for dealing with the separation of long chain molecules.

Materials and Methods

We performed Monte Carlo simulations in the Grand Canonical Ensemble to obtain adsorption isotherms of pure components. Based on these isotherms we used Ideal Adsorption Solution Theory to predict the adsorption of binary and multi-component mixtures. Additional Monte Carlo simulations for mixtures had also been performed to contrast the predictions from IAST. All simulations have been carried out using the RASPA code[3].

Results and Discussion

In this work we study the viability of MAF-6 as a potential candidate for separation processes involving alkanes of four, five, and six carbon atoms. Our study not only explores the separation between hydrocarbons of different length but also between their isomers.

Our computational results show that the adsorption of pure n-butane and isobutane is practically equal in MAF-6. Nevertheless in the case of C_5 isomers there are some differences. The adsorption of the three considered isomers is almost the same at low

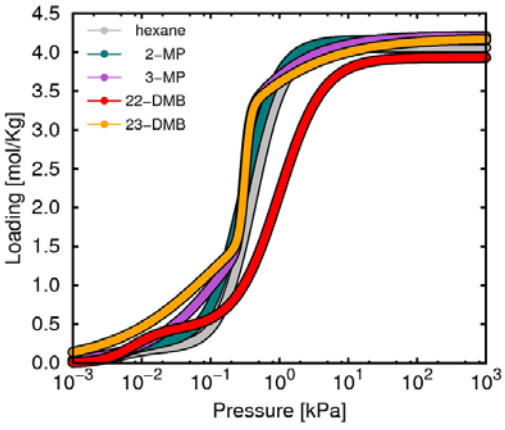

Fig. 1. Adsorption isotherms of pure C_6 isomers in MAF-6.

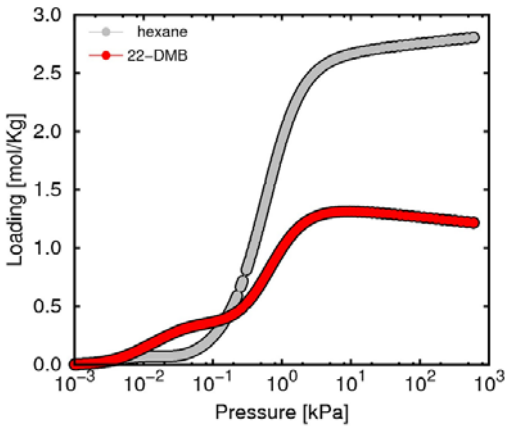

Fig. 2. Adsorption isotherms of binary mixture of hexane – 2,2-dimethylbutane in MAF-6.

pressure, but the saturation for 2,2-dimethylpropane is significantly lower. This is consequence of the better packing of the more linear isomers. For the C_6 isomers we also find interesting results. As can be seen in figure 1, the adsorption of all C_6 hydrocarbons is similar except for the 2,2-dimethylbutane isomer, and just at saturation pressure the adsorption of this isomer is slightly lower than for the rest. In striking contrast and in spite of the small differences in the pure isotherms, we obtain an unexpected trend in the adsorption of the binary mixture. In figure 2, we can observe that MAF-6 favors the adsorption of 2,2-dimethylbutane at low pressure while at high pressure the most adsorbed component is hexane. A further anaylsis of the adsoption selectivity and the distribution of molecules in the structure provides insights on the potential of this material as selective adsorbent of C_6 isomers at certain conditions.

Acknowledgements

This work has been supported by the European Research Council (ERC2011-StG-279520-RASPA) and the Spanish MINECO (CTQ2013-48396-P).

References

1. Gutiérrez-Sevillano, J. J.; Dubbeldam, D.; Bellarosa, L.; Lopez, N.; Liu, X.; Vlugt, T. J. H.; Calero, S., JPCC, 117 (40), 2013, 20706-20714
2. He, C.-T.; Jiang, L.; Ye, Z.-M.; Krishna, R.; Zhong, Z.-S.; Liao, P.-Q.; Xu, J.; Ouyang, G.; Zhang, J.-P.; Chen, X.-M, JACS, 137(22), 2015, 7217-7223.
3. D. Dubbeldam, S. Calero, D. E. Ellis, and R. Q. Snurr, Mol. Simul., 2016, 42, 81-101.

Adsorbent Particle Design for Application in Gas Adsorption Processes

C. L. Antunes[a], A. U. Garate[a], M. G. Plaza[b], R. P. P. L. Ribeiro*[a], I. A. A. C. Esteves*[a], José P. B. Mota[a]

[a] LAQV, Requimte, Chemistry Dept., Faculty of Sciences and Technology, Universidade NOVA de Lisboa, 2829-516 Caparica, Portugal

[b] Instituto Nacional del Carbón, INCAR-CSIC, Apartado 73, 33080 Oviedo, Spain

**iaesteves@fct.unl.pt, rpp.ribeiro@fct.unl.pt*

Introduction

Carbon Capture and Storage (CCS) is a mid to long term strategy for cost effective CO_2 capture [1]. An alternative to the energy intensive amine scrubbing is adsorption processes using solids for CO_2 capture [2], such as Pressure Swing Adsorption (PSA) [3].

A proper adsorbent for CO_2 capture is vital for the applicability of CCS adsorption processes. The topical adsorbents for CO_2 capture are usually in the form of powder. Examples of these solids are Metal Organic Frameworks (MOFs). MOFs are coordination polymers made by metal clusters (inorganic building blocks) and organic linkers, which give to these solids nanometer-sized(50-90% porosity), high crystallinity, highly ordered geometries with fine-tuned functionalities and large surface areas (1000-8000 m^2/g), thus having high potential for gas separation/storage by adsorption[4]. Despite this fact, it is impractical to pack a MOF powder into fixed-bed adsorption columns due to heavy pressure drops raised by using such small particles.

Formulation and shaping of MOFs from porous powders into a macroscopic shape enables an enhanced structure with high mass transfer, low pressure drop, good heat management, high mechanical, chemical and attrition stability to be used as an adsorbent in a PSA process at large-scale level. Yet, shaping MOFs into mechanically robust particles with efficient adsorption capacity for CO_2 removal by PSA is still scarce in open literature [5], which opens a window for topical research in this field.

Materials and Methods

MOFs densification is proposed by using two approaches: binderless mechanical compression and binder-containing extrusion. The effect of compression force (0.5, 1 tnf) and binder (Polyvinyl alcohol, PVA aqueous solutions)/MOF ratio were studied, along with CO_2 sorption equilibria on the formulated samples at 30ºC, using a volumetric/manometric unit [4]. Two MOF were used: i) ZIF-8 (Zeolitic Imidazolate Framework, 2-methylimidazole zinc) and ii) MIL-53(Al) (hydrophilic aluminum terephthalate), powders made by BASF SE. Mechanical, structural and physico-chemical analyses were done to compare the formulated solids with their original powder. Similarly, the CO_2 sorption equilibria were compared for the two forms.

Results and Discussion

The results obtained (Fig. 1) for MIL-53(Al) show that the binderless granules compressed at 0.5 tnf show the most promising results with approx. 20% adsorption capacity loss (above 4 bar) in comparison with the original powder, whereas pellets with less percentage of binder exhibit higher adsorption CO_2 capacity, but lower mechanical

resistance compared to samples with more than 5% of PVA in MIL-53(Al). The binder-containing pellets show approx. 30% less adsorption capacity towards CO_2 (above 4 bar) when compared to the respective powder. Despite the adsorption capacity losses, due to binder blockage of the micropores and the compression effect in the crystalline structure, the best formulated solids can pack a column to perform fixed-bed experiments targeted for the advance of PSA processes using MOFs as adsorbents.

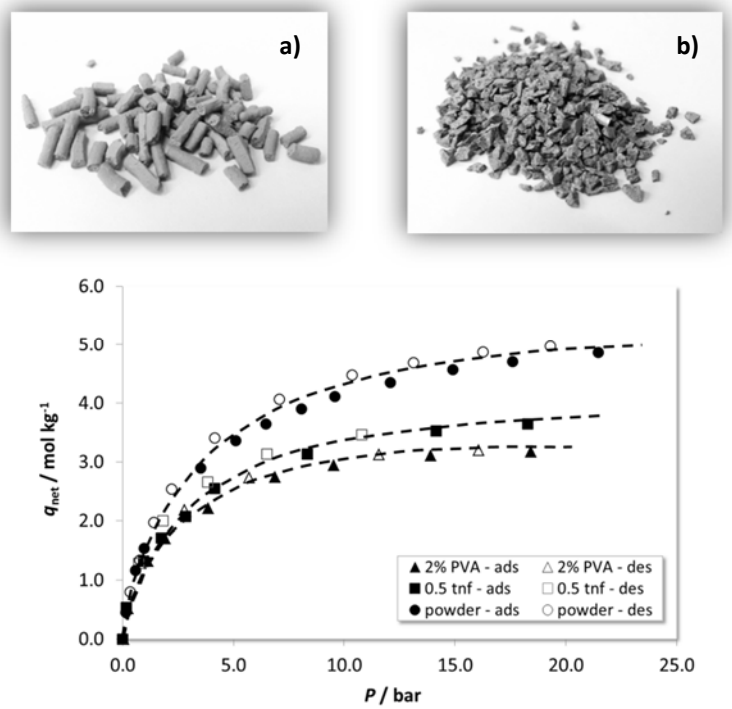

Fig. 1. Top: formulations of MIL-53(Al): a) binder-containing pellets, b) binderless granules. Bottom: sorption equilibria results of CO_2 at 30ºC on MIL-53(Al) original powder (•), pellets with 2% PVA binder (■) and binderless granules with 0.5 tnf (▲). Filled/empty symbols denotes adsorption/desorption data. Dashed lines are guides to the eye.

Acknowledgements

Contract Investigador FCT, IF/01016/2014 (I.A.A.C. Esteves), grant SFRH/BPD/103533/2014 (R.P.P.L. Ribeiro) and projects EXCL/QEQ-PRS/0308/2012, PTDC/AAC-AMB/108849/2008 and ELAC2014/BEE0367 from FCT/MEC(PT) are gratefully acknowledge. The work was supported by LAQV-REQUIMTE which is financed by PT funds from FCT/MEC (UID/QUI/50006/2013) and co-funded by the ERDF in the PT2020 Partnership Agreement (POCI-01-0145-FEDER - 007265).

References

1. M.K. Mondal et al., Energy 46(1) (2012) 431–441. EEA Technical Report 14/2011. Copenhagen: EU Environm. Agency (2011) 66. DOI: 10.2800/84208.
2. S. Choi et al., Chem.Sus.Chem 2(9) (2009) 796–854. A.A. Olajire, Energy 35(6) (2010) 2610-2628. Y. Liu et al., Env. Sci. & Technol.45(13) (2011) 5710–5716.
3. D.M. Ruthven et al., PSA, VCH Pub.:NY, 1994. D.M. Ruthven, Principles of Adsorp.&Adsorp. Proc., Wiley:NY, 1984. I.A.A.C. Esteves et al., Ads.Sci. & Technol.25(9) (2007) 693-715.
4. B.C.R. Camacho et al., Sep. Pur. Technol. 141 (2015) 150-159. A. Lyubchyk et al., J. Phys. Chem. C 115(42) (2011) 20628-20638. J. Liu et al., Chem. Soc. Rev.41(6) (2012) 2308–2322.
5. D. Bazer-Bachi et al., Powder Technol.255 (2014) 52–59. F. Rezaei et al., Microp. & Mesop. Mat.204 (2015) 34-42. V. Finsy et al., Microp. & Mesop. Mat.120(3) (2009) 221-227.

Membranas de Polisulfona con Óxido de Grafeno como Soportes de Membranas de Osmosis Directa

Sergio Morales-Torres*, José L. Figueiredo, Adrián M.T. Silva
Laboratory of Separation and Reaction Engineering – Laboratory of Catalysis and Materials (LSRE-LCM), Faculdade de Engenharia, Universidade do Porto, Rua Dr. Roberto Frias, 4200-465 Porto, Portugal
**semoto@fe.up.pt*

Introducción

El crecimiento exponencial de la población junto con el cambio climático está provocando un aumento drástico en la demanda de agua a nivel mundial. Las actuales reservas hídricas se agotan y, por tanto, son necesarias nuevas estrategias que incentiven la producción de agua limpia a partir de fuentes alternativas, como la desalinización de agua de mar o aguas salobres [1]. El proceso de osmosis directa (FO) ha ganado interés en el tratamiento de aguas, debido a su baja energía de operación y a la baja desactivación de sus membranas. Sin embargo, las actuales membranas impiden que el proceso de FO sea competitivo comparado con la osmosis inversa. Por otro lado, los materiales de carbón tales como, los nanotubos de carbono y el grafeno han demostrado tener un enorme potencial para mejorar las propiedades de las membranas aplicadas en desalinización [2-3]. En este trabajo, membranas de polisulfona (PSf) con óxido de grafeno (GO) se prepararon por el método de inversión de fase, estudiando parámetros de síntesis como la carga de material y la composición del baño de coagulación. Las membranas de PSf fueron usadas como soportes de membranas de compuestos de lámina delgada (TFC), cuyo comportamiento fue estudiado en FO de agua salada con diferentes configuraciones de membrana.

Materiales and Métodos

Las membranas de PSf (9 % peso) con diferentes contenidos (0.05 – 0.20 % peso) de GO fueron preparadas por el método de inversión de fase, empleando agua destilada (DI) o agua/isopropanol (70:30) como baños de coagulación. La caracterización física-química de las membranas fue analizada por diferentes técnicas tales como, microscopía electrónica de barrido (SEM), medidas de porosidad, FTIR, termogravimetría y determinación del ángulo de contacto. La permeabilidad de las membranas de PSf fue determinada por medidas de filtración con agua DI a una presión de 0.5 bar. Finalmente, las membranas de PSf fueron usadas como soportes de membranas de TFC, las cuales fueron preparadas por el método de polimerización interfacial [3]. Las membranas de TFC fueron analizadas usando agua DI y una solución acuosa de NaCl (0.6 M) como disoluciones de alimentación y permeado, respectivamente, estudiando diferentes configuraciones: capa activa de la membrana orientada hacia la disolución de permeado (modo PRO) y orientada hacia la alimentación (modo FO).

Resultados y Discusión

Las membranas de PSf presentaron una estructura típica asimétrica formada por una capa superior delgada-densa y una sub-capa porosa (Fig. 1a). La adición de cualquier

cantidad de GO a las membranas de PSf provocó cambios en sus propiedades físicas y químicas. En general, membranas con GO presentaron una estructura más porosa compuesta por poros en forma de dedos (Fig. 1b), mientras que sólo macrohuecos fueron mayoritariamente observados en la membrana de PSf pura (Fig. 1a). Además de mejorar la estructura de las membranas, la adición de GO produjo membranas con menores ángulos de contacto y consecuentemente, una mayor hidrofilicidad superficial. Por otro lado, las membranas obtenidas con baño agua/isopropanol presentaron una porosidad mayor que aquellas formadas con sólo agua. Estos cambios estructurales inducidos tanto por el uso de GO como isopropanol, podrían ser justificados por las diferentes velocidades de intercambio disolvente/no-disolvente producidas durante la formación de las membranas. La estructura porosa con poros en forma de dedos y la mejor hidrofilicidad superficial de las membranas de GO produjeron permeabilidades superiores que membranas de PSf pura en los ensayos de filtración.

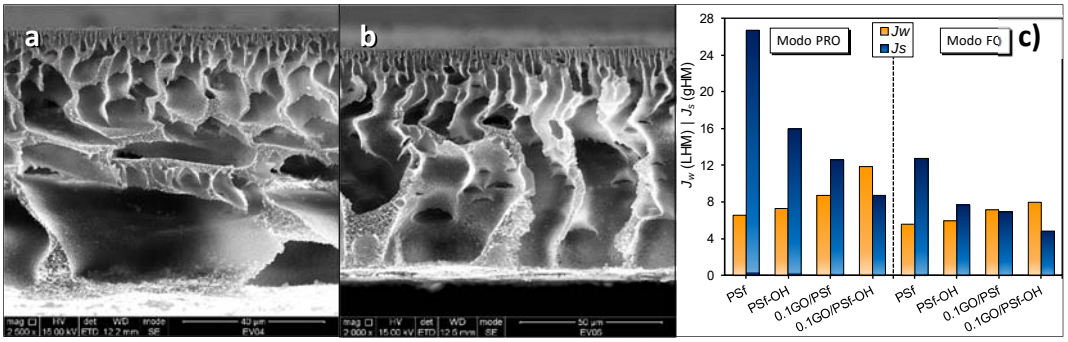

Fig. 1. Imágenes de SEM de las membranas de a) PSf pura y b) con 0.1% de GO. c) Flujo de agua (J_w, L h^{-1} m^{-1}) y flujo inverso de soluto (J_s, g h^{-1} m^{-1}) obtenidos en modos PRO y FO para algunas membranas de TFC.

Las membranas de TFC obtuvieron mayores flujos de agua (J_w) en la configuración PRO que FO (Fig. 1c). Este comportamiento se debe al mayor efecto de concentración de polarización interna cuando la capa activa de la membrana está orientada hacia la disolución de alimentación (modo FO). En general, las membranas con GO presentaron mayor J_w y menor flujo de soluto inverso (J_s) que las respectivas membranas de PSf pura, independientemente del tipo de baño usado y de la configuración estudiada. La membrana de TFC más eficiente fue aquella preparada con un soporte de PSf con 0.1 % de GO y formada en un baño agua/isopropanol.

Agradecimientos

Este trabajo fue financiado por el Proyecto POCI-01-0145-FEDER-006984 – *Associate Laboratory LSRE-LCM* financiado por fondos FEDER, a través de COMPETE2020 – *Programa Operacional Competitividade e Internacionalização* (POCI) – y por fondos nacionales a través de la FCT – *Fundação para a Ciência e a Tecnologia*. Este trabajo fue parcialmente co-financiado por QREN, ON2, FCT y FEDER (NORTE-07-0124-FEDER-000015). SMT (SFRH/BPD/108981/2015) y AMTS (IF/01501/2013) también agradecen a la FCT su financiación personal.

Referencias

1. T.-S. Chung, S. Zhang, K.Y. Wang, J. Su, M.M. Ling, Desalination 287 (2012) 78-81.
2. H.M. Hegaba, L. Zoua, J Mem Sci 484 (2015) 95-106.
3. T.L.S. Silva, S. Morales-Torres, J.L. Figueiredo, A.M.T. Silva, Desalination 357 (2015) 233-245.
4. D. Emadzadeh, W.J. Lau, T. Matsuura, A.F. Ismail, et. al., J Mem Sci 449 (2014) 74-85.

Estudio Comparativo de la Entalpía de Interacción de Fenol y Ácido Salicílico a Diferente pH desde Solución Acuosa sobre Carbón Activado

Valentina Bernal[a,*], Liliana Giraldo[a]; Juan Carlos Moreno-Piraján[b]
[a] Departamento de Química, Universidad Nacional de Colombia, Cra 30 No. 45-03, Colombia.
[b] Departamento de Química, Universidad de los Andes, Cra. 1a No. 18A- 10, Colombia.
**vbernalf@unal.edu.co*

Introducción

El uso y desecho inadecuado de medicamentos genera que moléculas con actividad biológica aparezcan en aguas residuales, subterráneas y potables; aunque en concentraciones bajas se considera que no representan un riesgo toxicológico las propiedades fisicoquímicas de las moléculas permite su acumulación en tejidos corporales y suelos, elevando sus concentraciones a niveles que pueden generar actividad biológica [1].

El carbón activado es un adsorbente utilizado para el tratamiento terciario de aguas residuales debido a su porosidad, alta área y química superficial; este último factor adquiere relevancia para el proceso de adsorción de moléculas de uso farmacéutico teniendo en cuenta el carácter anfótero de los principios activos de los medicamentos [2]. Una forma de conocer las interacciones que tienen lugar entre soluciones acuosas de los fármacos y el carbón activado es la determinación de la entalpía de inmersión.

Materiales y métodos

Se emplearon dos carbones activados con diferente química superficial como adsorbentes, un carbón activado granular preparado a partir de cascara de coco y activación física con CO_2, CAG, y un carbón activado reducido a 1173 K en atmósfera de N_2.

Los carbones activados se caracterizan de forma física y química por adsorción de Nitrógeno a -77 K y acidez y basicidad total respectivamente.

Las isotermas de adsorción de los fármacos desde fase acuosa se realiza por adsorción en batch; la concentración en equilibrio se determina por espectroscopia uv-vis a 296 nm para el ácido salicílico y 268 nm para el Fenol, el tiempo de equilibrio se determinó previamente.

La calorimetría de inmersión se llevó a cabo en un calorímetro tipo Calvet de construcción local; se pesaron 100 mg de carbón activado en una ampolleta de vidrio de vidrio de pico frágil, se realizó desorción a 200 ^oC y 10^{-4} mmHg, y posteriormente se realizó la inmersión en soluciones de fármaco de diferentes concentraciones. Se realiza calibración eléctrica.

Resultados y Discusión

En este trabajo se compara la entalpia de inmersión de carbones activados en soluciones acuosas de diferente concentración de ácido salicílico y fenol a tres valores de pH, 2, 7 y 11, debido a que tanto el carbón activado como los fármacos presentan diferencias en su carga eléctrica a diferentes pH.

La Figura 1 muestra una curva calorimétrica obtenida para la inmersión de carbón activado granular en soluciones de 100 mg L^{-1} de ácido salicílico y fenol a pH 7.

Los valores de entalpía de inmersión del ácido salicílico se encuentran entre 7.53 y 22.5 J g^{-1}, y para el fenol entre 9.48 y 23.7 J g^{-1}.

Los resultados obtenidos permiten evidenciar que la entalpía de inmersión varía con el pH debido a cambios en las interacciones carbón activado-fármaco.

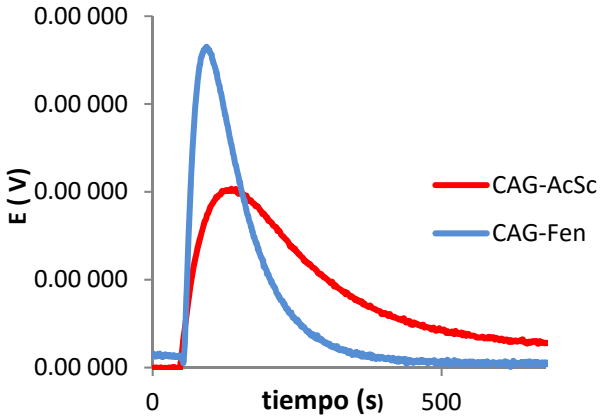

Fig. 1. Curva calorimétrica obtenida de la inmersion de ácido salicilico y fenol en carbón activado granular a pH7

Agradecimientos

Los autores agradecen al convenio marco entre la Universidad Nacional de Colombia y la Universidad de los Andes y al programa de becas de la fundación CEIBA por el apoyo económico para la realización de estudios doctorales.

Referencias

1. Nunes, B.; Campos, J.C.; Gomes, R.; Braga, M.R.; Ramos, A,S.; Antunes, S,C.; Correia, A.T. Environ sci.pollut r. 22 (2015), 667-678.
2. Aburub, A.; Wuster, D. Journal Colloid Interface Science , *J. Colloid Interface Sci.* 296 (2006), 79-85.

Glycerol from Biodiesel Production: Promising Activated Carbons Precursor

Mary K. S. Batista[a,b]*, Ana S. Mestre[a], Isabel M. Fonseca[b], Ana P. Carvalho[a]
[a]Centro de Química e Bioquímica, Faculdade de Ciências da Universidade de Lisboa, 1749-016 Lisboa, Portugal
[b]Departamento de Química REQUINTE, CQFB, FCT, Universidade Nova de Lisboa, Quinta das Torre, 2829-516 Caparica, Portugal
**mkbatista@fc.ul.pt*

Introduction

In the search for alternative fuels to petroleum, biodiesel has gained expression in the market and its production has been increasing steadily. In fact, biodiesel production through transesterification reaction of triglycerides (vegetable oils and animal fats) is rapidly increasing due to strong governmental policies and incentives. Sustainable biodiesel production requires optimization of the production process and drastic increase in the utilization of glycerol, the principal by-product of the process. With the introduction of large volumes of glycerol coming from biodiesel production, it is imperious to find new applications for this chemical; otherwise the economic feasibility of the biodiesel as a renewable fuel can be impaired [1,2]. Recent studies report the use of glycerol for the production of chars [3,4] so in the present study we aim to synthetize glycerol-based activated carbons *via* a two-step procedure involving carbonization followed by activation, and test them as adsorbents for the removal of the pharmaceutical compounds from aqueous solution.

Materials and Methods

Glycerol-based activated carbons were prepared by combination of acid carbonization and chemical activation following the methodologies reported, respectively, in ref. 3 and 5. Two glycerol samples were assayed: sample GC (87%, Analar Normapur) and sample GI (84 %) supplied by a biodiesel producer (Iberol – Portugal). Briefly, glycerol and concentrated sulfuric acid were mixed in a flask and stirred at room temperature for 30 min until foaming ceased. Afterward, the mixture was heated in an autoclave at 180 °C for 6 h. The obtained char was washed several times using distilled water and dried at 100 °C. Thereafter, the char was impregnated with potassium carbonate solution for 2 h at room temperature, then dried at 100 °C. The mixture was activated in a horizontal furnace at under N_2 flow (5 cm^3 s^{-1}). The temperature was raised (10 °C min^{-1}) up to the activation temperature and kept for 1 h. After cooling, under N_2 flow, the sample was thoroughly washed with distilled water and dried at 100 °C. Different char:K_2CO_3 weight ratios and activation temperatures were assayed.

The textural properties were investigated through N_2 adsorption-desorption isotherms; and the chemical properties were discussed based on pH_{PZC}, elemental analysis and Fourier transform infrared (FTIR). The morphological characterization of the materials was performed by SEM.

Results and Discussion

The morphological analysis performed by SEM (Fig. 1(a)) reveals that the char prepared from commercial glycerol (sample GC) is constituted by interconnected spheres with diameters of ≈ 2 μm. The N_2 adsorption isotherms of the char revealed its incipient porosity development since according to the IUPAC classification [6] a type II isotherm was obtained ($A_{BET} \approx 10\ m^2\ g^{-1}$). The activation of the glycerol-derived char with K_2CO_3 allowed to prepare activated carbons with apparent surface areas higher than 1000 $m^2\ g^{-1}$ and presenting type I isotherms (Fig. 1(b)) revealing the presence of a well-developed micropore network.

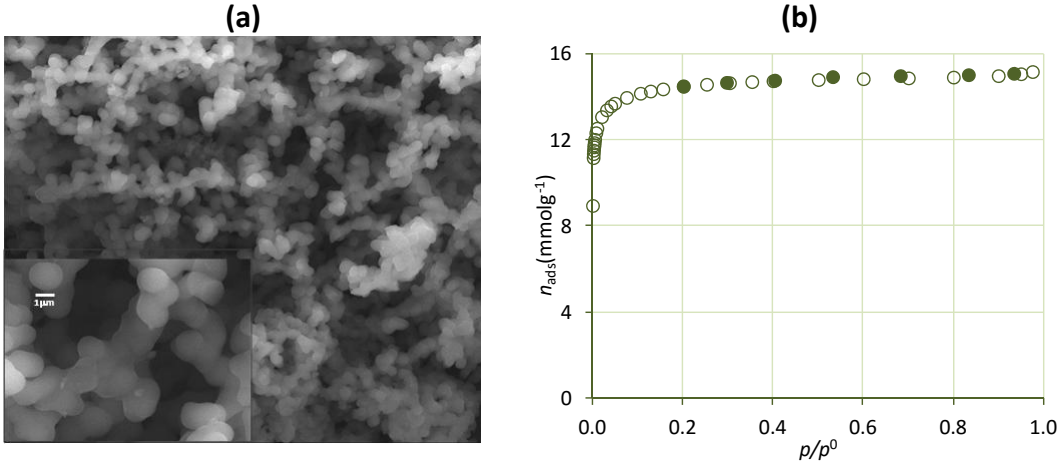

Fig. 1 (a) SEM photograph of the char prepared from sample GC and (b) N_2 isotherm at -196 °C of activated carbon prepared using 3 g of K_2CO_3 per gram of GC-char and 800 °C during 1h for the activation (closed symbols are desorption points).

The FTIR and pH_{PZC} data reveal numerous functional groups distributed on the carbon surface. Considering all the above facts, glycerol-derived activated carbons will be tested as adsorbents for pharmaceutical compounds in liquid phase.

Acknowledgements

The authors thank Fundação para a Ciência e Tecnologia (FCT, PT) for financial support through projects UID/MULTI//00612/2013 (CQB) and UID/QUI/50006/2013 (LAQV-REQUIMTE). MKSB (SFRH/PBD/84542/2012) and ASM (SFRH/BPD/86693/2012) also thank FCT for their Post-doc grants. IBEROL- Sociedade Ibérica de Oleaginosas for supplying the glycerol waste.

References

1. M.A. Betiha, H.M.A. Hassan, E.A. El-Sharkawy, A.M. Al-Sabagh, M.F. Menoufy, H.E.M. Abdelmoniem, Appl. Catal. B: Environ. 182 (2016) 15-25.
2. B.P. Pinto, J.T. Lyra, J.A.C. Nascimento, C.J.A. Mota, Fuel 168 (2016) 76-80.
3. B.L.A. Prabhavathi Devi, K.N. Gangadhar, K.L.N. Siva Kumar, K. Shiva Shanker, R.B.N. Prasad, P.S. Sai, J. Mol. Catal. A: Chem. 345 (2011) 96-100.
4. R.S. Ribeiro, A.M.T. Silva, M.T. Pinho, J.L. Figueiredo, J.L. Faria, H.T. Gomes, Catal. Today 240 (2015) 61-66.
5. A.S. Mestre, E. Tyszko, M.A. Andrade, M. Galhetas, C. Freire, A.P. Carvalho, RSC Advances 25 (2015) 19696-19707.
6. M. Thommes, K. Kaneko, A.V. Neimark, J.P. Olivier, F. Rodriguez-Reinoso, J. Rouquerol, K.S.W. Sing, Pure Appl. Chem. 87 (2015) 1051-1069.

Adsorción de Arsénico en Disolución Acuosa mediante un Sistema Combinado de TiO_2 y Hierro Metálico

J.M. Raez, A. Arencibia*, Y. Segura, J.M. Arsuaga, M.J. López-Muñoz
Grupo de Ingeniería Química y Ambiental, Universidad Rey Juan Carlos, C/ Tulipán s/n, Móstoles 28933, Madrid, España.
*amaya.arencibia@urjc.es

Introducción

La contaminación del agua por arsénico es un problema global que afecta a millones de personas. Debido a su peligrosidad, la OMS lo ha catalogado como uno de los diez elementos químicos más tóxicos y cancerígenos, recomendando una concentración máxima de 10 $\mu g \cdot L^{-1}$ en aguas de consumo [1]. Su presencia en el medio acuoso se debe tanto a fuentes naturales como antropogénicas y se encuentra comúnmente en sus formas inorgánicas arsenito, As(III), y arseniato, As(V), dependiendo del pH y potencial redox del agua [2].

Generalmente el tratamiento de aguas contaminadas con arsénico se lleva a cabo mediante una primera etapa de oxidación de As(III) a As(V), seguida de la posterior eliminación de As(V) mediante adsorción, co-precipitación, coagulación, filtración, o intercambio iónico [2,3], ya que la especie reducida es más difícil de eliminar de forma directa. En nuestro grupo de investigación se está estudiando la viabilidad de emplear un sistema combinado de dióxido de titanio (TiO_2) y hierro metálico (Fe^0), eliminando As(III) y As(V) simultáneamente mediante oxidación fotocatalítica y adsorción. Dentro de este trabajo global, el objetivo del presente estudio es estudiar el proceso de adsorción de As(III) y As(V) en disolución acuosa utilizando como adsorbentes TiO_2, hierro metálico y el sistema combinado de TiO_2 con hierro metálico. Para ello se ha evaluado la influencia de la concentración de arsénico en disolución, el pH inicial de la disolución de arsénico y la relación másica entre los dos adsorbentes.

Material y métodos

Los experimentos de adsorción de arsénico se llevaron a cabo en un reactor discontinuo de un litro de capacidad, en presencia de oxígeno y con agitación magnética. Las disoluciones acuosas de As(III) y As(V) se prepararon a partir de $NaAsO_2$ y $Na_2HAsO_4 \cdot 7H_2O$ (90% Aldrich) respectivamente, ajustando la concentración inicial entre 10 - 30 $mg \cdot L^{-1}$. La cantidad de TiO_2 P25 (Evonik) se mantuvo constante (0,25 g) y se modificó la cantidad de Fe^0 (97%, Aldrich) entre 0 - 0,20 g para dos valores de pH inicial (pH= 9 y pH=3). La concentración de arsénico en disolución se determinó a partir de un método colorimétrico basado en la formación del complejo molibdato-arsénico (V) empleando un espectrofotómetro UV-vis JASCO V-630.

Resultados y discusión

El estudio del proceso de adsorción se ha llevado a cabo analizando la disminución de la concentración de As(III) y As(V) durante 3 horas, observando diferencias significativas entre las capacidades de adsorción de los tres sistemas investigados. La Figura 1 muestra los porcentajes de adsorción de As(III) y As(V) obtenidos para

10 mg·L^{-1} a pH 9 y pH 3, utilizando 0,25 g/L de TiO_2 y 0,1 g/L de Fe^0. Como puede apreciarse, en general la adsorción es mayor en el sistema mixto (TiO_2+Fe^0), siendo más significativa a pH ácido.

En medio básico el porcentaje de adsorción de As(III) sobre TiO_2 es mayor (20%) que el de As(V) (10%). Sin embargo, en condiciones ácidas la tendencia se invierte presentando valores de un 3% y un 15%, para As(III) y As(V), respectivamente. Estas diferencias se atribuyen a los cambios de carga neta superficial que sufre el TiO_2 (punto isoeléctrico a pH 6,8) y a la especiación tanto de As(III) como de As(V) en función del pH. A pH básico la especie predominante de As(V) está cargada negativamente, $HAsO_4^{2-}$, siendo repelida por la superficie negativa del TiO_2, mientras que la especie neutra de As(III), H_3AsO_3, se ve menos influenciada por lo que se adsorbe mayor cantidad. Por el contrario, a pH ácido se adsorbe mayor cantidad de As(V), ya que su forma iónica $H_2AsO_4^-$ presenta mayor afinidad por el adsorbente con carga neta positiva que la especie neutra de As(III) [2 ,4].

El empleo de Fe^0 como adsorbente a pH básico no presentó adsorción significativa de ninguna de la especies de arsénico. Sin embargo, a pH ácido la adsorción fue de 48% y 56% para el As(III) y As(V), respectivamente. En el sistema combinado (TiO_2+Fe^0) también se aprecia un aumento significativo en la adsorción cuando el proceso se lleva a cabo a pH 3, llegando a eliminar un 69% y 79% de As(III) y As(V), respectivamente. Este aumento se debe a la formación de óxidos/hidróxidos de hierro en la superficie del adsorbente producidos durante la corrosión del hierro metálico [3]. Generalmente, estos óxidos presentan una carga positiva a pH 6 [4], lo que favorece la adsorción de As(V) con respecto al As(III).

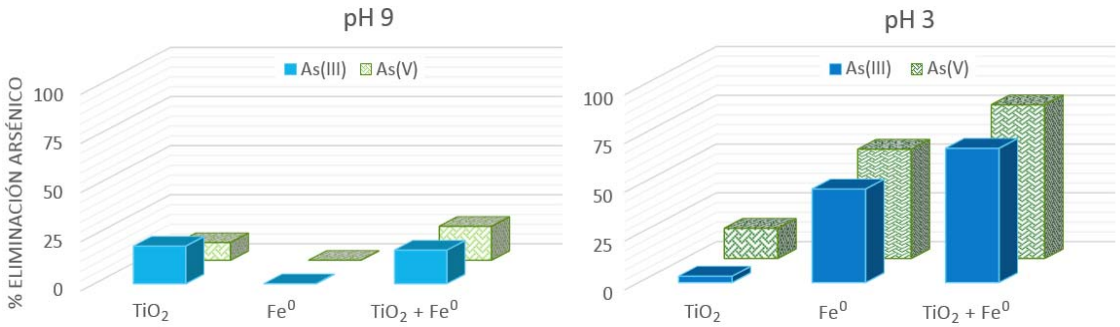

Fig. 1. Porcentaje de adsorción de As(III) y As(V) mediante TiO_2, Fe(0) y (TiO_2+Fe^0) a pH 9 y pH 3 (C_0= 10 mg/L).

Agradecimientos

Los autores agraden la financiación para la realización de este trabajo al Ministerio de Economía y Competitividad (proyectos CTM2012-34988 y CTM2015-69246-R) y a la Comunidad de Madrid (proyecto 2013/MAE-2716-REMTAVARES-CM)

Bibliografía

1. World Health Organization, Guidelines for drinking-water quality, 4th Ed., WHO, Geneva, 2011
2. P. K. Dutta, A. K. Ray, V. K. Sharma,F.J. Millero, J. Colloid. Interf. Sci. 278 (2004) 270-275.
3. F. Fu, D. D. Dionysiou, H. Liu, J. Hazard. Mater. 267 (2014) 194-205.
4. Y. Mamindy-Pajany, C. Hurel, N. Marmier, M. Roméo, Desalination 281 (2011) 93-99.

Computational Infrared Spectra of Zeolites as a Characterization Tool

Rocio Bueno-Perez[a], Salvador R. G. Balestra[a], Sofia Calero[a], Patrick J. Merkling[a*]
[a]Universidad Pablo de Olavide, Department of Physical, Chemical and Natural Physics, Ctra. de Utrera km. 1, 41013 Seville (Spain)
**pjmerx@upo.es*

Introduction

Zeolites are a type of nanoporous materials of great industrial and natural importance. Its frameworks are characterized by their regularity, and, due to this, they are typically modeled as rigid. However, these structures vibrate and generate infrared spectra showing some bands that are sensitive to structural details, such as topology, channel system, or chemical composition.

Moreover, the flexible force field used to model the zeolite might have an effect on the vibrational patterns obtained by simulation, depending on its accuracy and/or the target group of zeolites for which it was parametrized. Thus, the computation and comparison of infrared spectra can be an interesting tool to detect unexpected behaviors among a group of analogous zeolites or predict similar patterns in zeolites with different compositions.

Materials and Methods

Molecular Dynamics (MD) simulations were performed in the NVT ensemble at 298K with a time step of 0.5 fs to obtain the computational infrared spectra of 216 zeotypes. Keeping in mind that some zeotypes have different chemical compositions the corresponding minimised all-silica framework, whose crystallographic data is reported in the Database of Zeolite Structures [1], was taken as representative of each zeotype. These frameworks were modeled using the force field defined by Nicholas[2], which has been assessed to reproduce experimental infrared spectra [3]. Finally, the similarities and differences between several spectra were studied through the similarity index, explained in a previous work [3], and relationships were established using an algorithm based on graph theory [4]. Details on how best to perform this novel analysis will be given.

Results and Discussion

A total number of 216 infrared spectra were obtained, whose bands span from frequency values of 200 to 1400 cm^{-1}. In general terms, the vibrational pattern in the range of 900-1400 cm^{-1} involves Si-O bonds, while below 900 cm^{-1} the vibrational contribution belongs to tetrahedra bendings and external linkages.

The study of pairwise similarities over the 216 spectra results in a wide variety of values from 0.30 to 0.99 for pairs of zeolites. As an example, figure 1 shows the infrared spectra of the zeotypes AFG and LIO which share a similarity of 0.99, a similar chemical composition with a Si/Al ratio of 1, similar tiling arrangement and topology. On the contrary, CZP shows a similarity value around 0.3 against AFG or LIO. CZP is a very different, chiral topology obtained experimentally for a zincophosphate that has different tiling and a much more complex channel system. The network based on

pairwise relations suggests the existence of different communities generally related to chemical composition, topology and structural complexity.

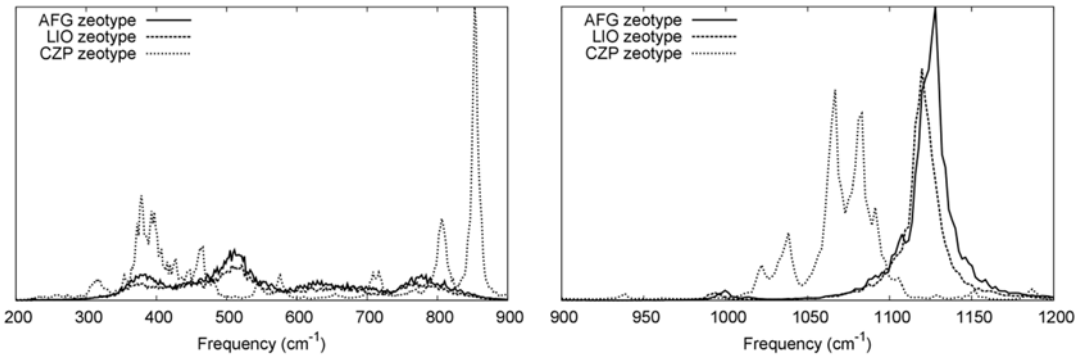

Fig. 1. Computational infrared spectra of all-silica framework corresponding to zeotypes AFG, LIO and CZP.

Among possible applications, this partitioning of the zeolites in communities based on zeotype and on composition (aluminosilicates, germanates, silicogermanates, and frameworks with any other composition) might give clues on the feasibility of the synthesis of a hypothetical framework/composition combination.

Acknowledgements

This work is supported by the European Research Council through an ERC Starting Grant (S.C., ERC2011-StG-279520-RASPA) and by the MINECO through an I+D project (CTQ2013-48396-P). S. R. G. thanks the MINECO for his predoctoral fellowship.

References

1. Ch. Baerlocher and L.B. McCusker, Database of Zeolite Structures: http://www.iza-structure.org/databases/

2. J. B. Nicholas, A. J. Hopfinger, F. R. Trouw, L. E. Iton. J. Am. Chem. Soc. 1991, 113 (13), 4792-4800

3. R. Bueno-Perez, S. Calero, D. Dubbeldam, C. O. Ania, J. B. Parra, A. P. Zaderenko, P. J. Merkling. J. Phys. Chem. C 2012, 116, 25797-25805

4. S. Gomez, P. Jensen, A. Arenas, Phys. Rev. E 2009, 80, 016114

Scaled-up Cork-Derived Activated Carbon: Performance as Pharmaceuticals Adsorbent

Marta A. Andrade[a*], Ana S. Mestre[a], Susana P. Silva[b], Ana P. Carvalho[a]
[a] Centro de Química e Bioquímica, Faculdade de Ciências, Universidade de Lisboa, 749-016 Lisboa, Portugal
[b] Corticeira Amorim, S.G.P.S., S.A., Rua do Ribeirinho, 202, 4536-907 S. Paio de Oleiros, Portugal
mvandrade@fc.ul.pt

Introduction

Cork transformation is one of the most important and sustainable industries in the Portuguese and Mediterranean region economies, producing several materials beyond the traditional ones, from agglomerates to composites, applied in a series of end products. The manufacturing process originates a set of by-products, as is the case of granules of expanded corkboard, among many others.

Integrated in a previous QREN project, industrial expanded corkboard granules were explored as precursors for the preparation of activated carbons at the lab-scale which proved to perform as efficient adsorbents for pharmaceutical compounds from liquid phase [1]. In the present study we investigate the performance of the activated carbon obtained from the scale-up of the patented activation methodology [2]. The potentialities of this material in liquid phase assays are herein evaluated, aiming a future application in synthetic and real water matrixes, in the context of project LIFE Impetus ”Improving current barriers for controlling pharmaceuticals compounds in urban wastewater treatment plants”.

Materials and Methods

The preparation of carbon S800/Lab was reported elsewhere [1]. Briefly, granules of expanded corkboard (obtained from Amorim Isolamentos, Portugal) were used as precursor, being activated at 800 °C for 1 h, with steam generated in a bubbler half full with distilled water at 90 °C and carried to the sample by a N_2 flow in a quartz reactor placed in a vertical furnace (Thermolyne, model 21100). Carbon S800/Scale-up was obtained from the scale-up of this procedure, involving the preparation of 10 activation batches of 15 dm^3 of expanded corkboard granules in a 50 dm^3 rotating stainless steel reactor. The potentialities of the prepared activated carbons as liquid phase adsorbents were evaluated through screening assays with six pharmaceutical compounds: ibuprofen (Ibu), paracetamol (Para), acetylsalicylic acid (ASA), caffeine (Caf), clofibric acid (Clof), and iopamidol (Iop). The removal efficiencies, after a contact time of 24 h (6 mg of carbon for 9 cm^3 of each pharmaceutical solution of 120 mg dm^{-3}), were determined using UV–vis spectrophotometry (Genesys 10S).

Results and Discussion

The nanotextural parameters of the activated carbons show that the scale-up has led to a less developed porous network. Actually, compared to lab-prepared carbon, sample

S800/Scale-up has half of the supermicropores volume and a quarter of the mesopore volume.

Table 1. Nanotextural properties of the studied activated carbons.

Sample	A_{BET} (m^2g^{-1})	V_{total} (cm^3g^{-1})	V_{meso} (cm^3g^{-1})	V_{ototal} (cm^3g^{-1})	V_{oultra} (cm^3g^{-1})	V_{osuper} (cm^3g^{-1})
S800/Lab	750	0.50	0.22	0.28	0.09	0.19
S800/Scale-up	590	0.44	0.05	0.18	0.10	0.08

Regarding the results of the screening assays for the removal of the pharmaceutical compounds, the efficiencies obtained using both carbons are displayed in Figure 1. The performance of carbon S800/Scale-up for most of the pharmaceutical compounds is similar or slightly inferior regarding the lab-made carbon (S800/Lab).

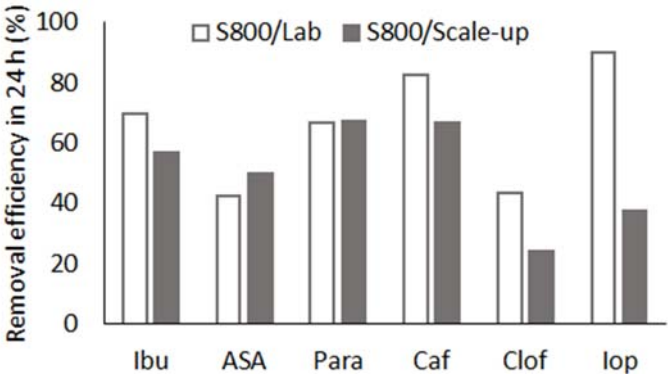

Fig. 1. Removal efficiencies for 24 h of the mentioned pharmaceuticals by carbons S800/Lab and S800/Scale-up.

An accentuated negative impact of the scale-up of the process is reflected only in the case of clofibric acid and iopamidol removal. The lower removal for iopamidol is certainly related with the smaller volume of supermicropores and mesopores of carbon S800/Scale-up, that causes diffusional constrains to this molecule, since the presence of agglomerates was reported in the studied experimental conditions [3]. However, from the perspective of an application in environmental conditions, it is expectable that S800/Scale-up material may reach similar iopamidol removal to that of lab-made carbon, since in the concentration range detected in real samples iopamidol is present as a monomer.

Acknowledgements

The authors thank EU funding through the Project LIFE 14 ENV/PT/000739-LIFE Impetus, Fundação para a Ciência e Tecnologia for financial support to CQB (PEst-OE/QUI/UI0100/2014), and COMPETE, AdI – QREN Project WaterCork (nº 5523). ASM thanks FCT for the Post-doc grant SFRH/BPD/86693/2012. The authors thank Hovione for the supply of iopamidol.

References

1. Mestre, A.S., Pires, R.A., Aroso, I., Fernandes, E.M., Pinto, M.L., Reis, R.L., Andrade, M.A., Pires, J., Silva, S.P., Carvalho, A.P., *Chem Eng J*, 253 (2014), 408-417.
2. Martins, S.P., Mestre, A.S., Carvalho, A.P. and Correia, P.B., 2012. Processo de produção de carvão activado a partir de material de cortiça, PT 106637 B, Portugal.
3. Mestre, A.S., Machuqueiro, M., Silva, M., Freire, R., Fonseca, I.M., Santos, M.S.C.S., Calhorda, M.J., Carvalho, A.P., *Carbon*, 77 (2014), 607-615.

Oxidative Destruction of Cyanide Species from Mining Effluents: Chemical vs Photocatalytic Oxidation

Juan José Viña Mediavilla[a], María C. Fernández de Córdoba[b], Inmaculada Velo Gala[b], Julia Ayala Espina[a], Begoña Fernández Pérez[a], Conchi Ania[b*]

[a] *Universidad de Oviedo, Oviedo, España*

[b] *ADPOR Group, Instituto Nacional del Carbón INCAR, CSIC), 33011, Oviedo, España*

**conchi.ania@incar.csic.es*

Introduction

Cyanide species (including thiocyanates) are formed in several industrial processes such as gold mining activities and the production of coke in steel factories. Although thiocyanates are less toxic than cyanides (in the mining industry they may be deliberately produced as a harmless form of cyanides for their disposal), they are more stable and difficult to destroy, and both pose a major environmental and health issue concern as they can be generated in high concentrations in the industrial effluents. With more stringent environmental regulations coming to force, the search of new and more effective methods to reduce the concentration of both cyanides and thiocyanates down to acceptable limits becomes a priority [1,2]. In this regard, much interest is currently being paid to the application of advanced oxidation processes (AOPs) as clean and efficient technologies for wastewater treatment, since they can promote the mineralization of pollutants through the generation of highly oxidative species. The objective of this work to investigate the oxidative destruction of cyanide species from wastewater effluents generated by the mining industry, using chemical and photoassisted oxdiation. The simultaneous degradation of cyanides and thiocyanates (and their mixtures) will also be envisaged.

Methods

Chemical oxidation was carried out using potassium permanganate as oxidant, as described elsewhere [3,4]; briefly, different amounts of $KMnO_4$ were put in contact with 100 mL of a solution containing ca. 25-500 ppm of cyanides (pH was adjusted to 12-14 with lime) and allowed to react under vigorous stirring for 20 min. The photoassited oxidation was carried out using cyanide (500-25 ppm) and thiocyanate (200 ppm) aqueous solutions in a batch reactor (250 mL) illuminated by a UV-Vis lamp (300 W] with a sunlike radiation spectrum, vertically suspended above the reactor. The photooxidation was explored in the absence and presence of catalysts (i.e., semiconductors). The catalysts suspensions (ca. loadings of 0.5 g/L) were initially equilibrated under mechanical stirring (900 rpm) and darkness, and then irradiated for 120 min providing a constant air flow of ca. 50 mL/min to ensure a constant oxygen concentration. During the irradiation, small aliquots of the solution (~1 cm^3) were taken out at predetermined time intervals and analyzed by flow injection analysis using a colorimetric method. All the experiments were done in duplicate with deviations below 5% in all cases; reported data represent the average values.

Results and Discussion

In this work, we have explored the effect of thiocyanates in the oxidation rate and conversion of cyanides from solution, comparing chemical and photoassisted methods. Figure 1 shows the dependence of the cyanides concentration with the dosage of permanganate (as oxidant) for the chemical oxidation of thyocianates. As seen, the concentration of cyanides in solution increases with the amount of permanganate used in the reaction; interestingly, the trend follows a plateau at dosages of permanganate of 1 mmol and above. This suggests that along with cyanides, permanganate is capable of inducing the breakdown of thiocyanates themselves, which has to be taken into account for the evaluation of the conversion when both species are simultaneously present in the solution. Also, the appearance of the plateau suggests that the rate of the chemical oxidation of thiocyanates is slow, compared to that of cyanides [3,4].

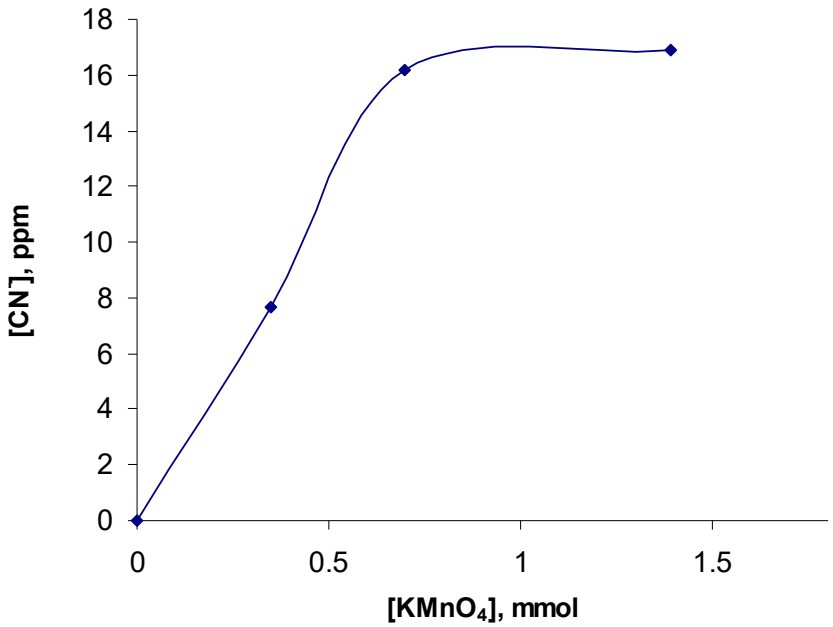

Fig.1. Dependence of the cyanides concentration with the amount of $KMnO_4$ for the oxidation of 0.35 mmol of thiocyanates.

Acknowledgements

Authors thank the financial support of Spanish MINECO (grant CTM2014-56770-R).

References

1. T.I. Mudder, M. Botz, K.A. Hagelstein. The Chemistry and Treatment of Cyanidation Wastes, 2001
2. W.D. Gould, M. King, B.R. Mohapatra, R.A. Cameron, A. Kapoor, D.W. Koren, Minerals Engineering 34 (2012) 38–47.
3. J.P. Sancho, B. Fernández-Perez, F. Bellón, 9th Int. Mine Water Congress 2005.
4. B. Fernández-Perez Desarrollo de un nuevo método para la eliminación de cianuro de aguas residuales de mina, PhD thesis, University of Oviedo, 2007.

Evaluación de la Captura de CO_2 en Heterostructuras Porosas Basadas en Montmorillonita Modificadas con Grupos Aminos

J.A. Cecilia[a*], E. Vilarrasa-García[b], D.C.S. Azevedo[b], C.L. Cavalcante Jr. [b], E. Rodríguez-Castellón[a]

[a] Universidad de Málaga, Departamento de Química Inorgánica, Cristalografía y Mineralogía, Campus de Teatinos, Facultad de Ciencias, 29071 Málaga, España

[b] Universidade Federal do Ceará, Departamento de Engenharia Química, GPSA-Grupo de Pesquisa em Separaçoes por Adsorçao, Campus do Pici, Fortaleza, Ceará 60455-760, Brazil

**jacecilia@uma.es*

Introducción

Los minerales de la arcilla son materiales muy versátiles con una gran variedad de aplicaciones principalmente en el campo de la adsorción y la catálisis [1]. Las propiedades texturales de estos materiales pueden mejorarse modulando sus propiedades fisicoquímicas como el área superficial y el volumen de poro mediante la adición de pilares entre dos láminas adyacentes. La metodología más usada es la incorporación de polioxocationes en el espaciado interlaminar. Otra estrategia sintética es la incorporación de un catión voluminoso que expande el espaciado basal y la posterior formación de pilares dando lugar a materiales de elevada alta área superficial y gran estabilidad térmica en comparación con los tradicionales polioxocationes [2,3].

En el presente trabajo estos materiales de origen natural se han evaluados en procesos de adsorción de CO_2. Para ello, tanto la montmorillonita natural como las heteroestructuras porosas basadas en montmorillonita han sido modificadas con la incorporación de grupos aminos mediante el anclaje de aminopropiltrietoxisilano o mediante la impregnación con polietilenimina o tetrapentilenimina.

Materiales y Métodos

Tanto la montmorillonita natural como las heteroestructuras porosas basadas en montmorillonita, así como los materiales funcionalizados con grupos aminos se caracterizaron por difracción de rayos X, espectroscopia de infrarrojo adsorción-desorción de N_2 a -196 ºC y análisis elemental para evaluar el contenido de nitrógeno de los materiales funcionalizados con grupos aminos.

Las isotermas de adsorción de CO_2 se midieron con un equipo Micromeritics ASAP 2020, mediante un análisis volumétrico a 25 ºC. Previamente al análisis, los materiales sintetizados fueron desgasificados a 115 ºC y una presión de 10^{-4} mbar durante toda la noche [4].

Resultados y Discusión

Los difractogramas de rayos X muestran como las reflexiones basales desaparecen cuando se forma la heteroestructura porosa basada en montmorillonita mientras las no basales se mantienen, lo que confirma la formación de una estructura pilareada a lo largo del eje *c*.

Las isotermas de adsorción-desorción de N_2 a -196 ºC muestran un incremento área

superficial desde 116 m^2g^{-1} para la montmorillonita hast 625 m^2g^{-1} para la heteroestructura porosa basada en montmorillonita, lo que indica la formación de una estructura de alta porosidad tras el proceso de expansión del espaciado basal y posterior pilareado.

La adsorción-desorción de CO_2 a 25 ºC (Fig. 1) de la heteroestructura mesoporosa basada en montmorillonita muestra una mayor capacidad de capturar CO_2 (0.62 mmol g^{-1}) que la montmorillonita de partida (0.11 mmol g^{-1}). La incorporación de grupos aminos en la heteroestructura porosa basada en montmorillonita produce un progresivo aumento de la adsorción de CO_2, obteniéndose unos valores máximos de 1.14 mmol g^{-1} para PCH-20A, 1.45 mmol g^{-1} para PCH-60P y 1.64 mmol g^{-1} para PCH-60T.

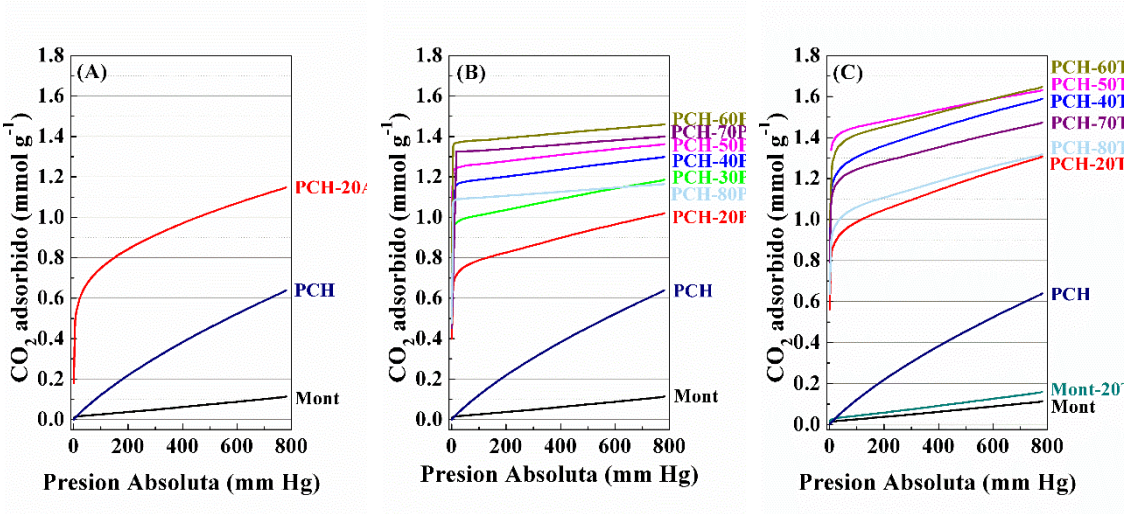

Fig. 1. Isotermas de adsorción de CO_2 a 25 ºC y 1 bar para la montmorillonita y las heteroestructuras basadas en montmorillonita funcionalizados con grupos aminos.

Agradecimientos

Los autores del presente trabajo quieren agradecer al Ministerio de Economía y Competitividad proyecto CTQ2015-68951-C3-3-R, Proyecto de Excelencia de la Junta de Andalucía P12-RNM-1565, Fondos FEDER y al Proyecto Europeo 295156 FP7-PEOPLE-2011-IRSES por su apoyo económico.

Referencias

1. A. Vaccari, Appl. Clay Sci. 14 (1999) 161-198.
2. A. Galarneau, A. Barodawalla, T.J. Pinnavaia, Nature 374 (1995) 529–531.
3. J.A. Cecilia, C. García-Sancho, F. Franco, Micropor. Mesopor. Mater. 176 (2013) 95-102.
4. E. Vilarrasa-García, E.M. Ortigosa-Moya, J.A. Cecilia, C.L. Cavalcante Jr., J. Jiménez-Jiménez, D.C.S. Azevedo, E. Rodríguez-Castellón, Micropor. Mesopor. Mater. 209 (2015) 172-183.

Activated Carbons Produced from Mixtures of Synthetic Polymers by Physical and Chemical Activation: Application in MCPA Removal

Cristóvão Ramiro Belo[a,b*], Isabel Cansado[a], Paulo Mourão[a]

[a] *Centro de Química de Évora and Departamento de Química, Instituto de Investigação e Formação Avançada and Escola de Ciências e Tecnologia, Universidade de Évora*

[b] *Departamento do Ensino de Química da Universidade Nacional Timor Lorosa'e, Dili, Timor-Leste*

**cristovaoramirobelo@ymail.com*

Introduction

Pollution of surface and ground waters causes risk to human health because of the potential health hazards of its contents in organic and inorganic compounds [1-3]. Pesticides belongs to this group of hazardous compounds that may pollute water due to their extensive application in agriculture, in particularly in developing countries like Timor Lorosa'e. In the other side, concerning the solids wastes, mainly the synthetics polymers, same restrictions affect the recycling possibilities and push them into the bin.

Carbon materials production is one of the areas with greatest interest of the scientific and industrial communities and in particular the possibility of using mixtures of waste materials as precursors for activated carbon (AC) production, which is environmental and economical favourable. Most AC are referred as an effective adsorbent for the separation and removal of unwanted compounds or substances from waste effluents, once they exhibit a developed porous structure, can be produced from a variety of carbonaceous raw materials and present also the possibility to be regenerated and reused [1-2]. In practice, coal, agricultural by-products or lignocellulosic materials are the main sources for the commercial AC production. Nevertheless, AC can be prepared from a wide variety of relatively low cost, natural or synthetic precursors by chemical or physical activation where the wastes can be economically valorised. The main innovative aspect of this work is the production of high porous AC, by physical or chemical activation, using CO_2 and the K_2CO_3 as activating agents respectively, from a synthetic polymeric mixture, with polyethyleneterephthalate (PET) and polyacrylonitrile (PAN) as precursors, for pesticides removals, such 4-chloro-2-methylphenoxyacetic acid (MCPA), from the aqueous phase.

Materials and Methods

AC have been produced from PET and PAN separately or in a mixture, by physical activation with carbon dioxide and chemical activation, with K_2CO_3, with a ratio of 2, at 1073K. All AC were chemical and structurally characterized using the most used techniques, such: determination of the point of zero charge (pzc), FTIR, elemental analysis and by nitrogen adsorption at 77 K. Selected AC were tested on the MCPA removals from the liquid phase, in an acidic medium, at 298 K. A fixed amount of adsorbent was added to a flask containing the same volume of aqueous solutions with different initial known concentrations of MCPA. The tests were completed with an equilibrium time of 1 day. The residual concentrations of MCPA were determined by UV-Vis spectrophotometry, at an appropriate wavelength.

Results and Discussion

The production of AC was achieved using the most common industrial and consumer solid waste, namely PET, alone or blended with another synthetic polymer such as PAN. The PET-PAN mixture (1:1 W/W %) was subjected to carbonization, with a pyrolysis yield off 31.9%, between that obtained with PET (16.9%) or PAN (42.6%) separately. By mixing PET, as a raw material, with PAN (different ratio), an improvement in the final yield of the AC production, for the same activation time, with CO_2, was found. An increase of the basic character, with a pzc around 10.5 and some characteristic bands on the FTIR spectra were identified on these AC. Some textural properties were enhanced and all AC revealed high apparent surface area getting 1400, 1230 and 1117 m^2g^{-1} and pore volume of 0.46, 0.56 and 0.50cm^3g^{-1} and an external surface area of 399, 20 and 13 m^2g^{-1}, respectively with PET, PAN and PET-PAN. The PET-PAN chemical activation, with K_2CO_3 allows to produce AC with a microporous structure well developed, presenting a higher surface area (superior to 2000 m^2g^{-1}) and micropore volume (0.95 cm^3 $g^{-1)}$, when compared with those prepared by physical activation.

Selected AC were tested on the MCPA removals from the liquid phase. Those prepared by physical activation exhibit a MCPA adsorption varying from 1.0 $mmolg^{-1}$ on PET-PAN-1:1-81200, 1.2 $mmolg^{-1}$ on PAN-8960 and to 1.7 $mmolg^{-1}$ on PET-8300. Those prepared by chemical activation presented a very high MCPA adsorption capacity, varying from 1.9 $mmolg^{-1}$ on PET-K_2CO_3, 3.5 $mmolg^{-1}$ on PAN-K_2CO_3 and 3.8 $mmolg^{-1}$ on PET-PAN-1:1-K_2CO_3. Concerning these adsorption systems, the controlling factor seems to be the porous volume and the mean pore size rather than the apparent surface area.

As a remarkable result is the use of different synthetic polymers wastes, which are often found mixed in the environment, as precursors for the AC production, with exceptional potential application on pesticides removals from the liquid phase.

Acknowledgements

This work was supported by Fundação Calouste Gulbenkian (Doctoral Grant nº 126541 by Fundação para a Ciência e a Tecnologia (Plurianual Finance Project Centro de Química de Évora (619)).

References

1. R.C. Bansal, Activated Carbon, Panjab University Chandigarh, India, 1988.
2. I.P.P. Cansado, P.A.M. Mourão, A.I. Falcão, M.M.L. Ribeiro Carrott, P.J.M. Carrott, Fuel Process Technol 103 (2012) 64-70.
3. P.J.M. Carrott, J.M.V. Nabais, M.M.L. Ribeiro Carrott, J.A. Menendez, Micropor and Mesopor Mat 47 (2001) 243-252.

HKUST-1 Confinado en las Cavidades de Materiales de Carbón Activado: Mejora en la Estabilidad Mecánica

Mirian E. Casco[a], Javier Fernández-Catalá [a], Manuel Martínez-Escandell[a], Enrique V. Ramos-Fernández[a], Joaquín Silvestre-Albero*[a].

[a] Laboratorio de Materiales Avanzados, Departamento de Química Inorgánica-Instituto Universitario de Materiales, Universidad de Alicante, Ctra. San Vicente-Alicante s/n, E-03690, España.

** joaquin.silvestre@ua.es*

Introducción

Los materiales porosos, incluyendo carbones activados y MOFs, han sido ampliamente propuestos en la literatura como adsorbentes prometedores en el almacenamiento de metano a altas presiones [1,2]. Mientras que los materiales MOF son capaces de alcanzar el nuevo valor fijado por el DOE de EEUU (263 v/v), a presiones moderadas (alrededor de 5 MPa en el caso específico de HKUST-1), materiales de carbón de alta superficie requieren presiones más grandes (cerca de 10 MPa) para llegar a este objetivo [1,2]. A pesar del comportamiento prometedor de los MOFs en comparación con los carbones activados, estos materiales presentan como inconveniente su baja estabilidad mecánica cuando se someten a una etapa de conformado, asociada a daños estructurales irreversibles. Estudios recientes de nuestro grupo de investigación han demostrado que la capacidad de adsorción de CH_4 en HKUST-1 puede disminuir hasta un 50% después de una etapa de conformado a 1,5 toneladas. Contrariamente a los MOFs, los carbones activados se caracterizan por una elevada estabilidad estructural y rigidez mecánica, de tal forma que estos materiales preservan sus excelentes propiedades de adsorción después de un conformado.

Con estos antecedentes, el presente trabajo plantea la síntesis y caracterización de materiales híbridos MOF@AC preparados mediante nucleación y crecimiento de nanocristales de MOF en las cavidades de un carbón activado perfectamente diseñado para este fin [3]. En una segunda parte del trabajo también se evaluó la nucleación de cristales de MOF en las cavidades de un monolito de carbón activado, con el fin de obtener monolitos híbridos.

Materiales y métodos

Para la síntesis de los materiales híbridos MOF@AC y para los monolitos se seleccionó como material huésped el MOF "HKUST-1", debido que este MOF presenta una elevada capacidad de adsorción, pero a su vez experimenta una disminución drástica de su capacidad cuando es sometido a una etapa de conformado.

Respecto a la matriz de carbón se escogió el material LMA726, procedente de activación química con KOH de un residuo de petróleo. Este carbón se caracteriza por una buena resistencia mecánica, una superficie aparente elevada (superior a 3000 m^2/g) y una estructura porosa muy desarrollada (contiene micro / meso y macroporos). En la formación de los monolitos híbridos también se utilizó una brea de mesofase como fuente de carbón, debido que estas breas tienen la propiedad de auto-sinterización, es decir, permiten obtener monolitos sin necesidad de un agente ligante. La síntesis de los

materiales MOF@AC se realizó modificando la síntesis del HKUST-1 realizada por J.T. Hupp y colaboradores [1]. En concreto, se añade el carbón activado inicialmente junto con el linker, después de 15 min se añade el precursor metálico y se utiliza agitación durante toda la síntesis. En la segunda parte del trabajo, los monolitos híbridos se sintetizaron confinando los cristales de HKUST-1 sin agitación y estudiando el efecto del etanol en la formación de los cristales confinados. Los materiales híbridos se caracterizaron mediante SEM, DRX, TG e Isotermas de adsorción de nitrógeno a 77K.

Resultados y discusión

Los estudios de adsorción de N_2 a 77 K y de difracción de rayos-X confirman que los materiales híbridos MOF@AC sintetizados en este trabajo son capaces de soportar una elevada compresión mecánica, preservando al mismo tiempo las excelentes propiedades de adsorción del MOF confinado y la estabilidad estructural (Figura 1). Estudios de adsorción de metano a 25ºC demuestran que tras el conformado los cristales confinados son capaces de mantener las propiedades de adsorción del material MOF original.

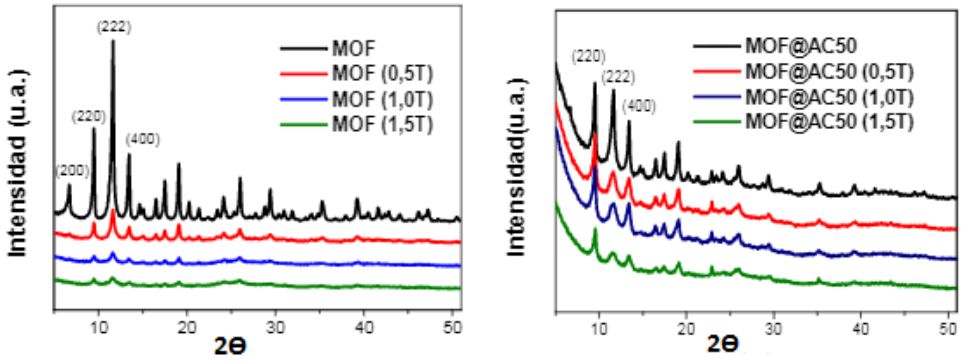

Fig. 1. Difracción de rayos X del MOF original y conformado, así como del hibrido con el 50% de carbón (MOF@AC50) original y después de conformar.

En la segunda parte del trabajo, los monolitos híbridos presentan una buena distribución de cristales de MOFs tanto dentro como en el exterior del monolito, y se caracterizan por tener una buena capacidad de adsorción, así como propiedades mecánicas mejoradas con respecto al monolito de carbón original.

Referencias

1. Y. Peng, V. Krungleviciute, I. Eryazici, J.T. Hupp, O.K. Farha, J.T. Yildirim, J. Am. Chem. Soc. 135 (32),(2013), 11887–11894.
2. M.E. Casco, M. Martínez-Escandell, E. Gadea-Ramos, K. Kaneko, J. Silvestre-Albero, F. Rodríguez-Reinoso, Chem. Mater. 27, (2015), 959−964.
3. M.E. Casco, J. Fernández-Catalá, M. Martínez-Escandell, F. Rodríguez-Reinoso, J.M. Ramos-Fernández, J. Silvestre-Albero, Chem. Commun. 51, (2015), 14191-14194.

Separation of Pentanol Isomers in ZIF-77

Rocío Bueno-Perez[a], Juan José Gutiérrez-Sevillano[a], Patrick J. Merkling*[a], Sofia Calero*[a]

[a]Universidad Pablo de Olavide, Department of Physical, Chemical and Natural Physics, Ctra. de Utrera km. 1, 41013 Seville (Spain)

**pjmerx@upo.es, scalero@upo.es*

Introduction

Pentanol isomers, also known as amyl alcohols, form a group composed of 1-pentanol (1P), 2-pentanol (2P), 3-pentanol (3P), 3-methylbutanol (3MB), 2-methylbutanol (2MB), 3-methyl-2-butanol (3M2B), 2-methyl-2-butanol (2M2B) and 2,2-dimethylpropanol (22DMP). They are often generated as side products in the chemical, pharmaceutical or biochemical industries. Their physicochemical similarities make the purification of these compounds difficult and require a multi-step process, which is economically and energetically costly, polluting and time consuming. Thus, alternative options for the purification of these isomers are highly desirable. In this study, we explore specifically the separation by adsorption with a specific, promising adsorbent material.

ZIF-77 is a framework from the Zeolitic Imidazolate family that is not based on any zeolitic topology [1]. The combination of zinc atoms and nitroimidazol generates a 2D system of channels which has been able to demonstrate high selectivities in hydrocarbons [2]. We used molecular simulations to evaluate the suitability of this structure for the separation of pentanol isomers and unravel how the adsorption selectivity is related to molecular structure.

Materials and Methods

Configurational bias Grand-Canonical Monte Carlo simulations yielded adsorption isotherms of each compound and equimolar mixtures, at room temperature and in a range of fugacities up to 100 kPa.

Results and Discussion

For a material to be an acceptable adsorbent, the first hurdle is that the guest molecule must be able to enter the structure and move within the structure. To illustrate the accessible part of the structure for each alcohol, the diffusion trail of a randomly inserted molecule is recorded (Figure 1). 1P is able to access both the z-channels and the narrower x-channels, 2P and 3M2B molecules are restricted to the z-channels, whereas 22DMP (and 2M2B) would only fit in the central region of a pore cavity due to their bulkiness. Therefore, the latter molecules cannot enter the structure and are discarded from further consideration. The preferential order of adsorption in ZIF-77 was determined based on permselectivities (Table 1): 1P >> 2P > 3P > 3MB > 2MB >> 3M2B. Two permselectivities are especially high, 1P over 2P, and 2MB over 3M2B.

For the sake of the discussion, the structural isomers of pentanol can be divided in four categories based on their heavy-atom skeleton: 1P would therefore be a linear molecule, 2P, 3P, 3MB and 2MB monobranched molecules, while 3M2B, 2M2B and

22DMP would be dibranched molecules. We find it useful to separate the latter three into molecules dibranched on different carbon atoms (3M2B) or on the same carbon atom (2M2B and 22DMP). Molecules from different categories can be separated very effectively, whereas molecules of the same category have similar permselectivities.

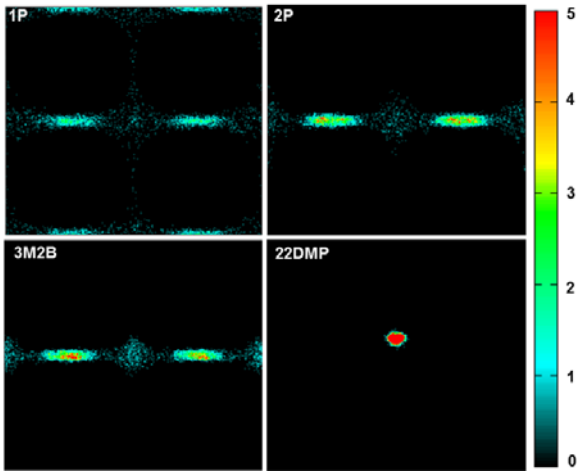

Fig. 1. Molecular dynamics trajectories of adsorbates within the framework in zx-view for four adsorbates: 1P, 2P, 3M2B and 22DMP.

Table 1. Permselectivity for alcohol molecules

Molecule *i*	Molecule *j*	Permselectivity
1P	2P	500
2P	3MB	4.0
3P	2MB	2.5
3MB	2MB	4.6
2MB	3M2B	39

Acknowledgements

The authors acknowledge Spanish MINECO for funding (CTQ2013-48396-P), including a predoctoral fellowship to R.B.-P.

References

1. R. Banerjee, A. Phan, B. Wang, C. Knobler, H. Furukawa, M. O'Keeffe, O. M. Yagui, Science 319 (2008) 939-943.
2. D. Dubbeldam, R. Krishna, S. Calero, A. O. Yazaydin, Angew. Chem. Int. Ed. 51 (2012) 11867 – 11871.
3. R. Bueno-Perez, J.J. Gutiérrez-Sevillano, D. Dubbeldam, P.J. Merkling, S. Calero, Chem. Phys. Chem. 16 (2015) 2735-2738.

Preparación de Carbón Activado mediante Activación con KOH. Influencia del Método de Impregnación sobre el Comportamiento Térmico

Carmen Lemus González, María Alexandre Franco[a], Carmen Fernández González, Vicente Gómez Serrano[a,*]

[a]Departemento de Química Orgánica e Inorgánica, Facultad de Ciencias, Universidad de Extremadura, Avda. de Elvas, s/n, 06006-Badajoz, España

**vgomez@unex.es*

Introducción

El carbón activado es cada vez más utilizado como adsorbente catalizador y soporte de catalizadores. El material de carbono puede prepararse a partir de una variada gama de materiales de partida por los métodos de activación física y activación química [1]. En este segundo caso, los agentes químicos más utilizados son H_3PO_4, $ZnCl_2$ y KOH. La selección del agente químico más apropiado para un fin determinado es fundamental ya que determina no solo el rendimiento del proceso, sino también, y lo que es igual o más importante, las propiedades texturales y químico superficiales del producto obtenido. Y también puede influir en el tamaño de partícula de producto final. KOH ha sido utilizado con bastante frecuencia como agente activante [2]. Con KOH, un factor esencial en relación sobre todo con el desarrollo textural conseguido es la forma de efectuar las impregnación, bien con el producto en disolución acuosa o en estado sólido. Los resultados obtenidos suelen ser discrepantes en ambos casos aun cuando cabe suponer que la impregnación del sustrato, ya sea en la etapa de carbonización o en la etapa de carbonización según el caso, tenga lugar mediante sucesivos procesos de mojado e imbibición. Aunque hasta la fecha se han publicado numerosos mecanismos de reacción [3-5], aún no está suficientemente claro las diferencias observadas en la generación de porosidad de distinto tamaño. Debido a ello, como comienzo en el desarrollo de una nueva línea de investigación sobre la activación con KOH, en esta comunicación de presentan los resultados preliminares obtenidos en el estudio de la influencia del método de impregnación de huesos de cereza sobre el comportamiento térmico de las muestras.

Materiales y Métodos

En este estudio se han utilizado huesos de cereza (HC) proporcionados en la Agrupación de Cooperativas del Valle del Jerte (Valdastillas, Cáceres). Los huesos fueron primero secados al aire y depués reducidos de tamaño y tamizados, seleccionándose la fracción de partículas de tamaño comprendido entre 1 y 2 mm. Para HC, los datos de los análisis aproximado (base seca) y elemental son: humedad, 5.4%; materia volátil, 75.8%; cenizas, 0.25%; carbono fijo, 23.9; C, 51.1%, H, 6.5%, N, 0.4%, S, 0.02%; O, 42.0%. La impreganción de HC se llevó a cabo por vía húmeda y vía seca. En el primer caso, la impregnación con KOH tuvo lugar a 25, 45 y 85 ºC. Además, a la disolución de impregnación se incoporó NH_3 o HCl y, con fines comparativos, también se utilizó una disolución de KCl. En el segundo caso, tan solo se emplearon KOH y KCl. El análisis de HC, KOH y de las muestras de HC impregnados se realizó por termogravimetría-espectrometría de masas (TG/DTG-EM) en una termobalanza Setaran, Setsys

Evolution-16, acoplada a un espectrómetro de masas Omnistar, Pfeiffer Vacuum, calentando entre 25 y 900 ºC a una velocidad de 10 ºC/min en atmósfera de helio (50 mL/min). Los gases analizados a la salida de la balanza fueron H_2O, CO_2 y CO.

Resultados y Discusión

Los resultados obtenidos en el análisis de las muestras ponen de manifiesto la existencia de notables diferencia en el comportamiento térmico de las muestras y en la composición de la mezcla de gases salientes, sobre todo cuando se emplea KOH sólido en comparación con KOH y KOH con HCl en disolución, y KCl; a diferencia de lo que sucede con NH_3 y efectuando la impregnación a distintas temperaturas. En relación con los cambios de composición, se ha de tener presente que los mismos son atribuibles tanto a la degradación térmica de HC y KOH como al efecto de activación química debida KOH. Los gases liberados son H_2O, CO_2 y CO a bajas temperaturas y CO también a temperaturas más altas. Además, la cantidad de este último gas es mucho más elevada solamente cuando se utiliza KOH sólido en el tratamiento de impregnación, como muestra la Fig. 1. Por otra parte, el número efectos térmicos que ocasionan liberación de gas es mayor para H_2O y CO que para CO_2.

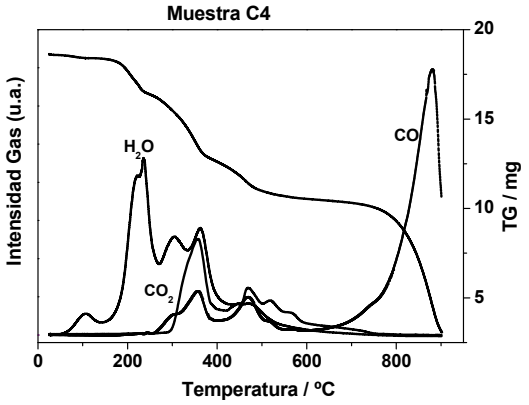

Fig. 1. Comportamiento térmico de la muestra preparada con KOH sólido. Variación de la masa de muestra y de la composición química de la mezcla de gases con la temperatura.

Agradecimientos

Los autores del presente trabajo agradecen al Gobierno de la Comunidad Autónoma de Extremadura la ayuda recibida, con la cofinanciación de FEDER, a este Grupos de Investigación.

Referencias

1. F. Rodríguez-Reinoso, in: H. Marsh, E. A. Heintz, F. Rodríguez-Reinoso (Eds.), Introduction to Carbon Techologies, Universidad de Alicante, Alicante, 1997, p. 35.
2. M. Olivares-Marín, C. Fernández-González, A. Macías-García, V. Gómez-Serrano, Appl. Surf. Sci. 252 (2006) 5980-5983.
3. P. Ehrburger, A. Addoun, F. Addoun, J.-B. Donnet, Fuel 65 (1986) 1447-1449.
4. M. A. Lillo-Ródenas, D. Cazorla-Amorós, A. Linares-Solano, Carbon 41 (2003) 267-275.
5. B. Y. Jibril, R. S. Al-Maamari, G. Hegde, M. Al-Mandhary, O. Houache, J. Anal. Appl. Pyrolysis 80 (2007) 277-282.

Metformin Adsorption onto Activated Carbons Prepared by Hydrothermal Carbonization and Activation

C. Laginhas[a], J.M. Valente Nabais[a*], M.M. Titirici[b]

[a]*Departamento de Química, Escola de Ciências e Tecnologia, Centro de Química de Évora, Universidade de Évora, Rua Romão Ramalho 59, 7000-671 Évora, Portugal*

[b] *Queen Mary University London, School of Materials Science & Engineering, Mile End Road, E14NS London, UK*

**jvn@uevora.pt*

Introduction

The hydrothermal carbonization can be considered an environmental friendly process for the production of carbon materials with tailored properties, such as regular porous structure and specific surface chemistry. This process is easy to perform and uses mild temperatures without the use of solvents or gases, which results in a positive environmental balance when compared with the usual pyrolysis process [1]. Diabetes affects more than 152 million people in Europe and is on the rise all over the World. Metformin is one of the most used drugs to treat type 2 diabetes. This drug is an endocrine disruptor with a potential negative impact in the environment due to the fact that metformin is almost not metabolized in the human body and the incorrect disposal into the domestic garbage. Another relevant aspect is the danger of overdose intake of the drug that can lead to lactic acidosis, which in extreme cases can be lethal. The work now reported study the in vitro adsorption of metformin onto activated carbons using simulated gastric and intestinal fluids.

Materials and Methods

The precursor chitosan (Agros Organics) was submitted to a hydrothermal carbonization process using an autoclave heated in an oven at 200ºC for 24h using a water:precursor ratio of 1:6. The resulting char (Q200-24) was then activated in a horizontal furnace with carbon dioxide at 800ºC for 1, 3 and 5h (AC-1, AC-2, AC-3) and by chemical activation with $CaCO_3$ by impregnation with a ratio 1:10(w/v) followed by pyrolysis at 800ºC for 1, 3 and 5h (ACa-1, ACa-2, ACa-3). The sample AC-5 was oxidized with nitric acid at 900ºC for 1h (AC-5Ox). All materials were characterised by SEM, FTIR, elemental analysis and nitrogen adsorption isotherms at 77K. The metformin adsorption was done at 37ºC using gastric and intestinal simulated fluids with pH 1.2 and 7.5, respectively.

Results and Discussion

The results of the samples' characterisation can be seen in table 1. Regarding the elemental analysis we can see a notewhorthy nitrogen content, between 6 and 10%, which is attributed to the precusor used, naturally rich on nitrogen. The porous structure was well developed with apparent surface area (A_{BET}) within the range 420-1400m^2g^{-1} and pore volume and external area, as estimated by the alfa-S method (V_s and A_{ext}, respectively) in the range 0.18-0.69cm^3g^{-1} and 21-224m^2g^{-1}. All activated carbon samples have basic properties with point of zero charge (pzc) superior to 8. The

oxidation with nitric acid has lead to a decrease of the pzc value but without any significant change on the porous structure. By FTIR it was possible to identify the presence of several surface functional groups, namely hydroxyl, amines, carbonyl and lactones. The sample AC-5Ox shows the presence of carboxylic acid and ester.

Table 1. Characterisation of the samples

Sample	pH_{pzc}	Elemental analysis / %				Porous structure			
		C	N	H	O	A_{BET} /m^2g^{-1}	V_s /cm^3g^{-1}	A_{ext} /m^2g^{-1}	V_0 /cm^3g^{-1}
Chitosan	-	40.38	7.72	7.81	33.70	-	-	-	-
Q200-24	6.01	59.62	10.07	4.97	16.42	10	-	-	-
AC-1	9.34	75.94	5.80	1.23	8.73	423	0.18	24	0.17
AC-3	8.76	83.20	5.23	0.25	10.69	1095	0.44	21	0.42
AC-5	8.77	81.08	5.93	1.00	11.92	1023	0.41	18	0.39
ACa-1	-	80.06	5.92	0.87	9.13	642	0.29	19	0.28
ACa-3	-	81.13	5.25	1.04	10.47	852	0.36	22	0.34
ACa-5	-	85.32	5.45	0.93	12.85	1432	0.69	222	0.54
AC-5Ox	2.54	44.02	3.22	0.77	23.92	1034	0.46	36	0.38

The metformin maximum adsorption capacity in gastric (FG) and intestinal (FI) fluids is shown in table 2. We can see that adsorption is higher when FI is used. This difference cannot be only explained with the porous structure of the materials but also with chemical interactions between the nitrogen functional groups and metformin, reason why the adsorption onto sample Q200-24 is so high. The adorption mechanism seems to include also the electrostatic interactions that can explain the low adsortion in FG, where metformin is totally ionised aquiring a positive charge like the surface of the activated carbon samples.

Table 2. Metformin adsorption

Sample	FG/mgg^{-1}	FI/mgg^{-1}
Q200-24	-	32.0
AC-1	-	24.0
AC-3	1.5	28.0
AC-5	2.2	44.2
ACa-3	0.7	22.4
ACa-5	2.1	11.5
AC-5Ox	9.0	18.5

Acknowledgements

The authors would like to thank Centro de Química de Évora (strategic project PEst-OE/QUI/UI0619) and to FCT COMPETE and QREN for the Carlos Laginhas PhD grant (SFRH/DB/82696/2011).

References

1. MMTitirici, A Thomas, M Antonietti. Adv. Functional Mat. 17 (2007) 1010-8.

Evaluación como Adsorbentes de CO_2 de MCM-41 y SBA-15 Modificados con Aminas

Marina González-Barriuso[a,b], Carmen Pesquera[a], Fernando González[a] , Ana Perdigón[a], Angel Yedra[b], Carmen Blanco[a,*]

[a]Dptº. de Química e Ingeniería de Procesos y Recursos. Universidad de Cantabria. 39005-Santander. Spain

[b]Fundación Centro Tecnológico de Componentes (CTC). Parque Científico y Tecnológico de Cantabria. 39011-Santander. Spain

**carmen.blanco@unican.es*

Introducción

Las emisiones de dióxido de carbono procedentes de los combustibles fósiles conllevan a una gran preocupación debido a su importante impacto en el ambiente. Se han propuesto varios métodos de captura de CO_2. Un amplio rango de materiales porosos adsorbentes se ha utilizado para este propósito, tales como, sólidos mesoestructurados, zeolitas, óxidos metálicos, materiales MOF ("Metal-Organic Framework"). Como es sabido, los grupos amina pueden mejorar potencialmente la quimisorción de CO_2. Además, los materiales nanoporosos se pueden modificar con grupos amina y, potencialmente, pueden mejorar el rendimiento de esta interacción [1, 2].

En este trabajo materiales nanoporosos de base silícica, MCM-41 y SBA-15, han sido elegidos como material de partida para su funcionalización con diferentes aminas, posterior caracterización, y evaluación como adsorbentes de CO_2.

Materiales y Métodos

Se ha utilizado el método "grafted" o de injerto para incorporar 3-aminopropiltrimetoxilane (APTMS), introduciendo grupos amino por reacción química entre los grupos silanoles de la superficie de los materiales nanoporosos y aminosilanos. Los materiales sintetizados se van a denominar: MCM-41(x) o SBA-15(x) donde "x" representa los milimoles de APTMS por g de soporte.

Además, se ha utilizado el método de impregnación húmeda con polietilenimina (PEI) de bajo peso molecular. Los materiales sintetizados se van a denominar: PEI-MCM-41(y) o PEI-SBA-15(y) donde "y" representa el porcentaje de PEI incorporado en el soporte.

La evaluación y el análisis de la adsorción de CO_2 fue llevado a cabo por dos métodos. En el primer método, se han llevado a cabo isotermas de adsorción-desorción de CO_2 puro a 298K con una presión entre 0-1 atmósferas (at), en un equipo Micromeritics ASAP 2010. Antes de cada análisis se llevó a cabo la desgasificación de las muestras a 383K, bajo vacío durante 6h. También se han realizado estudios de captura de CO_2 a 298K utilizando un equipo Setaram Setsys Evolution-1700 de termogravimetría (TG) con diferentes relaciones de concentración N_2/CO_2. Paralelamente, se evaluó la idoneidad de las muestras para un uso cíclico. Un aumento de masa en las muestras durante el experimento es considerado como la capacidad de adsorción de CO_2 de las mismas.

Resultados y Discusión

A partir de los datos de la Tabla 1 se observa que la adsorción de CO_2 para los materiales funcionalizados presentan un comportamiento diferente al de los materiales de partida de sílice nanoporosa (MCM-41 y SBA-15). Para la mayoría de los materiales funcionalizados la diferencia de captura de CO_2 es pequeña independiente del intervalo de presión utilizado, indicando un proceso de quimisorción [3]. Sin embargo, los valores de captura de CO_2 de los materiales de partida (MCM-41 y SBA-15) se aprecian que existe una gran diferencia dependiendo del rango de presión, y también una completa reversibilidad del proceso de desorción debido a un mecanismo de adsorción física**.**

En la Tabla 2 se encuentra la captura máxima (porcentaje en peso) de CO_2 obtenidos por TG para dos ciclos ensayados. Aunque estos valores son menores, son consistentes con los obtenidos a partir de las isotermas, considerando que aquel era un proceso estático con CO_2 puro y ahora es flujo dinámico con una relación del 10% de CO_2. Por otra parte, se observa que en los materiales amino-funcionalizados la captura de CO_2 es siempre menor en el segundo ciclo que en el primero. Este hecho indica que la regeneración no es completa debido a que la contribución del proceso de quimisorción impide la regeneración total.

Tabla 1. Capacidad de adsorción de CO_2 de las muestras a 1.0 y 0.1 atmósferas (at), obtenidas a partir de las isotermas de adsorción de CO_2 a 298K.

Muestra	CO_2(1.0 at) /cm^3/g	CO_2(0.1 at) /cm^3/g	Muestra	CO_2(1.0 at) /cm^3/g	CO_2(0.1at) /cm^3/g
SBA-15	20.8	3.5	MCM-41	20.7	2.1
SBA-15(4)	45.5	34.3	MCM-41(5)	29.5	22.1
SBA-15(20)	23.2	15.2	MCM-41(7.5)	33.5	27.6
SBA-15(40)	3.1	0.9	MCM-41(10)	39.1	29.4
PEI-SBA-15(20)	9.9	5.7	PEI-MCM-41(20)	6.3	4.1
PEI-SBA-15(40)	34.4	29.0	PEI-MCM-41(40)	7.0	4.4
PEI-SBA-15(60)	22.3	18.0	PEI-MCM-41(60)	18.1	11.9

Tabla 2. Porcentaje de captura de masa de CO_2 (%) por TG en el primer y segundo ciclo.

Muestra	CO_2 (%) Ciclo 1	CO_2 (%) Ciclo 2	Muestra	CO_2 (%) Ciclo 1	CO_2 (%) Ciclo 2
SBA-15	0	0	MCM-41	0	0
SBA-15(4)	4.3	4.2	MCM-41(7.5)	4.2	4.0
PEI-SBA-15(40)	4.7	4.5	PEI-MCM-41(60)	1.9	1.8

Agradecimiento: A la Universidad de Cantabria, España, por el Proyecto Nº 51.DI03.648 asociado al "Doctorado Industrial" 2015-2018.

References

[1] C. Chen, J. Kim, W. S. Ahn, Korean J. Chem. Eng. 31(11) (2014) 1919-1934.
[2] Z. Liu, Y. Teng, K. Zhang, H. Chen, Y. Yang, J. Energy Chem. 24 (2015) 322-330.
[3] T. Yokoi, Y. Kubota, T. Takashi, Applied Catalysis A: General 421-422 (2012)14-37.

Aprovechamiento de un Nuevo Precursor para su Uso como Adsorbente: el Aguaje

Beatriz Ledesma[a*], Rosario Sun-Kou[b], Silvia Román[a], J. F. González[a]

[a]Dpto. Física Aplicada, Univ. de Extremadura, Avda. de Elvas s/n, Badajoz, España
[a]Dpto. Ciencias, Sección Química, Pontífica Univ. Católica de Perú, Avda. Universitaria 1801, San-Miguel, Lima 32, Perú
**beatrizlc@unex.es*

Introducción

El crecimiento continuo del mercado de carbones activados (CAs) ha movido a la comunidad científica a intensificar la búsqueda de nuevos precursores renovables y de bajo costo, que puedan servir para la producción de materiales adsorbentes altamente porosos, con alta capacidad de adsorción, versátiles y con grupos funcionales "a la carta" para diferentes aplicaciones. Así, en el marco de los materiales lignocelulósicos, son muchos los estudios conducentes a estudiar la potencialidad de cáscaras, huesos o maderas de diversos tipos.

En este trabajo, se han preparado diferentes carbones activados (CA) a partir de semilla de Aguaje, un fruto muy abundante y consumido en países del centro y norte de Sudamérica. Mediante procesos de activación física (AF) y química (AQ), así como por hidrocarbonización (HC), se prepararon materiales adsorbentes carbonosos, con diferencias en su porosidad y química superficial. Su aplicabilidad en el tratamiento de aguas fue estudiado con dos compuestos orgánicos: el fármaco Ácido Nicotínico, y el tinte, Azul de Metileno.

A partir de las isotermas de adsorción y su correspondiente modelamiento se determinaron los parámetros característicos de cada adsorbente y se estudió el mecanismo de adsorción implicado.

Materiales y Métodos

Los adsorbatos empleados han sido el ácido nicotínico ($C_6H_5NO_2$, Sigma Aldrich S.A), y azul de metileno ($C_{16}H_{18}ClN_3S$, Panreac). El precursor utilizado fue la semilla de Aguaje, procedente de la región amazónica del Perú.

Se prepararon cinco tipos de CAs, tres por AF ($C\text{-}_{Steam}$ mediante vapor de agua a 850 ºC, 12 min.; C_{CO2} mediante CO_2 a 850 ºC, caudal de 40 mL min^{-1}, 10 min.), uno por HC (C_{HC}, obtenido a 220 ºC, 20 horas) y dos por AQ empleando ácido fosfórico al 80% con una relación 0,75 g_{H3PO4}/ $g_{precursor}$ (Chem-60 durante 60 min y Chem-90 durante 90 min.)

Para caracterizar los CAs se utilizaron las técnicas de adsorción de N_2 a 77K (AUTOSORB-1, Quantachrome) y punto de carga cero (mediante volumetría).

Los ensayos de adsorción en equilibrio siguieron el método de inmersión manteniendo en contacto en régimen de agitación y temperatura constantes, una determinada cantidad del sólido con un volumen de disolución de cada adsorbato de concentración conocida hasta alcanzar el equilibrio. La concentración de las suspensiones fue determinada mediante espectrofotometría UV-Vis. (UNICAM, Helios).

Resultados y Discusión

Los resultados del análisis de porosidad de los CAs mostraron que el tipo de tratamiento condiciona claramente el desarrollo de la porosidad obtenida en el material. Así, los carbones preparados mediante AF y AQ fueron microporosos, y el carbón obtenido mediante HC presentó escasa porosidad, concentrada en la zona de mesoporos. Además, la AQ condujo a mayores valores de la superficie específica del carbón (valores de S_{BET} de hasta de 938 m^2/g) comparado con la AF, la cual, a su vez, fue más efectiva cuando se utilizó vapor de agua. Se encontraron asimismo diferencias significativas en cuanto a la química superficial de los adsorbentes. De este modo, los carbones preparados por AQ fueron muy ácidos, los de AF, muy básicos, y el HC presentó un punto de carga cero cercano al pH neutro.

Las mencionadas disimilitudes afectaron de forma diferente a los procesos de adsorción, en función del adsorbato empleado. En la Fig. 1 se presentan las isotermas de adsorción. En dicha representación, la línea continua muestra el ajuste de los resultados experimentales obtenidos mediante la aplicación del modelo de Langmuir en su forma no lineal.

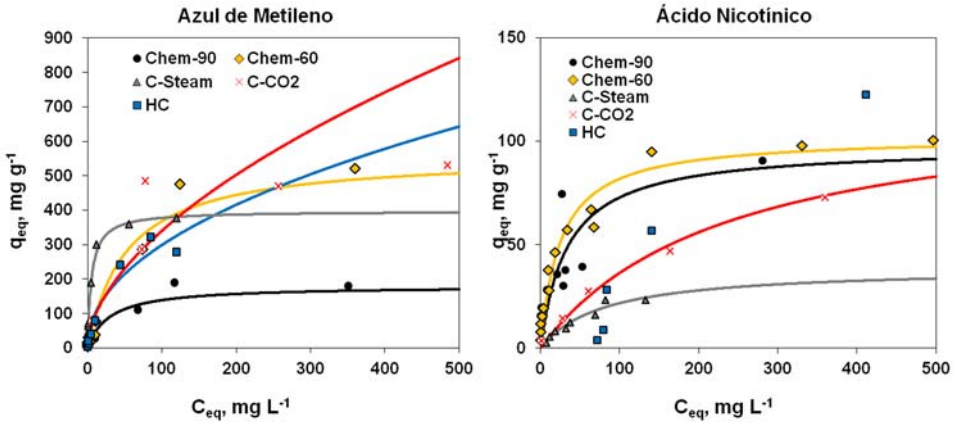

Fig. 1. Isotermas de adsorción obtenidas para los adsorbatos estudiados

Como puede observarse, para bajas concentraciones de Azul de Metileno el CA que presenta mayor afinidad es el C-Steam, poniendo de manifiesto que las interacciones más influyentes son las Π-Π para los CA básicos. En cambio, para concentraciones mayores del adsorbato se observa que las curvas de C-$_{CO2}$ y Chem-60 siguen creciendo mostrando mayor capacidad de adsorción y presentando mayor afinidad.

En el caso del ácido nicotínico las isotermas con mayor pendiente son las pertenecientes a los CA químicamente, comportamiento que se atribuye al carácter ácido de dichos CA, teniendo en cuenta que la molécula se encuentra protonada en esas condiciones. También se aprecia que un aumento del tiempo de contacto en la AQ no favorece la afinidad con el adsorbato (posiblemente debido a una posible obstrucción de los poros que se observó en este caso).

Agradecimientos

Los autores agradecen la financiación recibida de la Junta de Extremadura a través del proyecto GR15034, en el marco de las "Ayudas para el fortalecimiento de los de Grupos de Investigación de Extremadura", al Ministerio de Economía y Competitividad por el proyecto CTM2014-55998-R y a la Sección Química de la PUCP por las facilidades recibidas.

Activated Carbons from Polyethylene Terephthalate for CO_2 Capture

P.A.S. Moura[a], D.C.S. Azevedo[a], C.O. Ania[b], J.B. Parra[b*]
[a] *Grupo de Pesquisa em Separações por Adsorção, Universidad Federal do Ceara, Fortaleza, Brazil*
[b] *ADPOR Group, Instituto Nacional del Carbon (INCAR), CSIC, Oviedo, Spain*
**jbparra@incar.csic.es*

Introduction

Mitigation of global climate change requires urgent and drastic reduction of carbon dioxide emission from the combustion of fossil fuels [1]. Among various technologies, a number of solid sorbents including zeolites, functionalized porous silica, metal–organic frameworks (MOFs), and carbonaceous materials have proved to be effective for carbon dioxide capture and storage [2]. There is no ideal adsorbent, and each one possesses particular advantages and drawbacks. However, the use of carbon-based materials is especially promising because of their relatively low cost and easy regeneration. Hence, the objective of this work was to synthesize and characterize activated carbons using a plastic waste as precursor, and to explore their potentialities towards CO_2 capture considering different emission scenarios.

Materials and Methods

PET wastes were used as precursor to synthesize nanoporous carbons. Details on the experimental conditions have been reported elsewhere [3,4]. Briefly, the plastic wastes were pyrolyzed under a N_2 flow at 10 mL min^{-1} (i.e., 120 °C for 1 h, followed by 300 °C for 2 h and then 500 °C for 2 h) to produce a char. Subsequently, the char was activated under CO_2 atmosphere (i.e., 925 ºC at 10 mL min^{-1}) for 12 and 24 hours to generate samples with different burn-of degrees. The samples were labelled as ACPX-Char (after carbonization), and ACPX-t being *t* the time of activation in hours. The textural characterization of the prepared carbon materials was carried out by means of N_2 and CO_2 adsorption isotherms at, respectively, -196 and 0 ºC. The distribution of pore sizeds (PSD) was obtained using the 2D-NLDFT-HS model applied to the nitrogen adsorption isotherms [5]. Further characterization was carried out by helium density, thermogravimetric analysis, surface pH and elemental analysis. The CO_2 capture was evaluated at equilibrium and dynamic conditions at 20-100 °C.

Results and Discussion

Figure 1 shows the N_2 and CO_2 adsorption/desorption isotherms of the prepared samples. The corresponding main textural parameters obteind from the gas adsorption data are compiled in Table 1. As seen, the char resulting from the carbonization of the PET waste at high temperature exhibits a rather high porosity (i.e., apparent surface are of 450 m2/g). The activation under carbon dioxide atmosphere incresed significantly the porosity (as expected), giving rise to the formation of new pores and the enlargement on the existing narrow micropores (as inferred from the CO_2 adsorption isotherms).

Table 1. Main textural parameters of the prepared carbon materials obtained from gas adsorption.

	S_{BET} *[m² g⁻¹]*	C_{BET}	$V_{TOTAL\ PORES}$ [A] [cm³ g⁻¹ S.T.P.]	Wo, N_2 [B] *[cm³ g⁻¹]*	Wo, CO_2 [C] *[cm³ g⁻¹]*
ACPX-Char	450	-	106	-	0.234
ACPX-22	985	1120	264	0.367	0.367
APCX-41	1365	490	380	0.502	0.495
[A] Total pore volume, evaluated at relative pressure of 0.99					
[B] Evaluated from the NLDFT method					
[C] Evaluated from Dubinin-Stoeckli method					

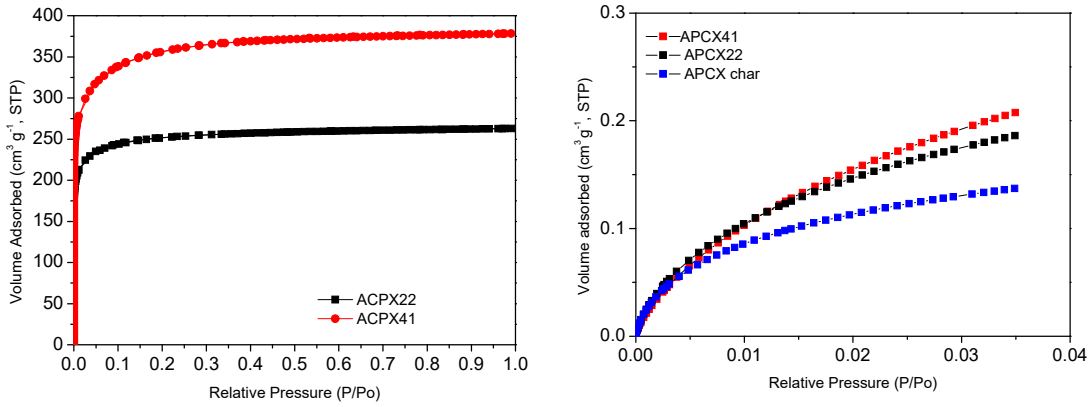

Figure 1. N_2 and CO_2 adsorption isotherms obtained, respectively at -196 and 0ºC of the synthesized carbons.

Acknowledgements

The authors thank *Coordenação de Aperfeiçoamento de Pessoal de Nível Superior – CAPES* and *Conselho Nacional de Desenvolvimento Científico e Tecnológico – CNPq for financial support*.

References

[1] IPCC, Summary for policymakers, in: climate change 2014, mitigation of climate change. contribution of working group III to the 5th assessment report of the intergovernmental panel on climate change, 2014. http://report.mitigation2014.org/spm/ipcc_wg3_ar5_summary-for-policymakers_approved.pdf.

[2] N. MacDowell, N. Florin, A. Buchard, J. Hallett, A. Galindo, G. Jackson, C. S. Adjiman, C. K. Williams, N. Shah and P. Fennell, An overview of CO_2 capture technologies, Energy Environ. Sci., 2010, 3, 1645–1669.

[3] J.B. Parra, C.O. Ania, A. Arenillas, F. Rubiera, J.J. Pis, High value carbon materials from PET recycling, Appl. Surf. Sci. 238 (2004) 304–308. doi:10.1016/j.apsusc.2004.05.229.

[4] J.B Parra, C.O. Ania, A. Arenillas, J.J. Pis, Textural characterisation of activated carbons obtained from poly(ethylene terephthalate) by carbon dioxide activation, in: Stud. Surf. Sci., Elsevier Masson SAS, 2002: pp. 537–543. doi:10.1016/S0167-2991(02)80178-1.

[5] J. Jagiello, C.O. Ania, J.B. Parra, C. Cook, Dual gas analysis of microporous carbons using 2D-NLDFT heterogeneous surface model and combined adsorption data of N2 and CO2, Carbon N. Y. 91 (2015) 330–337. doi:10.1016/j.carbon.2015.05.004.

Aplicação de Carvões Ativados de Precursores Lenhocelulósicos de Origem Angolana na Adsorção de Diuron

Emílio Tchikuala[a,b,*], Paulo Mourão[a], João Nabais[b]
[a] *Centro de Química de Évora, Departamento de Química, Escola de Ciências e Tecnologia, Instituto de Investigação e Formação Avançada, Universidade de Évora, Évora, Portugal*
[b] *Departamento de Ciências Exatas, Universidade Katyavala Bwila, Benguela, Angola*
** tchikuala@hotmail.com*

Introdução

As questões ambientais e de saúde pública estão cada vez mais presentes na agenda internacional. Em particular as consequências indesejadas da utilização de pesticidas na agricultura, em países em desenvolvimento, são um dos tópicos de maior atenção tanto ao nível político, social como científico [1].

Entre as técnicas mais utilizadas para a redução ou remoção destes poluentes a partir de águas contaminadas (naturais, consumo ou residuais) está a adsorção recorrendo a carvões ativados [2]. Esta estratégia ganha importância quando é possível valorizar os desperdícios de recursos endógenos de cada região.

Este trabalho segue esta linha, pela via do aproveitamento de desperdícios lenhocelulósicos de origem angolana na produção de carvões ativados para utilização na remoção de um pesticida de largo espectro de aplicação na agricultura.

Materiais e Métodos

Os carvões ativados foram produzidos a partir de desperdícios de dois tipos de madeira característicos da região de Benguela, o *Embondeiro* e a *Candeia*. Os adsorventes foram preparados por ativação física com dióxido de carbono (CO_2) num forno horizontal, em condições térmicas ajustadas e tempos de ativação distintos, de forma a obter materiais com propriedades estruturais distintas.

O precursor e as amostras preparadas foram caracterizadas química e estruturalmente, recorrendo às técnicas mais comuns neste tipo de ensaios, nomeadamente, termogravimetria, FTIR, análise elementar, pcz e adsorção de nitrogénio a 77 K.

Algumas amostras selecionadas foram testadas na adsorção do pesticida Diuron, 3-(3,4-Dichlorophenyl)-1,1-dimethylurea, em solução aquosa a 298 K. Ensaios cinéticos iniciais permitiram estabelecer um tempo de equilíbrio para estes sistemas de 24 h. A determinação da concentração do pesticida foi efetuada por UV-Vis a um comprimento de onda caraterístico.

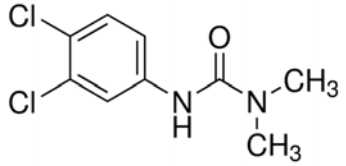

Fig. 1. Molécula de Diuron.

Resultados e Discussão

A caracterização das amostras produzidas permitiu verificar o potencial destes precursores para a produção de carvões ativados. Estes apresentam propriedades estruturais e químicas semelhantes a outros que surgem na bibliografia da especialidade [3]. Os materiais produzidos são essencialmente microporosos tendo-se observado que um incremento do tempo de ativação com CO_2 leva a um aumento da área superficial especifica, do volume poroso e pequenas variações da área superficial externa. Os valores obtidos com o precursor *Embondeiro* mostram valores de área superficial aparente na ordem dos 1148 m^2g^{-1}, volume poroso de 0,52 cm^3g^{-1} e uma área externa de 64 m^2g^{-1}, para uma amostra com um grau de queima, GQ, intermédio de 64%. Em termos de química de superfície todos os carvões ativados mostram um caracter básico.

Amostras selecionadas foram testadas na adsorção de Diuron com desempenhos distintos que podem ser explicados essencialmente pelas suas diferenças estruturais. Observa-se um incremento da quantidade adsorvida do pesticida quando a área superficial e o volume poroso aumentam. A título de exemplo, para a amostra com um GQ de 64% alcançou-se uma quantidade adsorvida de ~350 mg por grama de adsorvente, para uma concentração de equilíbrio de ~10 mgL^{-1}.

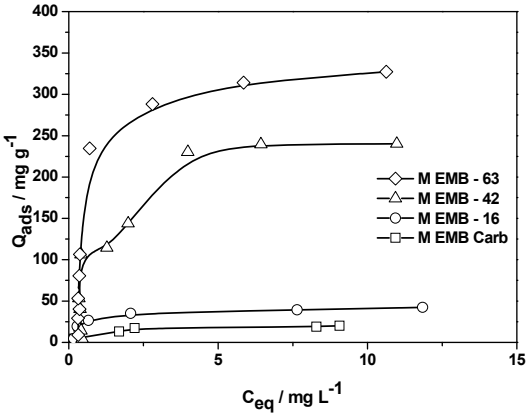

Fig. 2. Isotérmicas de adsorção de Diuron numa série de amostras preparadas a partir de Embondeiro.

Agradecimentos

E. Tchikuala agradece ao Centro de Química de Évora e Departamento de Química da Universidade de Évora por terem acolhido o seu projeto de Doutoramento, e ao Governo da República de Angola pela atribuição da sua Bolsa de Doutoramento.

Referências

1. E. Stokstad, G. Grullon, Science 341 (2013) 730−731.
2. H. Marsh, F. Rodríguez-Reinoso, Activated Carbon, Elsevier Science & Technology Books, 2006.
3. P.A.M. Mourão, C. Laginhas, F. Custódio, J.M.V. Nabais, P.J.M. Carrott, M.M.L. Ribeiro Carrott, Fuel Process. Technol. 92 (2011) 241-246.

Theoretical Study of the Stability of Template-Grown Ordered Metal Nanofoams

Jose Manuel Ortiz-Roldan[a], A. Rabdel Ruiz-Salvador*[a], Salvador R. G. Balestra, Sofía Calero[a], Elena García-Pérez[b], Francisco Montero-Chacón[b], Richard Catlow[c] and Said Hamad*[a]

[a] *Department of Physical, Chemical and Natural Systems, University Pablo de Olavide, Ctra. Utrera km. 1, 41013, Seville, Spain.*

[b] *Abengoa Research, Campus Palmas Altas, Calle Energía Solar 1, 41014, Seville, Spain.*

[c] *University College London, Kathleen Lonsdale Materials Chemistry, Department of Chemistry, 20 Gordon Street, London WC1H 0AJ, United Kingdom*

** said@upo.es, rruisal@upo.es*

Introduction

Foams can be defined as the materials formed when a liquid or a solid encloses gaseous regions, and they are a type of porous materials of increasing interest. In particular, metal foams are solid metal structures in which a large percentage of their structure is hollow, so that gas molecules can stay within, or diffuse through, the material. A number of possible applications of metal nanofoams (foams in which the size of the pores is of the order of nanometers) have been investigated[1]. The search for new materials has yielded interesting results regarding nanofoams.

There are several techniques with which to synthesize metal nanofoams, such as dealloying[2], sol–gel synthesis, nanosmelting, combustion synthesis, templating, etc[3]. With the help of appropriate templates it is possible to develop new nanoporous materials with unique structures, morphologies and properties[4]. One drawback of the metal nanofoams that have been investigated so far is that they have disordered pores[5], with sizes of the order of several nm[6,7]. In this work, we study a new type of metal nanofams, in which the pores are highly ordered and their sizes vary from 0.5 nm to less than 4 nm.

Materials and Methods

As templates for the formation of nanofoams with a range of porosities we have employed materials with different topologies, namely zeolites and Metal-Organic Frameworks (MOFs). A crystalline bulk metal structure is then superimposed with the template. We consider the sum of the metal Van der Waals radii and depending on the structure, the sulfur one or the hydrogen one. According to this, all metal atoms that are closer than this distance to a framework atom are removed.

We have constructed different zeolites using the cristobalite and the sodalite as initial structures. These ones are non-porous polymorph of quartz, but it is possible to synthesize highly porous zeolite structures with these topologies, but instead of having SiO_4 tetrahedra in the T sites, having tetrahedral structures composed of four SiO_4 tetrahedra, called T2 supertetrahedra. We named this material is named ST2. The porosity can be further increased by using T3 supertetrahedra, which are structural units built up by arranging four T2 supertetrahedra to form a larger tetrahedron, and consequently T4 supertetrahedra are composed of four ST3 supertetrahedra. The

structures are named ST3 and ST4 respectively. It is clear that ST3 is more porous that than ST2, but less than ST4. The use of supertetrahedra Tn clusters to form zeolite-like, 3D open-framework chalcogenide materials has been studied experimentally[8]. The tetrahedral sites of the zeolites are then substituted (employing the code TOBUNPOROUS[9]).

We carried out a simulation study of all these nanofoams, for five different metals, focusing on the influence that the level of porosity has on the mechanical properties of these materials. The first property we have focused on is the thermal stability of the structures. In order to predict which materials might be synthesized, we minimised the as-generated structures, and carried out MD simulations for increasing temperatures.

Results and Discussion

We found that some of the structures collapse right at the beginning of the MD simulations, but there are very stable topologies, for which the nanofoams can withstand very high temperatures and keep the crystallinity, such as SOD-ST3, SOD-ST4 and CRI-ST3 and CRI-ST4. We have also studied their thermal expansion coefficient within the range of temperatures where they are stable. In order to be used in gas separation of catalysis applications, the stable structures should be able to allow the flow of molecules. We therefore studied the diffusion of four relevant molecules (benzene, ortoxylene, metaxylene and paraxylene), within four of these materials, namely Ag-CRI-ST3, Pt-CRI-ST3, Pt-PCN6p and NDC-MIL101.

Acknowledgements

This work was supported by the spanish Ministerio de Economía y Competitividad (Sofía Calero, CTQ2013-48396- P). J. M. Ortiz-Roldan thanks Spanish MECD (FPU14/01094) for his predoctoral fellowship and ABENGOA RESEARCH for its joint venture agreement with University Pablo de Olavide.

References

[1] C. Zhu, D. Du, A. Eychmüller, Y. Lin, Chem. Rev. 115 (2015) 8896–943.
[2] J. Cai, J. Xu, J. Wang, L. Zhang, H. Zhou, Y. Zhong, D. Chen, H. Fan, H. Shao, J. Zhang, C. Cao, Int. J. Hydrogen Energy 38 (2013) 934–941.
[3] I. Vukovic, G. ten Brinke, K. Loos, Polymer (Guildf). 54 (2013) 2591–2605.
[4] Y. Liu, J. Goebl, Y. Yin, Chem. Soc. Rev. 42 (2013) 2610–53.
[5] J. Biener, A. Wittstock, L.A. Zepeda-Ruiz, M.M. Biener, V. Zielasek, D. Kramer, R.N. Viswanath, J. Weissmüller, M. Bäumer, A. V Hamza, Nat. Mater. 8 (2009) 47–51.
[6] H.-J. Qiu, J.L. Kang, P. Liu, A. Hirata, T. Fujita, M.W. Chen, J. Power Sources 247 (2014) 896–905.
[7] A. Slabon, F. Krumeich, F. Wächter, R. Nesper, ChemElectroChem 1 (2014) 536–538.
[8] Y. Lin, W. Massa, S. Dehnen, J. Am. Chem. Soc. 134 (2012) 4497–500.
[9] D.W. Lewis, A.R. Ruiz-Salvador, A. Gómez, L.M. Rodriguez-Albelo, F.-X. Coudert, B. Slater, A.K. Cheetham, C. Mellot-Draznieks, CrystEngComm 11 (2009) 2272.

Hierarchical Y Zeolite through CTAB Mediated Methodology

João P. Moutinho[a], Angela Martins[a,b], Ana P. Carvalho[a]
[a] *Centro de Química e Bioquímica, Faculdade de Ciências, Universidade de Lisboa, 749-016 Lisboa, Portugal*
[b] *ADEQ, ISEL, IPL, Rua Conselheiro Emídio Navarro, 1959-007 Lisboa, Portugal*
**ana.carvalho@fc.ul.pt*

Introduction

Zeolites are crystalline microporous aluminosilicates that have been widely used as heterogeneous catalysts and also as adsorbents, due to a combination of properties such as high thermal and mechanical stability, well defined pore sizes and intrinsic acidity. However, in the presence of large molecules, the diffusion limitations hinders the use of these materials. In this sense, efforts have been made to incorporate mesopores into zeolites. Recently, Garcia-Martinez et al. [1], proposed an alkaline treatment in the presence of surfactant molecules in order to generate hierarchical zeolite materials with controlled size mesoporosity. In the present work Y zeolite (FAU structure) was submitted to alkaline treatment with NH_4OH in the presence of CTAB surfactant, under autogenous pressure. The influence of the pH of the reaction mixture in structural and textural properties of the obtained materials was investigated.

Materials and Methods

The parent material Y zeolite was supplied by Zeolyst (CBV500; lot. 50006N00322B), that according with the technical report has a SiO_2/Al_2O_3 = 5.2. The samples were prepared according to the procedure described in [1]. The parent material was submitted to a pre-treatment with citric acid (1 mmol of acid per gram of zeolite) to obtain sample HY. To promote the envisaged textural changes, 0.35 g of HY was suspended in 21.3 mL of a 0.37 M solution of NH_4OH containing 0.25 g of cetyltrimethyl ammonium bromide (CTAB), under stirring for 30 min. The mixture pH was adjust at 10 and 11 using, when necessary, HCl 1M. The mixture was heated at 150 °C under autogenous pressure during 12 h. The solid was recovered by centrifugation, washed and dried at 60 °C overnight. To remove the occluded surfactant samples were heated in a N_2 atmosphere from room temperature to 500 °C (5 °C min^{-1}), then the atmosphere was switched to air and the temperature increased to 550 °C and kept for 8 h.

The samples where characterized by X-ray powder diffraction on a Pan'Analytical PW3050/6oX'Pert PRO with automated data acquisition, the diffractograms were obtained between 5° to 40° 2θ, using a monochromatized CuK_α as incident beam. The textural characterization was made by N_2 adsorption isotherms at -196 °C measured in an automatic apparatus Micromeritics ASAP 2010, before the isotherms acquisition the samples were outgassed for 2h at 300° C, under vacuum better than 10^{-2} Pa.

Results and Discussion

The obtained results (Table 1) clearly show that the alkaline treatment assisted with CTAB surfactant had no severe impact on the zeolite crystallinity but produced changes in the textural properties of Y zeolite. In fact, the adsorption isotherms presented in

Figure 1 prove that the treatments made on HY zeolite transformed a fundamentally micropore sample (type I isotherm) into a hierarchical structure (type IV isotherms). The influence of the pH on the development of mesoporosity is also shown since, between p/p^0 of 0.4 and 0.5, a somewhat steeper curve is observed in the case of sample HY/NH_4OH 11, what results in a higher volume of micropore + narrow mesopore ($V_{micro+meso}$), as estimated by the analysis of the data by α_S method.

Table 1. Percentage of mass loss, degree of crystallinity, C_{XRD}, and textural parameters evaluated from N_2 adsorption isotherms – micro+narrow mesopore ($V_{micro+meso}$) and wider mesopore volumes (V_{MESO}) and external area (A_{ext}) – of the samples

Sample	Mass loss (%)	C_{XRD} (%)	$V_{micro+meso}$ [a] (cm^3g^{-1})	V_{MESO} [b] (cm^3g^{-1})	A_{ext} (m^2g^{-1})
HY	-	100	0.29	0.08	51
HY/NH_4OH 10	38.5	83	0.32	0.08	69
HY/NH_4OH 11	29.5	79	0.36	0.04	38

[a] Volume of micro + narrow mesopore estimated back extrapolation of the α_S plot linear region defined by the high relative pressure points (α_S >1).

[b] Volume of wider mesopores: $V_{MESO} = V_{total} - V_{micro+meso}$, considering V_{total} as the volume adsorbed at $p/p^0 = 0.95$

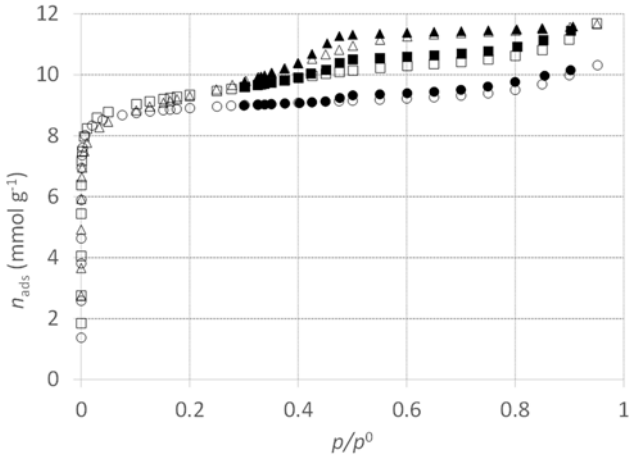

Fig. 1. Nitrogen adsorption-desorption isotherms at -196 °C on HY (○) and modified samples HY/NH_4OH 10 (□) and HY/NH_4OH 11 (Δ)

The promising results obtained so far encourage us to extend the study by changing other experimental parameters such as: duration of the treatment, other bases (e.g. NaOH), or the ratio base: surfactant in the reaction mixture.

Acknowledgements

The authors thank the Fundação para a Ciência e Tecnologia (FCT), Portugal, for financial support to CQB through the project PEst-OE/QUI/UI0100/2014

References

1. Garcia-Martinez J, Johnson M, Valla J, Li KH, Ying JY., **2012**. *Catal Sci Technol*, 2(5) (2012), 987-994.

Checking the Values of the Activation Energy in Isoconversional Methods for Thermal Solid State Reactions

Isabel Iglesias[a], José A. Huidobro[b], Belén F. Alfonso[a,*], Camino Trobajo[c], José R. García[c]

[a] *Departamento de Física, Universidad de Oviedo, 33204 Gijón, Spain*

[b] *Departamento de Matemáticas, Universidad de Oviedo, 33204 Gijón, Spain*

[c] *Departamento de Química Orgánica e Inorgánica, Universidad de Oviedo-CINN, 33006 Oviedo, Spain*

**mbafernandez@uniovi.es*

Introduction

Thermal stimulated solid-state reactions are commonly described by the equation

$$\frac{\mathrm{d}\alpha}{\mathrm{d}t} = A \exp\left(-\frac{E}{RT}\right) f(\alpha) \qquad (1)$$

where *t* (s) is the time, *T* (K) the temperature, *R* (Jmol^{-1}K^{-1}) the universal gas constant, *A* (s^{-1}) the pre-exponential factor, *E* (Jmol^{-1}) the activation energy, α the extent of conversion and *f*(α) the reaction model function [1].

In order to determine the so called kinetic triplet (*A*, *E*, *f*(α)), model fitting methods consider a particular reaction model function which is assumed to represent the conversion dependence on the reaction rate, but, as has been reported, these methods present uncertainties and their use is not recommended [2,3].

As an alternative, isoconversional methods allow calculating values of the activation energy as a function of the extent of conversion without knowing the pre-exponential factor or the model function [4]. The methods of Friedman, KAS and Vyazovkin are probably the most used [5] to perform kinetic analysis. In any case, the values of the activation energy should be checked before being accepted. An elementary test consists on solving the differential equation (1) and to compare the solution with the experimental data. But, apart from *E*, the knowledge of *A* and *f*(α) is required and these parameters are not computed in the isoconversional methods. The aim of this work is to propose a method to test the activation energy.

Materials and Methods

The compounds, $Cr_xFe_{1-x}NH_4(HPO_4)_2$, were hydrothermally synthesised in a stainless steel Teflon-lined vessel at 453 K under autogenous pressure. After 7 days and a molar ratio C/P = 0.25 and P/Fe = 10 the pale pink crystals of x = 0 solid were obtained. When the molar ratio was C/P = 0.25 and P/M = 15 (M = Cr, Fe) and after 10 days, the pale green x = 0.34 crystals were obtained. Five different heating rates were used for the kinetic analysis.

Eq. (1) can be written in the form

$$\frac{\mathrm{d}\alpha}{\mathrm{d}T} = \frac{c_\alpha}{\beta} \exp\left(-\frac{E_\alpha}{RT}\right) \qquad (2)$$

where $c_\alpha = Af(\alpha)$ and β is the constant heating rate. Considering different heating rates, for a fixed value of α, E_α is computed by a isoconversional method. To check these values, we use Eq. (2) and then, by fitting to the experimental data, the coefficient c_α

can be obtained. Now, for a given heating rate and since all quantities in the right hand side are already known, a numerical method can be applied to find the solution of the differential equation (2).

Solving Eq (2) for the same heating rates β_i, i = 1, …, n as in the experimental measures, theoretical curves of the extent of conversion are obtained which can be plot and compared with the experimental ones. This procedure has the advantage of being independent of the method used to compute the activation energy.

All computations in this study have been implemented in MatLab.

Results and Discussion

The procedure has worked efficiently in two theoretical simulations and it was applied to the thermal decomposition of $Cr_xFe_{1-x}NH_4(HPO_4)_2$, x = 0, 0.34. The agreement between the calculated and the simulated/experimental curves is generally good. This has been carried out by comparing the $\alpha - T$ plots and analysing the sum of the square errors given by

$$R^2 = 1 - \frac{SSE}{SST} \text{ , where } SSE = \frac{1}{n}\sum_{i=1}^{n}(\alpha_i^* - \alpha_i)^2 \text{ and } SST = \frac{1}{n}\sum_{i=1}^{n}(\alpha_i - \bar{\alpha})^2 \quad (3)$$

with α_i^* the calculated values, α_i the simulated/experimental values and $\bar{\alpha} = \sum_{i=1}^{n}\alpha_i /n$ the average. When $R^2 = 1$ all points lie on the curve with no scatter.

Acknowledgements

This work was supported by "Ministerio de Economia y Competitividad" (MAT2013-40950-R, MAT2011-27573-C04-02), "Gobierno del Principado de Asturias" (GRUPIN14-060 and GRUPIN14-037), and FEDER.

References

1. S. Vyazovkin, C.A. Wight, Annu. Rev. Phyis. Chem. 48 (1997) 125-149.
2. P. Deb, Kinetics of Heterogeneous Solid State Processes, 1nd Ed., Springer Science, New Delhi, 2014.
3. S. Vyazovkin, A.K. Burnham, J.M. Criado, L.A. Pérez-Maqueda, C. Popescu, N. Sbirrazzuoli, Thermochim. Acta 520 (2011) 1-19.
4. H.L. Friedman, J. Polym. Sci., Part C: Polym. Symp. 6 (1964) 183-195.
5. Y. Han, Theoretical study of thermal Analysis kinetics Theses and Dissertations. Paper 35. University of Kentucky (2014) http://uknowledge.uky.edu/me_etds/35

Using Different Co-Adjuvant Activating Agents to Improve Activated Carbon Adsorption Capacities

Isabel Cansado*, Paulo Mourão, Peter Carrott, Manuela Ribeiro Carrott
Centro de Química de Évora, Instituto de Investigação e Formação Avançada, Departamento de Química, Escola de Ciências e Tecnologia, Universidade de Évora, Colégio L. A. Verney, 7000-671 Évora, Portugal
** ippc@uevora.pt*

Introduction

Activated carbon (AC) has proved to be an effective adsorbent for the removal of an assortment of organic and inorganic pollutants from aqueous or gaseous media. However, the pursuit for more effective and cheaper AC is still very active and a diversity of textural and chemical treatments are described as a way to expand their applications. It is well known that the surface area and surface chemistry of AC strongly affect their adsorption capacity [1-3]. In particular, an increase in the nitrogen content has been related to an increase of the basic character and also to the development of the porous structure. In most published work this was achieved through an AC post treatment, including either a reaction with nitrogen containing reagents, such as ammonia, nitric acid, or a diversity of amines. However, the AC prepared directly from a nitrogen rich precursor through a physical or chemical activation is referred to as presenting the best characteristics, namely high nitrogen content, high basic character, low nitrogen leaching and also good thermal stability [4].

To improve the adsorption capacities of AC, prepared from cork or poly(ethyleneterephthalate) (PET) precursors, for acidic pesticide removal from the aqueous phase, we intend to improve the porous structure and to introduce nitrogen containing groups directly in the AC matrix by chemical activation with potassium hydroxide and using different co-adjuvant activating agents as nitrogen sources.

Materials and Methods

Highly activated AC have been produced by chemical activation, at 973 K, from PET or cork using a mixture of KOH with a co-adjuvant activating agent. The co-adjuvant agents were substances which contain nitrogen, namely urea, (2-hydroxyethyl)urea, 2-chloro-4,6-diamino-1,3,5-triazine and polyethylenimine. The precursors were dry mixed with KOH and a co-adjuvant agent, in a fixed mass ratio, and each mixture was submitted to pyrolysis, in a steel container, for 30 min at a final temperature of 973 K achieved using a heating rate of 10 K min^{-1}, with a flow of dry nitrogen of 85 cm^3 min^{-1}.

The characterization of the AC involved determination of the pH of point of zero charge (pH_{pzc}), elemental analysis, thermogravimetric analysis and nitrogen adsorption at 77 K. Selected AC were tested for the removal of the pesticide 4-chloro-2-methylphenoxyacetic acid (MCPA) from the liquid phase. In the present work fixed amounts of AC were added to aqueous solutions of known pesticide concentrations in an acidic medium. The equilibrium was attained after one day and the residual pesticide concentration was determined by UV-Vis spectrophotometry.

Results and Discussion

The experimental procedure used in this work allowed direct introduction of nitrogen into the AC matrix, reducing nitrogen leaching and improving the AC thermal stability determined by thermogravimetric analysis. The AC produced from cork with the four co-adjuvant agents presented basic character, as shown by an increase of the pH_{pzc} when compared with the cork AC activated without a co-adjuvant. With PET, this feature was not observed and the AC presented mainly neutral character.

All AC were characterised by nitrogen adsorption at 77 K and the adsorption isotherms obtained were characteristic of microporous materials. A really large improvement of the textural properties was observed when any of the four co-adjuvants were used with both cork and PET. The co-adjuvants interact in different ways with the two precursors. Nevertheless, an increase in the apparent specific surface area and pore volume was also accompanied by a widening of the mean pore size. The AC tested for the removal of MCPA from the liquid phase presented excellent adsorption capacity, reaching values as high as 3.7 $mmolg^{-1}$ with four of the samples. Those which exhibited a higher MCPA adsorption capacity, also presented highest micropore volume and broader mean pore size. It should be highlighted that the co-adjuvants tried in this work can be used as a way to improve considerably the apparent specific surface area and the pore volume and the AC performance in specific applications.

Acknowledgements

This work was financed through the Fundação para a Ciência e a Tecnologia (FCT, Portugal) with national funds (PEst-OE/QUI/UI0619/2014).

References

1. M.F.R. Pereira, S.F. Soares, J J.M. Órfão, J.L. Figueiredo, Carbon 41 (2003) 811–821.
2. I.P.P. Cansado, P.A.M. Mourão, A.I. Falcão, M.M.L. Ribeiro Carrott, P.J.M. Carrott, Fuel Proc. Technol. 103 (2012) 64-70.
3. A. Bhatnagar, W. Hogland, M. Marques, M. Sillanpaa, Chem. Eng. J. 219 (2013) 499–511.
4. J.M. Valente Nabais, P.J.M. Carrott, M.M.L. Ribeiro Carrott, J.A. Menéndez, Carbon 42 (2004) 1315–1320.

Resorcinol-Formaldehyde Carbon Xerogel for Biogas Upgrading

J.F. Vivo-Vilches[a], A.F. Pérez-Cadenas[a], F.J. Maldonado-Hódar[a], F. Carrasco-Marín[a*], M.J. Regufe[b], A.M. Ribeiro[b], A.F.P. Ferreira[b], A.E. Rodrigues[b]

[a](Carbon Materials Research Group, Department of Inorganic Chemistry, Science Faculty, University of Granada, Campus Fuentenueva s/n, ES18071-Granada,Spain)

[b](Laboratory of Separation and Reaction Engineering - Laboratory of Catalysis and Materials, Department of Chem. Eng., Faculty of Engineering, University of Porto, Rua Dr. Roberto Frias, PT4200-465-Porto, Portugal)

**fmarin@ugr.es*

Introduction

Carbon materials obtained from polymers are more and more frequently used. The main advantage of these materials is the possibility of tailoring porosity depending on the application, since synthetic methods are highly reproducible. From them, resorcinol formaldehyde carbon gels have been largely studied since Pekala patented the first one [1] due to the easiness and versatility of the process; several variables such as catalyst, solvent, resorcinol to catalyst and resorcinol to solvent ratios, drying or shape can be modified to obtain materials with very different properties. Moreover, similarly to traditional carbon materials obtained from natural sources, activation or functionalization with heteroatoms can be performed in order to modify surface chemistry and porosity. In our work, a carbon xerogel obtained by polymerization catalyzed by Cs_2CO_3, thermal drying and carbonization was employed as CO_2 selective adsorbent for biogas upgrading.

Materials and Methods

A carbon xerogel was obtained by carbonization of a polymer made by resorcinol and formaldehyde. The recipe used to obtain this xerogel was very similar to one already published by our group[2]. Briefly, resorcinol and formaldehyde in a 1:2 molar ratio were dissolved in water (R/W=0.07), then the polymerization catalyst, which was Cs_2CO_3(R/C=300), was added. Once reactants and catalyst were totally dissolved, solution was transferred to cylindrical glass moulds with 6 mm of inner diameter, and moulds were sealed. Then, a temperature program was selected to perform the gelification and curing of the RF hydrogel (1 day, 25°C; 1 day, 50°C and 5 days, 80°C). The polymeric precursor was then removed from glass moulds, cut into pellets of 2-3 cm and dried in a furnace at 110°C till constant weight to obtain the organic xerogel. This xerogel was carbonized at 900°C (1.5°C min^{-1}) on nitrogen. The sample was labelled as XCsP6.

Textural properties of the sample were obtained from the analysis of N_2 adsorption-desorption isotherms at -196°C and CO_2 adsorption ones at 0°C, as well as bulk density by Mercury Intrusion Porosimetry. Scanning Electron Microscopy (SEM) microphotographs were also obtained.

After characterizing the samples, isotherms of target compounds (CH_4 and CO_2) were obtained at 30, 50 and 70°C in a pressure range from 0 to 10 bar using a magnetic suspension balance (Rubotherm, Germany). Breakthrough experiments were performed under different conditions to test the adsorptive behaviour of this sample.

Results and Discussion

XCsP6 is a micro-mesoporous solid with a relatively high W_0 (N_2) and S_{BET} (Table 1). It presents a large volume of macropores very regular in size (around 100nm) determined by Mercury Intrusion Porosimetry, and, therefore, a low bulk density.

Once porous texture of samples was characterized, adsorption-desorption isotherms for the target gases, CO_2 and CH_4, were obtained. Experimental data were fitted with Langmuir or Toth model depending on the suitability of each one. Figure 1 illustrates the CO_2 and CH_4 adsorption-desorption isotherms at 30°C for XCsP6. Breakthrough experiments were performed under different conditions, by changing composition of the inlet gas and pressure. All of them were conducted at 30°C. Figure 2 shows the breakthrough curves obtained at atmospheric pressure for a 20% CH_4 10% CO_2 mixture (dilution was performed by adding He to the mixture). XCsP6 presented a very promising behaviour as CO_2 selective adsorbent for CO_2/CH_4 mixtures.

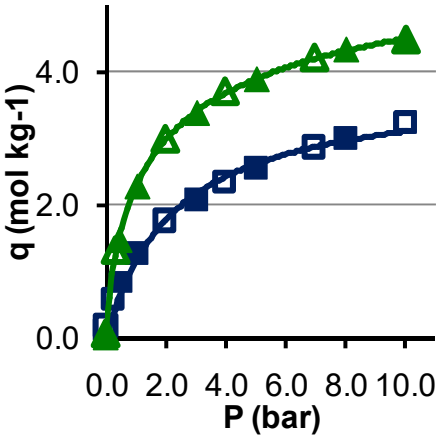

Fig. 1. CO_2 (▲) and CH_4 (■) isotherms at 30°C for XCsP6.

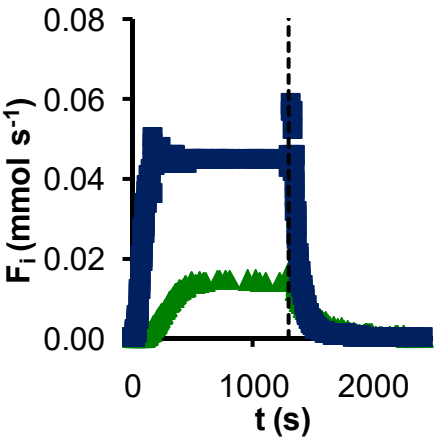

Fig. 2. Breakthrough curves for binary adsorption of CO_2 (▲) and CH_4 (■).

Table 1.Textural properties of XCsP6.

Sample	S_{BET} / $m^2 \cdot g^{-1}$	$W_0(N_2)$ / $cm^3 \cdot g^{-1}$	$W_0(CO_2)$ / $cm^3 \cdot g^{-1}$	$L_0(CO_2)$ / nm	ρ_{Hg} / $g \cdot cm^{-3}$
XCsP6	591	0.23	0.34	0.73	0.58

Acknowledgements

This research is supported by the FEDER and Spanish projects CTQ2013-44789-R (MINECO) and P12-RNM-2892 (Junta de Andalucía). This work was partially financially supported by: Project POCI-01-0145-FEDER-006984 – Associated Laboratory LSRE-LCM funded by FEDER funds through COMPETE2020 - Programa Operacional Competitividade e Internacionalização (POCI). The author Vivo-Vilches is grateful to Spanish MECD for his FPU grant.

References

1. R.W. Pekala, US Patent 4997804.
2. S. Morales-Torres, F.J. Maldonado-Hódar, A.F. Pérez-Cadenas, F. Carrasco-Marín, *Micro and Meso Mats,* 153(2012) 24–29.

Textural Properties of Waste Marble Powder Samples Used as Cheap CaO-based Sorbents for Calcium Looping Cycle CO_2 Capture Process

Carla I.C. Pinheiro[a*], Auguste Fernandes[a], Maria F. Ribeiro[a]
[a]CQE-Centro de Química Estrutural, Instituto Superior Técnico, Universidade de Lisboa, Avenida Rovisco Pais 1, 1049–001 Lisboa, Portugal.
**carla.pinheiro@tecnico.ulisboa.pt*

Introduction

One of the most promising CCS post-combustion technologies is the Ca-looping cycle process, which endeavours to scrub CO_2 from flue gases by using CaO-based sorbents [1]. This regenerative cyclic process is based on the well known capacity of CaO in reacting with gaseous CO_2 at high temperatures (600-750°C) by forming solid $CaCO_3$ [1,2]. Natural sorbents, such as limestone and dolomite, have been considered by several researchers as suitable candidates due to their low price, availability and re-use as feedstock for the cement industry [3], though they become less reactive upon cyclic operations due to sintering, during the high temperatures calcination step [1,3].

Up-to-date there are no studies in literature on the use of natural waste marble powder (WMP) resources, as cheap sorbents for Ca-looping cycle CO_2 capture. The high volume of marble production is associated with considerable amounts of WMP generated as by-product during cutting and polishing procedures, that negatively impacts the surrounding environment. A recent study by these authors demonstrates the ability of WMP to be used as possible cheap and effective CaO-based sorbents with high carrying capacity efficiency upon Ca-looping cycle CO_2 post-combustion capture process. Multiple carbonation-calcination cycles over the WMP sorbents are characterized by a gradual decay of the CO_2 sorption capacity. The main goal of this study consists in investigating the evolution of the textural properties of WMP samples used as CaO-based sorbents in the Ca-looping cycle CO_2 capture, with multiple cycles of carbonation-calcination.

Materials and Methods

Two natural WMP samples (WMP_α and WMP_β) collected from two Portuguese marble producer plants in the region of Estremoz were used as precursors of CaO-based sorbents. The as-received WMP samples were manually grinded in powder form and sieved through CISA sieves (sizes of 63, 125, 250 and 355 μm) and different particle size fractions were obtained. The samples were oven dried at 120 °C. The composition of the fresh WMP samples was determined by chemical analysis.

The BET surface area (S_{BET}) and the pores size distribution (PSD) of the fresh dried, calcined and used (after 10 cycles of carbonation-calcination) samples were determined by N_2 sorption, at -196 ˚C, using a Micromeritics ASAP 2010 apparatus. Before measurement, the samples were outgassed under vacuum at 90 ˚C for 1 h and then at 350 ˚C for 4 h. The total porous volume (V_p) (excluding macropores volume) was calculated from the adsorbed volume of nitrogen for a relative pressure P/P0 of 0.99. Surface areas were calculated by applying the BET equation, while PSD was obtained by using BJH method (desorption branch).

Results and Discussion

The presence of $CaCO_3$ (calcite) as the main compound of the fresh non calcined WMP_{α} and WMP_{β} sorbents dried at 120 ˚C, was confirmed by chemical elemental analysis and by XRD patterns. In addition to Ca, C and O, the chemical elemental analysis of both WMP sorbents show the presence of other elements in trace amounts including Si, Mg, Al and Fe, with a molar ratio of trace element/Ca lower than 0.05, being Si the major trace element for both WMP sorbent samples.

The pores size distributions curves from BJH desorption branch from 50 Å to ca. 1000 Å for the different samples, show that the WMP fresh calcined sorbents have low porous volume but very large mesopores (maxima centered at ca. 950 Å for WMP_{α} samples and ca. 550 Å for WMP_{β} samples). The isotherms obtained for the used samples $WMP_{\alpha\text{-}10cycles}$, $WMP_{\beta\text{-}10cycles}$, and $WMP_{\alpha\text{-}250\text{-}355\text{-}10cycles}$, correspond to type IV with a type H1 hysteresis, both typical of mesoporous solid materials. During the multiple carbonation-calcination cycling process of the WMP samples, there is an increase of V_p mainly due to the formation of mesopores with smaller d_p than in the initial fresh calcined sorbents. This increase of mesopores volume with smaller d_p can explain the observed unexpected increase of the S_{BET} with increasing number of carbonation-calcination cycles for these WMP sorbent samples. The results obtained for sample $WMP_{\beta\text{-}3cycles}$, show that this unusual increase in S_{BET} and V_p is gradual with the increase of the number of cycles.

Typical results found in literature for nitrogen sorption analyses of natural limestones sorbents show that CO_2 cycling of the original sorbent leads to a decreased surface area, which is usually accounted for by sintering and loss of pores surface area due to shrinkage of smaller pores, usually accompanied by growth of macropores [4].

The new and unexpected result highlighted by this work in the case of WMP sorbents with non–differentiated particle sizes WMP_{α} and WMP_{β} and with the higher range particle sizes $WMP_{\alpha\text{-}250\text{-}355}$, is that along with a significant increase of the S_{BET} and of the mesopores volume with smaller d_p observed with the increasing number of carbonation-calcination cycles, there is a decrease of the CaO carbonation conversion. This apparent contradiction can be explained by a deactivation mechanism of blocking of the small pore mouths in the case of narrow bottleneck pore mouths, by the formation of $CaCO_3$ with density significantly lower than that of CaO during the fast stage of the CaO carbonation step at a pore mouth, which makes the CaO sites inside the pores unavailable for the progress of the reaction with CO_2 during carbonation.

Acknowledgements

The authors gratefully acknowledge the financial support by Fundação para a Ciência e Tecnologia, through research project PTDC/AAG-MAA/6195/2014.

References

1. E.J., Anthony, Grenhouse Gas Sci. Technol. 1 (2011) 36-47.
2. E.T., Santos, C., Alfonsín, A.J.S., Chambel, A., Fernandes, A.P., Soares Dias, C.I.C., Pinheiro, M.F., Ribeiro, Fuel. 94 (2012) 624-628.
3. M.C., Romano, M., Spinelli, S., Campanari, S., Consonni, G., Cinti, M., Marchi, E., Borgarel, Energy Procedia. 37 (2013) 7091-7099.
4. P., Sun, J.R., Grace, C.J., Lim, E.J., Anthony, AIChE Journal. 53(9) (2007) 2432-2442.

MDF and PB Composites Wastes used in the Production of Activated Carbons by Physical Activation

José Gomes*, Paulo Mourão, Isabel Cansado, João Nabais, Peter Carrott, Manuela Ribeiro Carrott

Centro de Química de Évora, Instituto de Investigação e Formação Avançada, Departamento de Química, Escola de Ciências e Tecnologia, Universidade de Évora, Colégio L. A. Verney, 7000-671 Évora, Portugal

** jose.gomes.cb@gmail.com*

Introduction

The development of carbon materials remains, at present, one of the areas of great interest within the scientific and industrial communities [1]. Special attention is given to the valorisation of industrial residues of low economic value, trying in this way to solve problems of managing large quantities of waste [2]. Of particular note we highlight the potentially dangerous wastes according to data from the Food and Agriculture Organization of the United Nations (FAO) [3].

The development of new materials for the furniture industry, wood substitutes, has generated an enormous diversity of products but also of waste. The most common are composite materials, among them particle board (PB) and medium density fibreboard (MDF), which have registered an increase of consumption in Europe of 1.3% and 4.3%, respectively, even in times of economic crisis such as the one we are going through [3].

The objective of the present work is to study the potential of these residues for the production of activated carbons (AC) in monolithic forms, generating a product with a high added value and innovative characteristics for subsequent application in adsorption processes.

Materials and Methods

The precursors for the production of activated carbons were modelled according to Fig. 1 in order to obtain mechanically stable structures with large area external to the micropores.

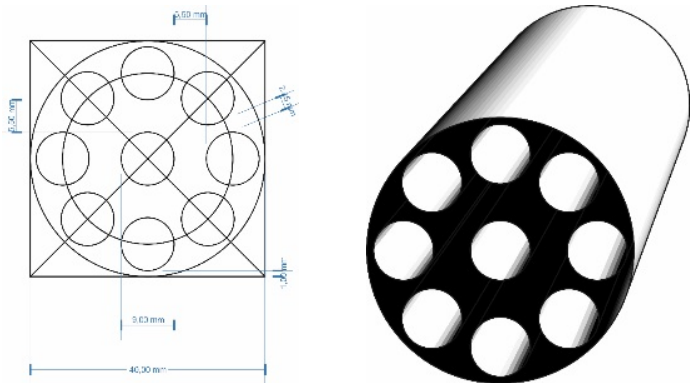

Fig. 1. Model of the monoliths produced, scaling and 3D rendering.

The adsorbent materials were produced by physical activation with carbon dioxide in a horizontal tubular furnace at a final temperature of 1073 K, varying the time of activation in order to obtain AC with distinctive porous structures.

The characterisation of each of the samples involved adsorption of N_2 at 77 K, X-ray diffraction, Fourier transform infrared spectroscopy, CHNSO elemental analysis, determination of pH of point of zero charge (pH_{pzc}) and determination of ash content.

Results and Discussion

The samples produced retained the shape of the precursor, with a decrease of volume and mass, characteristic of the activation process, but in most cases maintaining mechanical integrity.

It can be concluded that the increase in the degree of burn-off of the materials results in an overall increase of the porous structure of the adsorbents, reaching maximum values of apparent BET area of 1259 and 1349 $m^2 g^{-1}$, for AC prepared from MDF and PB, respectively. The elemental analysis results are characteristic of materials produced from lignocellulosic precursors, there being noticed an increased carbon content with the activation process, while the levels of the other heteroatoms decreased during this process. An increase in the percentage of ash and in the pH_{pcz}, dependent on the degree of burn-off of the AC produced from MDF and PB, was also found.

The materials produced in the form of monoliths demonstrate very interesting qualities for applications in the field of adsorption from gas and liquid phases, in line with those prepared in powder form [4].

Acknowledgements

This work was supported by national funds through the Fundação para a Ciência e a Tecnologia (FCT, Portugal), and co-financed by the Fundo Europeu de Desenvolvimento Regional (FEDER) through COMPETE – Programa Operacional Fatores de Competitividade (POFC), within the framework of the projects EXPL/AAG-REC/1181/2013 (FCOMP-01-0124-FEDER-041551) and PEst-OE/QUI/UI0619/2014. We also thank SONAE Indústria for the supply of the wood composites and J. M. A. Figueira (Dep. Física) for the furnace adaptation.

References

1. H. Marsh, F. Rodríguez-Reinoso, Activated Carbon, Elsevier Science & Technology Books, London, 2006.
2. T.M. Letcher, D.A. Vallero, Waste: A Handbook for Management, Academic Press, Boston, 2011.
3. UNECE/FAO Forest Products Annual Market Review, 2013-2014, United Nations Publications, Geneva, 2014.
4. P.A.M. Mourão, J.A.F.L. Gomes, I.P.P. Cansado, J.M.V. Nabais, P.J.M. Carrott, M.M.L. Ribeiro Carrott, in XXXIX Reunión Ibérica de Adsorción, 2014, 175-176.

Utilização de Nanoplaquetas de Grafeno XGNP® para Adsorção do Corante Textil Amarelo Direto Chrysophenine

Eveline Haiana Costa de Oliveira[a*], Marilda Nascimento Carvalho[a], Marcos Gomes Ghislandi[b], Elenora Maria Pereira de Luna Freire[a], Luciana Pereira[c], Mauricio Alves da Motta Sobrinho[a]

[a]Universidade Federal de pernambuco, Recife, Pernambuco, Brasil.

[b] Universidade Federal Rural de Pernambuco address, Cabo de Santo Agostinho, Pernambuco, Brasil.

[c] Universidade do Minho, Braga, Portugal

**oleveline@hotmail.com*

Introducão

O gerenciamento de resíduos especialmente da indústria têxtil tem sido um desafio nos dias atuais (Oliveira, 2015). Os corantes utilizados nos processos de tingimento têm propriedades complexas o que dificulta seu tratamento e disposição final. Apesar dos vários métodos de remediação de efluentes utilizados atualmente (coagulação, floculação, separação por membranas etc) todos eles esbarram em alguma limitação como não resolver o problema totalmente e/ou o alto custo de operação. Dentre estes processos as técnicas de adsorção têm se destacado pela sua eficiência e facilidade de manuseio e operação (Kanchi, 2013). Quando se trata de alternativas tecnológica nos últimos anos os nano materiais têm sido considerados de grande importância incluindo os derivados do carbono, dentre eles destaca-se o grafeno por suas importantes propriedades (Martinez, 2013)

Este estudo teve como objetivo o estudo do processo de adsorção em batelada, utilizando como adsorvente o grafeno xGnP® para a remoção do corante sintético – Amarelo Direto Chrysophenine.

Materiais e metodos

O grafeno utilizado como adsorvente neste estudo foi adquirido comercialmente e consiste em nanofolhas de grafite esfoliado (xGnP®). *Adsorvato* – Corante amarelo direto Chrysophenine foi obtido comercialmente pela empresa Sigma – Aldrich®.

Caracterização do adsorvente: O material foi caracterizado por de microscopia eletrônica de transmissão (MET) das nanofolhas. A caracterização de grafeno também foi realizada por microscopia de força atômica (AFM) além da difração de raio X e a determinação do ponto de carga zero (pHpcz).

Planejamento Fatorial: Foi realizado um planejamento factorial experimental 2^3 para avaliar a influência das variáveis independentes (massa do adsorvente, concentração do corante e tempo) sobre a variável resposta (quantidade adsorvida), a fim de determinar as melhores condições de trabalho e para avaliações futuras sobre o processo. A variável resposta ou variável dependente corresponde à quantidade adsorvida (mg g^{-1}) do corante no adsorvente está representada na Equação 01:

$$q_e = \frac{(C_0 - C_e)V}{m} \qquad (01)$$

q_e é a quantidade adsorvida no equilíbrio (mg g^{-1}), C_0 concentração inicial do corante (mg L^{-1}), C_e a concentração do corante no equilíbrio (mg L^{-1}), V o volume da solução do corante (L) e m a massa do adsorvente (g).

Resultados e discussão

Quando o sistema alcança o equilíbrio, o grafeno comporta-se como um tampão, e isto ocorre em um pH final entre 3,6 a 3,9. O ponto de carga zero foi determinado realizando-se uma média aritmética desses valores, obtendo-se o valor de 3,78, indicando então o pHpcz do grafeno. O difratograma de raio X da amostra de grafeno, mostrou pico em 2Θ igual 26,48 e 44,34, planos de difração característicos de grafite.

As imagens de MET mostraram que as nanofolhas de grafeno estavam, em sua grande maioria, empilhadas ou dobradas umas sobre as outras. A dimensões da área lateral (diâmetro médio) das amostras analisadas (~20) variam em torno de 1-2 um. Através das análises de AFM foi possível estimar que a espessura média correspondeu ao indicado pelo fornecedor. O planejamento experimental mostrou as variáveis que interferiram no processo de adsorção, estão ilustradas na figura 1, mostrando que a concentração e massa exerceram influencia positiva ao passo que o tempo não foi significativo:

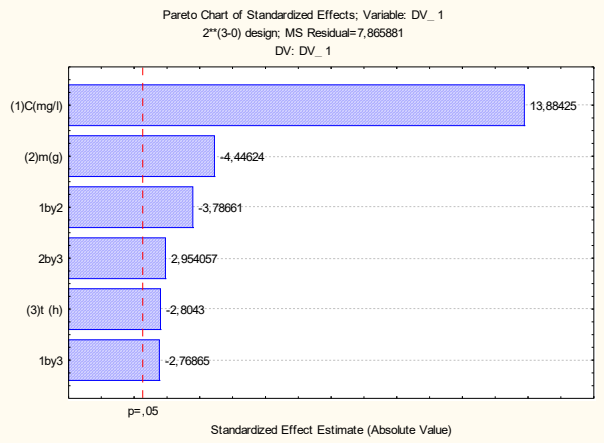

Fig. 1. Grafico de pareto das variaveis que influenciam no processo de adsorção do corante amarelo direto chysophenine

Agradecimentos

Ao programa de pós gradução em Engenharia Química da UFPE

Referencias

1.Kanchi, S.; Bisetty, K.; Kumar, G.; Sabela, M.I.. Arabian Journal of Chemistry, 2013.

2. Martinez, L.M.P., Torres, S.M., Gomes, H.T., Silva, A. M.T. Nanotubos e grafeno: os primos mais jovens da família do carbono! Quim, 128, p 21-27, 2013

3. Oliveira, E.H.C., Mendonça, E. T. R., Barauna, O.S., Ferreira, J.M., Sobrinho, M. A. M. Adsorption Jornal. Vol 21. Pag 1 – 11. . (2015).

Multifunctional Tannic Acid Nanoparticles for Imaging and Therapeutic Applications

J. R. Aguilera[a], V. Venegas[a,b], J. M. Oliva[a], M. J. Sayagués[c], M. de Miguel[d], J. A. Sánchez-Alcázar[a], M. Arévalo-Rodríguez[e], S. Calero[a] and A. P. Zaderenko[a,*]

[a]Departamento de Sistemas Físicos, Químicos y Naturales. Universidad Pablo de Olavide, Spain

[b]Centro de Investigación Cooperativa en Biociencias, Spain

[c]Instituto de Ciencia de Materiales de Sevilla, Spain

[d]Departamento de Citología e Histología Normal y Patológica. Universidad de Sevilla, Spain

[e]Biomedal S.L., Spain

**apzadpar@upo.es*

Introduction

Tannic acid (TA) is a natural product belonging to the family of polyphenols, which exerts multiple effects against cancer [1,2]. The role of TA in cancer therapy is especially promising in those types of cancer that overexpress the epidermal growth factor receptor (EGFR), as TA modulates its activation and downstream signaling pathways, triggering programmed cell death [3].

We have developed a method that generates stable TA nanoparticles (TAN) in a single step [4]. Our nanoparticles were shown to take up extremely high amounts of TA, and were only toxic for the tumoral cells. The uptake assay demonstrated that they were able to enter the cells through a receptor-mediated mechanism. In addition, fluorescent markers could be grafted on the nanoparticles, endowing them with simultaneous imaging and therapeutic applications.

Materials and Methods

TA nanoparticles were synthesized by self-assembly of TA with a neutral polymer (poly(vinyl alcohol); PVA) through hydrogen bonding in aqueous medium, and characterized by dynamic light scattering, Fourier transform infrared spectroscopy and scanning electron microscopy. Nanoparticles were then coated with polyethylene glycol (by a liquid-state adsorption process) and subsequently with protein G, and conjugated to an antibody to EGFR.

Results and Discussion

The physicochemical characterization of nanoparticles showed that they are spherical with a hydrodynamic diameter of 211 nm, a zeta potential of -21 mV and an entrapment efficiency of 92% TA, which is remarkably high and makes our synthesis very effective and compliant with green chemistry principles. The presence of both components, TA and PVA, in the nanoparticles was confirmed by FTIR (Fig. 1).

The cytotoxicity assay showed that our nanoparticles are not toxic for the non-tumoral HDF cell line whereas they are markedly toxic for the tumoral epidermoid carcinoma cell line A431, a cell line widely used as model to study the effect of therapeutic approaches directed to EGFR (Fig. 2).

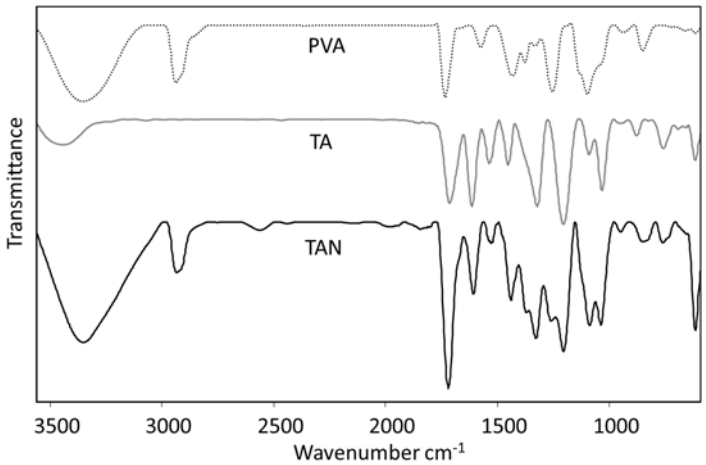

Fig. 1. FTIR spectra of PVA, TA and TA nanoparticles.

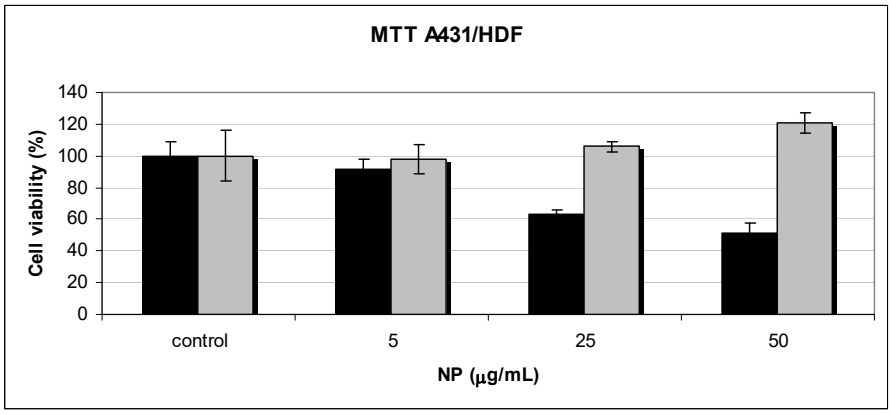

Fig. 2. Dose-dependent cytotoxicity of TAN-Ab nanoparticles in A-431 (black) and HDF (grey). n=3. *P<0.05.

To analyze the cellular uptake of our nanoparticles, a set of nanoparticles was labeled with a water-soluble fluorescent marker, propidium iodide, which is not able to cross intact cell membranes itself. Our results shown that TAN nanoparticles are able to enter the cells through a receptor-mediated mechanism.

Acknowledgements

This work was supported by Junta de Andalucía (Proyecto de Investigación de Excelencia P10-FQM-6615 and PAIDI FQM-319) and Ministerio de Economía y Competitividad, Gobierno de España (Proyecto de Excelencia CTQ2013-48396-P).

References

1. F. Majed, S. Rashid, A. Q. Khan, S. Nafees, N. Ali, R. Ali, R. Khan, S. K. Hasan, S. J. Mehdi and S. Sultana, Mol. Cell. Biochem. 399(2014) 217-228.
2. N. Sahiner, S. Sagbas and N. Aktas, Mater, Sci. Eng. C 49(2015) 824-834.
3. M. Cichocki, M. Dałek, M. Szamałek and W. Baer-Dubowska, Nutr. Cancer. 66(2013) 308-314.
4. J. R. Aguilera, V. Venegas, J. M. Oliva, M. J. Sayagués, M. de Miguel, J. A. Sánchez-Alcázar, M. Arévalo-Rodríguez, A. P. Zaderenko, RSC Adv. 6(2016) 7279-7287.

Adsorption of CO_2 in Carbon Aerogels at Ambient Temperature

Luísa M. Marques, Peter Carrott*, Manuela Ribeiro Carrott
Centro de Química de Évora, Instituto de Investigação e Formação Avançada, Departamento de Química, Escola de Ciências e Tecnologia, Universidade de Évora, Colégio L. A. Verney, 7000-671 Évora, Portugal
** peter@uevora.pt*

Introduction

Carbon aerogels are a remarkable form of electrically conducting monolithic carbon which have a number of advantages over other forms of carbon material. They are most frequently prepared by sol-gel polymerisation of resorcinol and formaldehyde followed by supercritical drying and carbonisation of the resulting organic gel. The particle size and aggregation can be controlled during the sol-gel synthesis and retained during the drying and carbonisation steps with the result that the final product can have a very high specific surface area and extremely high and homogeneous mesoporosity [1], which makes them interesting materials for use in a diverse range of applications related to energy and environmental technologies. These include fuel cell components, supercapacitors, laser experiments, nuclear particle detection, thermal insulation, catalysts, adsorbents for water purification and solvent recovery, molecular sieves for separation of fuel gases and adsorbents for capturing CO_2, amongst others. The success of CO_2 capture with solid adsorbents is dependent on the development of new adsorbent materials with high CO_2 selectivity and adsorption capacity [1].

Materials and Methods

Polymer aerogels were prepared from 2,4-dihydroxybenzoic acid (DHBA) or resorcinol (R) and formaldehyde (F) under basic conditions using the procedure given in [1]. All the aerogels were synthesized from 100 mL of precursor solution, using the stoichiometric R/F molar ratio (0.5) and a dilution ratio of 80. The dilution ratio parameter is defined as the molar ratio between the total amount of solvent and the total amount of reactants. Carbon aerogels were obtained using a vertical tube furnace by heating individual monoliths in a 90 mL min^{-1} N_2 flow to 1073 K at a rate of 5 K min^{-1} and maintaining at this temperature for 180 min. For porosity characterisation each sample was outgassed and the N_2 isotherm at 77 K determined. Analysis of the adsorption isotherms by the α_S, quenched solid density functional theory and Barrett–Joyner–Halenda methods was carried out. A Perkin-Elmer STA6000 analyzer was used to measure the adsorption-desorption of CO_2 at 298 K and a total pressure of approximately 1 bar [1].

Results and Discussion

The N_2 adsorption-desorption isotherms determined on polymer and carbon aerogels were found to be Type IV of the IUPAC classification with well-defined hysteresis loops [1]. Preliminary studies of CO_2 adsorption–desorption were very promising. The adsorption–desorption cycles of CO_2 at ambient temperature are shown in Figure 1. After multiple adsorption-desorption cycles the carbon aerogel showed no significant

alteration in adsorption capacity, confirming the reproducibility and the stability of the material. The results also show that the adsorption and the desorption are very fast, reaching about 90 % of full capacity 2 minutes after switching the carrier gas from He to CO_2 and complete desorption in less than 10 min after switching back to He.

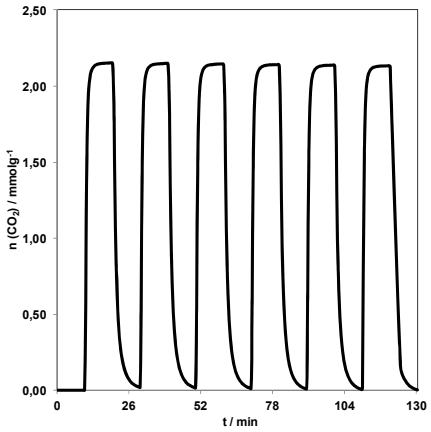

Fig. 1. Repeat cycles at 298 K of CO_2 adsorption–desorption on DHBAF aerogel.

Table 1 lists CO_2 adsorption capacities of the adsorbents used in this work, as well as of some other carbon materials. The comparison of CO_2 adsorption capacity indicates that the results obtained with the carbon aerogels are similar to those obtained with other carbon adsorbents. The results will be considered in more detail in the presentation.

Table 1. Comparison of CO_2 adsorption capacities of carbon adsorbents at 298 K

Sample	n_{ads} / mmol g^{-1}
DHBAF	2.13
RF	1.89
Carbosieve	2.15
Maxsorb	1.87
Takeda 4A	1.15

Acknowledgements

The work was financed through the Fundação para a Ciência e Tecnologia (FCT, Portugal) with national funds (PhD grant SFRH/BD/70543/2010 and project PEst-OE/QUI/UI0619/2014) and co-financed with european (FEDER, programme COMPETE of QREN) funds (project FCOMP-01-0124-FEDER-007307).

References

1. P.J.M. Carrott, L.M. Marques, M.M.L. Ribeiro Carrott, Micropor.Mesopor. Mater. 131 (2010) 75-81.

2. L.M. Marques, P.J.M. Carrott, M.M.L. Ribeiro Carrott, Adsorpt. Sci. Technol. 31 (2013) 223-232.

Removal of Cr(III) in Aqueous Solution by Low-Rank Coals

Delfina Gallardo-López, María F. Alexandre Franco, Carmen Fernández-González, Eduardo M. Cuerda-Correa*, Vicente Gómez-Serrano

Department of Organic and Inorganic Chemistry. University of Extremadura. Avda de Elvas s/n ES06006, Badajoz, Spain

** emcc@unex.es*

Introduction

The necessity to develop alternative technologies for the treatment of polluting industrial effluents has led to make important investments in investigation aimed at preparing more profitable adsorbents. Natural materials that are available in large quantities from industrial or agricultural wastes are excellent candidates for the preparation of the so-called low-cost adsorbents. Among these materials, lignin, different types of biomass, zeolites, seaweed, etc are to be mentioned.

From the biological standpoint, chromium is an essential element involved in the metabolism of lipids and carbohydrates, thyroid metabolism, in some enzyme systems, and in stabilizing proteins and nucleic acids. However, in high concentrations, chromium causes serious environmental problems due to its use in industries such as tanneries, electroplating, pigments, fertilizers, etc. An excess of chromium may also cause severe health problems in humans as, for instance, mutagenic effects, skin lesions, lung disease and several forms of cancer. Chromium compounds are known in all oxidation states ranging from (I) up to (VI). Nevertheless, the chemistry of Cr (I), Cr (IV) and Cr (V) is extremely restricted, while Cr (VI) is a strongly oxidizing species. The most stable chromium species is Cr (III). Taking into consideration all the above exposed, in this work, three low-rank coals such as peat, lignite and leonardite and the derived ashes have been used as the adsorbents with the aim of removing Cr(III) from aqueous solution. The adsorption process has been studied in terms of kinetics, thermodynamics and equilibrium.

Materials and Methods

The peat used in this work was kindly provided by the Spanish subsidiary of the Canadian company Biomatrix Gold. The lignite and leonardite were supplied by SEPHU (Sociedad Española de Productos Húmicos, S.A.). Chromium (III) was used in the form of $Cr(NO_3)_3 \cdot 9H_2O$ (Analytical grade, Panreac Química, Barcelona, Spain).

The adsorbents were characterized in terms of particle size, ash content, physical adsorption of gases (N_2, 77K), FT-IR spectroscopy and point of zero charge.

For the study of the adsorption kinetics, 0.1 g (± 0.0001 g) of adsorbent and 20 mL of aqueous solution of Cr(III) were placed in screw-capped test tubes and maintained in a Selecta Unitronic-OR C thermostatic shaker bath under agitation (50 rpm) and at constant temperature (25 ± 0.1 ºC).

For the determination of the adsorption equilibrium isotherms, a solution of Cr (III) of initial concentration equal to $4 \cdot 10^{-3}$ M was kept in contact with different amounts of adsorbent comprised between 0.01 and 0.5 g under constant stirring (50 rpm) at different temperatures (15, 25, 35 and 45ºC) for a period of time longer than that strictly

necessary to reach equilibration. In both cases, the concentration of Cr(III) in the supernatant liquid was determined by AAS with the aid of a Thermo Electron S Series spectrofotometer.

Results and Discussion

The N_2 adsorption isotherms (Fig. 1, left) show that both peat and leonardite exhibit a limited development of porosity and specific surface. Textural parameters are more developed in lignite. The thermal treatment of leonardite and lignite produces a remarkable increase in the specific surface area and pore volumes relative to the initial samples.

The FT-IR analysis of the samples reveals the presence of a remarkable variety of oxygenated functional groups (hydroxyls, carboxylic acids, ketones, ethers, esters and epoxides) as well as aromatic structures on the surface of the peat. However, the number of organic functional groups gradually decreases with increasing the rank of the coal, probably due to the increase in the content of mineral matter.

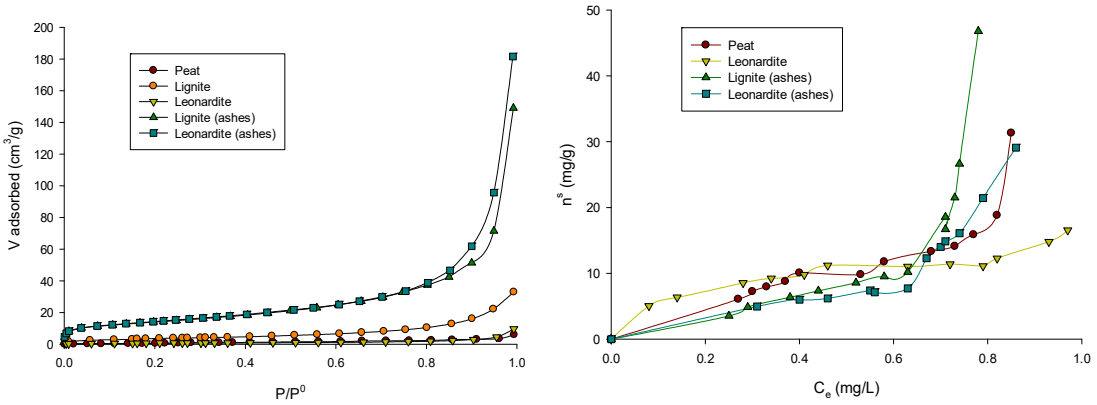

Fig. 1. N_2 adsorption isotherms at 77K (left) and Cr(III) adsorption isotherms (right) by the low-cost adsorbents.

Specific adsorption rates (k_a) were of the order of 10^{-3} s^{-1} although major differences in this parameter ($0.88\text{-}289\cdot10^{-3}$ s^{-1}) have been observed. The influence of diffusion on the overall adsorption process has also been analyzed by applying the methods proposed by Banerjee [1] and Carman and Haul [2]. The values of the diffusion coefficient are around 10^{-8} cm^2/s, although important differences between the systems under study were found.

From the adsorption equilibrium isotherms of Cr(III) in aqueous solution (Fig.1, right) adsorption capacities ranging from 13 up to 130 mg/g have been obtained.

Acknowledgements

The authors gratefully acknowledge Biomatrix Gold and SEPHU for kindly providing the adsorbents used in this study.

References

1. Crank, J. The Mathematics of Diffusion, 2nd Ed., Clarendon Press, Oxford, 1993.
2. Carman, P.C.; Haul R., Proc. Roy. Soc. A. 222 (1954) 109-117.

Europium(III)-Titanium(IV) Phosphates Synthesized *via* Propylamine

Jorge García-Glez[a], Sergei A. Khainakov[b], Zakariae Amghouz[b], Camino Trobajo[a,*]
[a] *Department of Organic and Inorganic Chemistry, University of Oviedo-CINN, 33006 Oviedo, Spain*
[b] *Scientific and Technical Services, University of Oviedo, 33006 Oviedo, Spain*
** ctf@uniovi.es*

Introduction

Ortíz-Oliveros et *al.* [1] have been published the synthesis, physical-chemical characterization and preliminary evaluation of α-$Ti(HPO_4)_2 \cdot H_2O$ (α-TiP) sorption of Eu^{3+}. These authors concluded that the retention process for Eu^{3+} can take place on the surface and in the cavities of the solid in two stages: (i) diffusion into the cavities of the material and (ii) chemisorption. In this work, we will show that the uptake process is limited to surface of the α-titanium phosphate (the interlayer space is inaccessible to the europium species when the α-TiP hydrogen form is used as sorbent), while the diffusion into internal cavities is possible when basal spacing is previously expanded.

Materials and Methods

α-TiP was obtained by using 10 M H_3PO_4 and reflux times of 50 h. Propylamine intercalation compound, α-$Ti(HPO_4)_2 \cdot 2C_3H_7NH_2 \cdot H_2O$ (α-TiPPr), was obtained by placing α-TiP in an atmosphere saturated with propylamine vapor during 6 days at room temperature. In bath, the α-TiP (or α-TiPPr) was equilibrated with europium nitrate solutions (T = 25.0 ± 0.1 ºC, t = 72 h, solution/solid ratio = 20 mL/1 g). The prepared samples were designated as TiP_x (or TiPPr_x), where x indicates the molar concentration europium nitrate solution in the starting solutions, $[Eu^{3+}]_i$.

Results and Discussion

TiP_10^{-4} and TiP_0.1 samples are highly crystalline and their PXRD patterns are identical, corresponding to the α-TiP. Both samples maintain the typical platelet-like pseudo-hexagonal morphologies (length: 0.2-0.8 μm; thickness: 10-30 nm). In TiP_0.1, an additional phase ($EuPO_4 \cdot H_2O$) with nanorod-like morphology (thickness of *ca.* 10 nm) has been formed. The photoluminescence properties of TiP_10^{-4} and TiP_0.1 were investigated. The emission spectrum (λ_{ex} = 394) of TiP_10^{-4} does not show any transition line due to the sorption of Eu^{3+}, while TiP_0.1 spectrum shows the typical emission transitions of Eu^{3+} (attributed to $EuPO_4 \cdot H_2O$ nanorod-phase).

PXRD patterns of TiPPr_10^{-4} to TiPPr_0.1 show a structural order in the direction perpendicular to the plane of the sheet. In the range 0.0001-0.0625 M, the interlayered distance of the sheets remains substantially constant (16.0 Å). However, a new diffraction peak at 2ϑ = 7.3º corresponding to d-spacing of 12.0 Å appears when the concentration is increased to 0.0750 M, which became the only observed peak when the $[Eu^{3+}]_i$ is raised to 0.1000 M. Moreover, the carbon content of the resulting solids continuously decreases with increasing concentration of europium nitrate in the starting solutions, in agreement with the results of STEM-EDS elemental mapping, which obviously indicates that the removal of the amine increases as the ionic strength of the

solution increases. As a result, the behaviour TiPPr_x can be divided into four different zones (A-B-C-D) depending on the concentration of Eu^{3+} in the initial solutions. In the A-zone of low concentrations, the material consists of slightly wrinkled thin films with lateral dimensions varying from about 0.1 μm to 1 μm and thicknesses of *ca* 6.0 nm, maintaining long-range order in the direction of the crystallographic *c*-axis, while a certain order is still maintained in *ab* plane. The propylamine content decreases, being undetectable the presence of Eu. Additionally, the emission spectrum does not show any transition line due to the sorption and/or intercalation of Eu^{3+}. In the region of intermediate concentrations (B-zone) the layers are stacked in the direction perpendicular to the plane of the titanium phosphate sheet, where the interlayered distance is slightly lower than in the starting material TiPPr, but it is essentially constant (16.0 Å), being preserved the pseudo-hexagonal morphologies. The amine content gradually decreases and thus the Eu-content increases in solid phase, reflected in the decrease of carbon content and the appearance of $^5D_0 \rightarrow {}^7F_{0\text{-}4}$ transition peaks in the emission spectrum. Assuming that an ion-exchange process is taking place between the propylammonium cations, $C_3H_7NH_3^+$, and the hexahydrate species of europium, $[Eu(H_2O)_6]^{3+}$, the following tentative formula, $(C_3H_7NH_3)_{2\text{-}3y}[Eu(H_2O)_6]_yTi(PO_4)_2{\cdot}[(H_2O)_6]_{y/2}$, has been proposed for the resulting materials. At higher concentration (C,D-zones) the particles maintain their pseudo-hexagonal morphologies, and besides the presence of interlayered distance of 16.0 Å (the appearance of a new phase with *d*-spacing of 12.0 Å is also observed). In D-zone, the low carbon content suggests that almost all the alkylammonium cations have been involved in the ion-exchange process, thus leading to the formation of a material with the idealized formula $[Eu(H_2O)_6]_{2/3}Ti(PO_4)_2{\cdot}[(H_2O)_6]_{1/3}$, where $[Eu(H_2O)_6]^{3+}$ occupying 2/3 of the pseudo-zeolitic cavities so as to counteract the negatively charged titanium phosphate layer, and the rest of the pseudo-zeolitic cavities (1/3 of the total) will be occupied by water molecules (its crystal structure has been proposed by using DFT-calculations).

In conclusion, the Eu^{3+} uptake capacity of α-TiP and α-TiPPr was investigated by different characterization techniques (PXRD, SEM, TEM, TGA and PL). The Eu^{3+} sorption process takes place only on the surface of α-TiP rather than in its interlayer space, because of the following summarized observations: (i) at high $[Eu^{3+}]_i$ no change in the interlayer distance of α-TiP has been observed by PXRD, and (ii) Eu^{3+} was undetectable by EDX analysis or by PL emission spectra at low $[Eu^{3+}]_i$. However, the Eu^{3+} uptake is considerably improved with α-TiPPr as a consequence of an ion-exchange process into the expanded interlayer space, involving $C_3H_7NH_3^+$ cations and $[Eu(H_2O)_6]^{3+}$ species.

Acknowledgements

Financial support from Spanish *Ministerio de Economía y Competitividad* (MAT2013-40950-R) and *Gobierno del Principado de Asturias* (GRUPIN14-060), and FEDER funding are acknowledged.

References

1. H.B. Ortiz-Oliveros, R.M. Flores-Espinosa, E. Ordóñez-Regil, S.M. Fernández-Valverde, Chem. Eng. J. 236 (2014) 398-405.[1] S.A. Steiner, T.F. Baumann, J. Kong, J.H. Satcher, M.S. Dresselhaus, Iron-doped carbon aerogels: Novel porous substrates for direct growth of carbon nanotubes, Langmuir, 23 (2007) 5161-5166.

Capture and Separation of Dichlorodifluoroethene Isomers using Porous Materials

I. Matito-Martos[a], A. Martin-Calvo[a,b], and S. Calero*[a]
[a]*Department of Physical, Chemical and Natural Systems, University Pablo de Olavide, Sevilla 41013, Spain*
[b]*Department of Chemical Engineering, Vrije Universiteit Brussel, Brussels, 1050, Belgium*

Introduction

Molecular simulation has been extensively used to shed light over the mechanisms that govern separation of mixtures containing isomer molecules. However to the best of our knowledge, separation of geometric isomers in crystalline porous materials have not been deeply explored, and most work has been oriented to chain aliphatic hydrocarbons [1] and positional isomers of aromatic hydrocarbons [2].

This work deals with separation of 1,1-dichloro-2,2-difluoroethene and the *cis* (Z) and *trans* (E) isomers of dichloro-difluoroethene. The selection of these molecules is based on simplicity and potential polarizability, which can make the difference in adsorption and the orientation of the molecules inside the materials. Besides, the capture or the removal of these chlorofluorocarbons (CFCs), is also important from the environmental point of view. We use a group of well known Metal-Organic Frameworks (MOFs) in order to analyze the effects that the metal cluster, the organic linkers, and structural properties such as pore size/shape or accesible surface area, exert during the adsorption and separation processes.

Materials and Methods

We fit the guest-guest interaction parameterer of the Lennard-Jones potential to the vapor-liquid equilibrium curve. Simulations were performed using Gibbs-ensemble Monte Carlo. The Lennard-Jones parameters for the adsorbents were taken from Wiersum *et al.* [3] for UiO-66 (both for the hydroxylate and dehydroxylate structures) and from an internal comunication for MOF-74 (for structures with Co, Cu, Fe, Mn, Ni, and Zn as metal cluster). Since we consider them rigid, these parameters are only used for the interactions for the adsobate-adsorbent interactions, using Lorentz-Berthelot mixing rules. The Widom test particle method is used to explore the low coverage adsorption properties at room temperature. The complete adsorption isotherms are calculated with Monte Carlo simulations in the Grand Canonical ensemble (GCMC). All simulations have been performed using the code RASPA.

Results and Discussion

The results obtained from the Heats of Adsorption (HoA, figure 1a) show that the molecule of 1,1-dichloro-2,2-difluoroethene exhibits the highest interaction with all structures, while the E-/Z-isomers show small differences. Z-isomer interacs stronger with UiO-66 and weaker with MOF-74 than E-isomer. In any case, the strengh of the interaction between the molecule and the structure is stronger in UiO-66 than in MOF-74 since the former is formed by channels narrower in diameter. The relatively

large pore size of MOF-74 hinders the effect that the diferent metal clusters could exert on the adsorption and separation of these molecules. The computed adsortion isotherms from ternary mixture 1,1-dichloro-2,2-difluoroethene/Z/E (0.1:0.45:0.45)[4] in the two UiO-66 structures are depicted in figure 1b. The isotherms were calculated at room temperature exhibiting similar shape for the three molecules, and the largest saturation values for the Z-isomer. It is interesting to note the large differences in adsorption despite the low differences between the heats of adsorption (figure 1a), indicating that the adsorption in these structures is dominated by guest-guest interations. Another interesting observation is the large adsorption of the molecules of 1,1 dichloro-2,2-difluoroethene (which proportion in the mixture is only 10%), compared with these obtained for the Z/E-isomers. Small differences in the loading can be seen at medium pressure between the two UIO-structures, being a slighyly higher in the hydroxylated UiO-66. However at the highest pressures the adsorption of the E- and the Z-isomer increases and decreases, respectively in presence of –OH groups. Further studies on others well known MOFs are performed in order to obtain a wider map on the adsorption behaviour of these three molecules

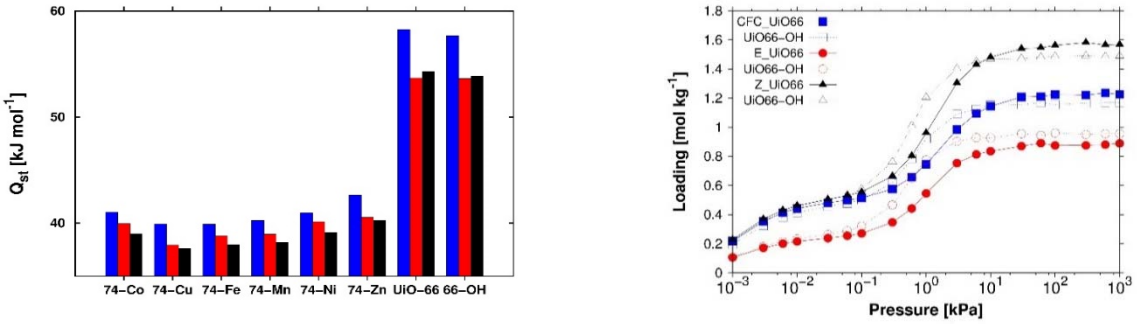

Fig. 1. Left: Isosteric heat of adsorption of 1,1-dichloro-2,2-difluoroethene (blue), Z-isomer (black) and E-isomer(red) in MOF-74 containing different metal clusters, and in UiO-66 hydroxylated and dehydroxylated. Right: adsorption isotherms for the ternary mixture (0.1:0.45:0.45) in UiO-66 hydroxylated (full symbols) and dehydroxylated (empty symbols) at room temperature.

Acknowledgements

This work was supported by the European Research Council through an ERC Starting Grant (ERC2011-StG-279520-RASPA), by the MINECO (CTQ2013-48396-P) and by the Andalucía Region (FQM-1851). I. Matito-Martos thanks the Spanish "Ministerio de Educación Cultura y Deporte" for his predoctoral fellowship.

References

1 M. Maes, L. Alaerts, F. Vermoortele, R. Ameloot, S. Couck, V. Finsy, J. F. M. Denayer and D. E. De Vos, J. Am. Chem. Soc. 132 (2010) 2284–2292.

2 B. Van de Voorde, B. Bueken, J. Denayer and D. De Vos, Chem. Soc. Rev. 43(2014) 5766–88.

3. A. D. Wiersum, E. Soubeyrand-Lenoir, Q. Yang, B. Moulin, V. Guillerm, M. Ben Yahia, S. Bourrelly, A. Vimont, S. Miller, C. Vagner, M. Daturi, G. Clet, C. Serre, G. Maurin and P. L. Llewellyn, Chem. - An Asian J. 6 (2011) 3270–3280.

4 Craig N. C. and Evans D. A., J. Am. Chem. Soc. 87 (1965) 4223-4230.

Recovery of Butanol from Model Fermentation Broths with an Adsorption-Desorption Process using Resin SP-207 ®

V. Ismael Águeda, José A. Delgado*, M Ángeles Uguina, José L. Sotelo, Álvaro García
[a]*Complutense University of Madrid, Madrid, Spain*
**jadeldob@quim.ucm.es*

Introduction

The interest for the fermentative production of butanol as bio-fuel or chemical has increased in the last years. In this process, a very low final butanol concentration is reached due to its toxicity towards the producing microorganisms. A downstream process to recover butanol during the fermentation, or at the end of it, must be developed to reduce this inhibition phenomenon and prolong the fermentation. The low butanol concentration achieved in the broths and the presence of a heteroazeotrope in the butanol-water system complicates the butanol recovery and usually leads to energy-intensive processes. In this context, adsorption as separation technique is considered one of the operations with more potential versus others conventional or not conventional techniques [1]. A cyclic adsorption-desorption process is proposed to carry out the butanol recovery, which consists of an adsorption step in liquid phase followed by a desorption step with hot air. The desorbed products are recovered by condensation and decantation (Figure 1). Previous results showed that the resin SP-207 is selective to butanol in presence of the typical solvents in the fermentation broths. A product stream with a butanol concentration of 77 % w/w is obtained with this process [2]. Few works in the open literature study the stability of the adsorbent with the adsorption-desorption cycles and give a clear desorption methodology including an energy requirement estimation. This contribution will focus on studying the stability of the resin SP-207 with the number of adsorption-desorption cycles, and will propose an energy-efficient desorption step which could make the bio-butanol recovery by adsorption feasible.

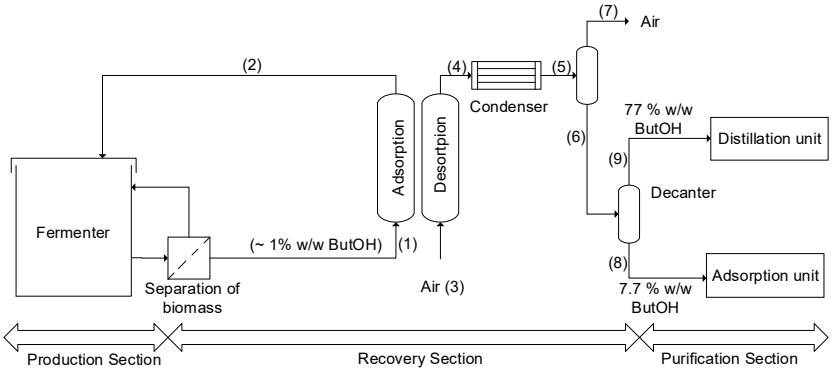

Figure 1. Adsorption-desorption process proposed to recover bio-butanol.

Materials and Methods

A commercial macroporous resin (Sepabeads SP-207®) with a hydrophobic nature has been used as adsorbent. The feed consists on an aqueous mixture with the main components found in a fermentation broth, acetone (0.28 % w/w), butanol (1 % w/w),

ethanol (0.28 % w/w), acetic acid (0.1 % w/w), butyric acid (0.1 % w/w) and glucose. The content of glucose in the mixtures range between 0 and 10 % w/w. The experimental conditions are shown in the Table 1.

Table1.Experimental conditions of adsorption-desorption cycles.

	Adsorption	Desorption	Condensation
Temperature (ºC)	60	60	-5
Flowrate (mL/min)	1 (Liquid)	200 (Air)	200 (Air)
Time (min)	70	60	60

Results and Discussion

The butanol breakthrough curves obtained in consecutive cycles are shown in Figure 2 (a). The butanol concentration in the adsorption effluent (2) after the first cycle is not zero because the column has not been regenerated completely in the previous cycle. The butanol breakthrough times and the shape of its curves do not vary from the cycle 2 to 35 indicating that a steady state has been achieved. Glucose is not adsorbed on the resin and its presence does not affect the butanol adsorption. The adsorption working capacity for butanol is about 50 g/kg in the steady state whereas the one for the others solvents is almost negligible (Figure 2 (b)). The glucose and the acids consumed in the metabolic pathway are recycled to the fermenter by the adsorption effluent (2). The condensed product (5) is separated by decantation giving stream (9) with 78 % w/w butanol, 21 % w/w water and 1 % w/w of acetone, ethanol and acids.

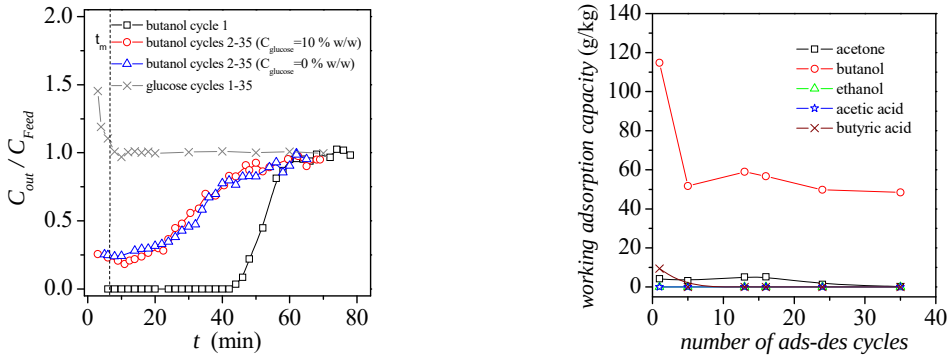

Fig. 2. Breakthrough curves (a); adsorption working capacity (b).

A mathematical model based on fundamental equations and validated experimentally has been used to estimate the energy requirement of the desorption-condensation step. It is assumed that the proposed process is heat-integrated with the whole process, enabling the use of waste heat for the desorption step. The condensation is performed in two steps in series, the first one at 10 ºC driven by a refrigeration cycle using waste heat and the second one at -5 ºC. An optimal interval of desorption time has been found with an energy cost of 1.4-1.7 MJ/kg_{but} and butanol recovery about 95 %.

References

1. N. Abdehagh, F. Handan T, Jules T, Biomas & Bioenergy 60; (2014); 222-24.
2. J.A. Delgado, V.I. Águeda, M.A.Uguina, J.L. Sotelo, A.García, Patente ES2478415, 30-05-2014.

Removal of 1-Bromopropane by Adsorption with Activated Carbons

Ana Beatriz Freitas[a], Auguste Fernandes[a], João M. Silva[a,c], A. Paula Matos [b], M. Filipa Ribeiro[a,*]

[a]*CQE-Centro de Química Estrutural, Instituto Superior Técnico, Universidade de Lisboa, Avenida Rovisco Pais 1, 1049–001 Lisboa, Portugal.*

[b] *TAP Manutenção e Engenharia, Aeroporto de Lisboa*

[c] *ADEQ, ISEL – Instituto Superior de Engenharia de Lisboa, Instituto Politécnico de Lisboa, R. Cons. Emídio Navarro, 1959-007 Lisboa, Portugal*

** filipa.ribeiro@tecnico.ulisboa.pt*

Introduction

Nowadays, people are more aware of the consequences of VOCs emissions to the atmosphere. In the aerospace industry, the cleaning of metal pieces was done, during many years, with vapor degreasing processes that used organic solvents as cleaning agents, for instance 1,1,1–trichloroethane and trichloroethylene. As a consequence of Montreal Protocol revision in the 90s, the use of those solvents became limited and it was necessary to introduce new solvents like 1-bromopropane (1-BP), as possible substitutes [1]. Nevertheless, certain precautions are still required in order to reduce VOCs emissions and to assure the compliance of the limiting emission values established by law. The adsorption process is the most common to remove VOCs from gaseous streams. The main costs associated with the implementation of adsorption systems are related with the type of adsorbent chosen that will also influence the efficiency of the process [2]. Activated carbons are the most common adsorbents since they have high surface areas and non-uniform pores that allow the adsorption of a large number of compounds simultaneously. In contrast to what happens with compounds like toluene and CFCs, there is a lack of studies focused in the removal of 1-bromopropane (1-BP). In this work, the removal of 1-BP was studied by adsorption in commercial activated carbons with different characteristics and shapes.

Materials and Methods

Several commercial activated carbon samples in different forms: granular (Norit RX3, Carbosorb b64, Merck 102514 AC and Filtracarb), fiber (ACF) and cloth (ACC) supplied by Kynol, were used as adsorbents. The adsorption study was performed using EnSolv® 5408 solvent containing around >90 wt.% of 1-BP and <3 wt.% of 2-butanol and 1-BP with 99% purity from Sigma-Aldrich. The characterization of the samples was carried out by nitrogen sorption at 77K using a Micromeritics ASAP 2010 apparatus and by thermal programed decomposition (TPD) to identify the functional groups that exist at the carbons surface (according to the procedure developed by Figueiredo et al. [3]). The adsorptions studies were performed through the determination of breakthrough curves obtained at atmospheric pressure and ambient temperature and using 1g of sample in a fixed bed column. The inlet concentration was composed by nitrogen and 1-BP (125; 172, 238; 330 mg/L). The outlet stream from the column was analyzed every 4 minutes by gas chromatography (GC). The amount of 1-BP adsorbed by each adsorbent, q_{exp}, was

determined from the integration of breakthrough curves from time t=0 and t=saturation. The breakthrough curves obtained were adjusted to different empirical models like Thomas and Bohart-Adams Models.

Results and Discussion

The breakthrough curves obtained during the adsorption of 1-BP with the different activated carbon samples are shown in Fig. 1. ACC sample was the one that adsorbed the highest amount of 1-BP and had higher breakthrough times. The adsorption models fit the experimental data reasonably well. The Bohart-Adams model was only used for comparison of the breakthrough times, since the model can only describe the beginning of the breakthrough curve. The adsorbed quantities obtained with this model cannot be used to describe the real amounts adsorbed. However, the breakthrough times were similar to the ones determined experimentally. In order to verify if the solvent impurities have any influence, an adsorption test was performed using 1-BP (99% purity) with a Carbosorb 64 sample and the adsorption capacities obtained in both cases were the same (2,37 mmol/g) and the breakthrough curves very similar. Using Norit R3, an increase of 1-BP concentration at inlet was observed, leading to identical adsorption capacities with saturation times decreasing from 72 to 24 minutes. TPD analysis showed that the presence of carboxylic groups in the carbon surface does not have any influence on the amount of 1-BP adsorbed by each sample. The results obtained in this study showed that the adsorption capacities are higher using samples in powder form than in granular. From the industrial point of view, the granular samples are preferable, but it was observed that samples with higher micropores volume adsorb higher amounts of 1-BP, except when preferential paths related with the shape of the granulated samples (extrudates or spheres) are present.

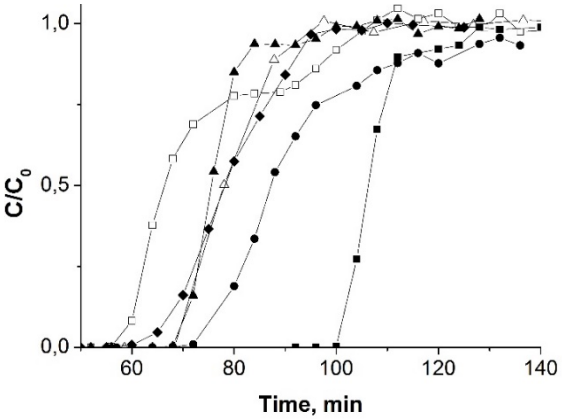

Fig. 1. Breakthrough curves for 1g of Norit RX3 (●), Carbosorb64 (♦), Filtracarb (▲), Merck (□), ACC (■) and ACF (Δ).

Acknowledgements

The authors thank Portuguese FCT for financial support PEst-OE/QUI/UI0100/2013

References

1. B.G. Travis, C. Boster, Plat. Surf. Finish 80 (1993) 20–22.
2. J. Rodríguez-Mirasol, J. Bedia, J.J. Rodríguez, Separ. Sci. and Technol. 40 (2005) 3113–3135.
3. J.L. Figueiredo, M.F. Pereira, M.M. Freitas, J.J. Órfão, Carbon 37 (1999) 1379–1389.

Magnetic Iron Oxide-Mesoporous Silicas for Adsorption of 5-Fluorouracil

Elisabete Palma Carreiro[a], Manuela Ribeiro Carrott[a,b,*], Peter Carrott[a,b], Anthony Joseph Burke[a,b]

[a]Centro de Química de Évora, Instituto de Investigação e Formação Avançada, Universidade de Évora, Colégio L.A. Verney, 7000-671 Évora, Portugal

[b]Departamento de Química, Escola de Ciências e Tecnologia, Universidade de Évora, Colégio L.A. Verney, 7000-671 Évora, Portugal

** manrc@uevora.pt*

Introduction

Magnetic mesoporous silica nanoparticles (MMSN) have been shown to be important materials for diverse biomedical applications, like imaging for diagnostic, biosensing, biocatalysis and drug delivery [1]. MMSN are attractive materials due to the conjugation of nontoxicity and biocompatibility with the magnetic properties of iron oxide together with the advantageous structural properties of mesoporous silica, such as tunable uniform pore size, large internal specific surface area and pore volume.

5-Fluorouracil (5-FU) is an important antineoplastic drug but, on the other hand, it is very toxic, causing severe side effects. The immobilization of 5-FU in nanomaterials by adsorption is one possibility for drug delivery systems in order to decrease the side effects. However, the studies of adsorption of 5-FU in mesoporous silica based materials are very scarce [2, 3].

The objectives of this work are to obtain and to characterise magnetic mesoporous materials consisting of iron oxide in mesoporous silica nanoparticles, with different characteristics, and to test their ability for adsorbing 5-FU. Two MMSN are considered in this work and the results are compared also with a pure silica grade.

Materials and Methods

The magnetic iron oxide nanoparticles, the materials with iron oxide in mesoporous silica (A and B) and a pure silica mesoporous material (C) were prepared with some differences in the procedures reported in the literature [4, 5].

The characterisation of the materials involved nitrogen adsorption at 77 K, scanning (SEM) and transmission (TEM) electron microscopy, X-ray diffraction and energy dispersive X-ray fluorescence spectrometry. Nitrogen adsorption-desorption isotherms were determined on a Quantachrome Autosorb iQ, using helium and nitrogen of 99.999% purity. SEM and TEM analyses were obtained, respectively, on Hitachi S2400 and on Hitachi 8100 electron microscopes. X-ray diffraction was carried out on a Bruker AXS D8 Advance diffractometer. Iron oxide content was determined by X-ray fluorescence and using calibration data determined, in an appropriate concentration range, on an Oxford Instruments X-Supreme 8000 spectrometer.

Adsorption of 5-FU from solutions was tested at 298 K and the amounts of 5-FU adsorbed were obtained from changes of its concentration as determined by spectrophotometry, after appropriate dilution to be in the concentration range of calibration data obtained, under the same conditions, on a Perkin Elmer Lambda 850 UV-Vis spectrophotometer.

Results and Discussion

As inferred from Fig. 1, materials with different characteristics were obtained, although, they have, in all cases, large specific surface areas and mesopore volumes.

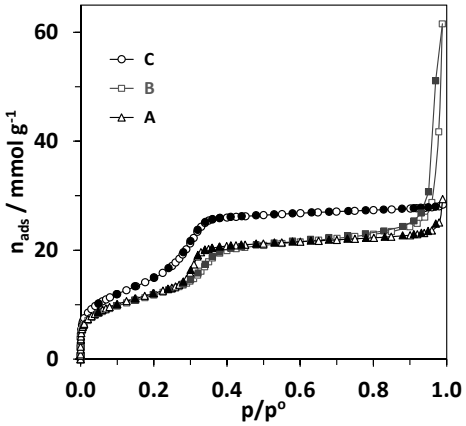

Fig. 1. Nitrogen adsorption-desorption isotherms, at 77 K, determined on mesoporous silicas A and B with magnetic iron oxide and on mesoporous silica C.

It is evident that material A has very uniform mesopore width, better than material B which, in addition, presents secondary mesoporosity. The materials A and B have similar specific surface area, while that of material C is larger although the mean pore width, obtained from the maximum of the pore size distribution calculated by NLDFT, is similar to that of material A. TEM showed differences in the shape of the mesoporous silica particles, namely that C consists of spherical particles, while B has mainly round particles and A has rod shape particles with uniform channels in consistency with the nitrogen adsorption. In addition, A and B present iron oxide nanoparticles in the silicas. The materials A and B, for which the iron oxide content was found to be similar, have advantage over pure silica grades of being easily recovered and for drug delivery, due to the magnetic properties of the iron oxide in the silica nanoparticles. The adsorption of 5-fluorouracil by the different materials will be compared in the presentation.

Acknowledgements

EPC is grateful for a post-doctoral research fellowship (SFRH/BPD/72182/2010). This work was financed through the Fundação para a Ciência e a Tecnologia (FCT, Portugal) with national funds (PEst-OE/QUI/UI0619/2014). We also thank Eng. Isabel Nogueira (MicroLab, Instituto Superior Técnico, Lisboa) for assistance with the electron microscopy analyses.

References

1. C. Argyo, V. Weiss, C. Braüchle, T. Bein, Chem. Mater. 26 (2014) 435-451.
2. A.M. Tomoiaga, B.I. Cioroiu, V. Nica, A. Vasile, Colloids Surf. B: Biointerfaces 111 (2013) 52-59.
3. X. She, L. Chen, C. Li, C. He, L. He, L. Kong, J. Nanomater. 2015 (2015) 1-9.
4. N.Z. Knezevic, I.I. Slowing, V.S.-Y. Lin, ChemPlusChem 77 (2012) 48-55.
5. M. Grün, K.K. Unger, A. Matsumoto, K. Tsutsumi, Micropor. Mesopor. Mater. 27 (1999) 207-216.

Adsorption of Water Vapour by Activated Carbon Fibres with Systematically Varied Micropore Sizes

Peter Carrott[a,*], Manuela Ribeiro Carrott[a], Paulo Correia[b]
[a]*Centro de Química de Évora, Instituto de Investigação e Formação Avançada, Departamento de Química, Escola de Ciências e Tecnologia, Universidade de Évora, Colégio L. A. Verney, 7000-671 Évora, Portugal*
[b]*Fisipe SA, Member of SGL Group - The Carbon Company, Apartado 5, 2836-908 Lavradio, Portugal*
** peter@uevora.pt*

Introduction

In many of their practical applications activated carbon materials are used in the presence of water vapour or liquid. Hence, the study of the interaction between water molecules and carbon surfaces is of some practical importance. It is generally believed that the mechanism of adsorption involves a number of stages. Initially, individual molecules adsorb on polar surface sites and these then act as secondary sites for the formation of clusters. As the relative pressure increases, the clusters grow and may eventually coalesce or may detach from the primary sites. Multimolecular clusters behave as larger more polarizable molecules and will therefore be able to adsorb in the micropores even if the walls are hydrophobic. On the basis of these general principles a number of models and corresponding isotherm equations for the adsorption of water vapour by microporous carbons have been proposed [1-4].

The objective of the present work was to obtain water vapour adsorption isotherms on series of purely microporous carbons covering a range of micropore sizes and to use these for the evaluation of a number of models. In the presentation we will consider just one model, referred to as the cooperative multimolecular sorption (CMMS) model [1]. According to this, the adsorption of water vapour is described by the equation

$$\frac{C}{C_{sat}} = \frac{K_o a}{(1 - K_{as} a)[K_o a + w^2(1 - K_{as} a)]}$$

where

$$w = \frac{1}{2}\left(1 - \frac{K_1 a}{1 - K_{as} a} + \sqrt{\left(1 - \frac{K_1 a}{1 - K_{as} a}\right)^2 + \frac{4K_o a}{1 - K_{as} a}}\right)$$

C and C_{sat} are the adsorption and adsorption capacity, a is the relative pressure and the K's are equilibrium constants for the different stages of adsorption.

Materials and Methods

The precursor used in this work was a modified acrylic fibre specially prepared by Fisipe SA, Member of SGL Group - The Carbon Company. A vertical tube furnace and constant gas flow of 85 $cm^3 min^{-1}$ were used. Each sample was carbonized by heating to 700, 800, 900 or 1000 ^oC at a rate of 10 $^oC\ min^{-1}$ under N_2. Activation was carried out by switching to a CO_2 flow for between 15 to 4320 min, then switching back to the N_2 flow and allowing the sample to cool to below 50 ^oC before removing from the furnace. The

samples are designated FXtq, where t is the activation temperature in °C divided by 100 °C and q is the burn-off. Each sample was subsequently characterized by adsorption of N_2 at 77 K using a Quantachrome Autosorb iQ.

The adsorption isotherms of water vapour were determined gravimetrically at 293 K using a CI Precision vacuum microbalance coupled to a Disbal control unit with pressure measurement by means of an Edwards Barocel 600 capacitance manometer. Fitting to the CMMS Equation was carried out using IGOR Pro vs. 6.3.7.2.

Results and Discussion

Fig.1 shows water vapour adsorption isotherms for 3 of the samples prepared at 900 °C. As the burn-off increases the adsorption capacity increases and the pore-filling step shifts to higher relative pressure. Similar results were obtained at other preparation temperatures, the most significant differences being that, considering a fixed value of burn-off, both the adsorption capacity and the relative pressure of the step increased with increasing preparation temperature. In addition, it was found that the isotherms exhibited hysteresis at pressures greater than about 0.25p° when the burn-off was high but were completely reversible when the burn-off was low. An estimate of mean pore size was obtained by application of the Dubinin-Astakhov Equation to the 77 K N_2 isotherms and it was found that, in general, there was a relatively linear relationship between mean micropore size and the point of inflection of the water vapour isotherms.

Fig.2 shows representive examples for the fitting of the CMMS equation. In all cases reasonable fits are obtained over a wide range of relative pressures for samples with very different burn-offs and mean micropore sizes (0.7 and 1.4 nm for 17 and 83 % burn-off, respectively). The results will be considered in more detail in the presentation.

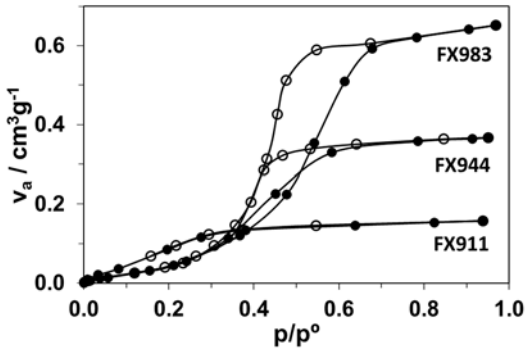

Fig.1. Representative water vapour adsorption isotherms

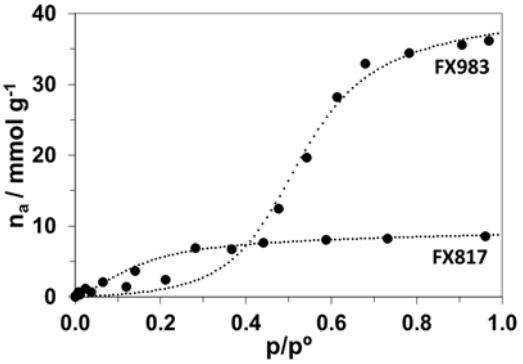

Fig.2. Representative examples of fitting the CMMS Equation

Acknowledgements

The authors are grateful to FISIPE SA (Portugal, Member of SGL Group - The Carbon Company) for the preparation of the precursor fibres. The work was financed through the Fundação para a Ciência e Tecnologia (FCT, Portugal) with national funds (project PEst-OE/QUI/UI0619/2014).

References

1. S.W. Rutherford, Carbon 41 (2003) 579-625.
2. D.D. Do, H.D. Do, Carbon 38 (2000) 767-773.
3. S. Lagorsse, M.C. Campo, F.D. Magalhães, A. Mendes, Carbon 43 (2005) 2769-2779.
4. S. Furmaniak, P.A. Gauden, A.P. Terzyk, G. Rychlicki, Adv. Colloid Interface Sci. 137 (2008) 82-143.

ÍNDICE DE AUTORES

APÊNDICE

Esquema do Programa

Hora	5 de setembro de 2016 (segunda-feira)	6 de setembro de 2016 (terça-feira)	7 de setembro de 2016 (quarta-feira)
8.00	Entrega de documentação Sessão de Abertura		
9.00	Conferência Plenária	Conferência Plenária	Reunião do Grupo de Adsorção
10.00	4 Comunicações Orais	4 Comunicações Orais	4 Comunicações Orais
11.00	*Coffee Break*	*Coffee* e Comunicações em Poster	*Coffee Break*
12.00	4 Comunicações Orais	4 Comunicações Orais	4 Comunicações Orais Sessão de Encerramento
13.00	Almoço	Almoço	Almoço
14.00	Comunicações em Poster	Visita Turística	
15.00	4 Comunicações Orais		
16.00	*Coffee* e Comunicações em Poster		
17.00	4 Comunicações Orais		
18.00			
19.00	Receção		
20.00		Jantar do Congresso	
21.00			